Universidad de Valladolid

Escuela de Doctorado Universidad de Valladolid

PhD PROGRAM IN BIOMEDICAL RESEARCH

PhD DISSERTATION:

Effect of the Gluten-Free Diet on the Intestinal and Circulating Immunome from Patients with Coeliac Disease

Submitted by Aida Fiz López to obtain a PhD degree
from the University of Valladolid

Supervised by:
Eduardo Arranz and David Bernardo

A mi madre.

En primer lugar, quiero expresar mi más sincero agradecimiento a David por darme la oportunidad de realizar esta tesis, por su confianza y apoyo a lo largo de estos años. Ha sido un mentor excepcional, siempre dispuesto a recordarme que los errores forman parte del aprendizaje y abierto a cualquier propuesta. Gracias por tenderme la mano en los momentos más difíciles.

También quiero agradecer a Eduardo por su apoyo y orientación, así como a todas las personas que han formado parte del laboratorio de Inmunología de las Mucosas durante este tiempo. He tenido la suerte de compartir este camino desde el principio con Elisa, aprendiendo juntas y compartiendo frustraciones, ha hecho que todo sea más fácil. A Ángel, quien además de mantenernos siempre alerta, ha demostrado una gran disposición para ayudar en todo momento, incluso asumiendo la responsabilidad de recoger las muestras en el hospital. A Carol, por su dominio excepcional de Excel, su paciencia infinita, su espíritu de equipo y su entusiasmo constante. A Álex, por ayudarme a crecer como mentora y por su apoyo en tantos experimentos. Y, por supuesto, a Candi, el mejor técnico que podríamos haber tenido. A todos los que habéis formado parte de este laboratorio Garrote, Paloma, Antonio, Juan, Sara y Marina gracias por acompañarme en este camino.

Al personal del IBGM, en especial a Lola, Diego y Nuria, por fomentar un ambiente de trabajo amable y cercano. También a Álvaro de la Unidad de Citometría por su dedicación y apoyo técnico.

Un reconocimiento especial a los equipos del Servicio de Gastroenterología del Hospital Universitario y del Hospital Universitario Río Hortega en Valladolid por su dedicación en la recolección de muestras, especialmente a Luis por sus valiosas ideas, así como a Sandra y Javier por sus contribuciones. Gracias también a todos los pacientes por su participación, gracias a ellos pueden llevarse a cabo todas nuestras investigaciones.

Gracias a Juan, de Ámsterdam UMC, y a todo su equipo por su cálida bienvenida y su inestimable ayuda durante mi estancia, en especial a Sara.

Finalmente, le agradezco a Javi su apoyo constante, tanto emocional como técnico. Gracias por estar a mi lado en cada proyecto que emprendo. Por último, gracias a mi familia y amigos por hacerme sentir válida ante cada desafío.

Contents

List of Figures

List of Tables

Abbreviations

APC Antigen presenting cells.
ASCT Autologous stem cell transplantation.

BTNL Butyrophilin-like protein.

C-GFD Coeliac disease patient on a gluten free diet.
C-NI Coeliac disease patient with no inflammation.
C-I.M1/2 Coeliac disease patient with mildly inflamed duodenum (Marsh 1/2).
C-I.M3 Coeliac disease patient with severely inflamed duodenum (Marsh 3).
C-I Coeliac disease patient with inflamed duodenum.
CCR C-C motif chemokine receptor.
CD Coeliac disease.
cDC Conventional dendritic cells.
CXCR C-X-C motif chemokine receptor.

DC Dendritic cells.
DTT Dithiothreitol.

EdgeR Empirical analysis of digital gene expression in R.
EDTA Ethylenediaminetetraacetic acid.
EPCAM Epithelial cell adhesion molecule.

FABP Intestinal fatty acid-binding protein.
FACS Fluorescent activated cell sorting staining.
FGID Functional gastrointestinal disorders.
FMO Fluorescence minus one.
FODMAP Fermentable oligosaccharides, disaccharides, monosaccharides and polyols.
FOXP3 Forkhead box protein P3.

GALT Gut-associated lymphoid tissue.
GFD Gluten free diet.
GIP Gluten-immunogenic peptides.

IBD Inflammatory bowel disease.
IEC Intestinal epithelial cells.
IEL Intraepithelial lymphocytes.

IFN Interferon.
Ig Immunoglobulin.
IL Interleukin.
ILC Innate lymphoid cells.

JAML Junctional adhesion molecule-like.

LP Lamina propria.
LPL Lamina propria lymphocytes.
LPMC Lamina propria mononuclear cells.

MFI Mean fluorescence intensity.
MRI Magnetic resonance imaging.

NC-I Non-Coeliac disease patient with inflammation.
NC-NI Non-Coeliac disease patient with no inflammation.
NK Natural killer cells.

PBMC Peripheral blood mononuclear cells.
pDC Plasmacytoid dendritic cells.

RCD Refractory coeliac disease.
RT Room temperature.

t-SNE t-distributed Stochastic Neighbor Embedding.
$\mathbf{T}_{\mathrm{reg}}$ Regulatory T cells.
TCR T cell receptor.
TEMRA Effector memory cells re-expressing CD45RA.
TG2 Tissue transglutaminase type 2 enzyme.
TGF Transforming growth factor.
Th T helper.
TLR Toll-like receptor.
TNF Tumor necrosis factor.

UMAP Uniform Manifold Approximation and Projection.

Summary

Introduction

Coeliac disease (CD) is an autoimmune disorder associated with gluten ingestion in genetically predisposed individuals, primarily affecting the small intestine but with systemic implications. Following the involvement of intraepithelial lymphocytes (IEL) and lamina propria lymphocytes (LPL), villous atrophy is induced in the duodenum. The immune response is not restricted to the small intestine as it can be also observed in the peripheral immune system, increasing the susceptibility to other autoimmune diseases and/or malignancies. The prevalence of CD is about 1 % in western countries, with an increase in the incidence, especially in children. Its diagnosis involves serology, histopathology, and genetic testing, with flow cytometry-based lymphograms as a helping test in complex cases. Early detection and improved diagnostic algorithms are crucial for timely intervention.

A gluten-free diet (GFD) is the primary and only treatment for CD, but adherence is challenging. Monitoring methods include serological tests and the detection of gluten immunogenic peptides in faeces. Flow cytometry, particularly spectral flow cytometry, helps CD research by enabling detailed immune profiling, and offer insights into immune dysregulation and potential therapeutic targets. However, more than half of the patients still exhibit villous atrophy despite adherence to a GFD, highlighting the need for improved monitoring and therapeutic approaches.

Hypothesis and aim

Given that recent evidence suggests that up to 50 % of CD patients exhibit persistent mucosal atrophy despite adherence to a GFD, we hypothesize that such lack of mucosal recovery may be associated with alterations in the mucosal and/or peripheral immune system. The aim of this thesis therefore is to study the effect of a GFD on the phenotype and function of immune cells from the intestinal mucosa and peripheral blood of CD patients.

Material and Methods

Due to the current limited knowledge regarding the phenotype and function of IEL, these cells have been characterized throughout the length of the human gastrointestinal tract, including the stomach, duodenum, ileum, and colon. Additionally, their enrichment and subsequent

cell culture were assessed. The study then focused on examining the effect of a GFD on the soluble and cellular immunome from CD patients. A detailed analysis was further conducted on duodenal LPL and peripheral blood mononuclear cells (PBMC) from non-celiac controls, newly diagnosed CD patients and CD patients on a GFD, who were further categorized based on the presence of symptoms and villous atrophy. Cytokines in the duodenal microenvironment and plasma samples from patients were also evaluated. Flow cytometry was the primary technique used for these analyses.

Results

The immune landscape in the gut showed notable shifts, with T$\gamma\delta$ IEL expanding and classical T IEL reduced in the duodenum, particularly in those cases with mucosal atrophy. While NK-like cells remain unchanged, CD7$^+$ cells are enriched in the duodenum.

Contrary to expectations, none of the IL-15R subunits were significantly increased in the IEL of CD patients. Moreover, a reduction in IL-15Rα expression was observed on T$\gamma\delta$ IEL in all CD patients. These results suggest the involvement of alternative cytokines in IEL cytotoxicity. However, IL-15Rα was elevated in the epithelial cells fraction of CD patients supporting the trans-presentation model, where IL-15 is transferred from epithelial cells to IEL.

A more direct role in IEL cytotoxicity can be attributed to NKG2D, which was upregulated on CD4$^+$ and CD4$^+$CD8$^+$ T IEL in CD patients, particularly in patients with atrophy. This suggests that NKG2D could serve as a potential target for immune therapies.

Despite improvements in mucosal structure following GFD, persistent atrophy was observed in 68.4% of patients. Additionally, a longer duration on the GFD was associated with increased gut-homing markers (Integrins α4, β7, CCR9, CCR2) and inflammatory markers (CD2, CD38) in the lamina propria. Symptomatic GFD-treated patients exhibited heightened gut-homing markers in CD8 T cells and memory B cells, with reduced CXCR3 and CD38 expression on regulatory T cells. Despite these alterations, the cytokine analysis revealed normalization of IL-18 and IL-12p70 post-GFD.

Last, when examining peripheral immunity, this study found that during the active phase of the disease in newly diagnosed patients, the immune profile follows expected patterns, characterized by sustained immune activation. Persistent immune activation was also observed in C-GFD patients wit atrophy and symptomatology. These findings suggest enhanced migration of active immune cells to the intestine, contributing to ongoing mucosal damage. Moreover, computational cytometry analysis revealed an inflammatory shift in active CD, with increased plasmablasts, whereas GFD patients showed more cDC2 and altered immune trafficking.

Discussion

Many patients continue to exhibit villous atrophy and immune activation despite strict adherence to the GFD, suggesting that while immune normalization may initially occur, it is often followed by unresolved chronic inflammation.

These findings support the hypothesis that persistent mucosal atrophy in CD patients on a GFD is associated with immune alterations at both mucosal and systemic levels. This persistent inflammation could be driven by factors such as microbial drivers or exposure to non-gluten dietary antigens, underscoring the need for a more comprehensive approach to treatment. Moreover, persistent villous atrophy may not solely be indicative of refractory coeliac disease (RCD), but rather reflects a more complex form of CD that does not align with the traditional definition of refractoriness. This raises the question of whether the concept of RCD should be reconsidered, viewing persistent atrophy as a marker of prolonged damage rather than a definitive sign of clinical refractoriness.

These findings highlight the urgent need for personalized therapeutic strategies that extend beyond gluten exclusion, focusing on immune regulation and addressing the underlying causes of chronic inflammation. By integrating advanced imaging techniques, immunological markers, and tailored dietary interventions, clinicians can better manage the diverse manifestations of CD as well as to improve long-term patient outcomes.

Conclusions

More than half of CD patients display persistent villous atrophy despite strict adherence to a GFD. Increased NKG2D expression on IEL is associated with atrophy, highlighting its potential as a target for immune therapies. Of note, the expression of the IL-15 receptor is not increased on these lymphocytes, suggesting that other cytokines may play a role in their cytotoxicity. While the GFD helps to restore the immune balance in LPL, symptomatic patients exhibit heightened gut-homing and inflammatory markers, which worsen with a longer time on a GFD. Atrophy and persistent symptoms are linked to peripheral immune activation, and the increase in inflammatory markers over time may reflect an initial phase of immune normalization followed by unresolved chronic inflammation, potentially driven by microbial drivers or other dietary antigens.

1 Introduction

1.1 Coeliac Disease

Coeliac disease (CD) is a chronic autoimmune disorder that affects multiple organs, primarily the small intestine, in genetically predisposed individuals. Gluten serves as the principal driver of immune activation in coeliac disease, although the precise trigger initiating the disease remains unknown[1].

The clinical manifestations of CD are gluten-dependent, with symptoms varying widely due to the systemic nature of the disease. Although gastrointestinal symptoms are most prevalent, extra-intestinal manifestations are also frequently observed, especially in those diagnosed in the adulthood[2]. CD is associated with increased infertility, spontaneous abortion, and a higher risk of various comorbidities, including ocular disorders (cataracts, uveitis, Sjögren syndrome), hematological issues (anemia, nutrient deficiencies), renal and hepatobiliary disorders, respiratory diseases, genetic conditions, musculoskeletal and endocrine disorders, autoimmune diseases, diabetes, cancer, cardiovascular diseases, psychiatric and neurological disorders as well as skin conditions[3].

CD can be categorized into different subtypes based on clinical, immunological, and histopathological features, including seronegative and slow-responders. Furthermore, a subgroup is referred to as "potential" CD, characterized by a normal small-bowel mucosa but positive CD serology and genetic[4].

In 2011, the Oslo Classification ranked the clinical presentation of CD in classical, non classical, subclinical and refractory[5]. Refractory CD (RCD) is defined by persistent or recurrent malabsorptive symptoms and villous atrophy despite strict adherence to a gluten-free diet (GFD) for at least 6-12 months in the absence of other causes of non-responsive treated CD and overt malignancy[6].

1.1.1 Genetics and Environmental Factors

The HLA-DQA1 and HLA-DQB1 genes play a crucial role in presenting gluten peptides as antigens, making the MHC-HLA loci the most significant genetic factor in the development of CD[7]. Most CD patients (90-95 % in some populations) carry the HLA-DQ2.5 heterodimers, encoded by DQA1*05 and DQB1*02 alleles, while 5-10 % carry either HLA-DQ8 or HLA-DQ2.2. A rare subgroup ($<$ 1 %) expresses DQ7.5. Homozygosity for DQ2.5 presents the highest CD risk (up to 30 %) compared to the 3 % risk for heterozygous individuals, with homozygosity also linked to more severe forms of CD[8,9]. While essential to CD pathogenesis, HLA risk alleles account for only 35-40 % of the genetic risk, with additional non-HLA genomic regions contributing to the disease's genetic heritability[10].

Genetic factors contribute to the development of CD, but environmental triggers also play a significant role. Gastrointestinal infections, especially those caused by reoviruses, have been associated with the onset of CD[11,12]. Other potential triggers include medications, pre- and perinatal factors, infant feeding practices, and variations in gut microbiota[13,14,15]. These factors can disrupt intestinal permeability, allowing antigens to interact with immune cells[14]. Furthermore, gluten immunogenic peptides (GIP) found in breast milk[16] may expose infants to gluten before its introduction into the diet, potentially influencing the development of CD. While gluten exposure is necessary for the development of CD, the duration of breastfeeding and the timing of gluten introduction do not appear to affect the risk of developing the disease[4].

1.1.2 Etiopathology

CD arises in genetically susceptible individuals who lose their immunological tolerance to dietary gluten found in wheat, barley, rye and some oat varieties. As shown in **Fig. I.1**, the exact mechanism by which gluten crosses the intestinal barrier remains unclear. Once in the LP gluten peptides are deaminated by tissue transglutaminases type 2 (TG2)[1]. Then gluten derived peptides bound avidly to MHC class II molecules that give CD predisposition (HLA-DQ2/8) and are presented by antigen presenting cells (APC) in the mesenteric lymph nodes to $CD4^+$ T cells. Furthermore, recent studies suggest that intestinal epithelial cells (IEC) can also present these peptides in to $CD4^+$ T cells[17].

The activation of these gluten specific $CD4^+$ T cells (T helper (Th)) in the lamina propria (LP) result in the release of proinflammatory cytokines such as interferon (IFN)γ, tumor necrosis factor (TNF)-α, and interleukin (IL)-21, sustaining a Th1 response and driving intestinal inflammation. This chronic inflammatory state results in epithelial infiltration by lymphocytes and structural alterations of the duodenal mucosa. Additionally, plasma cells produce antibodies against TG2 and deamidated gluten peptides, further contributing to the disease pathology[18].

Persistent inflammation leads to an expansion of $V\delta1^+$ T$\gamma\delta$ cells, which enhance IFNγ production. Gluten peptides also upregulate IL-15 and stress molecules on enterocytes. Elevated IL-15 levels promote a natural killer (NK)-like phenotype in $CD8^+$ T cells, contributing to enterocyte death. Some $CD8^+$ T$\gamma\delta$ cells may exert regulatory functions via transforming growth factor (TGF) β secretion[18]. The epithelial $CD8^+$ T cell response has been considered cytokine-driven and T cell receptor (TCR) -independent. However, recent findings suggest the presence of a clonally expanded, cytotoxic $CD8^+$ T cell population with biased TCR repertoires in the intestinal mucosa, suggesting a more direct role in disease pathogenesis[19].

Increased epithelial apoptosis and unequaled cell regeneration in crypts probably results in villous atrophy. The redirection of cell fate towards enterocyte regeneration may serve as a compensatory mechanism[20].

The role of innate immunity in CD remains poorly understood. Epithelial damage triggers the release of damage-associated molecular patterns, or alarmins, which interact with intestinal epithelial cells and type 1 innate lymphoid cells (ILC). Alarmins such as thymic stromal

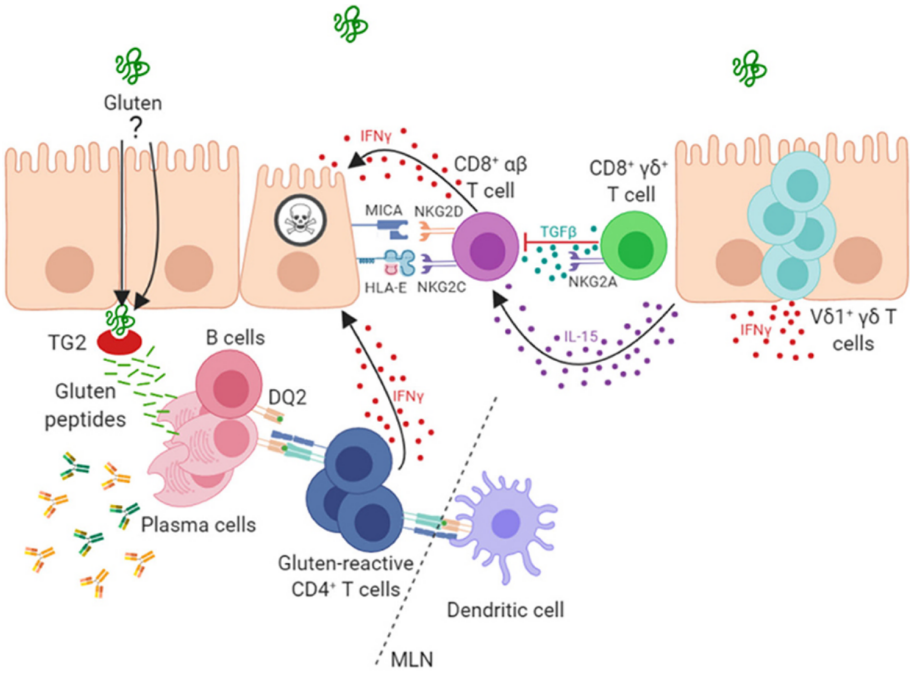

Figure I.1: Etiopathology of coeliac disease. *The exact mechanism by which gluten crosses the intestinal barrier remains unclear. Peptides derived from gluten are modified by transglutaminase type 2 (TG2) and presented by antigen presenting cells in mesenteric lymph nodes (MLN) to CD4⁺ T cells, leading to the differentiation into Th1 type cells that produce IFNγ and intestinal inflammation. Chronic inflammation leads to expansion and persistence of Vδ1⁺ T$\gamma\delta$ cells, which also contribute to IFNγ production. Gluten peptides induce the expression of IL-15 and stress molecules on enterocytes. In this environment CD8⁺ T cells, contribute directly to enterocyte apoptosis. A proportion of CD8⁺ T$\gamma\delta$ cells are thought to play a regulatory role through secretion of TGF-β. Plasma cells are also abundant in the lesion where many are induced to secrete antibodies that bind to TG2*[18].

lymphopoietin (TSLP), IL-33, and high-mobility group box 1 protein (HMGB1) may play a crucial role in initiating and sustaining inflammation[21].

Although CD primarily affects the intestinal mucosa, it is recognized as a multi-organ disease. Extraintestinal manifestations may result from mechanisms such as antibody cross-reactivity, immune-complex deposition, direct neurotoxicity, and, in severe cases, vitamin or nutrient deficiencies. Microbial imbalance and disruptions in the "gut-liver-brain axis" have also been implicated in CD-related neurological complications[22].

Overall, CD is a multifactorial autoimmune disorder driven complex interactions between gluten, HLA-DQ molecules, TG2 activation, and CD4⁺ T cells. Epithelial stress responses and intraepithelial cytotoxic T lymphocyte activation contribute to tissue destruction. However, the mechanisms of communication between LP T cells and epithelial cells remain unclear[23].

1.1.3 Epidemiology

Epidemiological studies on CD show varying prevalence estimates, depending on the methodology used, whether based on serological tests or biopsy results, with a prevalence of 1.4 % using serological tests and 0.7 % with biopsy results. Prevalence also varies by geographic location, sex and age[24]. In Western Countries CD is the most common food intolerance, with higher latitude regions showing greater serology-based prevalence[25]. In Spain the estimated prevalence is 1:204[26]. Additionally, is more frequent in women[27] and studies suggest that prevalence is greater in children than adults[28]. Early-life environmental exposures may play a critical role in the development of CD, as indicated by a shift in peak prevalence to older age groups in some pediatric cohorts[28].

While the global incidence of CD has reportedly increased by 7.5 % annually[29], consistent methodologies are necessary for valid cross-country comparisons. Population-based studies are crucial for accurate determination of the disease prevalence, as hospital records primarily assist in active case detection[30].

In clinical practice, CD testing should have a low threshold, even without abdominal symptoms, as many adults normalize their symptoms and remain undiagnosed. Most adult CD patients are undiagnosed but benefit from a GFD, which improves gastrointestinal symptoms and health-related quality of life[31].

Regarding comorbidities, a meta-analysis showed that the pooled seroprevalence of CD was similar for both overall and unexplained infertility, with a pooled proportion ranging from 1.3 % to 1.6 %. This suggests that individuals with infertility are three times more likely to have CD compared to controls[32]. Additionally, the pooled prevalence of CD was found to be 5.5 % among patients with iron deficiency anemia[33].

1.1.4 Diagnosis

The diagnosis of CD is guided by algorithms and recommendations proposed by the paediatric and gastroenterology societies, as well as by the health national systems. It is established through a combination of mucosal alterations and positive serological tests[34].

In the paediatric population the diagnosis can be made without the need for a duodenal biopsy in a specific clinical context[35]. However, in adults, the diagnostic approach remains a subject of ongoing debate, with discrepancies among different guidelines and a significant gap between clinical practice and official recommendations[4].

The standard diagnostic process typically involves genetic analysis, a gluten challenge, and serological follow-up. However, approaches vary depending on patient characteristics. In adults, an endoscopic duodenal biopsy is generally required to confirm the diagnosis based on the presence of characteristic histological lesions[4].

Developing diagnostic algorithms that are simple, cost-effective, and aligned with patient preferences could improve detection rates, particularly among individuals who do not seek medical consultation due to mild or non-specific symptoms. Many of these individuals may self-limit gluten consumption or already follow a GFD without an official diagnosis[36]. Consequently, they may remain unaware that they have CD, potentially leading to poor adherence to a strict GFD and an increased risk of comorbidities.

Serology

Immunoglobulin (Ig) A-TG2 antibody is the preferred single test for the detection of CD at any age. Total IgA levels should be measured alongside serology testing to assess whether they are adequate, as some cases may have IgA deficiency. In patients with selective total IgA-deficiency, IgG based testing (IgG-Deamidated gliadin peptides or IgG-TG2) should be performed at diagnosis and follow-up. All diagnostic serologic testing should be done while patients are on a gluten-containing diet[4].

Other diagnostic approaches that use blood samples include the identification of gluten-specific reactive T-cells by enzyme-linked immunospot (ELISPOT) and a test for HLA-DQ gluten tetramer for detection of gluten-specific $CD4^+$ T cells identification[37,38].

Endoscopy and Histopathology

When CD is suspected, duodenal biopsies are recommended even if the duodenum appears normal, as they are essential for diagnosis in adults[4].

The histological diagnosis of CD is based on the finding of increased intraepithelial lymphocytes (IEL) ($\geq$ 25/100 enterocytes), crypt hyperplasia, and villous atrophy in biopsy samples.

None of these elementary lesions is specific for CD; the diagnosis of CD is based on the identification of histological alterations accompanied by clinical and serological consistent data[39]. LP content should also be evaluated, as CD typically presents with infiltration of lymphocytes, plasma cells, eosinophils, and occasionally neutrophils. findings should be reported according to the modified Marsh classification[40,41].

The Marsh classification provides a structured approach to the evaluation of CD-related lesions. Marsh 1, or infiltrative lesions, are characterized by normal villous architecture with increased IEL. Marsh 2, or hyperplastic lesions, display both increased IEL and crypt hyperplasia. Marsh 3, or destructive lesions, present with varying degrees of villous atrophy and are further categorized into three subtypes: 3a, with mild villous atrophy and increased IEL; 3b, with moderate villous atrophy and increased IEL; and 3c, with total villous atrophy and increased IEL[39].

To improve clarity and facilitate communication between pathologists and clinicians, Corazza and Villanacci introduced a simplified classification. This system divides lesions into non-atrophic (Grade A) and atrophic (Grade B) categories. Grade A lesions exhibit normal villous structure but an increased IEL count. Grade B lesions, on the other hand, are further divided into B1, where the villous-to-crypt ratio is less than 3:1 with increased IEL and B2, where villi are completely absent, also with increased IEL[42]. While the histopathology analysis remains the gold-standard, alternatives for patients unwilling or unable to undergo a biopsy, such as video capsule endoscopy, are being developed. These alternative techniques, which are not used for initial diagnosis, may aid in monitoring after diagnosis[4].

Genetic Studies

Testing negative for HLA-DQ2/8 effectively rules out CD with a predictive value of over 99 %. It is recommended in specific cases, such as when individuals are already on a GFD before testing, when there are conflicting serology and histology results, in seronegative patients with Marsh 1-2 histology, to identify first-degree relatives of CD patients who may require monitoring and for individuals with autoimmune diseases or genetic disorders linked to CD. However, results should be interpreted carefully, as at-risk individuals should undergo serological testing before making dietary changes. The need for the screening of asymptomatic individuals remains debated, though some evidence suggests that a GFD may improve their quality of life[4].

Lymphogram

The lymphogram is assessed by flow cytometry and reflects changes in IEL populations that are characteristic of the chronic intestinal epithelial inflammation. However, this immune profile is not exclusive of CD, and the precise functional role of these immune cells remains incompletely understood[43,44].

This approach is particularly valuable in complex cases, such as when anti-TG2 antibodies are negative or when the patient is on a GFD at the time of diagnosis, especially if they adopted the diet due to conditions such as fibromyalgia or fertility issues[45,46,47].

In general, reference values for the lymphogram are over 14 % for T$\gamma\delta$ and under 4 % for CD3$^-$. Alternatively, a T$\gamma\delta$/CD3$^-$ ratio of ≥ 5 is considered a valid diagnostic parameter[48]. However, each center should stablish its own specific reference ratios.

Notably, T$\gamma\delta$ lymphocytes remain elevated in CD patients even after long-term adherence to a GFD, whereas this pattern is not observed in non-coeliac gluten sensitivity[49]. Furthermore, the lymphogram has proven to be particularly useful for the diagnosing of patients with Marsh 1 lesions, who may otherwise be overlooked by CD diagnostic criteria[50].

Lastly, it is recommended to document gluten intake at the time of diagnosis, as intraepithelial CD3$^-$ lymphocyte quantification may serve as an indicator of mucosal integrity[51]. This

is particularly relevant because chronic inflammation permanently alters resident immunity in the intestinal mucosa of CD patients[52].

Gluten Challenge

A gluten challenge can be essential for the diagnosing of CD in patients already following a GFD. Traditional protocols recommend consuming at least 10 g of gluten daily for 68 weeks[53]. Short-term gluten exposure, as brief as three days, may induce transient cytokine release detection of transient cytokine release such as IFN-γ, IL-2, IL-8 and IL-10, offering a potential diagnostic marker[54,55]. Moreover, activated $CD8^+$ T cells can also be detected on blood after 3 days gluten challenge on CD patients[51,56].

1.2 Gluten Free Diet

Gluten is a complex mixture of proteins found in cereal grains. The main proteins in the wheat grain are gliadin and glutenin. Glutenins contribute to the strength and elasticity of dough, while gliadins contribute to its viscosity. Similar proteins to gliadin are found in other grains such as secalin in rye, hordein in barley, and avenins in oats and are collectively referred to as gluten. Additionally, derivatives of these grains, such as triticale and malt, as well as ancient wheat varieties like spelt and kamut, also contain gluten[57]. Of note, the gluten content has not decreased due to wheat breeding, with similar trends observed in rye and barley. The modern wheat varieties contain relatively less gluten than ancient ones. Probably, selective breeding has prioritized the starch content in modern wheats to gluten[58,59].

The GFD remains the only effective treatment for managing symptomatology in CD patients[60]. Even asymptomatic individuals with CD benefit from a GFD[61].

Interestingly, the GFD has gained popularity among individuals without CD. Several factors may explain this rise in the adoption of GFD. There is a growing public perception that GFD is healthier and may alleviate non-specific gastrointestinal symptoms. Many individuals with self-diagnosed gluten sensitivity report improvement in gastrointestinal health after avoiding gluten-containing foods[62]. Additionally, GFD have been shown to help improve gastrointestinal symptoms in some individuals with inflammatory bowel disease[63] (IBD). The increased availability of gluten-free products in supermarkets and online retailers has also likely contributed to the growing trend[62].

1.2.1 Challenges of GFD

The GFD poses several challenges, including high costs, threat of gluten contamination, nutritional deficiencies and social and psychological barriers[64]. Studies indicate that $0.2 \ \ 3.2$ % of patients consuming uncertified gluten-free products still exhibit intestinal damage. Approximately 30 % of CD patients report ongoing symptoms, potentially due to cross-contamination, poor adherence or other food compounds[65]. Furthermore, about half of adult CD patients have persistent villous atrophy despite strict GFD adherence and even in asymptomatic individuals[66]. One possible cause is a persistent immune dysregulation, as long-term adherence to a GFD in CD patients normalizes Th2 gene expression but fails to fully correct the activation of the Th1 pathway in the intestinal mucosa[67].

1.2.2 Adherence Monitorization

Various methods have been used to monitor adherence, including periodic visits by nutritionists, clinical follow-ups, serological test and detection of GIP in stools and urine. GIP analysis offers a non-invasive method to directly assess gluten exposure[68]. Additionally, measuring serum intestinal fatty acid-binding protein (FABP) and fecal zonulin levels in coeliac patients enables

the evaluation of intestinal permeability and can serve as non-invasive markers for monitoring ongoing structural changes in the mucosa, eliminating the need for endoscopy[69].

1.2.3 Beyond Gluten: Other Contributing Factors

Beyond gluten, other dietary components may contribute to persistent symptoms in CD patients. Fermentable oligosaccharides, disaccharides, monosaccharides and polyols (FODMAP), have been identified as symptom triggers in some individuals, with studies suggesting that their impact may be more significant than gluten in self-diagnosed gluten-sensitive individuals[71,72].

Trace elements and contaminants play also a role in the persistence of symptoms. Deficiencies in zinc and copper may exacerbate symptoms, as low zinc levels have been linked to increased transglutaminase activity[73]. CD patients on a GFD frequently show elevated levels of heavy metals such as arsenic and mercury, raising concerns about dietary exposure[74,75]. Persistent organic pollutants have also been detected at elevated levels in individuals following a GFD[76].

Other dietary factors, such as amylase and trypsin inhibitors, have been implicated in immune activation via Toll-like receptor 4 (TLR4) stimulation, promoting inflammation[77]. Histamine intolerance, linked to a deficiency in diamine oxidase, has been associated with gastrointestinal and extra-intestinal symptoms, including migraines[78].

Given the complexity of dietary management in CD, a multidisciplinary approach that includes nutritional assessment, biomarker monitoring, and awareness of additional dietary components beyond gluten is essential to optimize patient outcomes.

1.2.4 Innovation in Gluten Free Products

In the development of gluten-free dough, there has been a notable shift towards innovative technologies and ingredient modifications. Among these advancements, enzymatic treatments, high-pressure processing, sourdough fermentation, and extrusion-based techniques have been proposed as viable solutions to replicate the structural and textural properties of wheat-based dough without the presence of gluten[79]. Additionally, genomic modifications are being explored as another promising avenue for enhancing gluten-free products[80,81].

1.3 The Gut Immune System

The gut immune system is anatomically structured into distinct layers that contribute to immune surveillance and tolerance. The intestinal mucosa consists of the epithelial layer, the LP, and the muscularis mucosae, with a protective mucus layer covering the epithelium. Various specialized cells, including enterocytes, goblet cells (mucus secretion), Paneth cells (antimicrobial peptide production), M cells (antigen sampling), and IEL, maintain barrier integrity and immune function on the epithelium. Tight junction proteins, such as occludin and claudins, regulate permeability, and their disruption can lead to increased antigen entry and inflammation[82].

As shown in **Fig. I.2**, beneath the epithelium, the LP contains diverse immune cells, including $CD103^+$ dendritic cells (DC), macrophages, plasma cells, and regulatory T cells (T_{reg}), which help sustain immune homeostasis. The gut-associated lymphoid tissue (GALT), comprising Peyer's patches, isolated lymphoid follicles, and the appendix, plays a central role in adaptive immune responses by promoting IgA production and antigen-specific tolerance[70].

Oral tolerance prevents excessive immune responses to dietary antigens and commensal microbes. M cells in Peyer's patches and $CD103^+$ DC in the LP capture antigens from the microbiota and the food, promoting gut specific forkhead box protein P3 ($FOXP3^+$) T_{reg} differentiation under the influence of retinoic acid and TGF-β. IL-10-producing C-X3-C motif chemokine receptor 1 (CX_3CR1^{hi}) macrophages further support T_{reg} expansion, contributing

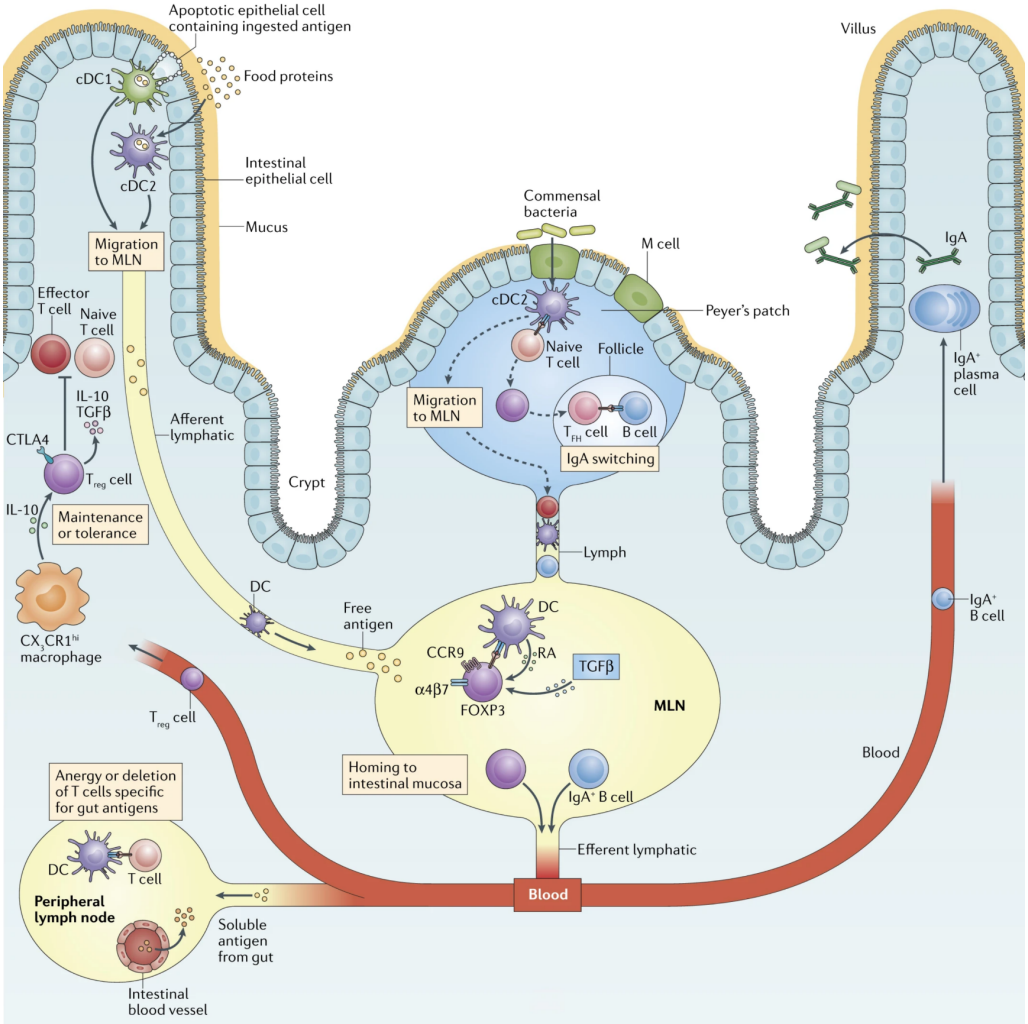

Figure I.2: Oral tolerance scheme. *Dendritic cells (DC) in the lamina propria capture antigens and migrate into the mesenteric lymph nodes (MLN). There, they interact with T cells. Production of retinoic acid (RA) by the DC induces the expression of forkhead box protein P3 (FOXP3) together with the gut-homing molecules C-C motif chemokine receptor 9 (CCR9) and $\alpha 4\beta 7$ integrin, on the T cells, leading to the generation of regulatory T (T_{reg}) cells capable of returning to the intestinal mucosa. The generation of T_{reg} cells is also promoted by the presence of transforming growth factor-β (TGFβ). These T_{reg} cells return to the intestine, suppressing immune responses by expression of cytotoxic T lymphocyte antigen 4 (CTLA4), which removes CD80 and CD86 from antigen-presenting cells (APC) and producing IL-10 and TGFβ, which inhibit both APC and T cells. IL-10 produced by resident C-X_3-C motif chemokine receptor 1 (CX_3CR1)^{hi} macrophages helps maintain FOXP3 expression by CD4$^+$ T_{reg} cells in the mucosa and is needed for their survival. It has been hypothesized that CD4$^+$FOXP3$^+$ T_{reg} cells that have been primed in the MLN and spent time in the mucosa may be involved in the systemic consequences of oral tolerance to protein antigens. An alternative explanation for systemic tolerance is that oral antigens can be found in the lymph and bloodstream, enabling access to resident DC in MLN and peripheral lymph nodes. For commensal microorganisms, antigens are primary taken up via M cells in Peyer's patches and isolated lymphoid follicles (ILC). DC present these antigens to naive CD4$^+$ T cells generating a FOXP3$^+$ T_{reg} cell that can migrate to the mucosa and CD4$^+$ follicular helper T (T_{FH}) cells that interact with B cells inducing a switch to immunoglobulin A (IgA) expression. IgA-switched B cells acquire CCR9 and $\alpha 4\beta 7$ integrin expression, exit from Peyer's patches and isolated lymphoid follicles via lymph and then migrate into the bloodstream to arrive to the lamina propria as plasma cells. Unlike soluble antigens, the tolerance to microbial antigens is confined to the intestine, and the systemic immune system normally remains ignorant of these materials*[70].

to systemic immune regulation[83]. These T_{reg} suppress inflammation via IL-10 and TGF-β, ensuring immune tolerance to dietary and microbial antigens[70].

Microbial exposure shapes immune differentiation, promoting $CD103^+$ DC, $ROR\gamma t^+$ Th17 cells, $FOXP3^+$ T_{reg} and IgA-producing plasma cells, which sustain homeostasis and prevent excessive inflammation[84]. GALT structures regulate immune responses by balancing tolerance to commensal microbes and defense against pathogens. B cell-rich follicles, T cell zones, and germinal centers generate memory B and T cells, while secretory IgA maintains gut barrier integrity[85]. Failure of these mechanisms contributes to conditions such as food allergies, IBD and autoimmune diseases like CD[85,70].

Early-life microbial colonization is critical for immune development. Maternal milk provides initial protection through secretory IgA and anti-commensal IgG, while post-weaning microbial colonization induces B cell class-switch recombination and IgA production. Disruptions in this process, such as antibiotic use, can increase susceptibility to immune-mediated diseases[84].

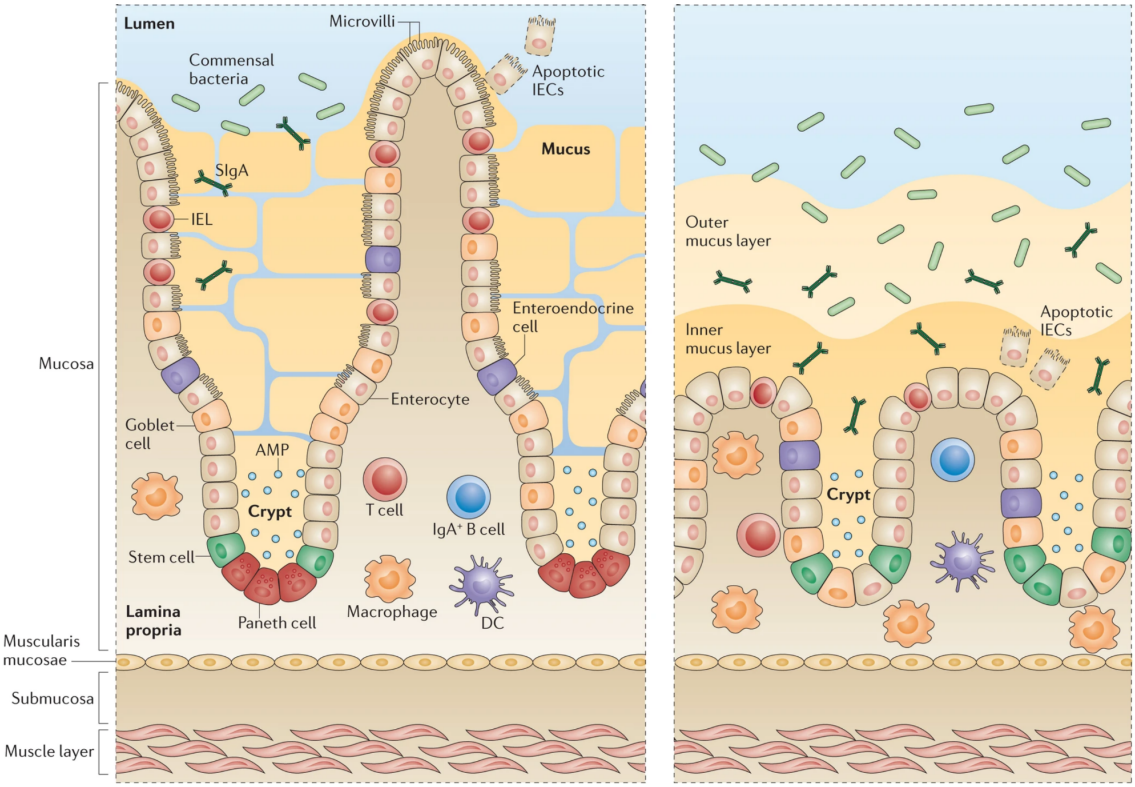

Figure I.3: Anatomy of the intestinal mucosa. *The intestine is divided into distinct segments, each with unique structural and functional characteristics. The small intestine has long, thin villi with an extensive brush border, optimized for nutrient absorption. It contains stem cells in crypts that produce various cell types, including absorptive intestinal epithelial cells (IECs), goblet cells, and Paneth cells. The ileum has shorter villi, more goblet and Paneth cells, and fewer intraepithelial lymphocytes (IEL). The large intestine begins with the caecum, which lacks villi and serves as a reservoir for commensal bacteria. It has numerous goblet cells and rare Paneth cells. The colon also lacks villi and has smaller crypts compared to the small intestine. Its primary functions are water reabsorption and acting as a barrier against commensal microbiota. The colon has many goblet cells producing a thick protective mucus layer, very rare Paneth cells, and fewer IEL than the small intestine[82]. AMP: Antimicrobial peptides; DC: Dendritic cells, Ig: Immunoglobulin; SIgA: Secretory IgA.*

The gut immune system exhibits regional specialization as shown in **Fig. I.3**. The small intestine, with its villi-lined surface, facilitates nutrient absorption and hosts tolerogenic DC. In contrast, the large intestine specializes in microbial processing and contains a higher proportion of Th17 and $T\text{-}bet^+$ Th1 cells. Other immune cells, including eosinophils, mast cells, and plasmacytoid DC (pDC), contribute to tissue repair, immune modulation, and antiviral defense.

Microbial metabolites, particularly short-chain fatty acids, play a crucial role in maintaining gut homeostasis and preventing inflammatory diseases[82].

Mouse models are widely used in immunological research, yet species-specific differences in T cell signaling, granulocyte responses, and B cell subsets impact translational studies. For instance, murine B-1 B cells primarily drive T cell-independent IgA production, whereas human IgA responses rely on T cell-dependent germinal center reactions. Additionally, T$\gamma\delta$ cells and mucosal-associated invariant T cells differ in distribution and function between species. Advanced techniques like mass cytometry improve model selection for drug development. Despite structural similarities, differences in lymphoid microenvironments, Th17 regulation, and IL-17 signaling necessitate caution when extrapolating murine findings to human immunity[86,87].

1.4 Flow Cytometry

Flow cytometry is a powerful technique for the analysis of individual cells within heterogeneous populations. This technique has been fundamental to biological research for over six decades. The process involves suspending cells in a fluid, typically a saline solution, which then enter a laminar flow in the cytometer. Through hydrodynamic flow, cells are aligned individually before crossing a laser beam, enabling the collection of information based on light dispersion[88].

A flow cytometer consists of several key components: a fluidic system controlling cell flow, an optical system with lasers and detectors, and an electronics and data acquisition system integrated with analysis software. While the basic principles have remained essentially unchanged, recent developments have significantly expanded its capabilities. Flow cytometry also enables cell sorting, where cells are physically separated based on their measured properties. This capability is invaluable for isolating specific cell populations for downstream applications such as genomics or proteomics[88].

Traditional flow cytometry relies on detecting fluorescence signals emitted by fluorochrome-labeled probes to analyze cellular properties and identify specific cell populations (**Fig. I.4A**). However, the introduction of spectral flow cytometry has enabled the simultaneous detection of a broader range of fluorochromes, addressing the limitations imposed by spectral overlap. Spectral flow cytometry uses a large bank of detectors to collect fluorescence signals across the entire spectrum, offering advantages in capturing complete fluorescence signals from all dyes without isolating each label's dominant spectral band (**Fig. I.4B**). This approach involves employing more detectors than utilized dyes, resulting in multiple representations of each label within the dataset[89].

To ensure reproducibility and robust data generation proper controls should be used and a careful panel design should be followed[90].

The abundance of high-dimensional data generated by these advanced cytometry techniques has led to the development of novel computational analysis approaches. Traditional gating strategies pose challenges in identifying novel cellular subsets, especially in high-dimensional datasets. To address these limitations, advanced computational techniques such as BayesFlow, Citrus, and semi-automated algorithms have been developed, enabling more systematic and unbiased analysis of immune cell populations[91,92,93].

Data visualization has evolved beyond traditional 2D dot plots, now utilizing advanced techniques like spanning trees, self-organizing maps, and manifold learning models (t-SNE: t-distributed Stochastic Neighbor Embedding, UMAP: Uniform Manifold Approximation and Projection and PHATE: Potential of Heat-diffusion for Affinity-based Trajectory Embedding) to reveal complex cellular relationships. These methods enable a better understanding of cellular heterogeneity and the identification of distinct cell populations[88].

Recent advances in flow cytometry analysis include the development of portable microfluidic diagnostic devices for point-of-care testing, which integrate microfluidics with flow cytometry to enable powerful measurements of multiple characteristics in biological samples[94,95]. Addi-

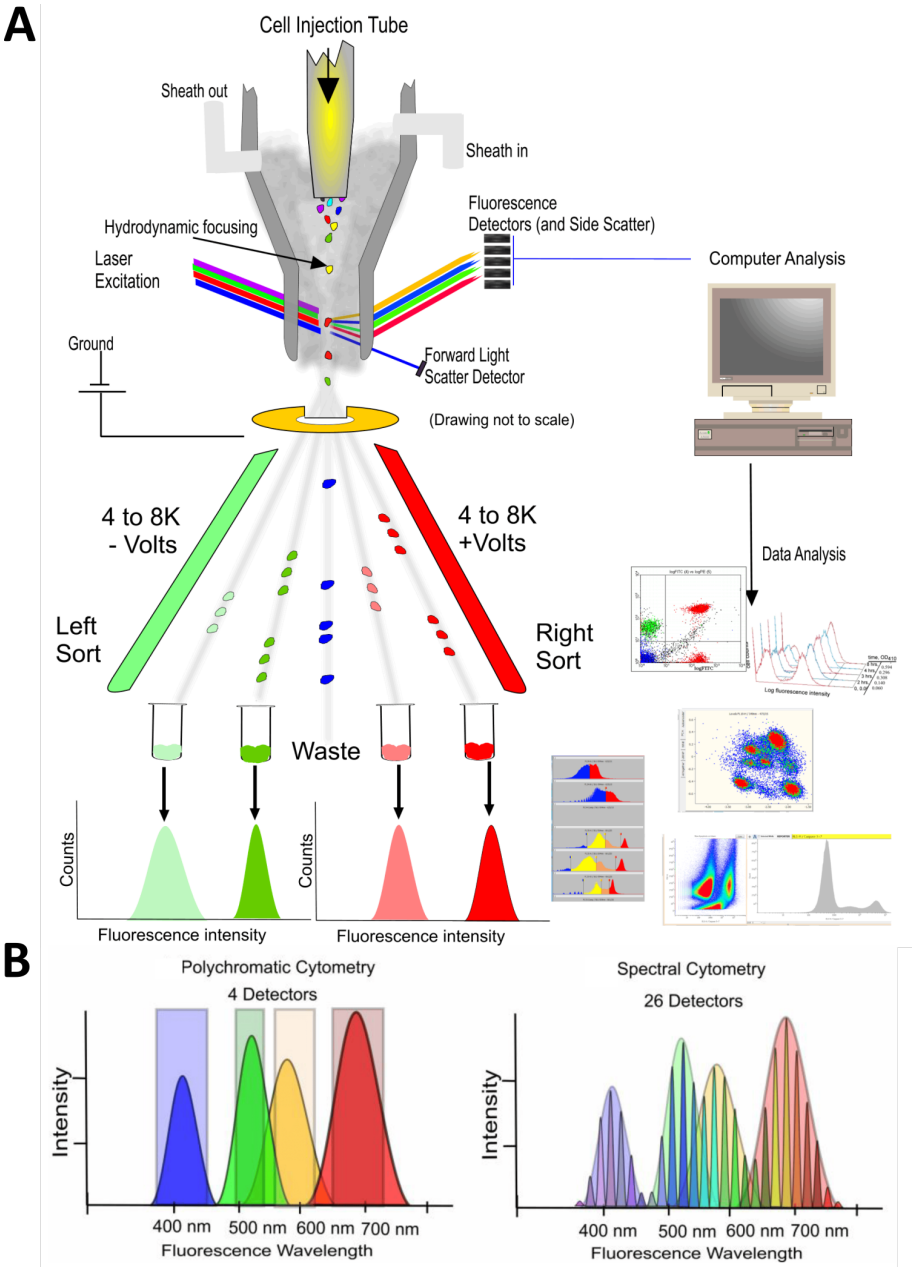

Figure I.4: Fundamentals of flow cytometry. *(**A**) General outline of a flow cytometer showing a sorting instrument and examples of data analyses (**B**) Comparison between polychromatic cytometry where each dye is collected by a single detector and spectral cytometry where many detectors are used to collect the entire spectrum of all dyes, enabling a process called spectral unmixing that can identify each dye*[88].

tionally, the automation of flow cytometry data analysis has been a focus[95] of research, aiming to improve efficiency and accuracy in processing and interpreting data[96,97,98].

New analysis algorithms and platforms, such as MetaGate, have been developed to handle the increasing complexity of flow cytometry data, offering interactive statistical analysis and capabilities of visualization for high-dimensional cytometry data[96,99,98]. Moreover, the integration of artificial intelligence with flow cytometry has shown promise in enhancing the analysis of massive datasets, paving the way for more efficient and insightful analyses in biotechnology research[99,98].

Looking into the future, the integration of flow cytometry with other omics data and artificial intelligence promises a more comprehensive understanding of cellular functions and

disease processes[100]. This will require collaboration between cytometrists, biologists, and data scientists to develop innovative analysis methods that combine flow cytometry profiles with other omics perspectives, potentially using multiview learning and other cutting-edge technologies.

In conclusion, flow cytometry remains an indispensable tool in biological research, continually adapting to new technological advancements while maintaining its core principles of single-cell analysis. Its ability to provide detailed, multi-parameter analysis at the single-cell level ensures its continued relevance in unraveling the complexities of cellular biology and disease processes.

2

Hypothesis and Objectives

Hypothesis

Given that up to 50% of coeliac disease patients exhibit persistent mucosal atrophy despite strict adherence to a gluten-free diet, this condition may be associated with alterations in the mucosal and/or peripheral immune system.

General Objective

To study the effect of a gluten-free diet on the phenotype and function of immune cells from the intestinal mucosa and peripheral blood of coeliac disease patients.

Specific Objectives

1. To characterize the phenotype, distribution, and function of intraepithelial lymphocytes in the stomach, duodenum, terminal ileum, and colon under non-inflammatory conditions and in the absence of gastrointestinal diseases.
2. To address the phenotype and function of duodenal intraepithelial lymphocytes from active celiac disease patients and from coeliac disease patients treated with a gluten free diet.
3. To identify alterations in the phenotype of immune cells in the lamina propria and peripheral blood from coeliac disease patients with a gluten free diet.
4. To study the impact of villous atrophy, the duration of gluten free diet, and the presence of symptoms on serum and tissue immune markers in coeliac disease patients treated with a gluten free diet.

3

Materials and Methods

3.1 Patient Cohorts: Inclusion Criteria and Group Definitions

This thesis involved the analysis of four distinct patient cohorts, each comprising groups stratified based on clinical diagnosis, histological findings and treatment status. Within these cohorts, subpopulations included non-coeliac controls, CD patients, and other relevant groups, selected according to the specific aims of the study. Patient grouping was based solely on these clinical criteria; demographic factors such as sex and age were not used as criteria for cohort stratification. Consequently, all eligible patients were included regardless of differences in sex distribution or age range, without exclusion due to imbalances between groups.

The first cohort was established to examine IEL across various regions of the gastrointestinal tract, including the stomach, duodenum, colon, and ileum, focusing on non coeliac controls. The second cohort aimed to investigate IEL, LPL and PBMC derived from controls, CD patients, and CD adhering to a GFD. This cohort specifically explored the impact of villous atrophy, clinical symptoms, and the duration of GFD adherence on duodenal IEL populations. The third cohort was designed to conduct cytotoxicity assays on IEL, utilizing samples from both control individuals and CD patients. Lastly, the fourth cohort focused on the enrichment of IEL and the establishment of primary cell cultures from these cells to facilitate further functional analyses.

Samples from these cohorts enabled a comprehensive evaluation of immune cell populations within the gastrointestinal tract and peripheral blood, allowing comparisons across different disease states, anatomical locations, and treatment conditions. Patients were categorized based on their diagnosis, mucosal histolopathology, and treatment status, as follows:

- Non-Coeliac disease patient with inflammation (NC-NI): Individuals with no clinical or histological evidence of CD or gastrointestinal inflammation, and without a history of autoimmune disorders or malignancies. An exception was made in the first cohort,

where resected tissue from colorectal cancer cases was included; in such cases, only macroscopically and histologically normal sections of the colon or ileum were used. All participants in this group exhibited normal mucosal architecture on endoscopic biopsy.

- Non-Coeliac disease patient with no inflammation (NC-I): This group consisted of patients who are not coeliac CD but showed histologically confirmed inflammation of the gastric or duodenal mucosa. These individuals served as inflammation controls unrelated to CD.

- CD patients: Diagnosis was confirmed based on the presence of CD-compatible HLA alleles (HLA-DQ2 and/or HLA-DQ8), positive serology for IgA anti-TG2 antibodies, and characteristic mucosal lesions classified according to the Marsh grading system. CD patients were further stratified into the following subgroups:

  - C-I (Coeliac disease with inflamed duodenum): Patients with active disease who had not yet initiated a GFD at the time of biopsy. These individuals exhibited both positive serology and histological evidence of mucosal damage. Based on the degree of villous atrophy, they were further classified as having mild (Marsh 12) or severe (Marsh 3) inflammation.
  - C-NI (Coeliac disease with no inflammation): Patients with no detectable mucosal inflammation, regardless of dietary status.

- C-GFD (Coeliac disease on a gluten-free diet): Patients who had adhered to a GFD for at least 12 months. Inclusion criteria for this group varied across cohorts: In the first and third cohorts, only patients with serological remission (negative anti-TG2 antibodies) and complete mucosal healing (Marsh 0) were included. These individuals are referred to as C-NI-GFD. In the second cohort, inclusion was based solely on self-reported adherence to the GFD, without requiring serological or histological remission.

- Unclassified patients: This group comprised individuals whose clinical or histological diagnosis remained inconclusive at the time of sample collection. These patients were retained for exploratory analyses, where appropriate.

Exclusion criteria were uniformly applied across all cohorts and included the presence of other autoimmune or gastrointestinal disorders, as well as systemic inflammatory conditions. Patients with active malignancies were excluded, except in the first cohort as noted above.

3.2 Sample Collection

Biopsies were taken during normal course of a gastroscopy or colonoscopy at the gastroenterology service from both Hospital Clínico Universitario and Hospital Universitario Río Hortega, from Valladolid (Spain) in the context of a routinary endoscopy or colonoscopy for the diagnosis and monitoring of the disease. Ileal and colonic resection were obtained from the proximal and distal ends from patients with colorectal cancer, with a minimum distance of 10 cm from the tumors. In all cases, samples were obtained following written informed consent after ethical approval from the local ethics committee from Valladolid Este (Valladolid, Spain) (PI19-1352, PI-19-1353 and PI-GR-20-1982). To ensure patient confidentiality, all samples were assigned unique identifiers that do not reveal any personal information using the coding system for later analysis. In all cases, samples were preserved in an ice-chilled medium for up to 4 h before arriving at the laboratory.

3.3 Cell Isolation

3.3.1 IEL Isolation

IEL were isolated as previously described[90]. Specifically, biopsies were collected in RPMI 1640 (Gibco, cat #11875093) and in most cases were cryopreserved in freezing media (RPMI supplemented with Fetal Calf Serum (Gibco, cat #10500064) and 10 % Dimethyl Sulfoxide (DMSO) (MP Biomedicals, cat #190186)). Cryopreservation was conducted in cryogenic vials (Fisherbran™, cat #300460-0020) in a CoolCell™ cell freezing container (Cornin™, cat #432001) at least 24 h at -80°C to ensure consistent freezing rates. Cells were cryopreserved at -80°C until further processed.

Biopsies were then either processed fresh or thawed and resuspended in HBSS (Gibco, cat #24020117) in tissue culture plates (Falcon™, cat #10212951) using a Pasteur pipette (Fisherbran™, cat #13439108). Cells were then incubated twice in 5 ml of IEL Isolation Medium consisting of HBSS, 1 mM dithiothreitol (DTT) (Sigma-Aldrich, cat #43816) and 0,5 mM ethylenediaminetetraacetic acid (EDTA) (Invitrogen, cat #11568896) in 15 ml tubes (Corning™, cat #10579691), at 250 rpm at 37°C for 30 min. After each incubation cells were filtered through a cell strained (Fisherbran™, cat #22363549) into a 50 ml tube (Corning™, cat #10334131) and centrifugated at 400 g during 10 min to remove debris.

In the case of intestinal resections, they were collected immediately following surgery in ice-chilled RPMI medium (4°C). Tissue was cleaned with HBSS and muscle and fat were removed using surgical scissors. As long as tissue was clean, it was cut it into pieces of about 1 cm. Then, the same procedure to obtain IEL as from biopsies was performed and the resulting cells were cryopreserved.

3.3.2 LPL isolation

After IEL isolation the remaining tissue was digested for a maximum period of 90 min in lamina propria mononuclear cells (LPMC) isolation medium (RPMI, 1 mg/mL of collagenase D (Roche, cat #11088882001), 20 µg/mL of Liberase™ TL Research Grade (Roche, cat #5401020001) and 0,025 U/µL of Universal nuclease for cell lysis Pierce™ (Thermo Scientific, cat #88702))Protocols already optimized and in use[101,102,103,104] were followed until reaching a suspension of LPMC, which was then filtered with a 100 µm strainer before staining the cells.

3.3.3 PBMC Isolation

PBMC were obtained by centrifugation over Ficoll-Paque PLUS (Amersham Biosciences, Chalfont St. Giles, UK) at 800 g 30 min without break. Next, cells were washed in DPBS (Cytiva, cat #SH30028.02) containing 1 mM EDTA and 0.02 % sodium azide (Sigma-Aldrich, cat #S2002-25G) (FACS buffer), centrifugated at 400 g 5 min, cultured when needed and stained with fluorochrome-conjugated antibodies as explained below.

3.4 Antibody Labelling

Extracellular staining was performed on the isolated cells in polystyrene tubes (Falco™, cat #352054). IEL staining was performed using viability dye Near-IR (Invitrogen, cat #10154363) and blocking the unspecific unions with Fc-block (BD Pharmingen, cat #564220) during 10 min at room temperature (RT). Cells were further washed in FACS buffer at 400g during 5 min. Extracellular stain was incubated for 20 min at 4°C.

When intracellular staining was conducted, Fix and Perm kit (Invitrogen, cat #GAS004) was used according to the manufacturer's instructions. Briefly, IEL were fixed with the medium

A for 15 min RT. Following a wash step, cells were permeabilized with Medium B and incubated with the first intracellular antibody during 20 min at RT. When a secondary antibody was used, after another wash, cells were stained with it for 20 min at RT.

LPMC were stained following a modified version of the OMIP-069 panel[105]. Briefly, cells were incubated with Live/Dead$^{\text{TM}}$ UV Blue (Invitrogen, cat #L23105). Brilliant Stain Buffer (BD Horizon$^{\text{TM}}$, cat #563794) and True-Stain Monocyte Blocker$^{\text{TM}}$ (BioLegend®, cat #426103) were also added prior to staining, as above. Cells were further fixed and preserved at 4°C until acquired.

In all cases, cells were further fixed with Fixing Medium (PBS) (Lonza, cat #17-516F) with 2 % Buffered Formalin (Protocol, cat #032-059)) for 10 min at 4°C. Cell were then washed in FACS buffer before they were acquired (within 48h) on a flow cytometer (Gallios Beckman Coulter or Aurora Cytek 5 lasers).

3.5 Statistical Analysis

Statistical analyses were conducted using GraphPad Prism version 8 for Windows (GraphPad Software, www.graphpad.com) and IBM SPSS Statistics version 29.0.1.1 (244) for Windows (www.ibm.com). The Shapiro-Wilk normality test was used to assess normality, followed by appropriate statistical tests based on the distribution of the data. Paired tests were applied when relevant, and corrections were applied only when group sample sizes exceeded 10. For comparisons between two groups, a t-test was performed on normally distributed data, while the Mann-Whitney U test was used for non-parametric data. One-way ANOVA was applied to compare multiple groups with normal distributions, while the Kruskal-Wallis test was employed for non-parametric groups. Pearson correlation was used for normally distributed data, and Spearman correlation for non-parametric data. A p-value of < 0.05 was considered statistically significant. Figures were assembled using Inkscape 1.3.2 (091e20e, 2023-11-25, custom, www.inkscape.org).

4

Intraepithelial Lymphocytes

4.1 Introduction

The first line of defense in the human gastrointestinal tract consists of IEL, specialized immune cells located within the epithelial layer. This diverse group is mainly made up of T cells, with a notable abundance of TCR$\gamma\delta^+$ cells[106]. Their strategic location enables them to rapidly respond to luminal antigens, supporting both oral tolerance and mucosal barrier integrity[107].

IEL are broadly categorized as either natural, that acquire an IEL fate in the thymus, or peripherally induced IEL that differentiate from conventional T cells activated in the intestinal-draining lymph nodes. Both can be further classified based on the expression of TCR$\gamma\delta$ or TCR$\alpha\beta$, and CD4, CD8$\alpha\beta$ or CD8$\alpha\alpha$. Natural IEL undergo agonist selection in the thymus and have restricted TCR diversity, while peripherally IEL follow conventional TCR selection and have a more diverse repertoire[44].

Despite their distinct developmental origins, IEL subsets share core traits including tissue adaptation, innate-like properties, cytotoxic potential, and limited TCR diversity. These adaptations promote robust but tightly controlled immunity at the epithelial barrier. IEL receive critical signals from the epithelial tissue, microbiota, and diet that influence their development, maintenance, and function. Dietary metabolites and microbial products can impact on the accumulation and functional programming of these cells[44].

To effectively fulfill their role, IEL must maintain a delicate balance between inhibitory and activating signals. This balance is crucial for regulating their cytotoxic potential and ensuring optimal immune surveillance[108]. However, this equilibrium can be disrupted in chronic inflammatory diseases, such as CD and IBD, where IEL may contribute to epithelial damage[109,110]. They also play a complex role in colorectal cancer: TCR$\gamma\delta$ IEL exhibit antitumor effects by targeting cancerous cells and producing IFN-γ, which lowers metastasis risk. However, other TCR$\gamma\delta$ IEL subsets expressing PD-1 and IL-17 may actually promote tumor growth[44].

4.1.1 IEL on CD

CD serves as a valuable model for studying gastrointestinal-related disorders, given that it is an autoimmune condition triggered by gluten intake in genetically predisposed individuals[34,111]. Despite the adherence to a GFD, many patients continue to experience symptoms, and the villus atrophy persists in 50% of the patients[66,112].

The upregulation of IL-15 plays a pivotal role in CD pathogenesis. Even in patients on a GFD, IL-15 and its receptor IL-15Rα remain elevated in the epithelium, promoting IEL activation and inflammation[113,114]. Studies in mouse models have demonstrated that overexpression of IL-15 in both the epithelium and LP is necessary for the development of villous atrophy[115]. The upregulation of IL-15 and activation of intestinal CD4$^+$ T cells by the dietary antigen are both necessary to drive the cytotoxic activation of CD8$^+$TCR$\alpha\beta^+$ IEL and the epithelial damage[116]. IEL are elevated in the CD mucosa and display a cytotoxic profile[117]. Consequently, TCR$\alpha\beta^+$CD8$\alpha\beta^+$ IEL drive inflammatory processes mediated by Fas ligand, perforin, granzyme B, and NKG2D, contributing to the development of small villous atrophy[118,119]. The increased expression of NKG2D on IEL, coupled with the upregulation of its ligand MICA on epithelial cells, drives cytotoxic activity and contributes to epithelial cell death[120].

CD patients exhibit alterations in the proportions of TCR$\gamma\delta^+$ and NK-like cells that have been identified as a valuable marker for the diagnosis of CD[51,121]. Additionally, IEL adjust to the different locations within the intestinal tract, as the immune environment systematically change through its length[82]. The small intestine harbors a higher proportion of memory IEL, experienced in responding quickly to familiar antigens, while the large intestine relies more on naïve IEL, which can adapt to novel antigens encountered less frequently[122].

4.1.2 IEL Isolation and Culture

Efficient isolation of IEL from human gastrointestinal samples is crucial for studying mucosal immunity. Density gradient centrifugation is a traditional method that separates cells based on their density[123,124,125]. Elutriation centrifugation offers a high yield ($>$ 85 %) and purity (55-75 %) for both mouse and human intestinal IEL without interfering with subsequent functional assays[126]. However, traditional methods like mechanical and biopsy culture are often limited by phenotypic alterations, and high contamination rates[127].

To overcome these challenges, various techniques have been developed to efficiently isolate IEL. Flow cytometry cell sorting offers a high precision and sensitivity, allowing the isolation of purified IEL populations[128].

Immunomagnetic bead-based separation is another effective method for IEL enrichment. This technique involves the use of magnetic beads conjugated with antibodies against cell surface markers. Negative selection strategies, such as depletion of epithelial cells using epithelial cell adhesion molecule (EpCAM)-specific beads, can also be employed to enrich IEL[129]. Alternatively, positive selection can be used based on the expression of surfer markers as CD8 or CD4[130,131]. León & Roy proposed the use of Annexin V-coated magnetic beads, taking advantage of the apoptosis-induced phosphatidylserine exposure on epithelial cells[132].

Once isolated, IEL can be cultured in vitro to study their activation, proliferation, and effector functions[133]. However, to maintain viability and functionality, selecting appropriate culture conditions is crucial. Anti-CD3 antibodies (αCD3) paired with a cytokine cocktail (IL-2, IL-15, IL-3, IL-4 and IL-15/IL-15R Complex) have been shown to sustain IEL activity in a murine model[134].

IL-15 is a potent T cell growth factor that promotes the expansion of memory and cytotoxic T cells[116]. In murine models IL-15/Il-15Rα signaling upregulates the serine/threonine kinases PIM1 and PIM2, which are essential for IEL to proliferate, grow and upregulate granzyme B in response to inflammatory IL-15. Interestingly, IEL from patients with CD show a high PIM expression and cells express the complete cytotoxic machinery, including granzyme B prior to IL-

15 activation. This suggests that additional factors might contribute to IL-15 driven cytotoxic responses[131]. It is likely that not only IL-2, but IL-21, which is produced by gluten-specific $CD4^+$ T cells, can cooperate with IL-15 to drive IEL activation[116].

In addition, IL-15 can modulate both stimulatory and inhibitory receptors on IEL[108], such as the activators junctional adhesion molecule-like (JAML) and CD100, potentially lowering the activation threshold for the T cell receptor, or other co-receptor involved in activation[131].

IEL subsets are differentially regulated by specific interactions in the gut. For instance, Butyrophilin-like protein 3 and 8 (BTNL3 and BTNL8) are key drivers of the expansion of $V\gamma4^+/V\delta1^+$ IEL in the human gut[135]. In active CD, the loss of BTNL8 expression is linked to a depletion of resident $V\gamma4^+/V\delta1^+$ IEL, which are replaced by $V\delta1^+$ lymphocites with heightened IFNγ production. A GFD restores BTNL8 expression but does not fully restore the physiological balance of resident IEL subsets[116,52].

IEL function is significantly influenced by the unique cytokine environment of the gut. When stimulated with αCD3, $CD8^+$ IEL produce TNFα,[136], whereas $CD4^+$ and $CD4^+CD8^+$IEL secrete IFN-γ, IL-5, IL-6 and IL-2[137]. Moreover, freshly isolated IEL expressed mRNA for IL-1β and IL-8,[138]. These cytokines influence epithelial cells, which, in response to IL-1β and TNFα produce IL-6[139] further contributing to the cytokine milieu. The intricate interplay of cytokine signaling with the epithelium, coupled with the expression of regulatory receptors on IEL surface and phenotype changes, highlight the sophisticated regulation of IEL-mediated immunity.

4.1.3 Study Objective and Research Gap

Building from that background, the phenotype, distribution and functional dynamics of IEL across the human gut were investigated. Given the central role that IEL elicit in the human gut, a special emphasis was made on duodenal IEL activation within the context of CD. By elucidating the distinct roles in both maintaining gastrointestinal homeostasis and contributing to disease pathogenesis, this research aims to enhance our understanding of IEL-mediated immune responses in the gut. Ultimately, these insights could inform the development of novel therapeutic strategies designed to modulate IEL function, thereby restoring immune balance and promoting a healthier intestinal environment in individuals affected by chronic inflammatory and autoimmune gastrointestinal diseases.

4.2 Materials and Methods

4.2.1 Patients Demographic

Cohort 1: IEL along the Gut

To assess the differences in the IEL compartment along the gut, samples from the most prominent parts have been obtained. Hence, gastric biopsies from 10 NC-NI (70 % women, 59 $\pm$ 12 years) without any inflammatory disease were collected from the body, incisure and antrum of the stomach of each patient. In addition, duodenal biopsies were also collected from 81 NC-NI (79 % women, 40 $\pm$ 15 years), and 30 NC-I (77 % female, 41 $\pm$ 14 years). A total of 59 patients with CD were included (78 % female, 39 $\pm$ 15 years). All of them had positive compatible genetics, serology (IgA anti-TG2) and duodenal lesion at diagnosis. Of the total 59 CD patients, 26 had been following a GFD for over a year. All GFD treated patietns had negative serology and no mucosal damage (Marsh Score 0) (C-NI-GFD)(81 % female, 39 $\pm$ 19 years). The remaining 33 patients were C-I (24 % female, 39 $\pm$ 13 years) with positive serology and mucosal damage at the time of endoscopy. They were further stratified, based on the Marsh score, into 22 patients severely inflamed with Marsh Score 3 (C-I.M3) (73 % female, 38 $\pm$ 14 years), and 11 patients mildly inflamed with Marsh score 1-2 (C-I.M1/2) (82

% female, 41 ± 11 years). Last, paired ileal and colonic samples were collected from resections from 19 NC-NI (26 % female, 71 ± 15 years) with not known autoimmune disease or other malignancies.

Cohort 2: Atrophy, Symptoms and Time on a GFD effect on duodenal IEL

Samples were obtained from three distinct groups as shown in **Tab. IV.1**. The first group consisted of 6 NC-NI, who had been referred for upper gastrointestinal symptoms such as dyspepsia and anemia but were found to have normal duodenal structure and no inflammation. The second group included 6 adult CD patients at disease onset. These patients exhibited clinical symptoms, had genetic susceptibility (HLA-DQ2/8^{+}), positive serology (IgA anti-TG2), mucosal enteropathy (Marsh score 3 or above) (CI-M.3), and had a compatible lymphogram. The third group was composed of 16 CD patients who had been on a GFD for at least 12 months (C-GFD). They all had negative serology, and only one of them was positive for the presence of GIP in stool.

	NC-NI	CI-M.3	C-GFD
Sample size (n)	6	6	19
Sex (% female)	83.3	66.7	84.2
Age (Mean ± SD)	47,3 ± 17,0	30,7 ± 10,4	39,4 ± 10,1
IgA TG2 (%)	0	100	0
Lymphogram (%)	0	100	73.7
Marsh Index	0 (83,3%), 1 (16,7%)	3 (16.7 %), 3B (66.7 %), 3C (16.7 %)	0 (31.6 %), 3A (68.4 %)
Atrophy (%)	0	100	68.4
GIP (%)	nd	nd	5.3
Symptoms (%)	nd	83.3	63.2
Months on GFD	0	0	81,1 ± 62,8
Initial Marsh Index	na	na	3A (26.3 %), 3B (31.6 %), 3C (36.8 %), 4(11.1 %)
Initial IgA TGT (%)	na	na	100

Table IV.1: Patient demographics of cohort 2. *C-GFD: coeliac on a gluten free diet; CI-M.3: coeliac Inflamed (Marsh 3); GIP: gluten immunogenic peptides; na: not applicable; NC-NI: non-coeliac not inflamed; nd: not defined; TG2: transglutaminase type 2.*

Cohort 3: Duodenal IEL Cytotoxic Assay

To assess the cytotoxicity of IEL. In total, 8 NC-NI (88 % female, 41 ± 7 years); 6 NC-I (83 % female, 29 ± 23 years) and 8 CD patients (50 % female, 40 ± 15 years) were recruited. Of the 8 CD patients, 3 were C-I.M3 (33 % female, 31 ± 16 years) and 5 were on a GFD and do not report inflammation (C-NI-GFD) (60 % female, 49 ± 8 years).

Cohort 4: Duodenal IEL enrichment and cell culture

The singularity of this cohort is that demographic data was not taken into account for the design of the experiments and the diagnosis was not known at the time of the assay since samples were used for enrichment or culture in fresh. A total of 17 patients were used. 15 duodenal samples were taken (73 % female, 40 ± 16 years): 5 from NC-NI (60 % female, 34 ± 14 years), 2 from NC-I (100 % female, 38 ± 23 years) and 5 from CD (83 % female, 48 ± 18 years). Only one of the CD patients was on a GFD. Moreover, duodenal samples from 2 patients (66 % female, 38 ± 17 years) that were unable to classify by the clinicians were also used on this study. Finally, 2 samples from ileum resections of NC-NI patients (demographic data not available) were collected.

4.2.2 IEL Enrichment and Culture

IEL enrichment on the isolated epithelial compartment was carried out using different strategies. Positive microbead selection with CD45 beads (Miltenyi, cat #130-045-801) was performed following the manufacturer's instructions. Briefly, cells were incubated with CD45 beads for 20 min RT, then passed through a magnetic column. $CD45^+$ cells retained on the column were then flushed with buffer to collect the enriched IEL population. Cells were used in fresh or cryopreserved as described above depending on the experiment.

For negative selection, EpCAM beads (Miltenyi, cat #130-061-101) were used. The same protocol as for CD45 enrichment was applied, with the key difference that $EpCAM^+$ cells retained on the column were discarded, while the flow-through containing $EpCAM^-$ cells was collected as the enriched IEL fraction.

When required, $EpCAM^-$ fraction was processed to a second step aiming to enrich $CD45^+$ cells with CD45 MicroBeads. Another strategy used for IEL enrichment was density gradient. It was performed by centrifugation of the previously isolated IEL over Ficoll.

For flow sorting, antibody labelling was performed as previously described. After Viability dye Near-IR and Fc-block staining, PE-Cy7 CD45 (BD, cat # 7313763) (1/800), was used for extracellular staining. Sorter was performed following the gate strategy showed in **Fig. IV.1** in BD FACSAria^{TM} II Cell Sorter and Cytek® Aurora^{TM} CS Cell Sorter.

4.2.3 IEL Culture

Cells were cultured in 96-well flat-bottom plates (Thermo Scientific^{TM}, cat # 167008) in AIM-V^{TM} medium (Gibco, cat #12055091) supplemented with 100 U/ml Penicillin-Streptomycin (Gibco, cat #11548876) and 60 µg/ml Gentamicin (Gibco, cat #11520506)) at a concentration of 1 million cells/ml for basal condition. For stimulation with anti-CD3 (αCD3) and anti-CD28 (αCD28) antibodies, plates were pre-coated with Ultra-LEAF^{TM} purified anti-human CD3 antibody (BioLegend, cat # 317347) and Ultra-LEAF^{TM} purified anti-human CD28 antibody (BioLegend, cat #302943) 18 h in advance. Cells were then cultured with 1 mg/ml of αCD28 and 5 µg/ml of αCD3 for 24 h, 48 h, 72 h and up to 120 h at 37°C and 5 % CO_2.

For IL-15 stimulation cultures of 24 h at 37°C and 5 % CO_2 in culture medium supplemented with IL-15 (BD, cat # 15800059) at concentrations of 10 ng/ml, 50 ng/ml or 100 ng/ml.

Prior to antibody labeling for intracellular staining, Golgi transport was blocked by culturing cells with Monensin (1:1000, BioLegend, cat #420701) for 4 h.

4.3 Results

4.3.1 Surface Markers

To characterize immune cell populations within the studied cohort, a comprehensive flow cytometry analysis was conducted. Flow Cytometry Standard files were analyzed using OMIQ software. To characterize immune cell populations within the studied cohort, a comprehensive flow cytometry analysis was conducted. The Peaco QC algorithm was used to clean the data prior to follow the gating strategy. For the first cohort, the analysis was performed using the panel shown in **Tab. IV.2**, where IEL were selected as SSC-A^{low} $CD45^+$ cells (**Fig. IV.2**). Then, singlet viable cells are identified and divided based on the T$\gamma\delta$ and CD3 expression on three groups: T$\gamma\delta$ (T$\gamma\delta^+$CD3$^+$), T cells (T$\gamma\delta^-$CD3$^+$) and NK-like cells (T$\gamma\delta^-$CD3$^-$). Within T$\gamma\delta$ and T cells, four more subsets were defined based on CD4 and CD8 expression, while NK-like cells were further defined based on CD7 expression. The percentage of cells expressing NKG2D, IL-15Rα and IL-2Rβ was also measured on each immune subset using the fluorescence minus one method (FMO) to set the positivity limits.

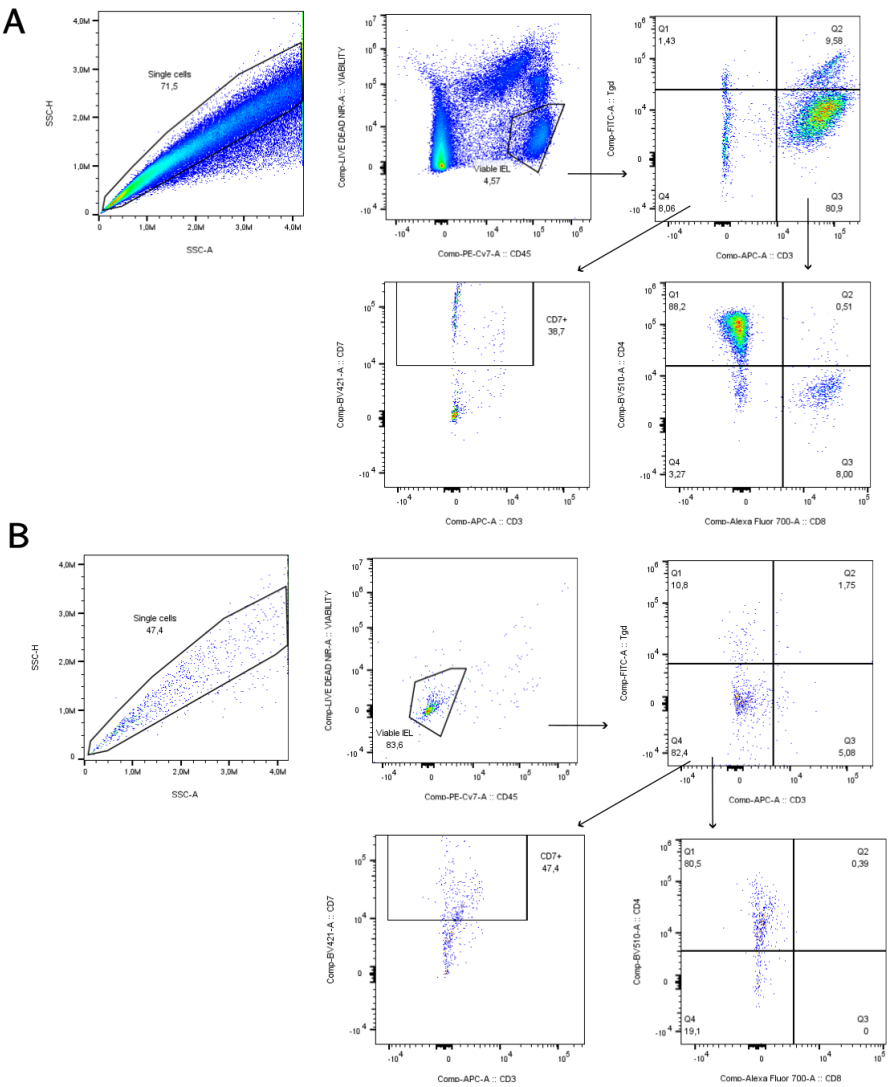

Figure IV.1: Identification of intraepithelial lymphocytes (IEL) with cell sorting. *(**A**) Within singlet cells CD45, viable cells were selected. Total IEL were further divided into subsets based on the expression of CD3 and Tγδ: $CD3^+ T\gamma\delta^+$ (Tγδ cells), $CD3^+ T\gamma\delta^-$ (T cells) and $CD3^- T\gamma\delta^-$. T cells were further subdivided based on CD8 and CD4 expression. CD7 expression on $CD3^- T\gamma\delta^-$ was also analyzed. (**B**) Same strategy was followed on the viable IEL fraction that was previously sorted. However, CD8 and CD4 expression was analyzed on $CD3^- T\gamma\delta^-$ cells.*

IEL Distribution along the Gut

The distribution of different IEL subsets across the non-coeliac and non-inflamed intestine was analyzed, as shown in **Fig. IV.3**.

TCRγδ$^+$ T cells were notably enriched in the colon compared to the small intestine (duodenum or ileum) and gastric mucosa (body, antrum, or incisura) (**Fig. IV.3A**), with a marked reduction in the CD4$^+$ subset in this region (**Fig. IV.3B**). In contrast, classical TCRγδ$^-$ T cells were found at lower levels in the colon compared to other gut areas (**Fig. IV.3C**), with no significant differences observed in the composition of their subsets throughout the gut (**Fig. IV.3D**). Finally, NK-like cell density remained consistent across tissue types (**Fig. IV.3E**), although the CD7$^+$ fraction was especially enriched in the duodenum (**Fig. IV.3F**).

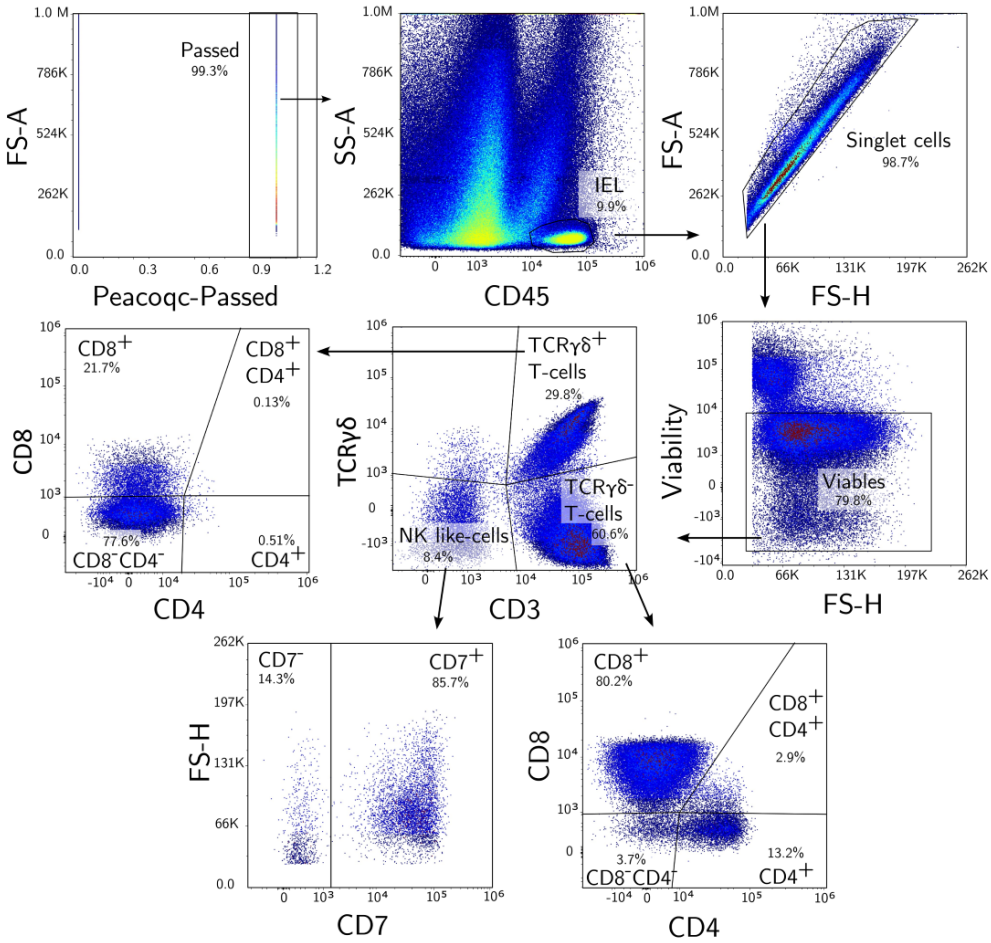

Figure IV.2: Identification of intraepithelial lymphocytes (IEL) subsets. *Total IEL were selected within the cells that passed the Peaco QC test as CD45$^+$ with low granularity (SS-A^{low}), singlet and viable cells. Total IEL were further divided into subsets based on the expression of CD3 and Tγδ: CD3$^+$Tγδ$^+$ (TCRγδ$^+$ T cells), CD3$^+$Tγδ$^-$ (TCRγδ$^-$ T cells) and CD3$^-$ Tγδ$^-$ (NK-like cells). T cells were further subdivided based on CD8 and CD4 expression while NK-like cells were categorized based on CD7.*

NKG2D is Highly Expressed on IEL throughout the Gut

Given the pivotal role of NKG2D in IEL functionality, its expression levels throught the gut was examined (**Fig. IV.4**). In Tγδ cells, NKG2D was expressed on nearly all cells, with a slightly reduced expression observed in the duodenum; however, this reduction was not linked to any specific subset (**Fig. IV.4B** and **C**). Due to an insufficient number of cells, satistical analysis was only perdormed in two subsets.

NKG2D expression was also high on classical T cells, though generally lower than in Tγδ cells, with notably increased expression in classical T cells from the ileum (**Fig. IV.4E**). Further analysis indicated a preference for NKG2D expression on CD8$^+$ classical T cells and, to a lesser extent, on CD4$^-$CD8$^-$T cells (**Fig. IV.4F**). Notably, NKG2D expression was elevated in CD4$^-$CD8$^-$ classical T cells from the ileum (**Fig. IV.4F**).

Finally, NKG2D was also detected on NK-like cells throughout the gut (**Fig. IV.4H**) with no significant regional variation, although its expression was higher in the CD7$^+$ fraction in the ileum and colon and lower in the CD7$^-$ fraction in the duodenum (**Fig. IV.4I**).

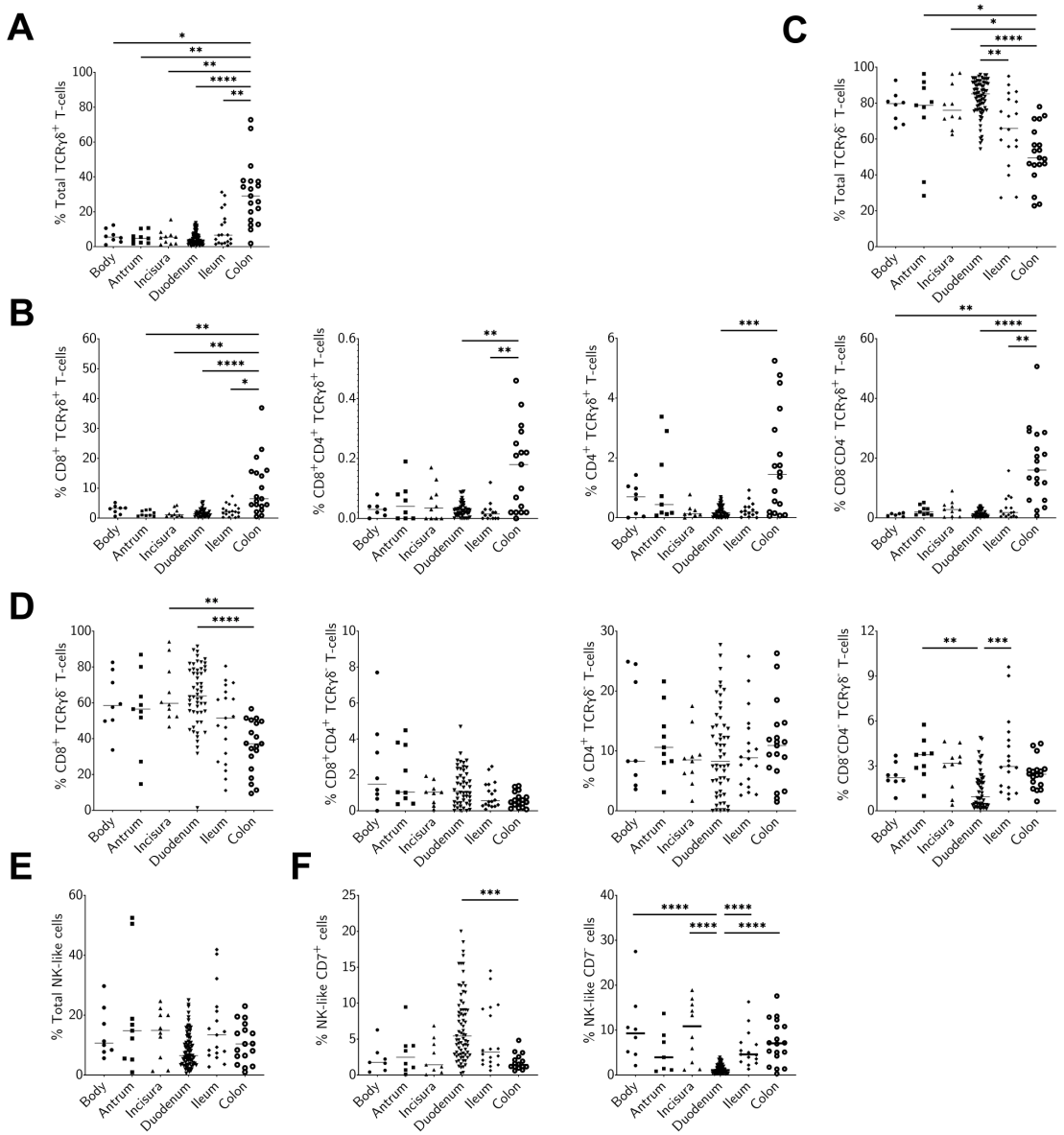

Figure IV.3: Intraepithelial lymphocytes (IEL) subsets through the gut. *Total IEL, as well as their different subsets, were identified as in* ***Fig. IV.2****. Their proportion was assessed in the gastric mucosa (body, antrum and incisura), as well as in the small bowel (duodenum and ileum) and colon from controls. The percentage of total TCR$\gamma\delta^+$ T cells is shown in (****A****), while their different subsets is displayed in (****B****). In a similar manner, the percentage of TCR$\gamma\delta^-$ T cells though the gut is shown in (****C****), with their different subsets in (****D****). Last, the percentage of total NK-like IEL, and their subsets through the gut is respectively shown in (****E****) and (****F****). Kruskal-Wallis test with Dunn's multiple comparisons test was applied in all cases. P-values < 0.05 were considered significant (*p < 0.05; ** p < 0.01; *** p < 0.001; **** p < 0.0001).*

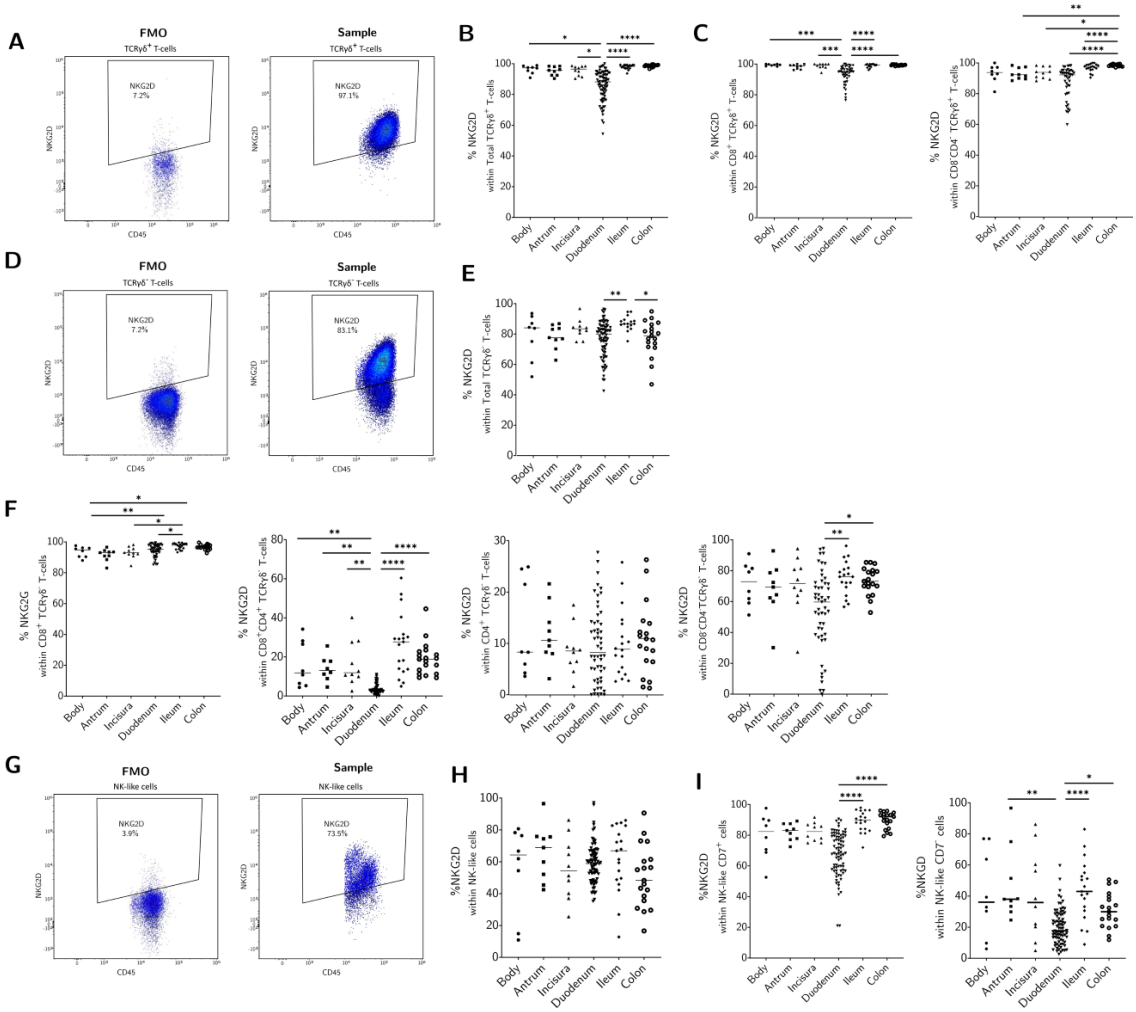

Figure IV.4: NKG2D expression on intraepithelial lymphocytes (IEL) through the gut. *IEL were identified as in* ***Fig. IV.2****. (**A**) NKG2D expression was determined on intraepithelial TCR$\gamma\delta^+$ T cells referred to their fluorescence minus one (FMO) control. (**B**) its expression was assessed on total TCR$\gamma\delta^+$ T cells, as well as on (**C**) TCR$\gamma\delta^+$ CD4$^-$ CD8$^+$ and CD4$^-$ CD8$^-$ T cells subsets. (**D**) NKG2D was also assessed on TCR$\gamma\delta^-$ T cells (**E**) through the gut and, within then, (**F**) in the different subsets based on the expression of CD4 and CD8. (**G**) Last, NKG2D was determined on total NK-like cells (**H**) both within total cells and (**I**) within their CD7$^+$ and CD7$^-$ subsets. Kruskal-Wallis test with Dunn's multiple comparisons test was applied in all cases. P-values < 0.05 were considered significant (*$p < 0.05$; ** $p < 0.01$; *** $p < 0.001$; **** $p < 0.0001$).*

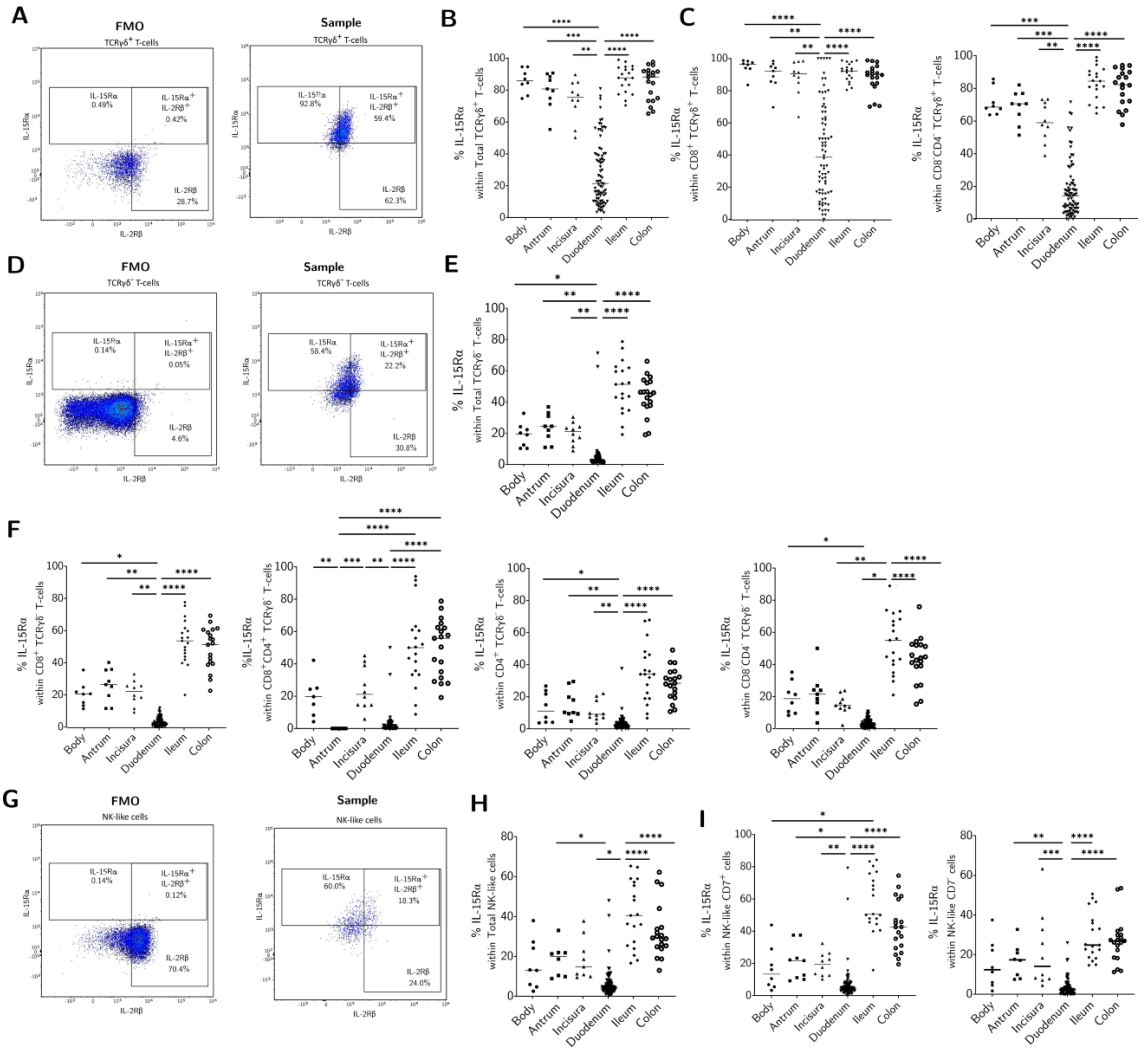

Figure IV.5: Expression of IL-15Rα on intraepithelial lymphocytes (IEL) through the gut. *IEL were identified as in* ***Fig. IV.2****. (**A**) IL-15Rα expression was determined on intraepithelial TCRγδ⁺ T cells referred to their fluorescence minus one (FMO) control. (**B**) its expression was assessed on total TCRγδ⁺ T cells though the gut, as well as on (**C**) its CD4⁺CD8⁺ and CD4⁻CD8⁻ subsets. (**D**) IL-15Rα was also assessed on TCRγδ⁻ T cells (**E**) through the gut and, within then (**F**) in their different subsets based on the expression of CD4 and CD8. (**G**) Last, IL-15Rα was determined on total NK-like cells, as well as through the gut, (**H**) both as total cells and (**I**) within their CD7⁺ and CD7⁻. Kruskal-Wallis test with Dunn's multiple comparisons test was applied in all cases. P-values < 0.05 were considered significant (*$p < 0.05$; ** $p < 0.01$; *** $p < 0.001$; **** $p < 0.0001$).*

Fluorochrome	Specifitity	Clone	Company	Cat N°
FITC	TCR$\gamma\delta$	B1	BD	559878
PE	IL15Rα	JM7A4	BioLegend	330208
PEDazzle594	NKG2D	1D11	BioLegend	320828
PerCP-Cy5.5	IL2Rβ	TU27	BioLegend	339012
PE-Cy7	CD45	HI30	BD	15879028
APC	CD3	HIT3a	BioLegend	300312
BV510	CD8	RPA-T8	BioLegend	301048
BV421	CD7	M-T701	BD	564018
Alexa Fluor 700	CD4	A161A1	BioLegend	357418

Table IV.2: Antibody panel for cohort 1 and 2 of intraepthelial lymphocytes. *Cat N°: Catalogue number.*

IL-15 Receptors are Specifically Decreased on Duodenal IEL

Recognizing IL-15's key role in regulating mucosal immune responses, the expression of IL-15Rα was examined across IEL in the gut. In T$\gamma\delta$ cells, IL-15Rα was expressed consistently throughout the gut, but showed a marked reduction in the duodenum affecting both $CD8^+$ and $CD8^-$ T$\gamma\delta$ cells (**Fig. IV.5B** and **C**). As previously mentioned, due to the low number of cells, statistical analysis was conducted only within two subsets of T$\gamma\delta$ cells. Notably, although IL-15Rα levels were generally lower in classical T cells compared to T$\gamma\delta$ cells (**Fig. IV.5B** and **E**), this decreased expression in the duodenum was similarly evident and not restricted to any particular subset (**Fig. IV.5F**).

Similarly, NK-like cells also expressed IL-15Rα throughout the gut, with a specific reduction observed in the duodenum, again without association to any distinct subset (**Fig. IV.5H** and **I**).

The expression of IL-2Rβ was assessed through the gut revealing that although it could be found on most IEL subsets through the gut, it was also decreased in the duodenum (**Fig. IV.6**). This renders such compartment, as opposed to the other sides of the gut, with no functional IL-15 receptor on classical T cells, and a very low expression on T$\gamma\delta$ cells (**Fig. IV.7**).

Intraepithelial Lymphogram in the Coeliac Duodenum

After identifying a specific reduction in IL-15Rα expression on IEL in the duodenum (**Fig. IV.5**) and considering the crucial roles of IL-15 and NKG2D in CD pathogenesis[140,141] the duodenal IEL in te context of CD was further investigated.

In CD patients, total T$\gamma\delta$ cells were expanded within the IEL compartment, regardless of mucosal status (**Fig. IV.8A**), consistent with previous findings[142,51]. A closer look revealed that, within total T$\gamma\delta$, the $CD4^-CD8^-$ subset was the most prevalent in the duodenum and showed a notable increase in CD patients, regardless of mucosal condition (**Fig. IV.8B**). In contrast, classical T cells were reduced in the CD duodenum, with a tendency toward higher levels of $CD4^-CD8^-$ cells in CD patients (**Fig. IV.8C** and **D**).

Additionally, NK-like cells were specifically reduced in CD patients with atrophy (C-I) irrespectively of Marsh index but remained unchanged in C-NI-GFD patients and non-CD controls (NC), both inflamed and non-inflamed (**Fig. IV.8E**), aligning with previous reports[121]. Finally, all CD patients, regardless of mucosal condition, showed a lower proportion of $CD7^+$ NK-like cells (**Fig. IV.8F**).

Atrophy, Symptoms and the Effect of Time on GFD on IEL Distribution

Further analysis was performed on the duodenal lymphogram of GFD-treated patients based on the presence of duodenal atrophy, presence of clinical symptoms or the duration of the GFD. IEL were classified into T$\gamma\delta$ cells, classical T cells and NK-like cells based on the

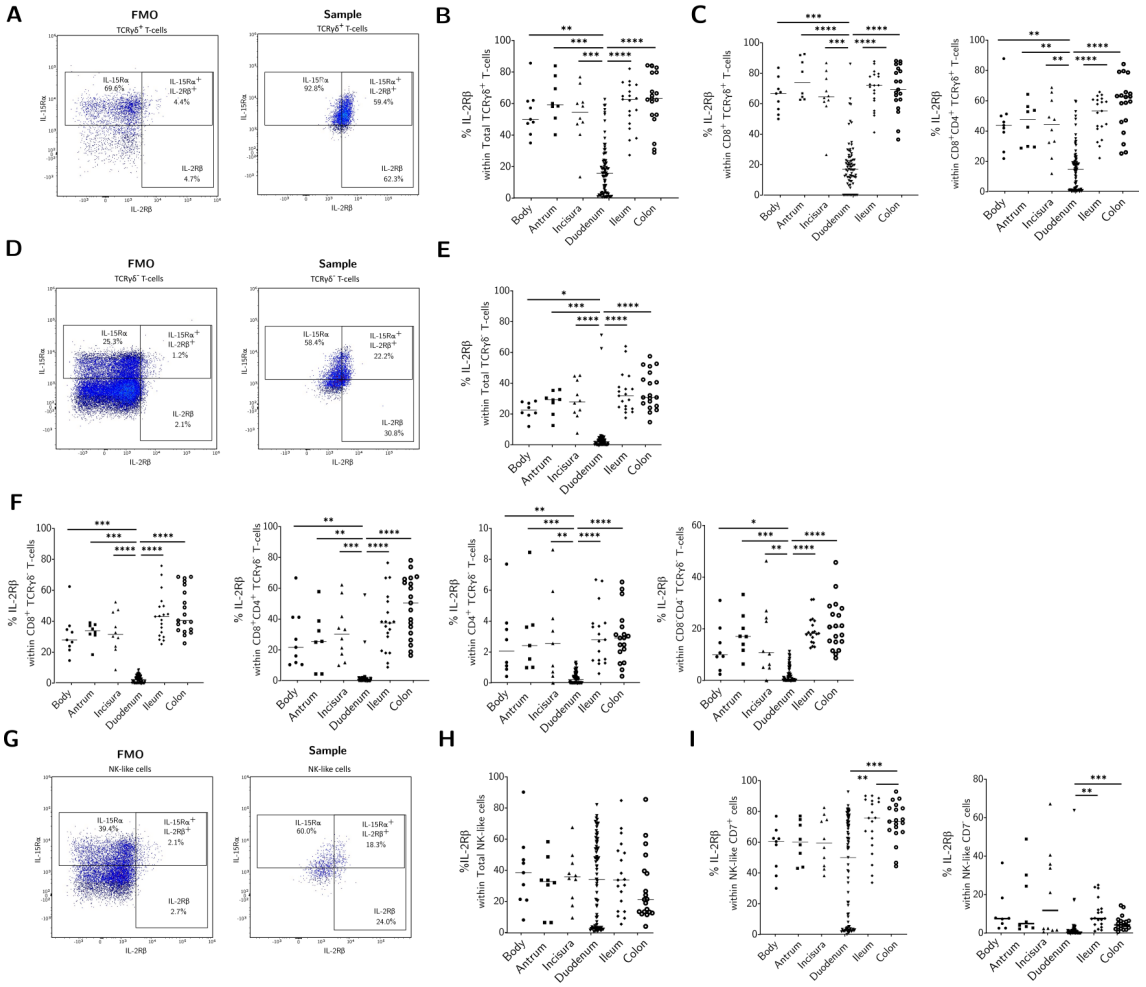

Figure IV.6: Expression of IL-2Rβ on intraepithelial lymphocytes (IEL) through the gut. *IEL were identified as in* ***Fig. IV.2****. (**A**) IL-2Rβ expression was determined on intraepithelial TCRγδ⁺ T cells referred to their fluorescence minus one (FMO) control. (**B**) its expression was assessed on total TCRγδ⁺ T cells though the intestine, as well as on (**C**) its CD4⁺CD8⁺ and CD4⁻CD8⁻ subsets. (**D**) IL-2Rβ was also assessed on TCRγδ⁻ T cells (**E**) through the gut and, within then, in (**F**) their different subsets based on the expression of CD4 and CD8. (**G**) Last, IL-2Rβ was determined on total NK-like cells through the gastrointenal, both as total cells (**H**) and (**I**) within their CD7⁺ and CD7⁻ subsets. Kruskal-Wallis test with Dunn's multiple comparisons test was applied in all cases. P-values < 0.05 were considered significant (*$p < 0.05$; ** $p < 0.01$; *** $p < 0.001$; **** $p < 0.0001$).*

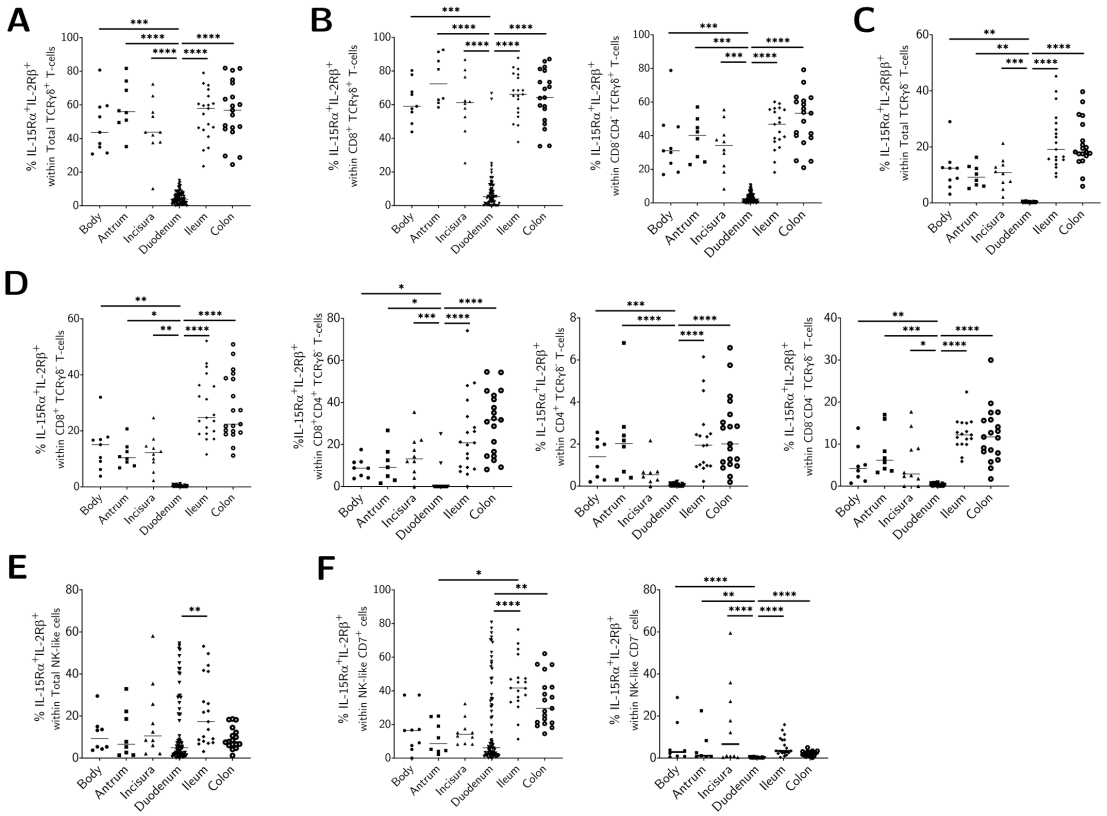

Figure IV.7: Active IL-15 receptor on intraepithelial lymphocytes (IEL) through the gut. *IEL were identified as in* ***Fig. IV.2****. (**A**) IEL expressing IL-15Rα^+IL-2Rβ^+ were identified on total TCR$\gamma\delta^+$ T cells though the intestine, as well as on (**B**) their CD4$^-$CD8$^+$ and CD4$^-$CD8$^-$ subsets. (**C**) The percentage of double positive cells also assessed on TCR$\gamma\delta^-$ T cells, through the gut and (**D**) within their different subsets based on the expression of CD4 and CD8. (**E**) Last, the proportion of IL-15Rα^+IL-2Rβ^+ cells was determined on total NK-like cells through the (**F**) within their CD7$^+$ and CD7$^-$ subsets. Kruskal-Wallis test with Dunn's multiple comparisons test was applied in all cases. P-values < 0.05 were considered significant (*p < 0.05; ** p < 0.01; *** p < 0.001; **** p < 0.0001).*

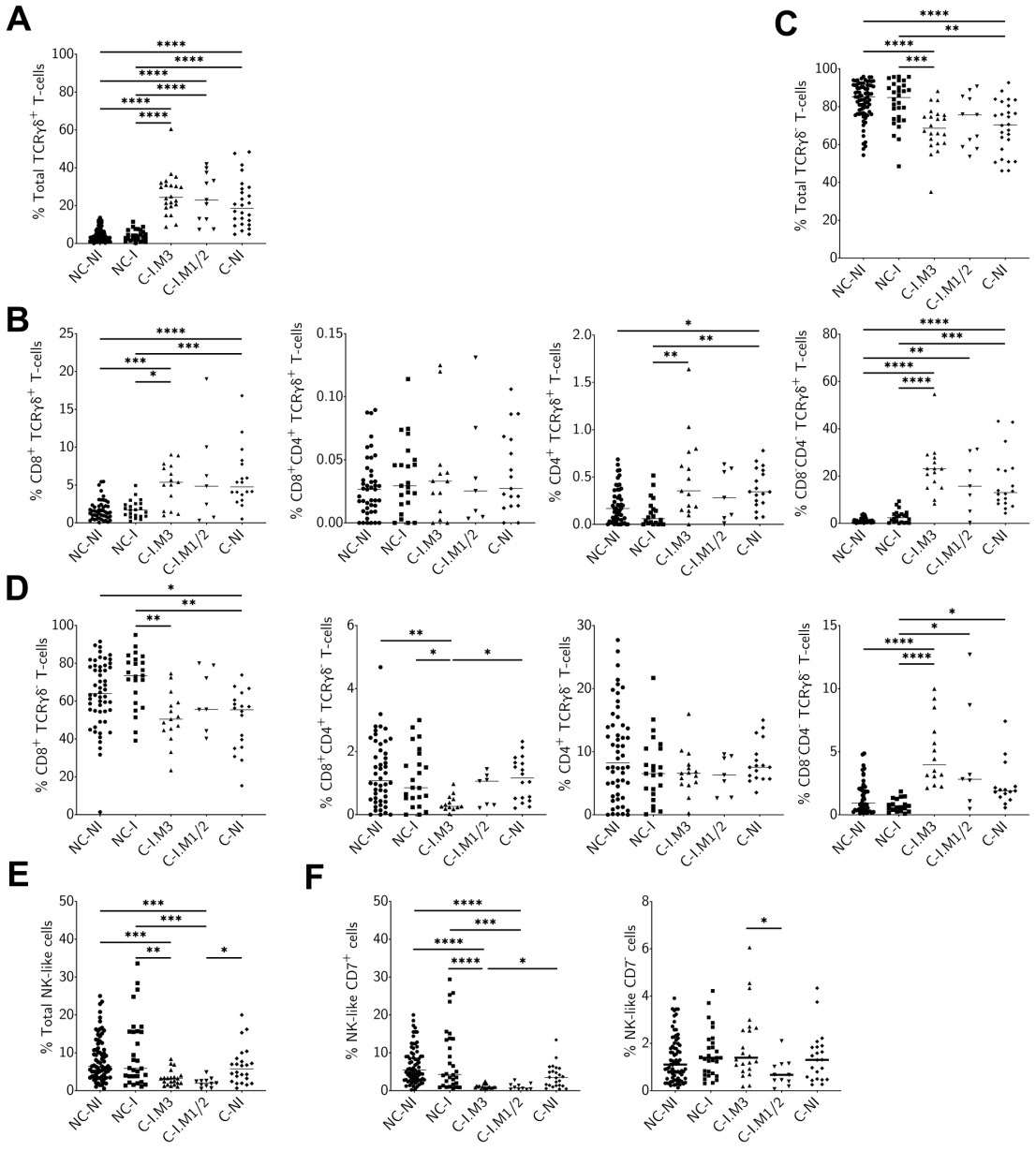

Figure IV.8: Intraepithelial lymphocytes (IEL) subsets in the duodenum. *IEL were identified as in* ***Fig. IV.2****, and their proportion determined in the duodenum from non-coeliac (NC) controls -both not inflamed (NC-NI) and inflamed (NC-I)- and from coeliac patients. Coeliac patients with different ranges of inflammation were included: Marsh 3 (C-I.M3), Marsh 2 or 1 (C-1.M1/2) and without inflammation (C-NI). The percentage of total TCR$\gamma\delta^+$ is shown in (**A**), with the relative proportion of their subsets based on the expression of CD4 and CD8 is shown in (**B**). The same applies for TCR$\gamma\delta^+$ T cells, both as (**C**) total cells and (**D**) their relative subsets; as well as for (**E**) total NK-like cells and (**F**) their subsets. Kruskal-Wallis test with Dunns multiple comparisons test was applied in all cases. P-values $<$ 0.05 were considered significant (*p $<$ 0.05; ** p $<$ 0.01; *** p $<$ 0.001; **** p $<$ 0.0001).*

expression of CD3 and T$\gamma\delta$ as previously explained on **Fig. IV.2**. CD patients were defined by a percentage over 10 % of total T$\gamma\delta$ cells within the IEL compartment in agreement with previous observations[48,143]. CD patients could be divided into newly diagnosed patients (C-I.M3) and C-GFD as shown in **Fig. IV.9** based on the proportion of NK-like cells. None of these variables (atrophy, presence of symptoms or duration of GFD) had a significant impact on the duodenal lymphogram (**Fig. IV.10**). Of note, there was a tendency (p=0,1) of an expansion of the T$\gamma\delta$ subset with time on a GFD.

Increased Expression of NKG2D on CD4$^+$CD8$^+$ and CD4 classical T cells from Patients with Severe CD.

Since NKG2D was consistently expressed across all T$\gamma\delta$ cells, its expression remained largely stable within this population and across its subsets, regardless of the duodenal mucosal condition (**Fig. IV.11A** and **B**). In classical T cells, NKG2D expression showed no significant variation across the conditions studied (**Fig. IV.11C**). However, in C-I.M3 patients, NKG2D expression was notably elevated in CD4$^+$CD8$^+$ T cells and, to a lesser extent, in CD4$^+$ T cells (**Fig. IV.11D**). In contrast, the NK-like cell population showed reduced NKG2D expression in C-I.M3 patients (**Fig. IV.11E**), with higher expression on CD7$^+$ cells and lower expression on the CD7$^-$ subset (**Fig. IV.11F**).

Reduced IL-15Rα Expression on Duodenal TCR$\gamma\delta^+$ T cells from CD Patients

IL-15Rα expression in duodenal IEL was also evaluated. L-15Rα expression was significantly reduced on T$\gamma\delta$ cells in all CD patients compared to non-CD controls, whether inflamed or non-inflamed (**Fig. IV.12A**). This reduction was not associated with any specific subset within the T$\gamma\delta$ cell population (**Fig. IV.12B**). In classical T cells, IL-15Rα expression showed no differences across conditions, whether assessed in total numbers or by cell subset (**Fig. IV.12C** and **D**), and similarly, NK-like cells exhibited stable IL-15Rα expression across all groups, whether in total or by subset (**Fig. IV.12E** and **F**).

For IL-2Rβ, expression levels did not vary across the studied conditions in the duodenum (**Fig. IV.13**). Indeed classical T cells in the duodenum lacked a functional IL-15 receptor (**Fig. IV.14C** and **D**), with no substantial differences observed in NK-like and T$\gamma\delta$ cells from CD patients (**Fig. IV.14A**, **B**, **E** and **F**).

Increased IL-15Rα Expression on Duodenal Epithelial Cells

To assess non-IEL cells, PeacoQC passed Singlets Viable CD45$^-$ cells were gated (**Fig. IV.15**). The percentage of cells expressing NKG2D, IL-15Rα and IL-2Rβ was analyzed following the gating strategy shown in **Fig. IV.4** to **IV.6**. The singlet, viable CD45$^-$ cell population in the duodenum, primarily consisting of IEC, exhibited significantly higher levels of IL-15Rα expression in patients with CD compared with controls. (**Fig. IV.16**).

4.3.2 IEL Cytotoxic Profile

Having therefore described the IEL phenotype and given that IL-15 did not seem critical on their cytotoxicity, immune activation markers were assessed next. Indeed, cytotoxic activity in inflammatory conditions was analysed using the antibody panel described in **Tab. IV.3**. A similar gating strategy was used but T$\gamma\delta$ cells were not subdivided and T$\gamma\delta^-$CD3$^-$ cells were further divided in NK cells (CD56$^+$) and CD3$^-$CD56$^-$ cells (**Fig. IV.17A**). Subsequently, both subsets were also divided based on CD7 expression. In addition, CD38, CD38^{hi}, Fas, Perforin and Perforin^{hi} subsets were defined as shown in **Fig. IV.17B**.

Although no significant differences were found in the immune activation based on the expression of CD38 (**Tab. IV.4**). Nevertheless, the proportion of CD38^{hi} cells was expanded

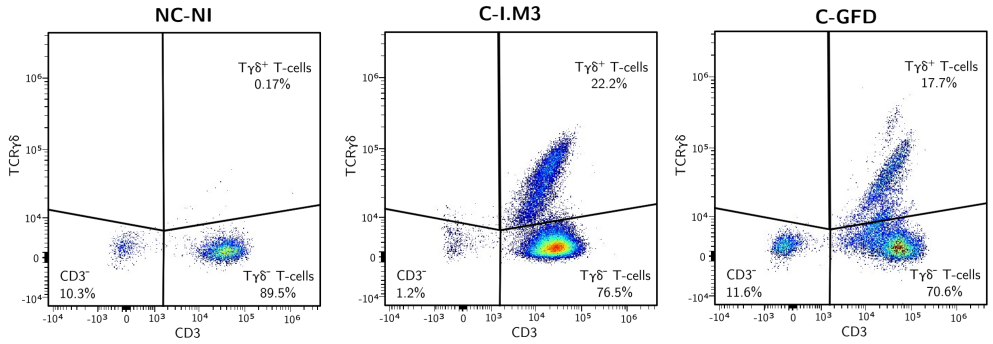

Figure IV.9: Tγδ and CD3⁻ cells on coeliac disease patients. *Identification of TCRγδ⁺ T cells (CD3⁺ TCRγδ⁺) and CD3⁻ cells within total intraepithelial lymphocytes on 3 different groups of samples: Non-coeliac not inflamed (NC-NI), coeliac inflamed (Marsh 3) (C-I.M3) and coeliac on a gluten free diet (C-GFD).*

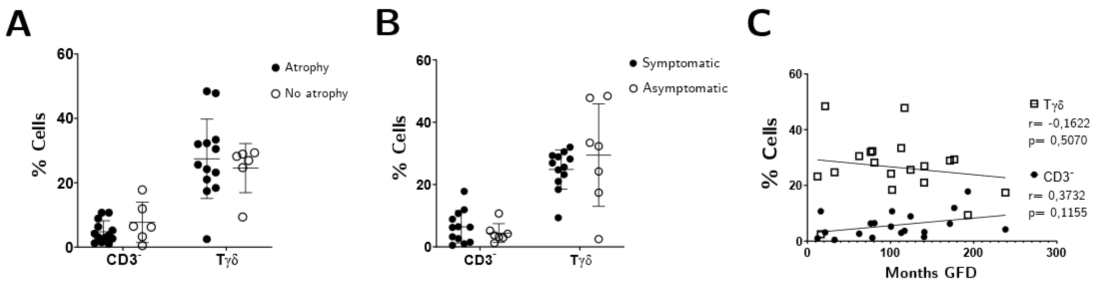

Figure IV.10: Lymphogram of gluten free diet coeliac patients. *The proportion of CD3⁻ and TCRγδ⁺ T cells on coeliac patients on a gluten free diet was assessed based on the presence of atrophy (**A**) atrophy, (**B**) symptoms and (**C**) correlation with time on the diet. T-test was performed on **A** and **B** while Pearson correlation was used for **C**. P-values < 0.05 were considered significant (*$p < 0.05$).*

Fluorochrome	Specifitity	Clone	Company	Cat. N°
Extracellular staining				
FITC	TCRγδ	B1	BD	559878
PE-Cy7	CD45	HI30	BD	15879028
APC	CD3	HIT3a	BioLegend	300312
BV510	CD8	RPA-T8	BioLegend	301048
BV421	CD7	M-T701	BD	564018
Alexa Fluor 700	CD4	A161A1	BioLegend	357418
BUV737	CD56	NCAM 16.2	BD	564447
APC-Fire 810	CD38	HB-7	BioLegend	356644
PE-Cy5	CD95	DX2	BioLegend	305610
Step 1 Intracellular staining				
NA	Perforin	polyclonal	Invitrogen	PA517431
Step 2 Intracellular staining				
Alexa Fluor 594	IgG anti rabbit	polyclonal	Invitrogen	A-11012

Table IV.3: Antibody panel for cohort 3 of intraepthelial lymphocytes. *Cat N°: Catalogue number; NA: not applicable.*

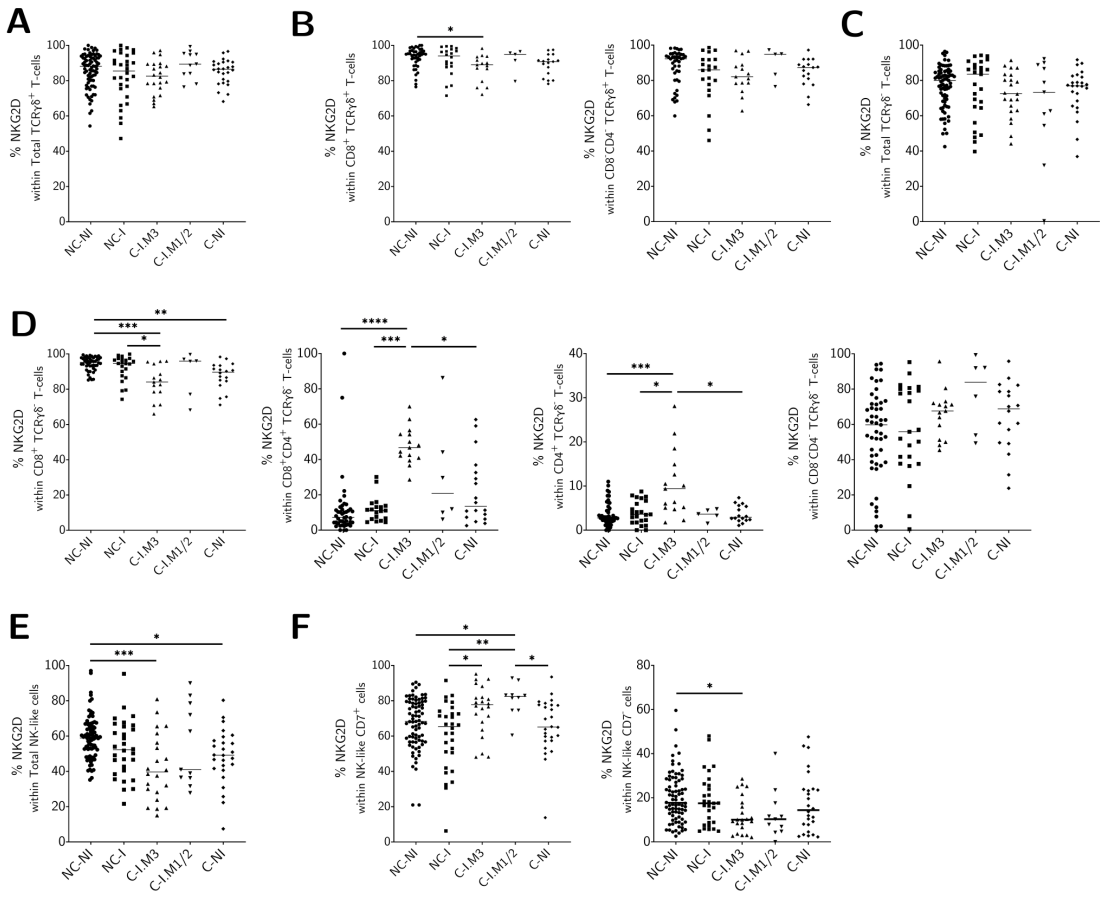

Figure IV.11: NKG2D expression on duodenal intraepithelial lymphocytes (IEL). *Duodenal IEL were identified as in* ***Fig. IV.2*** *in the duodenum of non-coeliac (NC) controls -both not inflamed (NC-NI) and inflamed (NC-I)- and from coeliac patients. Coeliac patients with different ranges of inflammation were included: Marsh 3 (C-I.M3), Marsh 2 or 1 (C-1.M1/2) and without inflammation (C-NI). Within them, the expression of NKG2D was determined on (**A**) TCR$\gamma\delta^+$ T cells and (**B**) their CD4$^-$CD8$^+$ and CD8$^-$CD4$^-$ subsets, as well as on (**C**) TCR$\gamma\delta^-$ T cells and (**D**) their CD4/CD8 subsets, together with the expression on (**E**) total NK-like cells and their CD7$^{+/-}$ compartment. Kruskal-Wallis test with Dunns multiple comparisons test was applied in all cases. P-values < 0.05 were considered significant (*$p < 0.05$; ** $p < 0.01$; *** $p < 0.001$; **** $p < 0.0001$).*

	NC-NI		NC-I		CI-M.3		C-NI		Test
	Media	SD	Media	SD	Media	SD	Media	SD	
T cells	9,4	12,5	38,4	47,1	34,5	54,1	17,2	14,8	0,53
CD8 T cells	9,3	12,6	38,1	47,6	35,4	54,3	18,6	16,3	0,56
CD4$^+$CD8$^+$T cells	9,8	19,0	47,7	42,1	66,7	57,7	7,2	16,0	0,07
CD4 T cells	9,6	14,2	36,3	48,3	33,2	56,4	5,4	10,1	0,45
CD4$^-$CD8$^-$ T cells	7,3	8,8	45,6	39,3	34,4	53,1	26,2	24,2	0,12
NK cells	47,0	32,1	62,2	48,5	46,4	45,7	84,4	7,4	0,37
CD7$^+$ NK cells	47,3	38,6	62,4	48,6	46,8	46,3	87,7	10,5	0,44
CD7$^-$ NK cells	66,67	51,64	66,68	47,14	51,97	39,74	25,00	35,36	0,56
CD3$^-$CD56$^-$ cells	48,6	30,2	59,3	43,4	54,0	30,8	80,5	5,5	0,37
CD7$^+$ CD3$^-$CD56$^-$ cells	63,9	39,2	62,4	47,4	40,2	44,0	90,0	5,2	0,55
CD7$^-$ CD3$^-$CD56$^-$ cells	21,1	17,0	45,7	39,2	56,9	28,4	43,7	19,6	0,15
T$\gamma\delta$ cells	34,4	35,0	59,8	44,7	35,4	53,7	54,7	13,7	0,40

Table IV.4: CD38 expression on intraepithelial lymphocytes. *CI-M.3: coeliac inflamed (Marsh 3); CI-NI: coeliac not inflamed; NC-I: non-coeliac inflamed; NC-NI: non-coeliac not inflamed.*

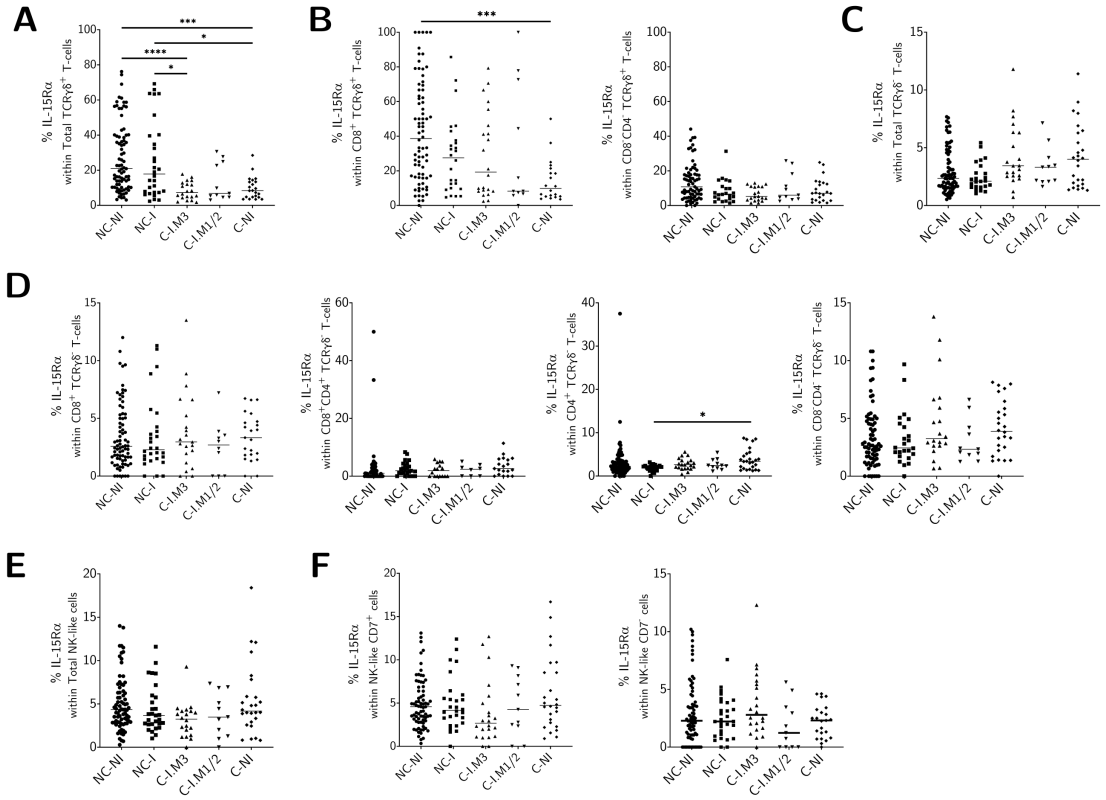

Figure IV.12: IL-15Rα expression on duodenal intraepithelial lymphocytes (IEL). *Duodenal IEL were identified as in* ***Fig. IV.2*** *in the duodenum of non-coeliac (NC) controls -both not inflamed (NC-NI) and inflamed (NC-I)- and from coeliac patients. Coeliac patients with different ranges of inflammation were included: Marsh 3 (C-I.M3), Marsh 2 or 1 (C-1.M1/2) and without inflammation (C-NI). Within them, the expression of IL-15Rα was determined on (**A**) TCRγδ$^+$ T cells and (**B**) their CD4$^-$CD8$^+$ and CD8$^-$ CD4$^-$ subsets, as well as on (**C**) TCRγδ$^-$ T cells and (**D**) their different CD4/CD8 subsets, together with the expression on (**E**) total NK-like cells and (**F**) their CD7$^{+/-}$ compartment. Kruskal-Wallis test with Dunns multiple comparisons test was applied in all cases. P-values < 0.05 were considered significant (*$p < 0.05$; ** $p < 0.01$; *** $p < 0.001$; **** $p < 0.0001$).*

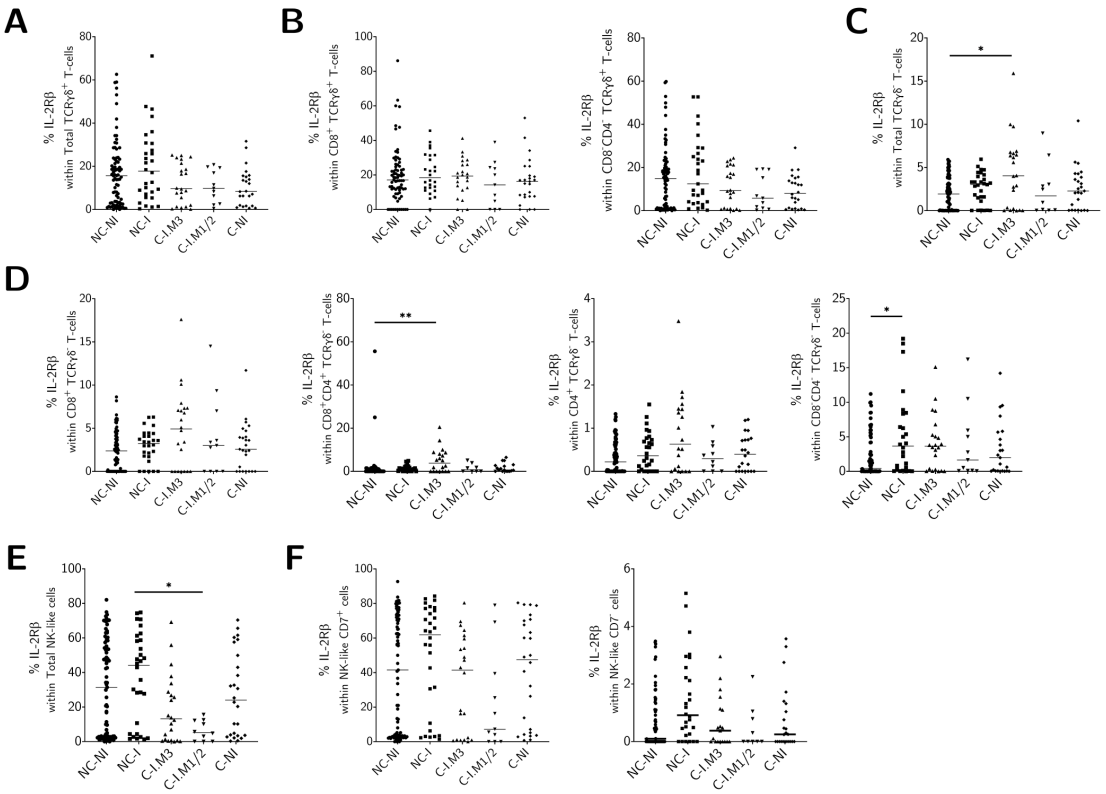

Figure IV.13: IL-2Rβ expression on duodenal intraepithelial lymphocytes (IEL). *Duodenal IEL were identified as in* ***Fig. IV.2*** *in the duodenum of non-coeliac (NC) controls -both not inflamed (NC-NI) and inflamed (NC-I)- and from coeliac patients. Coeliac patients with different ranges of inflammation were included: Marsh 3 (C-I.M3), Marsh 2 or 1 (C-1.M1/2) and without inflammation (C-NI). (**A**) Its expression is shown on total TCR$\gamma\delta^+$ T cells and (**B**) their CD4$^-$CD8$^+$ and CD8$^+$CD4$^-$ subsets, as well as (**C**) on total TCR$\gamma\delta^-$ T cells and (**D**) their different subsets based on the expression of CD4 and CD8, and (**E**) total NK-like cells and (**F**) their CD7$^+$ and CD7$^-$ subsets. Kruskal-Wallis test with Dunns multiple comparisons test was applied in all cases. P-values < 0.05 were considered significant (*$p < 0.05$; ** $p < 0.01$).*

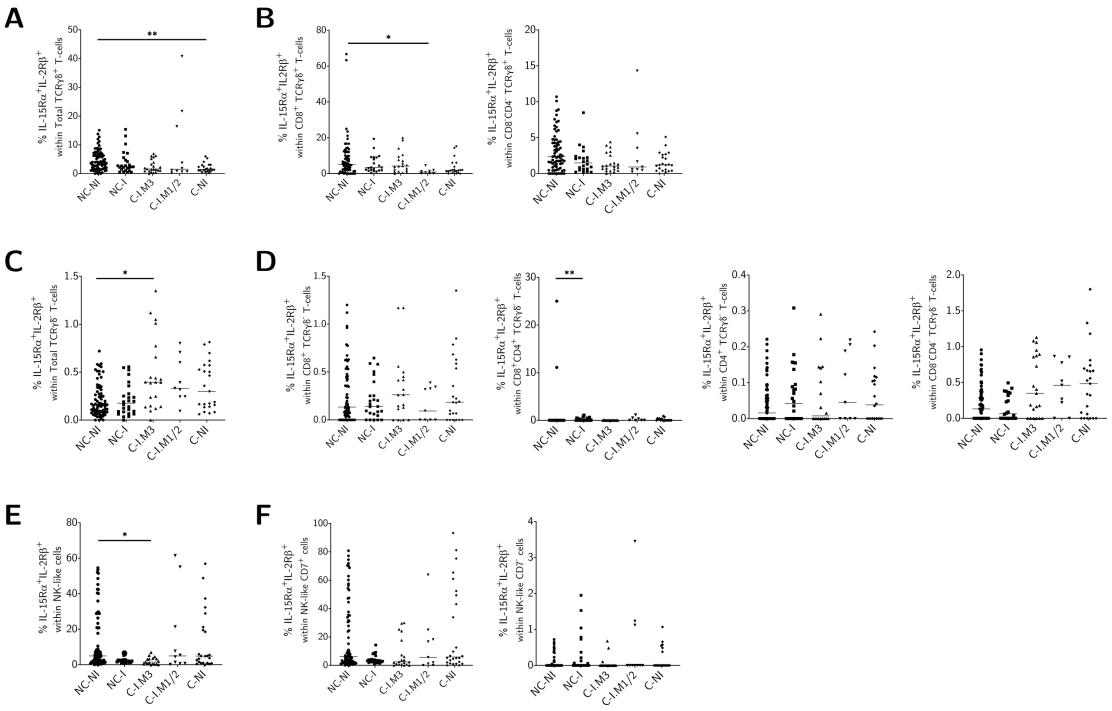

Figure IV.14: Active IL-15 receptor on duodenal intraepithelial lymphocytes (IEL). *The expression of active IL-15R (IL-15Rα^+IL-2Rβ^+) was determined on duodenal IEL as identified as in* ***Fig. IV.2*** *from non-coeliac (NC) controls -both not inflamed (NC-NI) and inflamed (NC-I)- and from coeliac patients. Coeliac patients with different ranges of inflammation were included: Marsh 3 (C-I.M3), Marsh 2 or 1 (C-1.M1/2) and without inflammation (C-NI). (**A**) total TCR$\gamma\delta^+$ T cells and (**B**) their CD4$^-$CD8$^+$ and CD8$^+$CD4$^-$ subsets, as well as (**C**) on total TCR$\gamma\delta^-$ T cells and (**D**) their different subsets based on the expression of CD4 and CD8, and (**E**) total NK-like cells and (**F**) their CD7$^+$ and CD7$^-$ subsets were identified. Kruskal-Wallis test with Dunns multiple comparisons test was applied in all cases. P-values < 0.05 were considered significant (*$p < 0.05$; ** $p < 0.01$).*

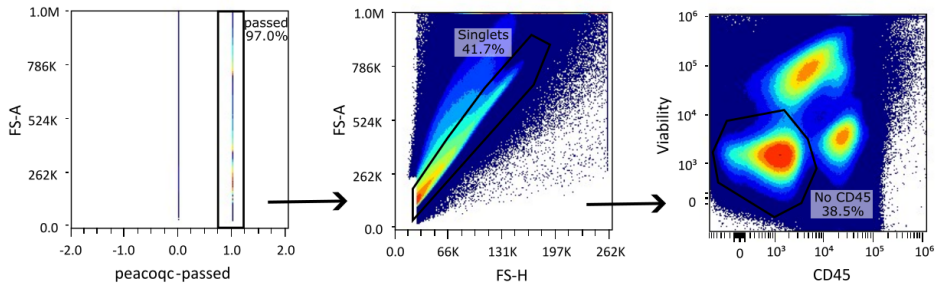

Figure IV.15: Identification of CD45$^-$ fraction on the duodenum. *CD45$^-$ fraction within the epithelial duodenal layer was selected as the cells that passed the Peaco QC test, singlet, viable and CD45$^-$ cells.*

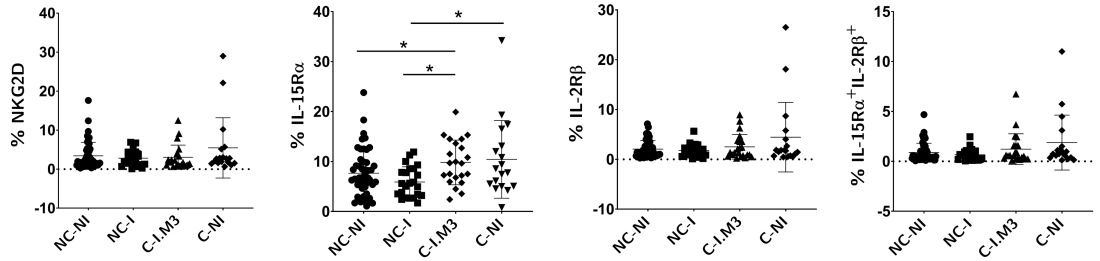

Figure IV.16: NKG2D and IL-15 receptor expression on the CD45⁻ fraction of the duodenum. *Expression of NKG2D, IL-15Rα, IL-2Rβ and IL-15Rα⁺IL-2Rβ⁺ on the CD45⁻ fraction of the epithelial layer identified as in* ***Fig. IV.15****. Comparisons within non-coeliac (NC) controls -both not inflamed (NC-NI) and inflamed (NC-I)- and from coeliac patients were performed. Coeliac patients with Marsh 3 (C-I.M3) and without inflammation (C-NI) were included. Kruskal-Wallis test with Dunns multiple comparisons test was applied in all cases. P-values < 0.05 were considered significant (*p < 0.05).*

on CD7⁻ NK cells of C-I patients while C-NI-GFD show enhanced expression of CD38^{hi} on CD3⁻CD56⁻ and CD3⁻CD56⁻ CD7⁺ cells (**Tab. IV.5**). A inflammatory state, marked by Fas expression, was enhanced in CD8 T cells, NK cells and T$\gamma\delta$ cells of the C-NI-GFD group (**Tab. IV.6**). No significant differences were found in the cytotoxic profile based on the expression of Perforin or Perforin^{hi} (**Tab. IV.7**,**Tab. IV.8**).

While cytotoxic capacity, as indicated by perforin expression, remained unchanged, the enhanced expression of CD38 and Fas in specific IEL subsets highlights an immune activation in the C-NI-GFD group.

4.3.3 IEL Enrichment Procedures

After describing the phenotypical differences of duodenal IEL among the distinct cohorts, the next step was to determine whether these differences translate into functional changes. For example, an increase in T$\gamma\delta$ is associated to CD irrespectively of the mucosal status, however, it is unknown whether their functionality changes. To investigate these potential differences, various cell isolation procedures were tested to establish IEL monocultures.

IEL enrichment using positive selection with CD45 magnetic beads on fresh samples resulted in low purity (32,9 %) and changes to the cell profile. Indeed, an aberrant CD3⁻T$\gamma\delta^+$ subset represented 11,8 % of the total cells (**Fig. IV.18**), as observed in cells cultured under resting conditions for 24 h. Furthermore, NK-like cells increased from 0,4 % to 17,2 % and similar changes were observed when using frozen samples. Additionally, changes in the CD4/CD8 profile were specifically observed in T cells (**Fig. IV.18**).

Given the phenotypic alterations caused by CD45 beads enrichment, cytometry sorting was explored (**Fig. IV.1**). However, sorter-based enrichment frequently resulted in no viable cells (**Fig. IV.19A**). Then, the focus was shifted to density gradient separation using Ficoll, expecting less cellular stress. While cell viability was less affected with this method, failed to enrich sufficiently the target population (**Fig. IV.19B**).

Combining the density gradient with magnetic negative selection using EpCAM beads yielded slight improvements (**Fig. IV.19C**), but the enrichment remained suboptimal. Moreover, negative selection altered the cell profile in 1 out of 5 experiments, particularly affecting the CD4/CD8 ratio in T cells (**Fig. IV.20**). Last, combining both negative and positive selection significantly disrupted CD4/CD8 profile (**Fig. IV.21**).

Hence, and although different approaches were tried, we did not succeed at implementing a protocol for enriching viable human IEL and set up functional approaches.

	NC-NI		NC-I		CI-M.3		C-NI		Test	NC-NI vs NC-I	NC-NI vs CI-M.3	NC-NI vs C-NI	NC-I vs CI-M.3	NC-I vs C-NI	CI-M.3 vs C-NI
	Mean	SD	Mean	SD	Mean	SD	Mean	SD							
T cells	1,2	1,5	23,1	32,6	13,8	23,1	5,1	6,2	0,63						
CD8 T cells	1,1	1,5	23,7	33,7	19,1	31,8	5,5	6,2	0,46						
$CD4^+CD8^+$T cells	4,0	5,3	33,9	43,0	65,7	56,9	4,7	10,6	0,08						
CD4 T cells	0,9	2,3	19,9	28,2	21,4	36,9	2,1	3,8	0,24						
$CD4^-CD8^-$ T cells	0,9	1,6	11,6	14,0	6,9	10,3	6,5	10,8	0,33						
NK cells	15,1	16,0	37,2	30,6	23,7	31,9	44,3	8,3	0,22						
$CD7^+$ NK cells	16,3	20,9	37,0	30,6	20,5	31,8	46,2	10,7	0,25						
$CD7^-$ NK cells	4,17	10,21	41,10	38,87	42,60	23,66	0,00	0,00	0,05	0,067	**0,022**	0,766	0,569	0,1	**0,041**
$CD3^-CD56^-$ cells	15,4	13,8	33,6	32,2	28,1	5,7	53,0	15,4	0,03	0,239	0,409	**0,003**	0,913	0,079	0,119
$CD7^+$ $CD3^-CD56^-$ cells	22,5	22,6	38,1	36,5	3,3	5,8	61,7	18,9	0,03	0,83	0,203	**0,031**	0,167	0,066	**0,004**
$CD7^-$ $CD3^-CD56^-$ cells	11,4	17,2	15,3	20,8	31,2	5,5	23,9	16,9	0,20						
T$\gamma\delta$ cells	7,7	9,6	35,3	40,3	12,6	20,6	12,6	13,1	0,44						

Table IV.5: Expression of $CD38^{hi}$ on intraepithelial lymphocytes. *CI-M.3: coeliac inflamed (Marsh 3); CI-NI: coeliac not inflamed; NC-I: non-coeliac inflamed; NC-NI: non-coeliac not inflamed.*

	NC-NI		NC-I		CI-M.3		C-NI		Test	NC-NI vs NC-I	NC-NI vs CI-M.3	NC-NI vs C-NI	NC-I vs CI-M.3	NC-I vs C-NI	CI-M.3 vs C-NI
	Mean	SD	Mean	SD	Mean	SD	Mean	SD							
T cells	24,3	26,9	36,4	32,3	49,8	17,1	66,7	8,6	0,05						
CD8 T cells	22,8	26,6	34,9	32,2	54,6	24,5	66,7	10,1	0,05	0,392	0,139	**0,006**	0,446	0,071	0,448
$CD4^+CD8^+$T cells	41,2	38,4	56,6	40,2	82,7	28,3	77,1	22,2	0,32						
CD4 T cells	35,8	34,2	40,8	34,3	56,6	19,9	77,5	4,8	0,18						
$CD4^-CD8^-$ T cells	24,3	20,9	25,9	31,0	33,4	4,3	56,8	6,8	0,06						
NK cells	38,0	22,3	28,9	31,2	19,0	24,1	64,7	7,4	0,03	0,461	0,263	0,053	0,611	**0,013**	**0,011**
$CD7^+$ NK cells	25,1	26,7	29,2	32,1	15,5	19,6	64,2	6,3	0,08						
$CD7^-$ NK cells	66,67	40,82	16,08	13,65	3,33	5,77	0,00	0,00	0,05						
$CD3^-CD56^-$ cells	35,6	26,8	38,5	29,2	20,7	4,5	72,8	6,8	0,07						
$CD7^+$ $CD3^-CD56^-$ cells	52,2	36,5	42,4	37,4	49,5	10,7	89,4	14,0	0,09						
$CD7^-$ $CD3^-CD56^-$ cells	11,9	14,8	17,0	9,6	16,4	7,0	17,8	7,3	0,56						
T$\gamma\delta$ cells	38,4	31,2	44,8	34,2	53,9	17,1	84,7	6,6	0,03	0,643	0,712	**0,003**	1	**0,019**	0,052

Table IV.6: Fas expression on intraepithelial lymphocytes. *CI-M.3: coeliac inflamed (Marsh 3); CI-NI: coeliac not inflamed; NC-I: non-coeliac inflamed; NC-NI: non-coeliac not inflamed.*

	NC-NI		NC-I		CI-M.3		C-NI		Test
	Mean	SD	Mean	SD	Mean	SD	Mean	SD	
T cells	55,1	35,2	77,1	32,3	50,2	44,5	82,1	37,9	0,18
CD8 T cells	53,9	35,9	76,3	32,2	51,4	45,1	82,1	38,0	0,15
$CD4^+CD8^+$T cells	67,4	37,7	82,7	32,0	44,1	50,4	82,6	38,9	0,21
CD4 T cells	61,9	35,0	80,7	32,1	43,6	48,0	83,1	37,1	0,08
$CD4^-CD8^-$ T cells	52,2	39,1	72,3	31,8	46,8	45,2	84,1	31,6	0,33
NK cells	66,4	29,7	85,9	26,2	54,8	40,7	88,0	23,1	0,27
$CD7^+$ NK cells	70,4	30,1	86,0	26,3	51,4	43,3	88,7	23,3	0,25
$CD7^-$ NK cells	79,17	33,23	94,63	7,88	50,50	37,21	75,00	35,36	0,29
$CD3^-CD56^-$ cells	74,1	28,3	86,9	18,4	59,3	33,2	90,2	20,2	0,16
$CD7^+$ $CD3^-CD56^-$ cells	79,3	29,4	85,6	19,3	69,7	25,9	91,1	19,8	0,23
$CD7^-$ $CD3^-CD56^-$ cells	61,4	34,3	86,5	25,9	57,0	36,2	85,3	27,1	0,31
$T\gamma\delta$ cells	51,9	42,6	73,5	37,5	43,9	46,0	82,9	36,5	0,40

Table IV.7: Perforin expression on intraepithelial lymphocytes. *CI-M.3: coeliac inflamed (Marsh 3); CI-NI: coeliac not inflamed; NC-I: non-coeliac inflamed; NC-NI: non-coeliac not inflamed.*

	NC-NI		NC-I		CI-M.3		C-NI		Test
	Mean	SD	Mean	SD	Mean	SD	Mean	SD	
T cells	11,5	17,3	28,4	30,0	17,6	27,4	47,9	35,4	0,42
CD8 T cells	10,8	16,7	26,4	28,7	14,6	21,6	47,5	34,5	0,34
$CD4^+CD8^+$T cells	21,2	32,8	40,8	39,6	18,8	25,7	50,6	48,5	0,72
CD4 T cells	16,5	21,7	33,7	33,6	10,4	17,4	53,4	37,9	0,16
$CD4^-CD8^-$ T cells	12,6	27,6	37,7	32,1	23,3	35,7	45,8	37,9	0,12
NK cells	23,0	28,2	42,7	40,7	22,4	20,5	70,9	37,0	0,21
$CD7^+$ NK cells	19,7	29,3	42,7	40,7	13,3	15,5	71,1	36,8	0,16
$CD7^-$ NK cells	50,00	54,77	68,45	46,14	21,30	36,89	50,00	70,71	0,66
$CD3^-CD56^-$ cells	28,8	33,0	58,3	37,0	19,2	20,8	69,8	34,8	0,18
$CD7^+$ $CD3^-CD56^-$ cells	32,3	33,8	54,3	43,2	28,8	36,4	73,2	37,6	0,34
$CD7^-$ $CD3^-CD56^-$ cells	22,8	29,7	60,4	29,2	18,9	19,9	61,9	29,2	0,06
$T\gamma\delta$ cells	18,9	27,3	30,6	33,1	19,2	30,8	48,2	36,3	0,48

Table IV.8: Expression of Perforin^{hi} on intraepithelial lymphocytes. *CI-M.3: coeliac inflamed (Marsh 3); CI-NI: coeliac not inflamed; NC-I: non-coeliac inflamed; NC-NI: non-coeliac not inflamed.*

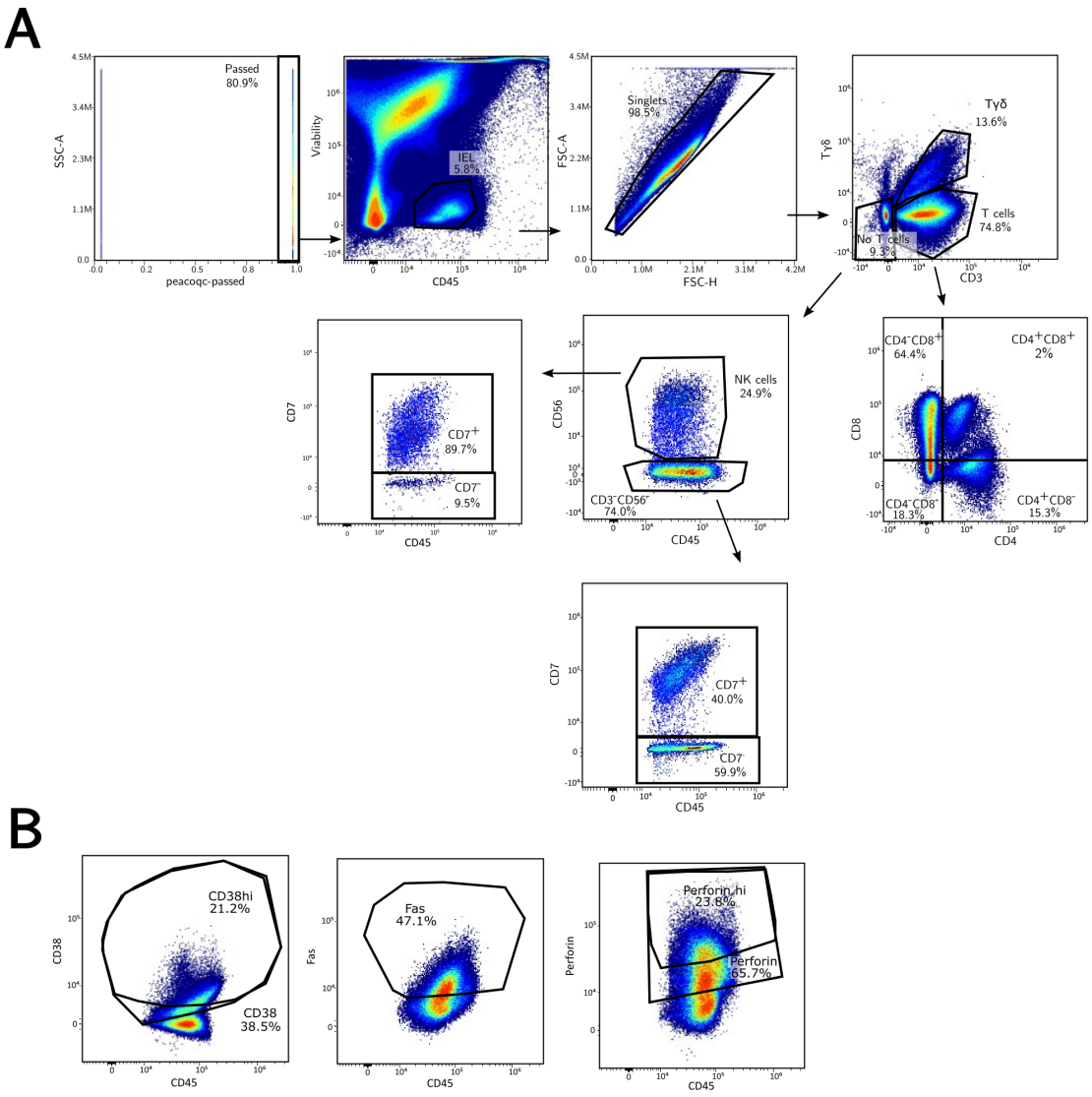

Figure IV.17: Identification of the cytotoxic profile on intraepithelial lymphocytes (IEL). *(**A**) Total IEL were selected within the cells that passed the Peaco QC test as CD45$^+$ viable, singlet cells. Total IEL were further divided into subsets based on the expression of CD3 and Tγδ: CD3$^+$Tγδ$^+$ (Tγδ), CD3$^+$Tγδ$^-$ (T cells) and CD3$^-$ Tγδ$^-$ (No T cells). T cells were further subdivided based on CD8 and CD4 expression. No T cells were categorized based on CD56 expression as NK cells and CD3$^-$CD56$^-$ cells. Both subsets were subdivided on CD7$^+$ and CD7$^-$ fraction. (**B**) For all IEL subsets expression of CD38, CD38^{hi}, Fas, Perforin and Perforin^{hi} was assessed.*

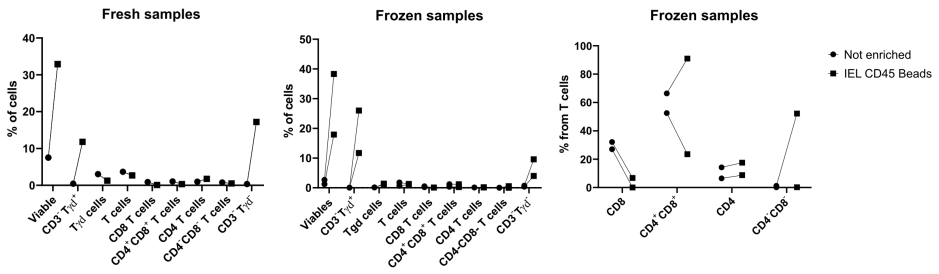

Figure IV.18: Immune profile of intraepithelial lymphocyte enriched with CD45 beads. *Fresh and frozen samples that were either enriched or not were used.*

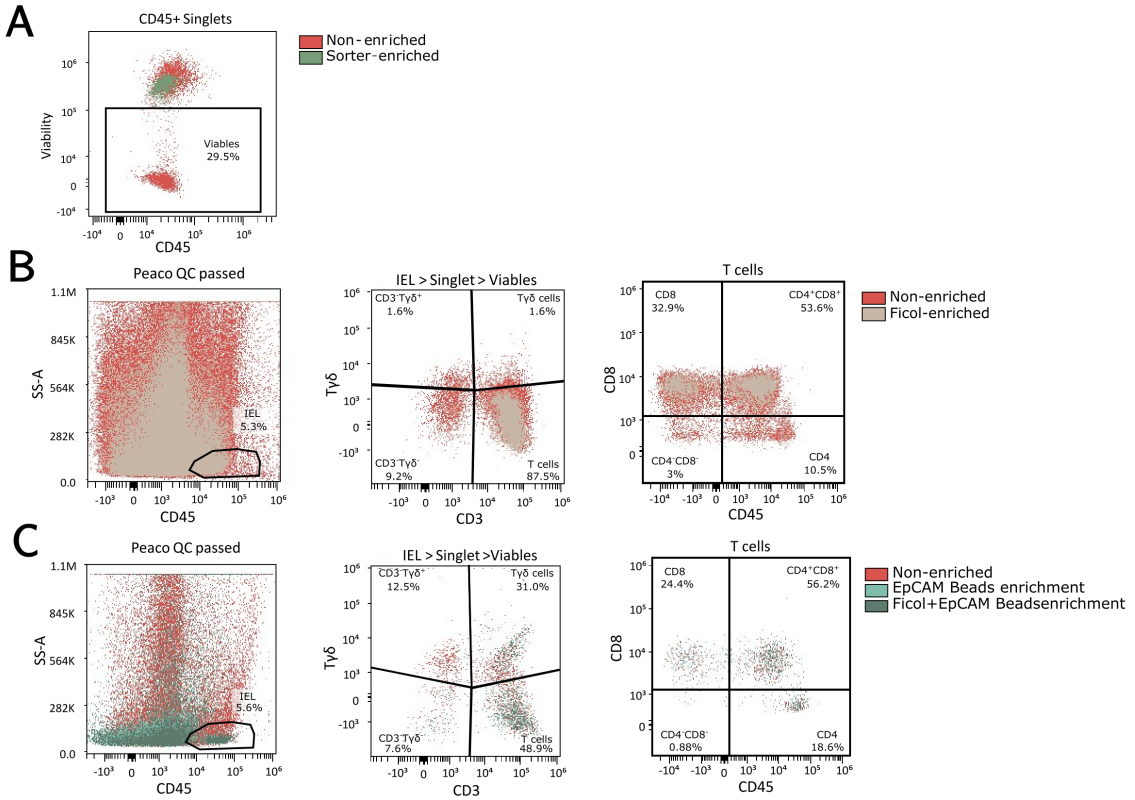

Figure IV.19: Intraepithelial lymphocytes (IEL) enrichment strategies. *(**A**) Viability and CD45 expression of non-enriched and CD45$^+$ sorter IEL. (**B**) Non enriched and enriched with ficol IEL identified as the cells that passed Peaco QC test, CD45$^+$ with low granularity (SS-A$^{\text{low}}$), singlet and viable cells. Total IEL were further divided into subsets based on the expression of CD3 and T$\gamma\delta$: CD3$^+$T$\gamma\delta^+$ (T$\gamma\delta$ cells), CD3$^+$T$\gamma\delta^-$ (T cells) and CD3$^-$ T$\gamma\delta^-$. T cells were further subdivided based on CD8 and CD4 expression. (**C**) Following the same strategy non enriched, enriched with negative selection with EpCAM beads and combining the beads with Ficol.*

4.3.4 IEL Stimulation Protocols

Given inability to establish monoculture of IEL, and that culture of IEL without enrichment do not alter their T$\gamma\delta$, CD4, CD4 and CD8 profile (**Fig. IV.22**), their functionality was assessed using stimulation protocols. The aim was to determine whether IEL from C-NI-GFD could respond differently to the inflamed milieu compared to those from C-I patients.

IFNγ and TNFα Expression after αCD3/αCD28 Stimulation

Cells, either cultured with or without enrichment, were stimulated with αCD3/αCD28 for 24 h, and stained with the antibody panel described in **Tab. IV.9** to assess the phenotype of the IEL based on the mean fluorescence intensity (MFI) of IFNγ and TNFα.

In our hands, cryopreservated IEL enriched using CD45 beads have higher IFNγ and TNFα levels, specially in the CD3 fraction compared with fresh CD45 beads-enriched IEL (**Fig. IV.23**).

αCD3/αCD28 led to a broad variability in IFNγ and TNFα expression when the experiments were performed with IEL enriched using positive selection with magnetic beads, either with fresh or frozen cells (**Fig. IV.24**). In contrast, non enriched cells obtained from frozen biopsy-isolated IEL displayed a consistent increase in IFNγ and TNFα expression within the CD3 population (**Fig. IV.24**), suggesting that IEL enrichment based on microbeads affects the stimulation response.

In resting conditions, fresh bead-enriched IEL show higher levels of IFNγ and TNFα than

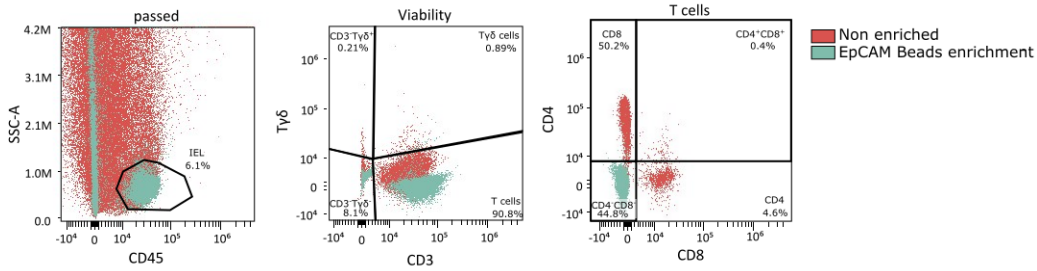

Figure IV.20: Example of intraepithelial lymphocytes (IEL) enrichment with EpCAM beads. *IEL were identified as the cells that passed Peaco QC test, CD45$^+$ with low granularity (SS-A$^{\text{low}}$), singlet and viable cells. Total IEL were further divided into subsets based on the expression of CD3 and Tγδ: CD3$^+$ Tγδ$^+$ (Tγδ cells), CD3$^+$ Tγδ$^-$ (T cells) and CD3$^-$ Tγδ$^-$. T cells were further subdivided based on CD8 and CD4 expression. Non enriched and IEL enriched with negative selection using EpCAM beads.*

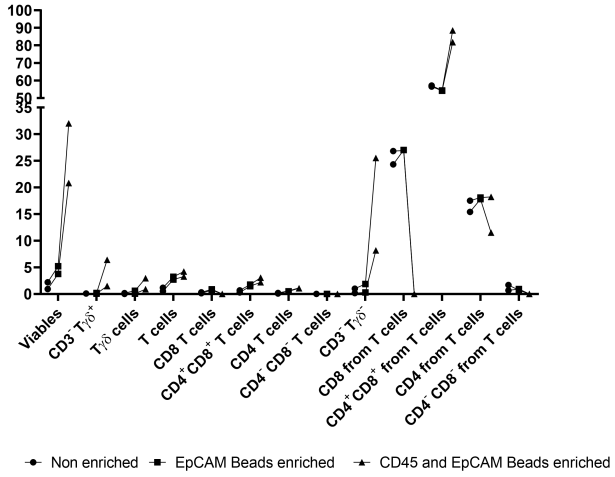

Figure IV.21: Immune profile of intraepithelial lymphocytes (IEL) enriched with negative selection. *Immune profile of IEL from the same patient that were non enriched, enriched with negative selection using EpCAM beads and combining this with CD45 beads positive selection.*

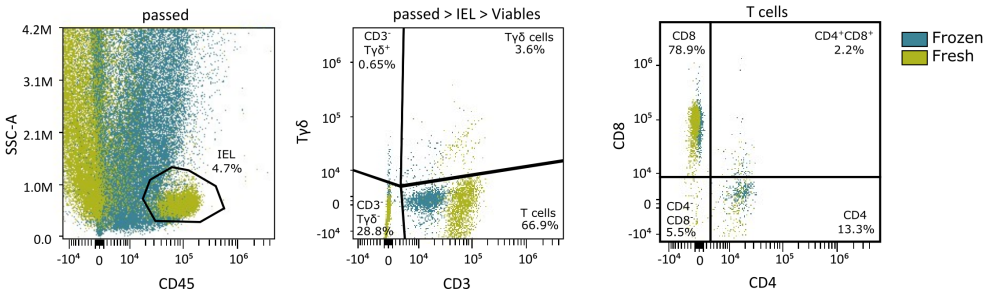

Figure IV.22: Intraepithelial lymphocytes (IEL) identification on frozen and fresh samples. *IEL identified as the cells that passed Peaco QC test, CD45$^+$ with low granularity (SS-A$^{\text{low}}$), singlets and viables. Total IEL were further divided into subsets based on the expression of CD3 and Tγδ: CD3$^+$ Tγδ$^+$ (Tγδ cells), CD3$^+$ Tγδ$^-$ (T cells) and CD3$^-$ Tγδ$^-$. T cells were further subdivided based on CD8 and CD4 expression. Scatterplots show the same sample treated freshly and after being frozen.*

Fluorochrome	Specifitity	Clone	Company	Cat. N°
Extracellular staining				
APC	CD3	HIT3a	BioLegend	300312
Intracellular staining				
PerCP-eFluor710	TNFα	MP6-XT22	Invitrogen	46-7321-80
PE-Cy7	IFNγ	XMG1.2	Invitrogen	25-7311-82

Table IV.9: Antibody panel to asessed IFNγ and TNFα on intraepithelial lymphocytes. *Cat N°: Catalogue number.*

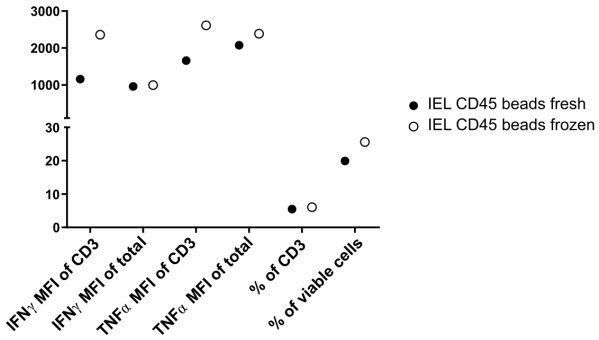

Figure IV.23: Cryopreservation effect on intraepithelial lymphocytes (IEL) enriched with CD45 beads. *Immune profile of IEL enriched with CD45 beads in the same sample treated freshly and after being frozen. After stimulation with αCD3αCD28 the mean fluorescence intensity (MFI) of IFNγ and TNFα of total viable cells and CD3 cells as well as their percentage were assessed.*

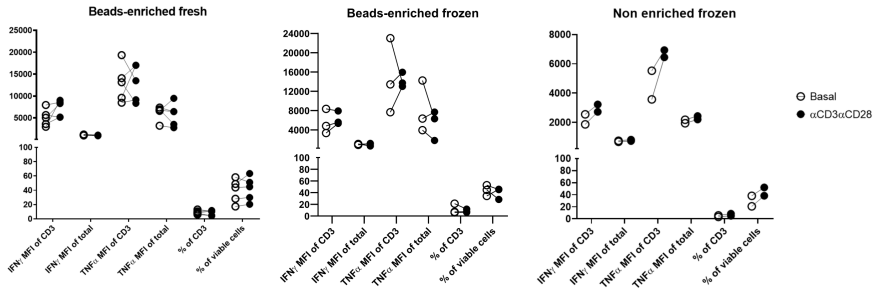

Figure IV.24: Stimulation effect on intraepithelial lymphocytes (IEL) enriched with CD45 beads. *Immune profile of IEL either enriched with CD45 beads treated freshly and after being frozen or non-enriched. Basal and after stimulation with αCD3αCD28 the mean fluorescence intensity (MFI) of IFNγ and TNFα of total viable cells and CD3 cells as well as their percentage were assessed.*

those stimulated with αCD3 αCD28 across different time points (**Fig. IV.25**). However, in frozen samples, the highest MFI values for IFNγ and TNFα were observed in the CD3 subset at 48 h (**Fig. IV.25**). Similarly, IEL enriched via sorting showed peak responses when cultured fresh at 24-48 h (**Fig. IV.25**). However, when cells were frozen there was a delayed peak at 72 h (**Fig. IV.25**). Together, these results suggest that both freezing and enrichment procedures may influence cytokine response dynamics in cultured IEL.

A direct comparison between fresh and frozen cultures at 24 h revealed similar trends in both stimulated and resting cells: a decrease in IFNγ and TNFα within the CD3 fraction (**Fig. IV.26**). Notably, during the first 24 hours of culture, cells that were frozen beforehand exhibited lower viability compared to fresh cells. However, after 72 hours, this trend reversed, suggesting that frozen cells exhibit greater robustness in longer cultures.

The unefficient stimulation on IEL with αCD3αCD28 rise doubts about the usefulness of the stimuli. Therefore, PBMC were cultured under this same stimulation to prove its efficacy. Of note, PBMC stimulation with αCD3 αCD28 for 24 h yielded more consistent outcomes, with robust IFNγ and TNFα responses even after freezing and despite the reduced percentage of viable CD3 cells (**Fig. IV.27**). This highlights the greater resilience and responsiveness of PBMC under similar conditions to IEL. Therefore, the implemented protocol although usefull for other type of cells is not convenient to stimulate IEL due to the particularities of these cells.

IL-1β and IL-6 Expression after IL-15 Stimulation

To determine if IL-15 would enhance cytokine expression in enriched IEL, cells were cultured with or without IL-15, enabling a comparison of cytokine profiles using antibody panel described in **Tab. IV.10**.

The gating strategy showed in **Fig. IV.28** was followed. Total IEL were further divided based on the Tγδ and CD3 expression on four groups: $T\gamma\delta^{+}CD3^{+}$ cells, Tγδ ($T\gamma\delta^{+}CD3^{+}$), T cells ($T\gamma\delta^{-}CD3^{+}$) and NK-like cells ($T\gamma\delta^{-}$CD3-). Within T cells, four more subsets were defined based on CD4 and CD8 expression. In addition, the $IL\text{-}6^{+}IL\text{-}1\beta^{+}$ subset was determined on singlet viable IEL. MFI of IL-6 and IL-1β was also measured.

After 24 h, a distinct $IL\text{-}1\beta^{+}IL\text{-}6^{+}$ subset emerged in bead-enriched IEL, a subset that was not present in non-enriched IEL cultures, and this pattern was independent of the IL-15 stimulation (**Fig. IV.29A**). However, this $IL\text{-}1\beta^{+}IL\text{-}6^{+}$ subset was not observed in frozen samples (**Fig. IV.29B**), underscoring the impact of the enrichment and cryopreservation on IEL development.

Fluorochrome	Specifitity	Clone	Company	Cat. N°
Extracellular staining				
FITC	TCRγδ	B1	BD	559878
PEDazzle594	NKG2D	1D11	BioLegend	320828
PerCP	CD45	HI30	Invitrogen	MHCD4531
APC	CD3	HIT3a	BioLegend	300312
BV510	CD8	RPA-T8	BioLegend	301048
BV421	CD7	M-T701	BD	564018
Alexa700	CD4	A161A1	BioLegend	357418
Intracellular staining				
PE	IL-1β	AS10	BD	340516
PE-Cy7	IL-6	MQ2-13A5	BioLegend	501120

Table IV.10: Antibody panel to asessed IL-6 and IL-1β on intraepithelial lymphocytes. *Cat N°: Catalogue number.*

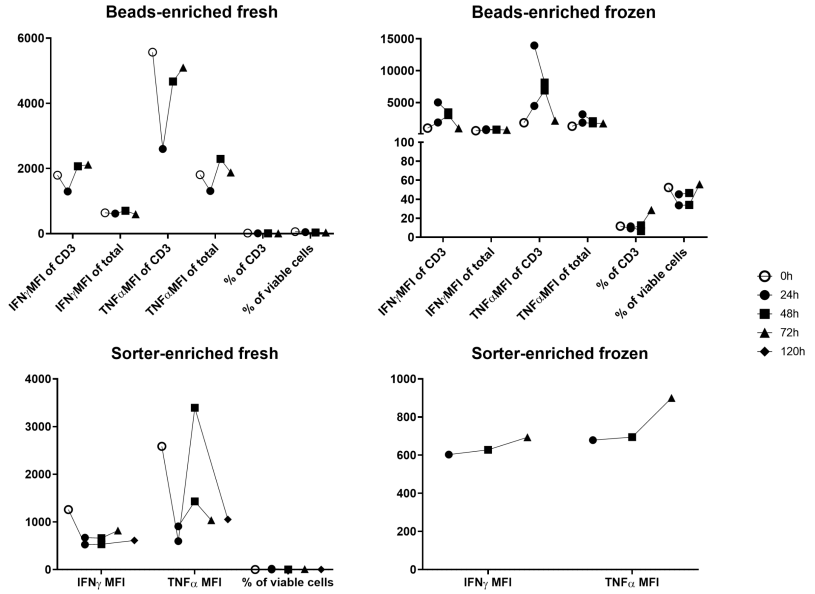

Figure IV.25: Culture of enriched intraepithelial lymphocytes (IEL) at different time points. *Immune profile of IEL either enriched with CD45 beads or CD45$^+$ sorted. For both enriched cells fresh and frozen samples have been cultured with αCD3αCD28. Resting (0 h) and after stimulation at different timepoints (24 h, 48 h, 72 h and 120 h) the mean fluorescence intensity (MFI) of IFNγ and TNFα of total viable cells and CD3 cells as well as their percentage were assessed.*

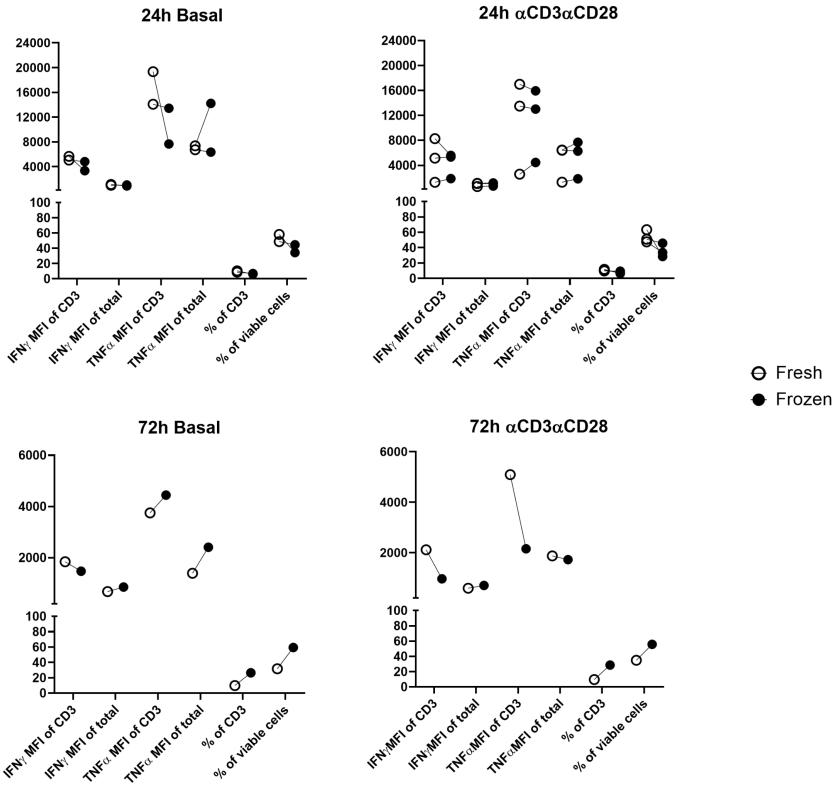

Figure IV.26: Cryopreservation effect at different time points. *Immune profile of IEL enriched with CD45 beads cultured freshly or after being frozen. Samples were cultured in resting conditions (basal) or stimulated with αCD3αCD28 for 24 h and 72 h. The mean fluorescence intensity (MFI) of IFNγ and TNFα of total viable cells and CD3 cells as well as their percentage were assessed.*

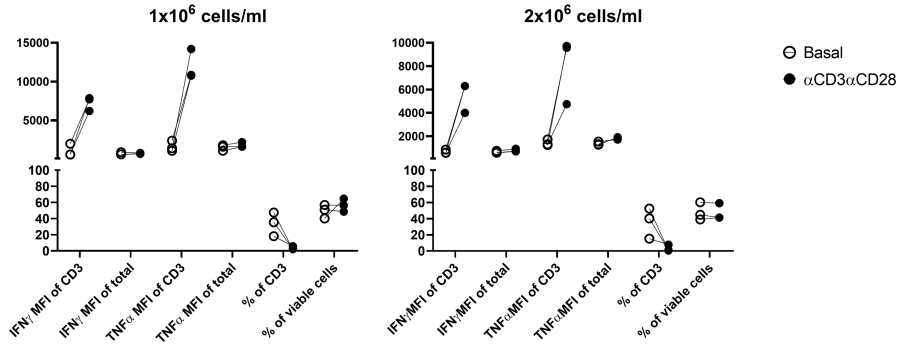

Figure IV.27: Peripheral blood mononuclear cells (PBMC) stimulation with αCD3αCD28. *PBMC were cultured in resting conditions (basal) or stimulated with αCD3αCD28 for 24 h either at 1 million cells/ml or 2 million cells/ml concentration. The mean fluorescence intensity (MFI) of IFNγ and TNFα of total viable cells and CD3 cells as well as their percentage were assessed.*

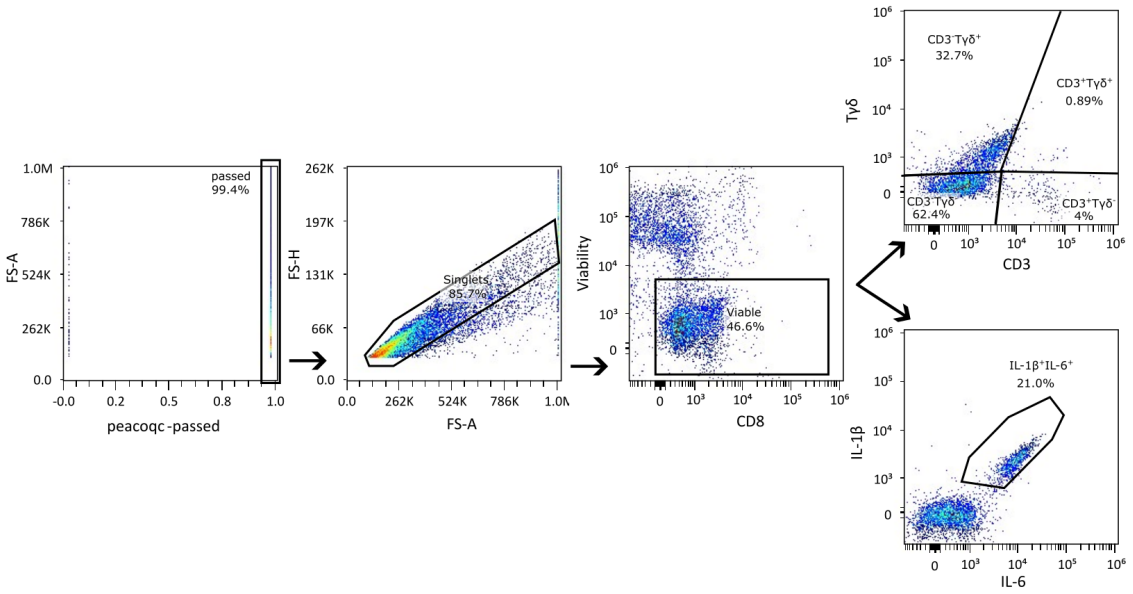

Figure IV.28: Identification of intraepithelial lymphocytes (IEL) producing IL-1β and IL-6. *IEL enriched with CD45 beads were identified as the cells that passed Peaco QC test, singlet and viables. Total IEL were further divided into subsets based on the expression of CD3 and T$\gamma\delta$. IL-1β^+IL-6$^+$ IEL were also gated.*

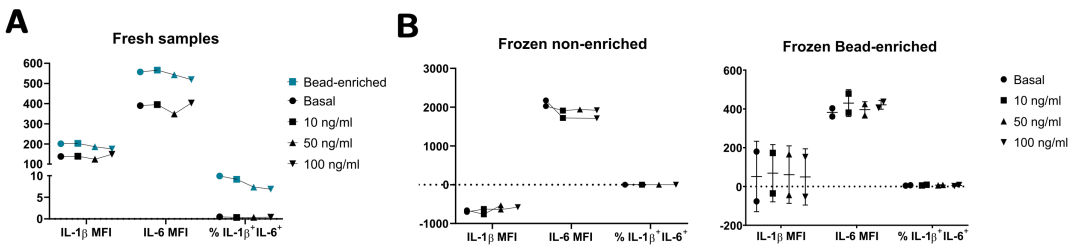

Figure IV.29: Stimulation of intraepithelial lymphocytes (IEL) with IL-15. *Mean fluorescence intensity (MFI) for IL-1β and IL-6 as well as the percentage of the IL-1β^+IL-6$^+$ subset on the IEL identifies as in **Fig. IV.28**. (**A**) Fresh samples as well as (**B**) frozen ones were used. In both cases non enriched and CD45 beads enriched IEL were used. Cells were cultures in resting conditions or with different concentrations of IL-15 (10, 50 or 100 ng/ml).*

4.4 Discussion

The properties of the immune system exhibit systematic variation along the length of the gut[84,82]. This study confirms that the profile of total IEL changes across the gut, revealing distinct characteristics in the duodenum, especially in the context of CD. One of the key findings is a lower expression of IL-15Rα in duodenal IEL when compared to other parts of the gut, a pattern that was more pronounced in CD patients. This suggests a unique functional profile of duodenal IEL, with potential implications for understanding oral tolerance and immune regulation in the gut.

Results also highlight also significant regional variation in the composition of IEL, with an increased proportion of T$\gamma\delta$ cells in the colon, confirming findings from previous studies[144]. Notably, the CD4$^+$ T$\gamma\delta$ cell fraction was virtually absent in the IEL compartment of the colon. Among all compartments examined, the duodenum stood out as the most distinct compartment, with expansions of classical T cells and CD7$^+$ NK-like cells. These duodenal cells exhibited a very low expression of IL-15Rα, particularly on classical T cells and NK-like cells, with expression on T$\gamma\delta$ cells also lower than in other regions of the gut. Additionally, there were virtually no functional IL-15R in T cells on this compartment and it was dramatically decreased on Tgammadelta and NK.like cells. Furthermore, IEL displayed lower activation levels, marked by decreased NKG2D expression on T$\gamma\delta$ cells. This suggests that duodenal IEL may possess a non-inflammatory, regulatory phenotype, which aligns with the immunoregulatory role attributed to this compartment[122,82].

When focusing specifically on CD, this study confirms previous observations of increased T$\gamma\delta$ cells in the duodenum of patients, regardless of mucosal status, while the NK-like cell fraction was reduced in patients with active disease[145,142]. This alteration in IEL composition in CD is likely related to the disease's pathogenesis, particularly the role of NKG2D in inducing intestinal epithelial cell apoptosis[119]. Besides, there is a direct link between the expression of NKG2D ligands and cellular stress in the inflamed mucosa from CD patients[146]. The data of this work show higher NKG2D expression on the CD4$^+$ T cell fraction of classical T cells and on the CD7$^+$ fraction of NK-like cells in CD patients, especially those with more severe disease. These results are in line with studies using murine models, where the recovery of mucosal function following a GFD led to a reduced NKG2D expression in the mucosa[147]. The correlation of NKG2D expression on IEL surface with villous atrophy suggests its potential as a target for immunotherapies.

The IEL profile is not always normalized following the instauration of a GFD[148,149,150,151]. However, in this study the percentage of CD3$^-$ and T$\gamma\delta$ cells on GFD treated patients showed a trend towards normalization that correlated with the duration of the GFD in months. Moreover, neither the presence of mucosal atrophy nor the symptoms impact this subset counts.

Given the central role of IL-15 in triggering immune responses in the gut[152], particularly in CD, where patients exhibit a lower immune response threshold to this cytokine[153], the expression of its receptor was examined. The findings indicate that IL-15Rα expression was markedly lower in duodenal IEL. Notably, the expression of IL-2Rβ, which shares its β chain with IL-15R[154], was also decreased in the duodenum compared to other regions of the gut (**Fig. IV.5**).

A lack of IL-15 or its receptor in the gastrointestinal epithelium hinders the development of intestinal IEL[155]. While the IL-2Rβ expression has been documented on IEL from some animal models[156], its presence and function in IEL require further investigation. The absence of an active IL-15R on the duodenum may therefore be a mechanism to mediate oral tolerance towards the nutrients and commensals[70].

Contrary to expectations, IL-15Rα expression was not significantly increased in the IEL of CD patients, and IL-2Rβ expression showed no major differences across the conditions studied. This suggests that the functional IL-15R is not actively operative in the duodenum

in CD, potentially reflecting a distinct immune regulatory mechanism specific to this region. Nevertheless, the importance of IL-15 is not discounted, particularly given the increase in IL-15Rα expression within the presumably IEC (CD45$^-$ fraction) in CD patients. These is in alignment with the trans-presentation of IL-15 from IEC to IEL for which a more in-depth study is necessary[157,158]. Traditionally, IL-15 has been considered as a key cytokine mediating IEL activation[115]. However, it might be relevant just at initial stages of CD[159] being transpresented by IEC[157,158]. Given the absence of a functional IL-15R in IEL, it is likely that other cytokines, such as IL-7, may have a more central role in CD pathogenesis, particularly in driving immune responses beyond disease onset[160].

This insight raises the possibility that IEL contribute to the persistent duodenal atrophy observed in CD, consistent with the abnormal phenotypes seen in RCD[161,162,163]. The continued presence of IEL in the gut lining after gluten withdrawal could signal an ongoing immune response, potentially to a non-gluten driver. Therefore, future research should focus on clarifying the role of IEL -and T$\gamma\delta$ cells in particular- in CD pathogenesis, as these immune cells may be key factors in the failure of mucosal healing. Furthermore, the presentation of IL-15 from IEC to IEL warrants further investigation. While CD patients exhibit increased IL-15Rα expression on IEC, no significant enhancement in IL-2Rβ expression has been observed.

An intriguing finding in this study was the elevated expression of Fas and Perforin^{hi} in asymptomatic CD patients. These results are counterintuitive, as they suggest that these individuals may harbor IEL with increased cytotoxic potential but without active inflammatory responses, possibly due to the absence of gluten exposure. This raises the possibility of irreversible changes in the IEL compartment in asymptomatic CD, which warrants further investigation.

Of note, this study is primarily descriptive, and further studies are needed to clarify the role of increased NKG2D expression on the CD4$^+$ fraction of duodenal classical T cells, as well as the precise function of IL-15 in the duodenum, both in health and in the context of CD. Future research should explore also the implications of the absence of a functional IL-15R on classical IEL T cells, which could suggest that IL-15's effects may be mediated via a trans-presentation mechanism in the coeliac duodenum[164]. A previous study[165] also reported selective upregulation of IL-15 and IL-21 in active CD patients, with both cytokines potentially contributing to tissue damage.

Distinct immune alterations in IL-2Rβ expression have been described in the duodenum of RCD. A downregulation of IL-2Rβ in specific CD3$^-$CD7$^+$ IEL clusters[166] as well as in CD127$^-$ innate IEL while being selectively expanded on CD127$^+$ innate cells[150].

In order to explore the functional implications of these differences in the IEL phenotype, to enrich and assess their function. Sorting, density gradient separation and capture beads for both positive and negative selection were explored. Either the viability or the immunological profile of IEL, defined by the expression of T$\gamma\delta$, CD3, CD4, and CD8, were altered during these isolation attempts, indicating that each method impacted the profile in distinct ways. Furthermore, achieving the desired purity of isolated cells was challenging across all methods, suggesting that further optimization is needed for a precise IEL enrichment.

Moreover, the influence of cell enrichment and freezing techniques on IEL cytokine responses further underscores the necessity for specialized culture conditions that take into account the distinct characteristics of IEL. The emergence of an IL-1β^+ IL-6$^+$ subset in bead-enriched IEL cultures, which was absent in non-enriched cultures and independent of IL-15 stimulation, suggests that the enrichment process may expose specific activation capacities within IEL populations. Moreover, while cryopreserved biopsy-derived IEL demonstrated initially a reduced viability, they retained their cytokine response after prolonged culture, highlighting the resilience of IEL to cryopreservation. These findings emphasize the plasticity of IEL under varying experimental conditions and reinforce the need for optimized activation protocols, distinct from those used for PBMC, to enhance the reproducibility and reliability of

IEL-based studies.

The potential impact of the isolation methods on IEL profiles was also observed by Leon and Roy (2004)[132], who noted a decrease in NK IEL proportions following enrichment with Annexin, likely due to an inferior viability, as these cells require IEC-derived cytokines like IL-7 and IL-15 for survival. Furthermore, the difficulties encountered with the enrichment process especially with regards to CD45 labeling raise concerns about potential misinterpretation due to contamination by epithelial cells. This highlights the importance of using optimized methods, such as direct isolation from fresh biopsies using DTT/EDTA, to prevent errors and to obtain a more accurate representation of IEL profiles.

In summary, the biological variability of IEL along the gut has been comprehensively characterized, providing new insights into regional differences and specific phenotypic and functional changes in IEL associated with CD. These findings not only enhance our understanding of the immune landscape in CD but also provide novel tools for the diagnosis and monitoring of CD. These also lay the groundwork for functional studies to investigate the precise role of IEL in CD pathogenesis.

Together, these studies emphasize the distinct IEL profile in CD, with altered IL-15 signaling capacity that likely impacts IEL functionality and highlights the heterogeneity and potential dysregulation of the IEL compartment in severe CD pathology. These findings reinforce the importance of further exploring the role of IL-15 and its receptor in both the immune response and pathology of CD, especially as it pertains to the function of IEL.

5

Lamina Propria Lymphocytes

5.1 Introduction

Nearly half of GFD-adherent patients continue to exhibit persistent villous atrophy despite the absence of symptoms or positive serology[66]. This phenomenon raises important questions about the underlying immune mechanisms and highlights a potential gap in our understanding of immune normalization in CD patients on a long-term GFD. Addressing this knowledge gap is critical to refining clinical monitoring approaches and developing new strategies to manage subclinical disease in CD.

The immune cell infiltrate in the duodenal mucosa of newly diagnosed CD patients is well-documented[167,168], but limited research has focused on immune profiles in GFD-treated patients who continue to exhibit villous atrophy. A comprehensive immune characterization of these patients could reveal key insights into the persistence of immune activity despite GFD adherence, as well as informing of targeted therapeutic interventions. This chapter aims to bridge this gap by examining the duodenal immune cell profile of GFD-treated CD patients with persistent atrophy, comparing it with both disease-onset CD and control profiles.

5.1.1 Immune Markers Related to Gluten in CD Pathogenesis

Several immune markers play critical roles in the pathogenesis of CD, particularly in the immune response to gluten. Among these, Toll-like receptor 4 (TLR4) has gained attention for its potential as a gluten-response receptor. Previous studies indicate that large supramolecular structures of 33-mer gliadin peptide aggregates activate TLR4 and TLR2, triggering pro-inflammatory cytokine release in CD[169,170]. Notably, TLR4 expression appears elevated in both blood samples and intestinal biopsies from active CD patients[171]. Park and Shin (2013) proposed a mechanism where gluten-reactive $CD4^+$ T cells activate TLR4 through IL-21 production in HLA-DQ2.5 CD patients[172]. These findings suggest that TLRs, particularly

TLR4, could play a relevant role in CD pathogenesis and could potentially serve as markers for gluten-related inflammation. However, more research is needed to fully establish TLR4's usefulness as a specific gluten-related marker in CD diagnosis and monitoring.

Research also has shown that gliadin, a component of gluten, binds to the C-X-C motif chemokine receptor 3 (CXCR3) in IEC, triggering a cascade of events leading to increased intestinal permeability in CD[173]. This interaction causes the release of zonulin, a protein that modulates intestinal tight junctions[174]. CXCR3 expression is elevated in active CD but normalizes with a GFD[173]. The gliadin-CXCR3 binding also induces IL-8 production in a CXCR3-dependent manner, but only in CD patients[175]. CXCR3 expression generally normalizes with a GFD, yet its role in cases with persistent atrophy remains unclear. Understanding the dynamics of CXCR3 expression in C-GFD-treated could enhance the ability to distinguish active immune processes from effectively suppressed ones. Therefore, any study investigating LPMC should consider including both receptors given their potential involvement in gluten recognition.

5.1.2 Mucosal Immune Markers

In addition to markers related to gluten recognition, markers associated with mucosal function should also be studied. Markers of mucosal immune function provide insights into the immune cell interactions within the intestinal microenvironment of CD patients.

C-X-C motif chemokine receptor 5 (CXCR5) plays a crucial role in mucosal immune function and can serve as a marker for recently activated memory $CD4^+$ T cells[176]. It is essential for the formation of ectopic lymphoid follicles in chronic infections and the development of solitary intestinal lymphoid tissue[177,178]. CXCR5-deficient mice exhibit impaired B cell homing and reduced humoral immune responses to oral immunization[177]. Indeed, following oral vaccination, activated T follicular helper-like cells expressing CXCR5 are mobilized into the blood, promote IgA production and express markers supporting gut-homing potential[179].

Similarly, CD95/Fas is associated with mucosal immune regulation in CD, where its expression promotes enterocyte apoptosis, contributing to the villous flattening observed in active disease[180]. Persistent elevation of these markers could indicate ongoing mucosal immune activation despite GFD adherence. Studies have shown increased expression of Fas and Fas ligand (FasL) on IEL and LPL in active CD compared to treated CD and controls[181,182]. Interestingly, IEL show decreased apoptosis in active CD, potentially contributing to autoimmune complications[182].

CD38 is a multifunctional protein expressed on immune cells and as a soluble form, serving as an activation marker upregulated by inflammatory mediators[183]. CD38 expression on gluten-specific T cells has emerged as a robust marker of gluten re-exposure in CD. Studies have shown that many $CD4^+CD62L^-CD38^+$ T cells are highly specific for mucosal antigens and can be used to monitor intestinal immune responses in peripheral blood[184]. In CD patients, CD38 expression on gluten-specific $CD4^+$ T cells increase consistently after gluten challenge[185]. The stability of CD38 as a gluten-response marker positions it as a useful tool for tracking immune activity and assessing the effectiveness of therapeutic interventions

Last, CD2 is a costimulatory receptor expressed on T and NK cells, fundamental in the formation of the immunological synapse and T cell activation[186]. It has been identified as a potential marker for mucosal immune function, particularly in LP T cells. CD2 signaling enhances IFN-γ secretion and activates STAT proteins in both peripheral blood and LPMC[187]. Evaluating these markers in GFD-treated patients allows for further elucidation of the extent of immune normalization in the intestinal mucosa and the identification of potential signatures of residual immune activity. Evaluating these markers in GFD-treated patients is essential for assessing mucosal immune recovery, identifying residual immune activity, and informing the development of more targeted therapeutic strategies in celiac disease.

5.1.3 Gut-Homing and Migration Markers

Understanding the mechanisms that regulate immune cell trafficking to the gut is critical for elucidating the pathogenesis of CD and for identifying potential targets for therapeutic intervention. Immune cell migration to the gut is a vital component of CD pathogenesis, mediated by gut-homing markers such as C-C motif chemokine receptor 9 (CCR9), C-C motif chemokine receptor 2 (CCR2), and integrins $\alpha 4$ and $\beta 7$. Circulating dendritic cells and monocytes from CD patients show increased gut-homing profiles, with gliadin peptides inducing different effects on conventional DC (cDC) phenotype and function[188].

CCR2 plays a key role in immune cell recruitment to the intestinal mucosa, where it facilitates the accumulation and localization of $CD4^+$ T lymphocytes, particularly during inflammation, making it a potential therapeutic target in gut-related immune diseases[189]. Additionally, CCR2 mediates DC migration to the intestine[101].

CCR9 is a gut homing migration marker, playing an important role in directing immune cells to the intestine and interacts with its ligand CCL25, primarily produced by gut epithelial cells[190]. Moreover, Integrin $\alpha 4\beta 7$ and its subunit $\beta 7$ are crucial markers for gut-homing lymphocyte migration. Integrin $\alpha 4\beta 7$ facilitates lymphocyte trafficking to gut-associated lymphoid tissues by interacting with Mmucosal addressin cell adhesion molecule-1 (MAdCAM-1)[191]. This integrin is selectively expressed on a subset of $CD4^+$ memory T cells with gut-trophic characteristics[192].

Assessing these markers in patients on a GFD can shed light on the persistence of inflammatory signals that may contribute to prolonged immune cell residence in the gut, potentially explaining persistent atrophy in some patients.

5.1.4 Study Objective and Research Gap

Despite significant advances in understanding the immune basis of active CD, the mechanisms driving persistent mucosal atrophy in GFD-treated patients remain elusive. This study seeks to address this knowledge gap by characterizing the duodenal immune infiltrate in GFD-adherent patients with persistent atrophy, comparing it with the profiles of active CD patients and healthy controls. The identification of immune markers that may signify ongoing subclinical immune activity aims to enhance CD management approaches and propose future strategies for monitoring disease progression in GFD-treated patients.

5.2 Material and Methods

5.2.1 Patients Demographics and Sample Processing

Samples were obtained from three distinct groups as shown in **Tab. IV.1**. Brifly, 6 NC-NI, 6 C-IM.3 and 16 C-GFD patients were recruited.

In all cases, a total of 10 duodenal biopsies per patient were obtained and immediately preserved on ice chilled RPMI.

Samples were transferred to the lab within 30 min. One biopsy was cultured and the remaining cryopreserved in Freezing Medium and stored in liquid nitrogen until processed.

5.2.2 Biopsy Culture

One biopsy per patient was cultured overnight in 0,5 ml of AIM V^{TM} in a 24 flat bottom plates at 37°C and 5% CO_2. After 18 h culture media was centrifugated at 400 g for 5 min, pellet was discarded, and the cell-free supernatant was cryopreserved at -80°C until use. Spontaneous cytokine production was measured using the LEGENDplex^{TM} Inflammation Panel 1 (13-plex) (BioLegend®, cat #740809) following the manufacturer protocol. Additionally,

Fluorochrome	Specifitity	Clone	Company	Cat. N°
PE- Dazzle 594	CCR9	L053E8	BioLegend	358918
BV785	CD103	Ber-ACT8	BioLegend	350230
eFluor 450	CD11c	3.9	ebiosience	48-0116-42
Super Bright 436	CD123	6H6	ebiosience	62-1239-42
APC-R700	CD127	HIL-7R-M21	BD	565185
Spark Blue 550	CD14	63D3	BioLegend	367148
BB515	CD141	1A4	BD	566017
BUV 496	CD16	3G8	BD	612944
PE/Cyanine7	CXCR3	G025H7	BioLegend	353720
Spark NIR 685	CD19	HIB19	BioLegend	302270
APC	CCR2	K036C2	BioLegend	357208
BV421	CCR7	G043H7	BioLegend	353208
Alexa Fluor 647	CD1c	L161	BioLegend	331510
PerCP/Cy5.5	CD2	TS1/8	BioLegend	309226
Pacific Orange	CD20	HI47	Invitrogen	MHCD2030
PE-Alexa 610	CD24	SN3	Invitrogen	MHCD2422
PE-Alexa 700	CD25	3G10	Invitrogen	MHCD2524
APC-H7	CD27	M-T271	BD	560222
BV650	CD28	CD28.2	BioLegend	302946
BV510	CD3	SK7	BioLegend	344828
APC/Fire810	CD38	HB-7	BioLegend	356643
BUV661	CD39	TU66	BD	749967
cFluorYG584	CD4	SK3	Cytek	R7-20041-100T
PerCP	CD45	2D1	BioLegend	368506
BUV395	CD45RA	5H9	BD	740315
BUV615	Integrin α4	9F10	BD	751596
BUV 737	CD56	NCAM16.2	BD	564447
BUV 805	CD8	SK1	BD	612889
PE-Cy5	Fas	DX2	BioLegend	305610
BV750	CXCR5	RF8B2	BD	747111
PE Fire 810	HLA-DR	L243	BioLegend	custom*
FITC	IgA	GOXHU	Invitrogen	AHI0108
BV480	IgD	IA6-2	BD	566138
BV605	IgG	G18-145	BD	563246
BV570	IgM	MHM-88	BioLegend	314517
BV711	Integrin β7	FIB504	Biolegend	321239
PerCP-eFluor710	TCR$\gamma\delta$	B1.1	ebiosience	46-9959-42
PE	TLR4	HTA125	BD	564404

Table V.1: Panel OMIPGut. *Lamina propria mononuclear cells antibody panel. Cat N°: Catalogue number*

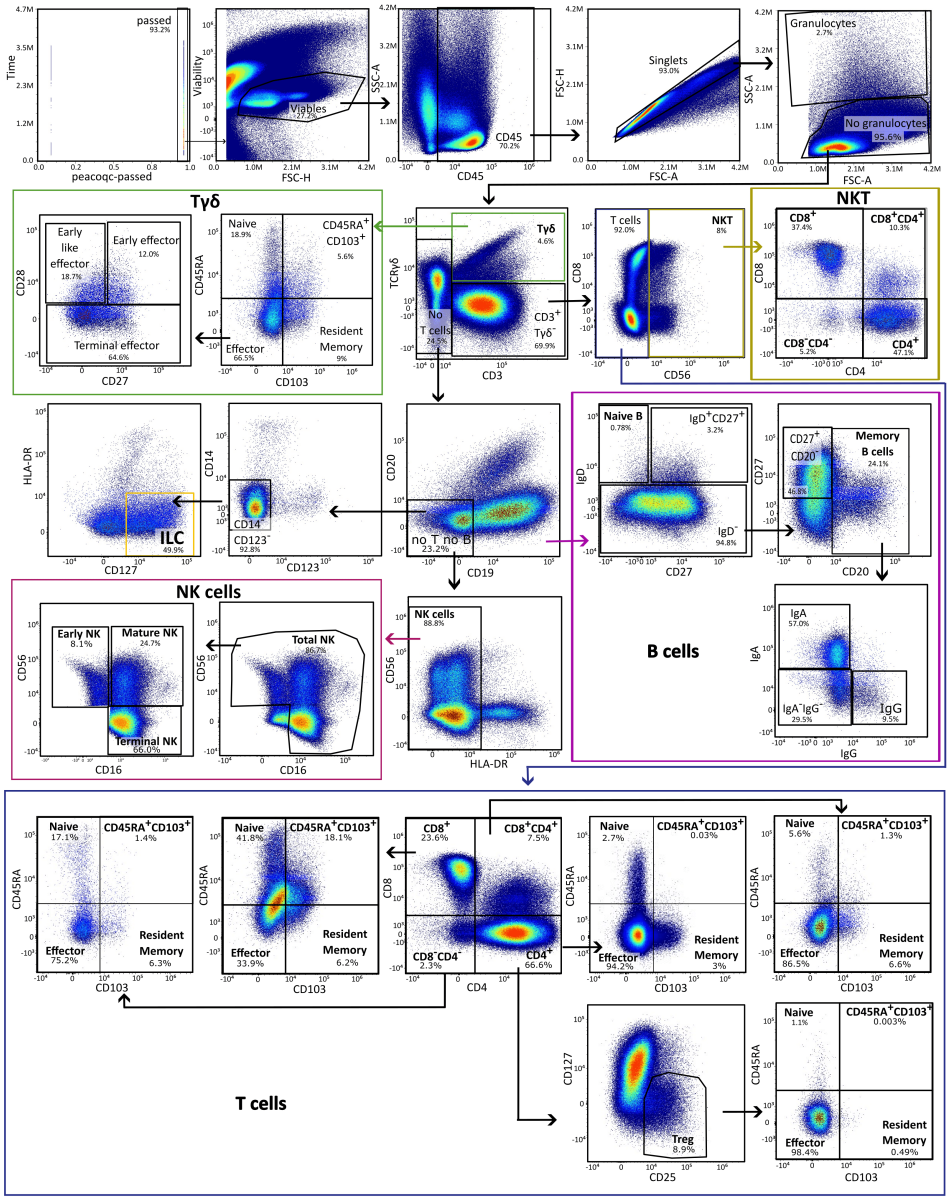

Figure V.1: Identification of the duodenal immunome in coeliac disease patients. *Total lamina propria leukocytes cells were selected, within the cells that passed the Peaco QC test, as singlet viable CD45$^+$. Granulocytes are identified based on their high scatter properties. The remaining cells were categorized into subsets based on the expression of CD3 and Tγδ: CD3$^+$Tγδ$^+$, (Tγδ$^+$), CD3$^+$Tγδ$^-$ and CD3$^-$ (No T cells). CD3$^+$Tγδ were further subdivided into T cells (CD56$^-$), NKT (CD56$^+$) and CD3$^-$ (No T cells). The latter were further divided into no T no B cells (CD19$^-$CD20$^-$) and B cells (CD20$^+$ and CD19$^+$CD20$^-$). B cells were categorized into naïve B cells (IgD$^+$CD27$^-$), IgD$^+$CD27$^+$ B cells and IgD$^-$ B cells. IgD$^-$ cells were further subdivided into CD27$^+$CD20$^-$ B cells and memory B cells (CD20$^+$). Memory B cells were classified based on IgA and IgG expression. No T and no B cells were also divided into Innate Lymphoid Cells (ILC) (CD14$^-$CD123$^-$HLA$^-$DR$^-$CD127$^+$) or total NK cells (excluding HLA-DR$^+$cells and CD56$^-$CD16$^-$cells). NK cells were further subdivided into early NK (CD56$^+$CD16$^-$), mature NK (CD56$^+$CD16$^+$) and terminal NK (CD56$^-$CD16$^+$). As for both T cells and NKT, they were further divided into CD8$^+$, CD8$^+$CD4$^+$, CD4$^+$and CD8$^-$CD4$^-$. Treg cells were within the CD4$^+$fraction as CD25$^+$CD127$^-$. Helper (CD4$^+$) and cytotoxic (CD8$^+$) T cells, as well as Tγδ were further divided into naïve (CD45RA$^+$CD103$^-$), effector (CD45RA$^-$CD103$^-$) and resident memory (CD45RA$^-$CD103$^+$) T cells.*

levels of FABP2 were determined by Enzyme-linked immunosorbent assay (ELISA) (Invitrogen, cat #EHFABP2) as a potential marker of intestinal lesion[193].

5.2.3 Cell Identification

Cells were acquired, within 48 h after staining, using panel described in **Tab. IV.1**, in a 5-laser and 67 detectors spectral cytometer (Aurora, Cytek). Data analysis was performed on the OMIQ Data Science platform (® Omiq, Inc. 2024). In all cases, the first step was to transform the fluorescence data using the scale parameters as suggested by the software. Subsequently, a cleaning algorithm (PeacoQC) was run on all samples. Then, "gates" were created to eliminate cell debris, doublets and select viable leukocytes ($CD45^+$ cells).

The gating strategy described in **Fig. V.1** allows the identification of up to 72 different duodenal subsets of granulocytes, DC, basophils, macrophages, ILC, T$\gamma\delta$ lymphocytes, NK cells, NKT cells, B cells and T cells. In addition, and within each immune subset, the expression of different markers related to potential gluten recognition (TLR4 and CXCR3) mucosal immune function (CXCR5, Fas, CD38 and CD2) and gut-homing migration (CCR2, CCR9, Integrin α4 and Integrin β7) was determined as in **Fig. V.2** using FMO method to stablish positive limits.

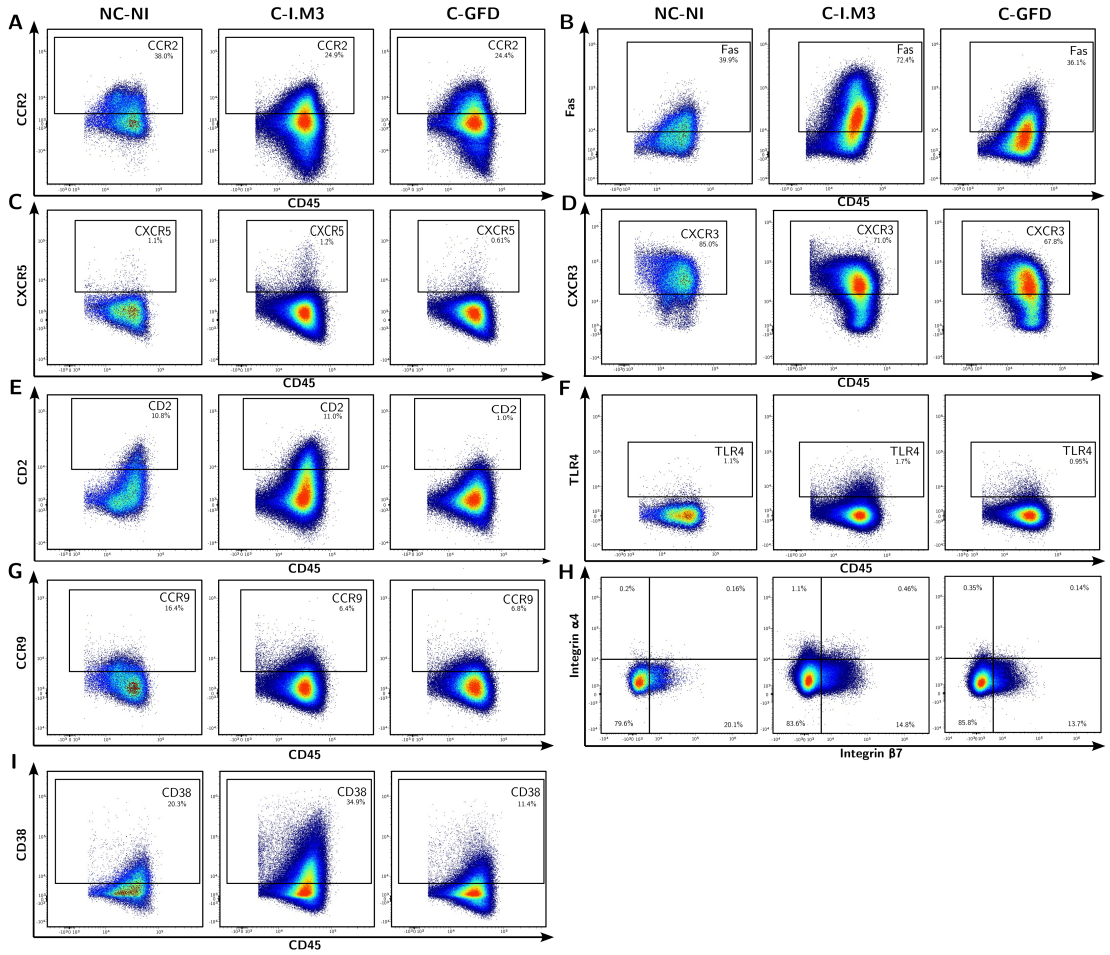

Figure V.2: Immunotyping of the duodenal infiltrate. *Total T cells were identified as in* ***Fig. V.1****, and assessed for the expression of CCR2, Fas, CXCR5, CXCR3, CD2, TLR4, CCR9, Integrin α4 and Integrin β7 and CD38 on non-coeliac not inflamed (NC-NI) controls, coeliac patients with inflammation (Marsh 3) (C-I.M3) and coeliac patients on a gluten-free diet (C-GFD). The same gating strategy to identify the percentage of positive cells for each marker, was further applied into all the different immune cell subsets described in* ***Fig. V.1****.*

5.3 Results

5.3.1 GFD-Treated CD Patients Display Persistent Villous Atrophy

GFD-treated CD patients, had positive genetics at the time of disease diagnosis, coupled with positive serology and villous atrophy (Marsh score ≥ 3). These patients had followed a GFD for a minimum of one year, with an average of 7 ± 5 years, and showed no analytical results suggesting poor clinical evolution or potential RCD.

Only one GFD-treated patient tested positive for GIP in faecal samples, indicating strong adherence to the diet within the cohort. However, despite good dietary adherence, 63.2% of these patients reported at least one symptom, and 68.4% continued to exhibit villous atrophy (Marsh score 3A), consistent with findings from previous studies[194,195]. Notably, the severity of villous atrophy in GFD-treated patients was generally lower than at the disease onset. Additionally, 73.3% showed a compatible lymphogram. Together, these findings reveal that all GFD-treated CD patients in the present cohort had at least one alteration in terms of villous atrophy, symptoms, or lymphogram compatibility (**Fig. V.3**).

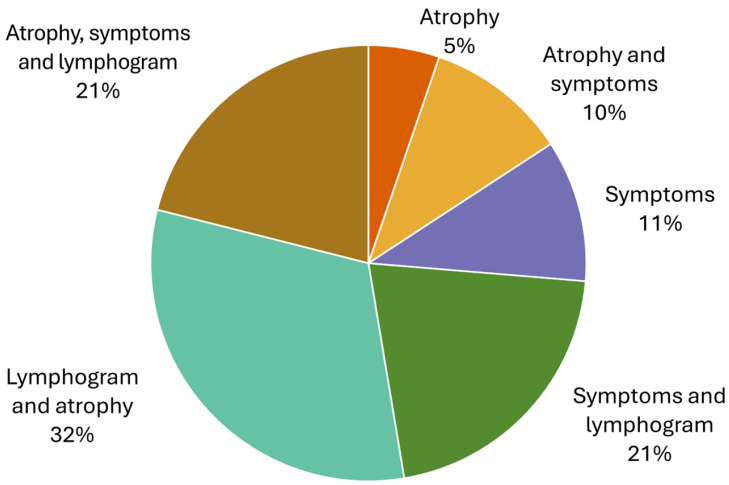

Figure V.3: Alterations on coeliac disease patients on a gluten free diet. *Distribution of atrophy, symptomatology and compatible lymphogram on coeliac disease patients following a gluten free diet.*

5.3.2 Restoration of LPL Phenotype in GFD-Treated Patients

In GFD-treated patients, the duodenal immune infiltrate was restored despite the lack of mucosal recovery. Previously, it was noted that 90% of GFD-treated patients displayed mucosal alterations, characterized by the presence of atrophy and/or a compatible lymphogram. Given the known alterations in the duodenal immunome in CD patients[168], the duodenal immune infiltrate of these patients was investigated to determine whether persistent mucosal abnormalities were linked to immune changes in the duodenum.

To assess this, a comprehensive analysis of the LP duodenal infiltrate in CD patients (both at diagnosis and after GFD treatment) and compared them with controls. Using the immune panel detailed in **Tab. V.1**, a total of 72 immune cell subsets were identified in the duodenum in the duodenum. However, for consistency and analytical rigor, the analysis focused on 47 subsets where at least 50 cells could be consistently and reliably detected across samples. **Tab. V.2** presents the mean and standard deviation of each immune cell subset's relative proportion within singlet viable $CD45^+$ LPMC population across the three study groups (controls, CD patients at diagnosis, and GFD-treated CD patients), with differentially expressed subsets highlighted in bold.

	NC-NI		C-I.M3		C-GFD		ANOVA	Tukey		
	Mean	SD	Mean	SD	Mean	SD		NC-NI vs C-I.M3	NC-NI vs C-GFD	C-I.M3 vs C-GFD
No granulocytes	96.3	3.9	95.3	2.1	97.3	1.7	0.27			
Total NK	5.6	3.9	17.3	15.3	4.1	1.8	**0.01**	**0.04**	0.91	**0.01**
Early NK	0.6	0.6	1.6	0.6	1.7	1.0	0.11			
Mature NK	0.5	0.4	4.1	4.6	1.1	0.7	**0.02**	**0.04**	0.88	**0.03**
Terminal NK	4.4	3.6	11.4	10.9	1.3	0.6	**0.00**	0.10	0.48	**0.00**
Total ILC	1.4	0.7	3.0	0.9	2.1	0.8	**0.02**	**0.02**	0.31	0.09
B cell	4.4	2.9	18.5	13.4	3.5	1.7	**<,001**	**0.00**	0.95	**<,001**
Memory B cells	2.7	2.3	4.7	2.9	2.1	1.5	0.07			
Memory B cells IgA	0.6	0.5	2.3	2.1	0.7	0.7	**0.03**	0.05	0.95	**0.03**
Memory B cells IgG	0.2	0.1	0.9	0.9	0.3	0.2	**0.03**	0.07	0.98	**0.04**
NKT cells	7.0	2.1	5.3	2.6	6.7	2.4	0.46			
NKT CD8	2.0	0.6	2.1	1.6	2.8	1.2	0.34			
NKT $CD8^+CD4^+$	1.2	0.8	0.5	0.3	0.7	0.5	0.12			
NKT CD4	3.5	1.3	2.4	1.2	2.7	1.4	0.42			
NKT $CD8^-CD4^-$	0.3	0.2	0.3	0.3	0.6	0.6	0.45			
T cells	78.3	6.7	59.3	12.2	76.8	5.1	**<,001**	**0.00**	0.91	**<,001**
CD8 T cells	13.5	4.5	14.3	5.6	17.7	7.8	0.42			
CD8 Naive T cells	5.1	2.5	6.5	3.8	8.0	3.7	0.29			
CD8 $CD45RA^+CD103^+$ T cells	3.9	3.3	1.6	1.5	2.3	2.0	0.25			
CD8 Effector T cells	3.6	2.9	5.8	3.5	6.5	4.9	0.43			
CD8 Early like effector T cells	0.8	0.6	1.3	0.6	2.0	2.2	0.41			
CD8 Terminal effector T cells	2.2	1.9	3.5	2.8	3.5	2.2	0.52			
CD8 RM T cells	0.9	0.9	0.5	0.5	0.9	1.6	0.84			
$CD8^+CD4^+$ T cells	12.5	6.3	3.9	1.6	7.6	4.1	**0.02**	**0.01**	0.09	0.25
$CD8^+CD4^+$Effector T cells	10.0	5.1	3.6	1.5	6.8	4.5	0.08			
$CD8^+CD4^+$Early like effector T cells	7.9	3.7	2.6	1.2	5.2	3.6	0.06			
$CD8^+CD4^+$Early effector T cells	0.6	0.5	0.5	0.1	0.6	0.5	0.76			
$CD8^+CD4^+$Terminal effector T cells	0.9	0.9	0.3	0.2	0.6	0.4	0.17			
CD4 T cells	50.9	10.4	39.6	8.1	49.3	6.5	**0.05**	0.08	0.92	0.06
CD4 Effector T cells	47.0	11.7	38.5	7.8	44.3	12.2	0.48			
CD4 Early like effector T cells	37.5	10.2	26.6	7.8	34.1	10.5	0.22			
CD4 Early effector T cells	4.0	1.0	7.5	1.8	5.7	3.2	0.14			
CD4 Terminal effector T cells	2.9	1.3	2.2	1.4	2.3	1.4	0.66			
CD4 RM T cells	3.5	3.9	0.8	0.9	1.1	1.5	0.09			
CD4 Early like RM T cells	2.8	3.3	0.6	0.7	0.8	1.0	0.07			
T_{reg}	0.5	0.4	4.3	1.6	1.5	0.9	**<,001**	**<,001**	0.20	**<,001**
T_{reg} Effector	0.5	0.4	4.3	1.6	1.4	1.0	**<,001**	**<,001**	0.25	**<,001**
T_{reg} Early like effector	0.4	0.2	2.4	1.1	1.1	0.7	**0.00**	**0.00**	0.17	**0.01**
$CD8^-CD4^-$ T cells	1.4	0.7	1.3	0.4	2.1	1.5	0.34			
$CD8^-$ $CD4^-$ Effector T cells	1.2	0.7	1.0	0.4	1.8	1.5	0.41			
$CD8^-$ $CD4^-$ Early like effector T cells	0.6	0.4	0.4	0.3	0.7	0.8	0.68			
$CD8^-$ $CD4^-$ Terminal effector T cells	0.3	0.2	0.4	0.2	0.7	0.6	0.20			
T$\gamma\delta$	2.0	1.0	5.4	2.1	4.2	1.4	**0.01**	**0.01**	**0.02**	0.33
T$\gamma\delta$ Naive	0.3	0.2	0.9	0.3	1.1	0.9	0.19			
T$\gamma\delta$ Effector	1.3	0.9	4.0	2.3	2.6	1.3	**0.03**	**0.02**	0.24	0.19
T$\gamma\delta$ Early like effector	0.8	0.5	0.8	0.6	0.6	0.3	0.61			
T$\gamma\delta$ Terminal effector	0.2	0.2	2.6	1.7	1.7	1.1	**0.01**	**0.01**	**0.05**	0.32
Granulocytes	3.0	3.6	3.0	1.4	1.8	1.2	0.39			

Table V.2: Lamina propria lymphocytes (LPL) variability among groups. *Lamina Propria Lymphocytes populations on non coeliac non inflamed (NC-NI) controls, coeliac patients with active inflammation with Marsh 3 (C-I.M3) and coeliac patients on a gluten-free diet (C-GFD). Mean and Standard Deviation (SD) of the percentage of lymphocytes within the viable, $CD45^+$ singlet cell population. One-way ANOVA was used to compare the groups (p-values shown). Post-hoc Tukeys multiple comparisons tests were performed where the difference was statistically significant ($p < 0.05$). ILC: Innate lymphoid cells; RM: Resident memory; T_{reg}: Regulatory T cells.*

The findings showed that, at diagnosis, CD patients had a specific expansion of NK cells, ILC, B cells, T_{reg} and T$\gamma\delta$ cells, alongside a reduction of total T cells, $CD4^+$ T cells, and $CD4^+CD8^+$ T cells. Importantly, these immune alterations largely reverted in GFD-treated patients, with the exception of persistently elevated T$\gamma\delta$ cells found in the mucosa from CD patients (consistent with their clinical utility as a biomarker[49,196]). This restoration of the immune cell composition occurred despite ongoing mucosal inflammation and/or the presence of a compatible lymphogram.

5.3.3 Restoration of Immune Markers in the Duodenum Infiltrate on GFD-Treated Patients

While the infiltrate normalizes in composition, as previously observed, its phenotype remains unknown, which underscores the importance of studying it. Active CD patients displayed an altered immune infiltrate compared to non-inflamed controls, a profile that normalized upon GFD treatment despite ongoing mucosal abnormalities. To determine whether this immune infiltrate could contribute to the lack of mucosal healing, its functional role was investigated.

Hence, the phenotype was determined in each immune subset as shown in **Fig. V.1**. On the 47 different immune subsets in which, at least, 50 cells could be consistently identified, markers related with potential gluten recognition (TLR4 and CXCR3), mucosal immune function (CXCR5, Fas, CD38 and CD2) and gut-homing migration and/or retention (CCR2, CCR9, Integrin $\alpha4$ and Integrin $\beta7$) were analysed. Given the large datasets, only results showing significant differences between groups are summarized in **Fig. V.4** and **Fig. V.5** .

Given the gut-homing capacity mediated by MAdCAM-1 through the $\alpha4\beta7$ integrin and considering that $\beta7$ can also be dimerized with CD103, the expression patterns of this integrin was analysed in the three the possible combinations $\alpha4^+$, $\beta7^+$ and $\alpha4^+\beta7^+$. The results revealed that active CD patients had an increased expression of both $\alpha4^+\beta7^-$ and $\alpha4^+\beta7^+$ (**Fig. V.4 A** and **B**) on different T cells subsets, along with a decreased expression of $\alpha4^-\beta7^+$ on early and early-like effector T cells (**Fig. V.4 C**).

Additionally, CD at diagnosis exhibited a reduced expression of CCR2 (**Fig. V.4 D**) and CCR9 (**Fig. V.4 E**). Expression of TLR4 and CXCR3, both associated with gluten, was also lower across several immune cells and were not just restricted to T cells (**Fig. V.4 F** and **G**). On the contrary, markers associated with T cell activation and inflammatory function -CD2, Fas and CD38- were increased on several T cell subsets from the inflamed mucosa of CD patients at diagnosis (**Fig. V.5**).

All these differences in the phenotype and function of the duodenal infiltrated from CD patients at diagnosis were nevertheless normalized on the GFD-treated patients despite the presence of persistent mucosal alterations.

5.3.4 Time on a GFD Correlates with an Increased Expression of Gut Homing Markers on Effector T Cells

Although 90% of GFD-treated patients displayed duodenal abnormalities (atrophy and/or a compatible lymphogram), their LP duodenal immunome, unlike that of newly diagnosed patients, showed no significant alterations in composition (**Tab. V.2**) or function (**Fig. V.4**) compared to non-inflamed controls. To understand the basis of this paradoxical inflammation, immune profiles in GFD-treated CD patients with persistent villous atrophy were compared to those with mucosal recovery.

Table V.3 highlights immune differences between these two groups. Notably, patients with mucosal recovery had higher levels of gut-homing markers and CD38 on certain duodenal T cells, NK cells, and NKT cells, alongside a lower expression of TLR4 in various immune populations. However, these differences were less pronounced than those observed in newly diagnosed CD patients with mucosal atrophy (**Fig. V.4**).

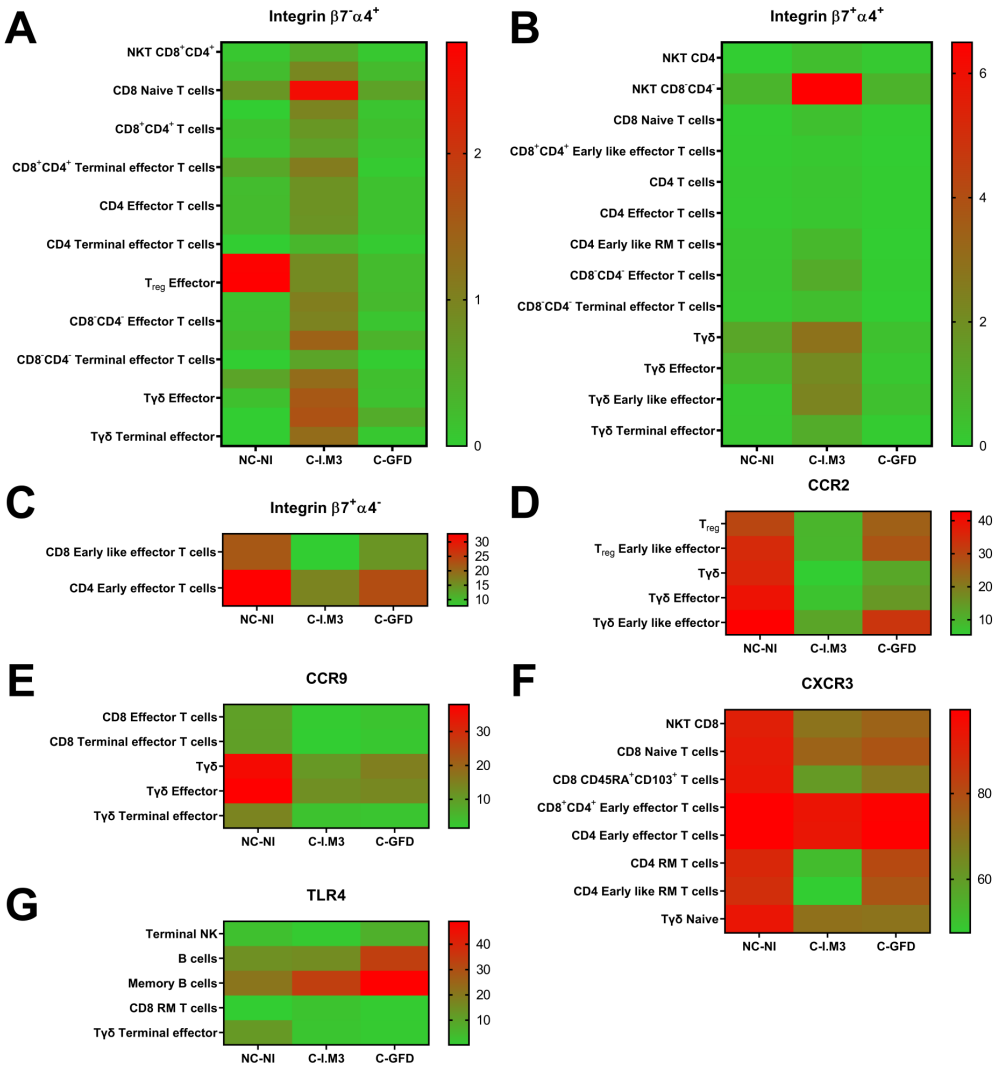

Figure V.4: Restoration of migratory and gluten related markers on coeliac disease patient on a gluten free diet. *Differences among the different duodenal immune subsets from non-coeliac not inflamed (NC-NI) controls, coeliac patients with inflammation (Marsh 3) (C-I.M3) and coeliac patients on a gluten-free diet (C-GFD) are shown for the expression of (**A**) Integrin $\beta7^-$ Integrin $\alpha4^+$ (**B**) Integrin $\beta7^+$ Integrin $\alpha4^+$ (**C**) Integrin $\beta7^+$ $\alpha4^-$, (**D**) CCR2, (**E**) CCR9, (**F**) CXCR3, (**G**) TLR4. Colours represent the median percentage of cells expressing the corresponding marker. For statistical analysis ShapiroWilk normality test followed by unpaired one-way ANOVA with uncorrected Fisher's LSD test and post-hoc Tukey's multiple comparisons test were used. Only those markers differentially expressed ($p < 0.05$) on the different immune subsets are included in the heatmap. RM: Resident memory; T_{reg}: Regulatory T cells.*

Finally, given that the GFD is the current treatment for CD patients, , the influence of time on a GFD on the duodenal immune profile was explored. Unlike the binary presence or absence of mucosal inflammation, GFD duration significantly affects duodenal infiltrate composition (**Tab. V.4**). Specifically, a positive correlation was observed between the time of GFD (in months) and levels of various T cell subsets, as well as a negative correlation with T_{reg} levels in the mucosa (**Tab. V.4**). Time on GFD was also positively correlated to increasing levels of gut-homing migration markers (Integrins $\alpha4$ and $\beta7$, CCR9, and CCR2), potentially explaining the higher mucosal T cell counts. Additionally, longer GFD adherence correlated with increased expression of gluten recognition markers (TLR4 and CXCR3) and inflammatory markers (CD2

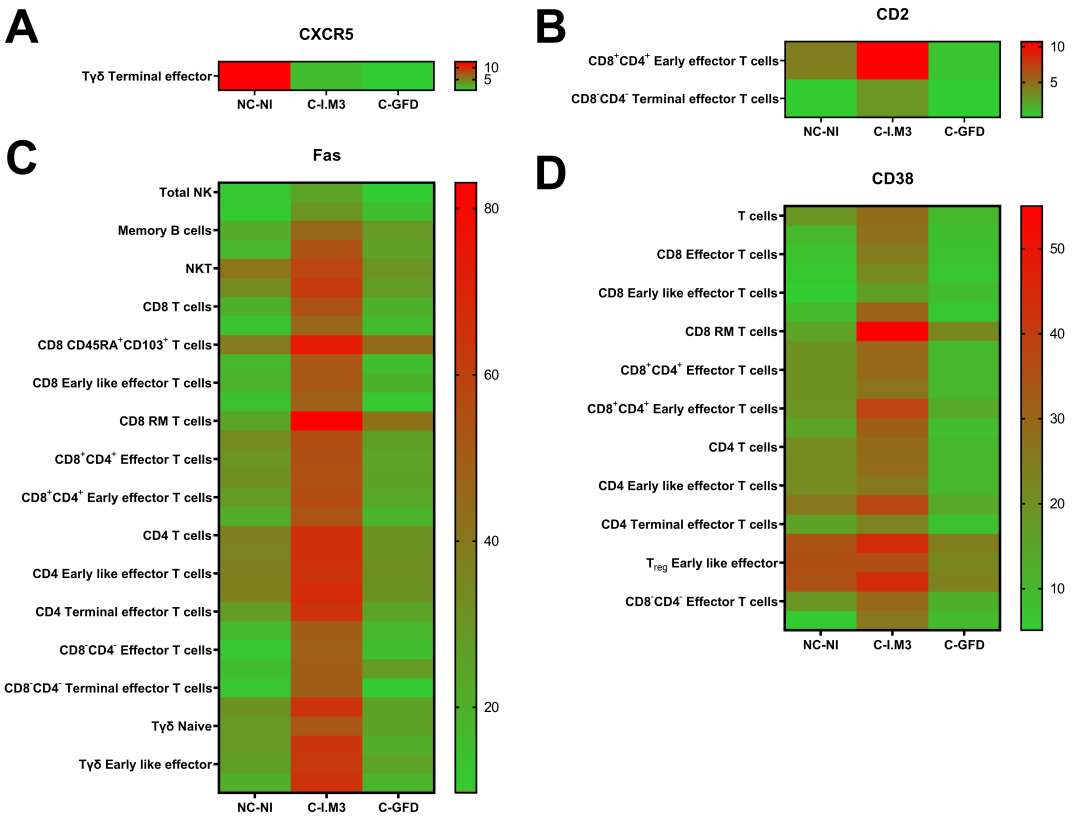

Figure V.5: Restoration of inflammatory markers on coeliac disease patient on a gluten free diet. *Differences among the different duodenal immune subsets from non-coeliac not inflamed (NC-NI) controls, coeliac patients with inflammation (Marsh 3) (C-I.M3) and coeliac patients on a gluten-free diet (C-GFD) are shown for the expression of (**A**) CXCR5 (**B**) CD2 (**C**) Fas (**D**) CD38. Colours represent the median percentage of cells expressing the corresponding marker. For statistical analysis ShapiroWilk normality test followed by unpaired one-way ANOVA with uncorrected Fisher's LSD test and post-hoc Tukey's multiple comparisons test were used. Only those markers differentially expressed ($p < 0.05$) on the different immune subsets are included in the heatmap.*

		No atrophy		Atrophy		T student
		Mean	SD	Mean	SD	
Integrin $\alpha4^+$ Integrin $\beta7^-$	CD4 T cells	0.3	0.2	0.1	0.1	0.049
	CD4 Effector T cells	0.3	0.2	0.1	0.1	0.046
	CD4 Early effector T cells	0.6	0.5	0.1	0.1	0.009
	$CD8^-$ $CD4^-$ T cells	0.7	0.8	0.1	0.2	0.043
	CD8-CD4- Early like effector	0.9	1.1	0.1	0.2	0.033
$\alpha4^+\beta7^+$	CD4 Early like effector T cells	0.03	0.02	0.01	0.01	0.026
$\beta7^+\alpha4^-$	NKT CD8	36.8	15.5	17.9	6.7	0.006
	NKT $CD8^+CD4^+$	29.3	11.7	16.8	8.5	0.044
	CD8 T cells	32.9	8.7	19.1	8.4	0.018
	T_{reg} Early like effector	3.7	4.4	10.0	4.6	0.039
CCR9	Total NK	22.9	11.8	10.8	8.0	0.044
	Mature NK	26.7	13.2	13.4	8.7	0.045
	Terminal NK	41.5	18.4	19.3	13.9	0.029
	CD8 T cells	6.2	6.4	2.0	0.6	0.049
	CD8 Effector T cells	6.2	6.3	1.8	1.1	0.041
	CD8 Early like effector T cells	6.4	6.6	1.7	1.7	0.049
	T$\gamma\delta$ Early like effector	37.7	9.1	16.1	9.8	0.003
TLR4	Total NK	6.4	3.9	2.9	1.9	0.039
	Mature NK	8.1	4.4	2.4	2.5	0.009
	Total ILC	2.8	2.6	0.6	0.5	0.019
	Memory B cells IgA	31.0	23.2	62.2	17.3	0.017
CD38	Mature NK	78.6	16.3	52.3	19.3	0.034

Table V.3: Atrophy effect on lamina propria lymphocytes populations of coeliac patients on a gluten-free diet. *Mean and Standard Deviation (SD) are shown only in the cases were the T student were significant ($p < 0,05$). ILC: Innate lymphoid cells; T_{reg}: Regulatory T cells.*

and CD38) on mucosal T cells.

5.3.5 Differences in Immune Profiles based on Symptom presence in GFD-Treated Patients

In GFD-treated patients who report symptoms, several immune markers showed differential expression compared to asymptomatic patients (**Tab. V.5**). Symptomatic patients displayed elevated Integrin $\beta7^-\alpha4^+$ levels on CD8 T cells and increased CCR2 expression on memory B cells, suggesting enhanced gut-homing potential in these cell types. Additionally, CD2 expression was elevated in naïve CD8 T cells among symptomatic individuals. Conversely, certain markers were decreased in symptomatic patients: CCR9 expression was lower on NK cells and B cells, and CXCR3 was reduced on NKT cells as well as $CD8^+CD4^+$T cells. Similarly, CD2 expression was diminished on CD4 early effector T cells, naïve T$\gamma\delta$ cells, and terminal effector T cells. Notably, symptomatic patients also exhibited lower CD38 levels on T_{reg} and effector T_{reg}, potentially reflecting an altered regulatory function in these cells.

5.3.6 Normalization of Inflammatory Soulble Immune Mediators on GFD-Treated Patients

Following the analysis in the cell-free culture secretomes of 13 cytokines and FABP2, it was revealed that only IL-18 and IL-12p70 were increased in CD patients at the diagnosis, being their levels normalized in the GFD-treated patients (**Fig. V.6**). Again, there was no major impact by the presence of atrophy (**Fig. V.7**), symptoms (**Fig. V.8**) and time on GFD (**Fig. V.9**) on these biomarkers. Only FABP2 levels correlate with the time on GFD (**Fig. V.9**).

		Months GFD				Months GFD	
		Correlation	p value			Correlation	p value
% Cells	NKT $CD8^-CD4^-$	0.56	0.037	TLR4	Total NK	0.65	0.011
	CD8 Naive T cells	-0.76	0.002		Terminal NK	0.77	0.001
	$CD8^+CD4^+$ Early effector T cells	0.59	0.026		Total ILC	0.55	0.043
	CD4 Early effector T cells	0.8	<,001		Memory B cells IgG	-0.56	0.049
	T_{reg}	-0.55	0.041		$CD8^-CD4^-$ T cells	0.54	0.048
	T_{reg} Early like effector	-0.54	0.046		CD4 Terminal effector T cells	0.57	0.033
CCR2	NKT CD8	0.65	0.011		$CD8^+CD4^+$ T cells	0.61	0.021
	NKT $CD8^+CD4^+$	0.57	0.032		$CD8^+CD4^+$ Effector T cells	0.83	<,001
	CD4 Effector T cells	0.54	0.044		$CD8^+CD4^+$ Early like effector T cells	0.61	0.021
	CD4 Early like effector T cells	0.53	0.049	CXCR3	CD8 T cells	0.59	0.025
	CD4 Early effector T cells	0.63	0.015		CD8 Effector T cells	0.55	0.04
	Tγδ	0.7	0.005		CD8 Resident Memory T cells	0.77	0.027
	Tγδ Effector	0.66	0.01		CD4 Resident Memory T cells	0.58	0.048
	Tγδ Early like effector	0.65	0.013		$CD8^-CD4^-$ T cells	0.67	0.009
CCR9	Terminal NK	0.66	0.01		$CD8^-CD4^-$ Effector T cells	0.62	0.018
	NKT	0.78	<,001		$CD8^-CD4^-$ Early like effector T cells	0.53	0.05
	NKT CD4	0.62	0.018		$CD8^-CD4^-$ Terminal effector T cells	0.65	0.013
	T cells	0.68	0.007		Tγδ Terminal effector	0.59	0.032
	CD8 T cells	0.6	0.023	CD2	$CD8^+CD4^+$ Terminal effector T cells	-0.58	0.031
	CD8 Naive T cells	0.6	0.022		$CD8^-CD4^-$ T cells	0.6	0.025
	CD8 Effector T cells	0.59	0.026		$CD8^-CD4^-$ Effector T cells	0.59	0.026
	CD8 Terminal effector T cells	0.71	0.004		$CD8^-CD4^-$ Early like effector T cells	0.61	0.022
	CD8 Resident Memory T cells	0.73	0.04		Tγδ	-0.56	0.037
	$CD8^+CD4^+$ Effector T cells	0.57	0.032	CD38	Memory B cells IgA	-0.63	0.015
	$CD8^+CD4^+$ Early like effector T cells	0.56	0.037	CXCR5	CD8 T cells	0.54	0.049
	CD4 T cells	0.59	0.025		CD4 Terminal effector T cells	0.67	0.009
	CD4 Effector T cells	0.64	0.013		$CD8^-CD4^-$ T cells	0.71	0.004
	CD4 Early like effector T cells	0.55	0.041		$CD8^-CD4^-$ Effector T cells	0.83	<,001
	CD4 Early effector T cells	0.75	0.002		$CD8^-CD4^-$ Early like effector T cells	0.67	0.008
	CD4 Terminal effector T cells	0.65	0.012	$\beta7^+$ $\alpha4^-$	CD8 Effector T cells	0.57	0.033
	$CD8^-CD4^-$ T cells	0.78	0.001		CD8 Early like effector T cells	0.57	0.035
	$CD8^-CD4^-$ Effector T cells	0.84	<,001		CD4 T cells	0.55	0.04
	$CD8^-CD4^-$ Early like effector T cells	0.63	0.016		CD4 Effector T cells	0.62	0.017
	Tγδ	0.56	0.039		$CD8^-CD4^-$ EffectorT cells	0.73	0.003
	Tγδ Effector	0.66	0.01		$CD8^-CD4^-$ Early like effector T cells	0.68	0.007

Table V.4: Correlation of months on a gluten free diet on coeliac disease patients and percentage of different lamina propria lymphocytes subsets for the percentage of cells. *Integrin $\beta7^+\alpha4^-$, CCR2, CCR9, TLR4, CXCR3, CD2, CD38 and CXCR5 expression. Correlation and p values are shown only for the cases were the Pearson correlation test were significant ($p < 0.05$). ILC: Innate lymphoid cells; T_{reg}: Regulatory T cells.*

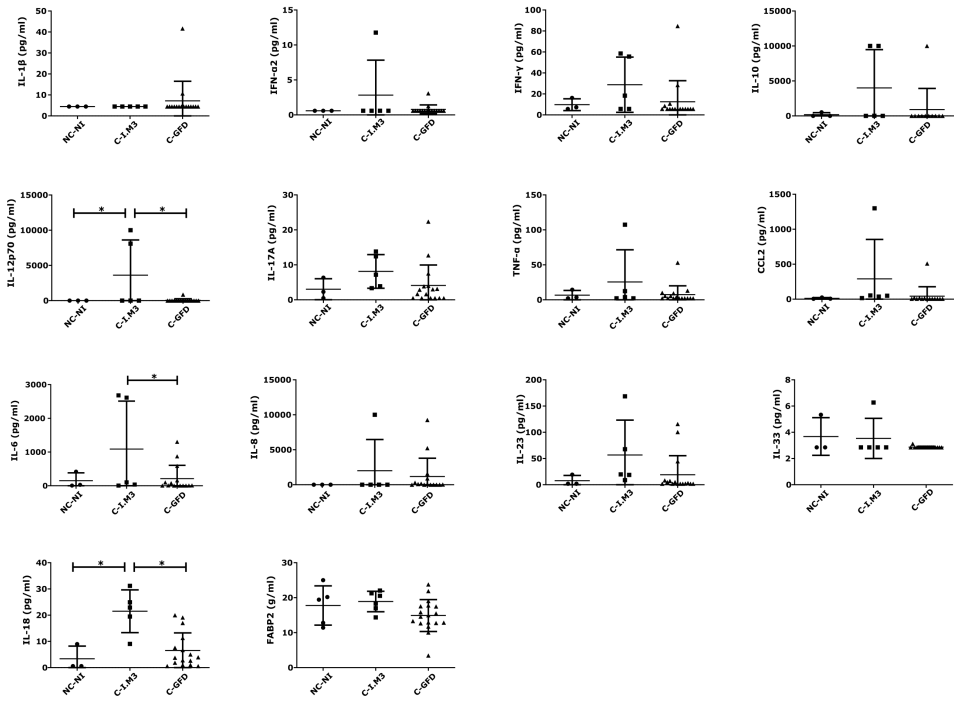

Figure V.6: Cytokines on biopsy supernatants of coeliac disease patients. *Expression of IL-1β, IFN-α2, IFN-γ, IL-10, IL-12p70, IL-17A, TNF-α, CCL2, IL-6, IL-8, IL-23, IL-33, IL-18 and FABP2. Data shown as pg/ml except for FABP2 which is in ng/ml. One-way ANOVA with uncorrected Fishers LSD test was applied in all cases. P-values < 0.05 were considered significant (*$p < 0.05$).C-GFD: coeliac on a gluten free diet; C-I.M3: coeliac Inflamed (Marsh 3);NC-NI: Non-Coeliac Not inflamed.*

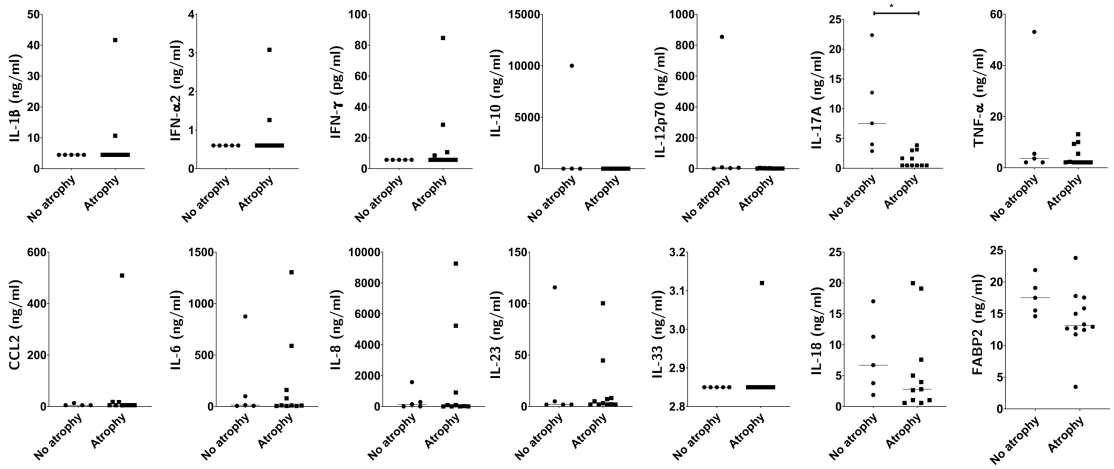

Figure V.7: Atrophy effects in biopsy supernatants of coeliac disease patients on a gluten free diet. *Expression of IL-1β, IFN-α2, IFN-γ, IL-10, IL-12p70, IL-17A, TNF-α, CCL2, IL-6, IL-8, IL-23, IL-33, IL-18 and FABP2. Patients have been grouped based on the presence of gut atrophy. Data shown as pg/ml except for FABP2 which is in ng/ml. Unpaired non parametric t test was performed in all cases. P-values < 0.05 were considered significant (*$p < 0.05$).*

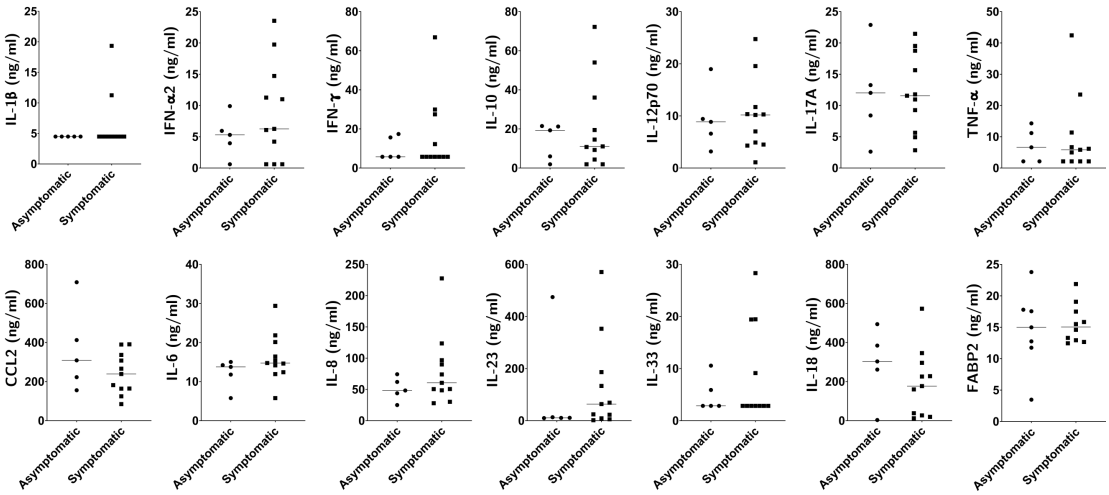

Figure V.8: Effect of symptoms on cytokines on biopsy supernatants of coeliac disease patients on a gluten free diet. *Expression of IL-1β, IFN-α2, IFN-γ, IL-10, IL-12p70, IL-17A, TNF-α, CCL2, IL-6, IL-8, IL-23, IL-33, IL-18 and FABP2 grouping patients based on the presence of symptoms. Data shown as pg/ml except for FAB2 which is in ng/ml. Unpaired non parametric t test was performed in all cases. P-values < 0.05 were considered significant.*

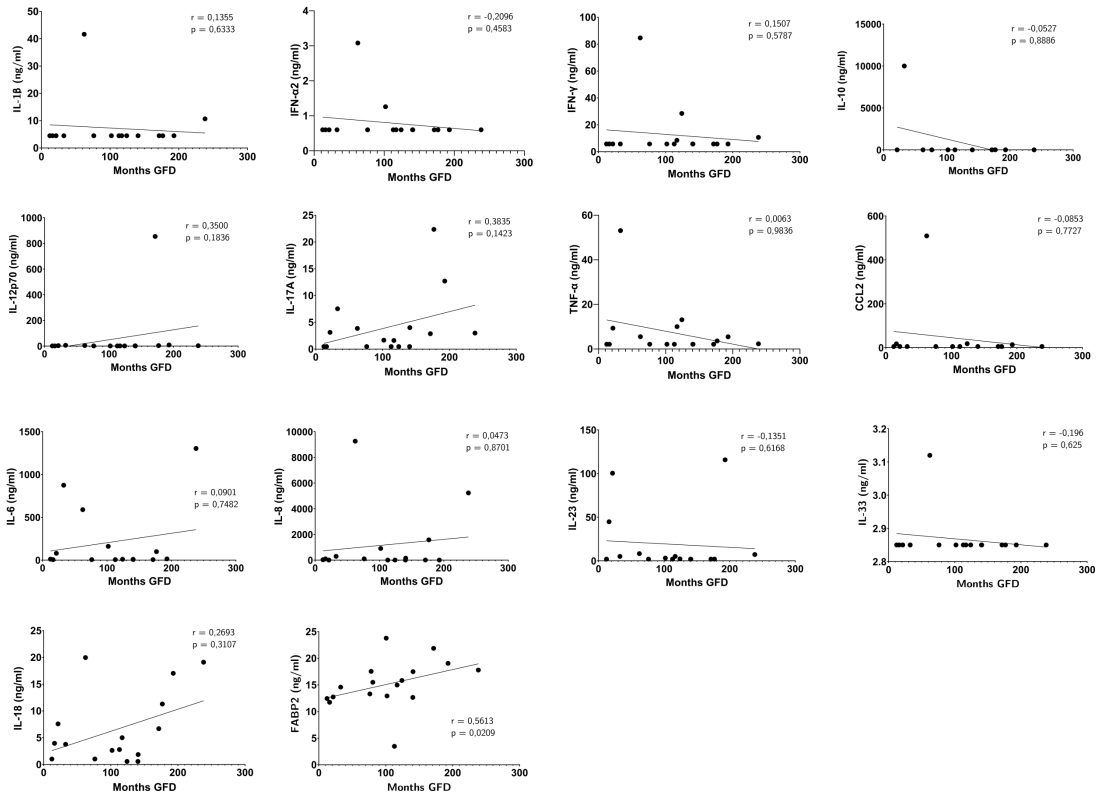

Figure V.9: Effect of time on gluten free diet in biopsy supernatants of coeliac disease patients. *Expression of IL-1β, IFN-α2, IFN-γ, IL-10, IL-12p70, IL-17A, TNF-α, CCL2, IL-6, IL-8, IL-23, IL-33, IL-18 and FABP2. Data shown as pg/ml except for FAB2 which is in ng/ml. Spearman test was performed in all cases. P-values < 0.05 were considered significant.*

		Asymptomatic		Symptomatic		T student
		Mean	SD	Mean	SD	
$\beta7^-\alpha4^+$	CD8 T cells	0.2	0.3	0.5	0.2	0.020
	CD8 CD45RA$^+$CD103$^+$ T cells	0.4	0.5	1.9	1.2	0.011
CCR2	Memory B cells	4.0	3.9	19.5	11.4	0.004
	Memory B cells IgA	4.8	5.1	21.3	10.5	0.002
	CD8$^-$CD4$^-$ Early like effector T cells	35.8	17.5	15.2	9.1	0.023
CCR9	Total NK	19.2	10.4	7.7	6.2	0.035
	Mature NK	22.4	12.1	10.1	5.8	0.042
	B cells	33.5	21.0	13.9	5.9	0.047
CXCR3	NKT CD8$^+$CD4$^+$	76.5	16.8	56.4	15.4	0.041
CD2	CD8 Naive T cells	1.6	0.1	2.0	0.3	0.034
	CD4 Early effector T cells	1.0	0.3	0.7	0.3	0.031
	T$\gamma\delta$ Naive	26.2	43.4	12.4	17.2	0.097
	T$\gamma\delta$ Terminal effector	27.8	51.5	20.0	16.8	0.048
CD38	Effector T_{reg}	29.6	11.2	19.3	5.8	0.044
	T_{reg}	30.0	11.7	19.3	5.8	0.043

Table V.5: Effect of symptoms on lamina propria lymphocites from coeliac patients on a gluten-free diet. *Mean and Standard Deviation (SD) are shown only in the cases were the T student were significant ($p < 0,05$).T_{reg}: Regulatory T cells.*

5.4 Discussion

Most C-GFD patients still show mucosal atrophy despite the presence of a negative serology, in agreement with previous observations[194,195]. Of note, in this chapter it has been proved that despite sucn persistent mucosal atrophy, LP immune infiltrate gets normalized following the GFD.

The duodenal immunome of CD patients at the disease onset displays major alterations in its composition and function, as an expansion of NK cells, ILC and T$\gamma\delta$ cells[197,166,168]. This is coupled with a reduction in total T cells, CD4$^+$ T cells, T_{reg} and CD4$^+$CD8$^+$ T cells. Interestingly, these alterations were reversed following a GFD, however this was not mirrored by a recovery of the mucosal architecture. Besides, time on GFD, but not the persistence of mucosal atrophy, correlated with an increased expression of gut-homing migration markers on mucosal effector T cells suggesting an influx of T cells towards the mucosa. The findings suggest that while the GFD effectively restores aspects of the immune composition and function, specific immune abnormalities remain in C-GFD patients, especially in those with symptoms. This indicates that the persistent immune dysregulation, particularly in gut-homing and inflammatory markers, may contribute to the ongoing symptoms.

This study underscores that monitoring CD should not solely rely on tracking circulating levels of IgA TG2 antibodies, as mucosal healing was absent in most patients despite adherence to a GFD. Although antibody levels can assist in CD diagnosis under specific conditions without endoscopy[198], these results confirm that antibody negativity is an inadequate indicator of mucosal healing since all C-GFD patients on the study had negative serology[199]. This limitation points to a critical need for novel biomarkers capable of accurately assessing mucosal healing without requiring invasive gastroscopy, especially given the long-term health risks associated with persistent villous atrophy[200].

In pediatric patients, following the diagnosis of CD and the instauration of a GFD, clinical parameters are not normalized until more than 3 years after starting the diet[201]. For adult CD patients, who likely have experienced prolonged mucosal damage prior to the diagnosis and starting the GFD, achieving complete mucosal healing may require an even more extended period of recovery. Although more than 68% of adult patients in this study continued to show mucosal atrophy, the Marsh severity score was consistently lower compared to baseline

at diagnosis, suggesting a gradual but incomplete trend towards mucosal recovery.

Interestingly, time on GFD, rather than the presence of mucosal atrophy alone, influenced the composition and function of the duodenal immune environment in these patients. This collective evidence indicates that, unlike pediatric patients, adult CD patients may need significantly more time on a GFD to achieve full mucosal recovery and clinical remission.

Although a strict GFD effectively normalized inflammatory markers and immune cell populations in the LP, many patients continued to exhibit mucosal lesions. Notably, longer adherence to the GFD was associated with an increase in gut-homing markers for effector memory T cells and a decrease in regulatory T cells, suggesting that restoring immune balance in the gut may take longer than anticipated, even if structural damage persists. The continued presence of immune markers linked to gut-homing and inflammation in symptomatic, C-GFD patients underscores the need for additional therapeutic approaches beyond the GFD to address residual immune dysregulation and to improve patient outcomes.

In conclusion, this study reveals the composition of the LP immune infiltrate in CD patients, showing that while a GFD can normalize aspects of the immune environment, it does not fully restore mucosal structure. The length of time on a GFD influences the duodenal immune profile, with longer adherence linked to increased T cell recruitment, activation, and inflammatory markers, regardless of mucosal healing status. These results indicate that immune changes continue to accumulate with the ongoing GFD adherence. However, the immunological factors driving persistent villous atrophy in patients strictly following a GFD remain poorly understood, highlighting the need for further research on immune-targeted therapies to achieve complete mucosal recovery in CD.

6

Peripheral Blood Mononuclear Cells

6.1 Introduction

The studies on the effects of a GFD reveals complex immunological consequences. In healthy individuals, adherence to a GFD reduces beneficial gut bacteria while harmful strains are increased, along with a decreasing immune stimulation of PBMC[202,203]. Furthermore, gene expression studies reveal that even after prolonged GFD adherence, CD patients exhibit aberrant PBMC gene expression associated with immunity, inflammation, metabolism, and cell proliferation[204]. Recent advances in single-cell RNA sequencing facilitate a deeper understanding of PBMC involvement in CD pathogenesis. For instance, the analysis of PBMC profiles before and after CD development in children has made it possible to identify potential early biomarkers for CD[205]. These findings highlight the need for further research into the long-term immunological effects of a GFD on both CD and NC individuals.

6.1.1 High Dimensional Cytometry Challenges

Flow cytometry is a widely used technology for the analysis of immune cell populations at the single-cell level[206,207]. However, traditional gating strategies pose challenges in the identification of novel cellular subsets, especially in high-dimensional datasets[208].

In this chapter, both supervised gating and unsupervised analyses will be applied to PBMC. To facilitate the interpretation of high-dimensional datasets, techniques of dimensional reduction and clustering algorithms are commonly used[209]. The uniform manifold approximation and projection (UMAP)[210] outperforms other methods of dimensionality reduction in speed and accuracy for imaging flow cytometry data[211]. Moreover, UMAP is particularly effective in detecting rare cell populations when combined with supervised classification techniques[212].

Similarly, the clustering algorithm FlowSOM, which utilizes self-organizing maps, provides an overview of marker behavior across all cells and helps to detect subsets that might be missed by traditional analysis methods[213]. However, clustering is susceptible to batch and experimental viability. To minimize the batch-associated effect, a balanced design was carried out and experimental groups were distributed across batches as recommended by other groups[214].

6.1.2 Study Objective and Research Gap

Despite significant advances in understanding the immune mechanisms underlying CD, the persistence of immune abnormalities in GFD-treated patients remains incompletely defined. This study aims to address this gap by investigating PBMC immune profiles and plasma cytokine levels in C-GFD patients, comparing them with those from active CD patients and NC controls. By identifying peripheral immune markers associated with ongoing immune activation, this research seeks to enhance current CD monitoring strategies and to provide insights into potential interventions for long-term disease management.

6.2 Material and Methods

6.2.1 Patients Demographics and Sample Processing

The same samples used in the previous LPL chapter were employed, as described in **Tab. IV.1**. Briefly, 6 NC-NI, 6 CD patients at the disease onset with mucosal enteropathy (Marsh score 3 or above) and 16 C-GFD.

Three 5 ml lithium-heparin tubes of blood were collected in all cases and preserved at 4°C until transferred to the laboratory within 30 min. Plasma was obtained by centrifugation at 400 g for 5 min while PBMC were isolated as described on **Sec. 3.3.3**. PBMC were cryopreserved in Freezing Medium and stored in liquid nitrogen, while plasma was stored at -80°C until analysis.

Before assays, plasma was defrosted and diluted 1:2 with PBS. The same procedure that was used to measure spontaneous cytokine and FABP2 levels on biopsy supernatants was followed for plasma samples. Briefly, spontaneous cytokine production was evaluated using the LEGENDplex™ Inflammation Panel 1 (13-plex) (BioLegend®, cat. # 740809) following the manufacturer's protocol and FABP2 levels were measured by ELISA (Invitrogen, cat. # EHFABP2).

6.2.2 Cell Identification

PBMC were thawed and stained using the panel described on **Tab. V.1**. Within 48 h of staining, cells were acquired using a 5-laser, 67 detectors spectral cytometer (Aurora, Cytek) and analysed on the OMIQ Data Science platform (©Omiq, Inc. 2024). Scale parameters were adjusted, and a cleaning algorithm (PeacoQC) was applied to all samples. Cells were identified with the strategy shown in **Fig. VI.1**, **Fig. VI.2** and **Fig. VI.3**.

Within each immune subset, the expression of CCR2, Fas, CXCR5, CXCR3, TLR4 and CCR9 was assessed using the FMO method to define positive populations as with LPL (see **Fig. V.2**). Additionally, the proportion of T and T$\gamma\delta$ cells expressing CD2 was determined. The expression of Integrin α4 and Integrin β7 was analysed across all subsets (**Fig. VI.4**).

Statistical analysis of marker expression was conducted only for subsets containing more than 50 cells through all groups.

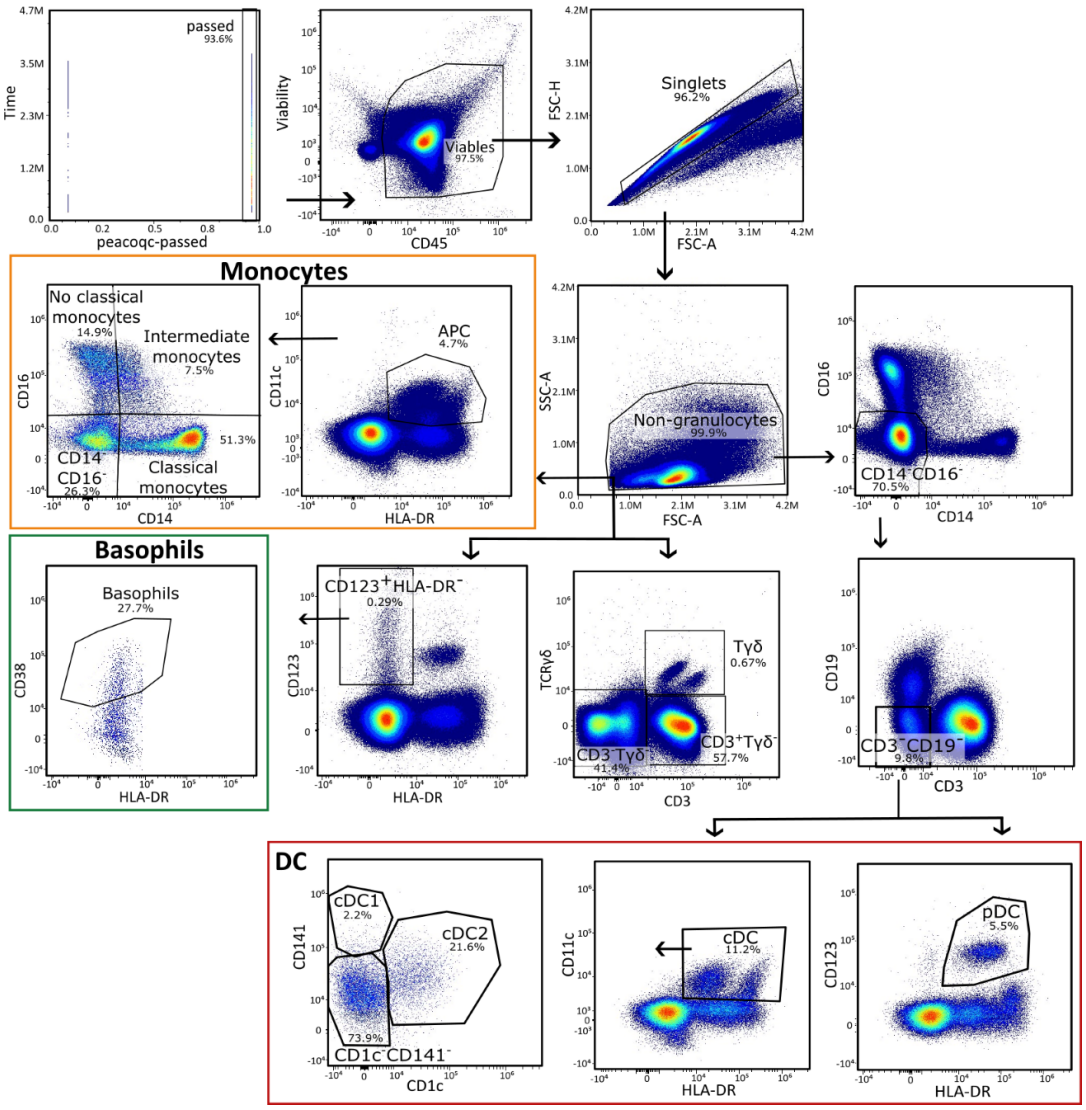

Figure VI.1: Identification of dendritic cells, monocytes and basophils. *Total leukocytes from peripheral blood mononuclear cells were selected, within the cells that passed the Peaco QC test, as singlet viable CD45⁺. Non-granulocytes were identified based on their high scatter properties and categorized into subsets. Monocytes were identified within antigen presenting cells (APC) (CD11c⁺HLA-DR⁺) and classified as no classical (CD16⁺CD14⁻), intermediate (CD16⁺CD14⁺), classical (CD16⁻CD14⁺) and CD14⁻CD16⁻ monocytes. Dendritic cells (DC) were identified as CD14⁻CD16⁻CD3⁻CD19⁻ and divided into plasmacytoid (pDC) (CD123⁺HLA-DR⁺) and conventional (cDC) (CD11c⁺HLA⁻DR⁺). cDC were further divided: DC1 (CD141⁺CD1c⁻), cDC2 (CD1c⁺) and CD1c⁻CD141⁻. Basophils are identified as CD123⁺HLA⁻DR⁻CD38⁺. Last, non-granulocytes were divided into: CD3⁺Tγδ⁺ (Tγδ⁺), CD3⁺Tγδ⁻ and CD3⁻ Tγδ⁻.*

6.2.3 Unsupervised Analysis

Cells were subsampled automatically to a total of 4 million cells per analysis group: NC-NI, C-IM.3 and C-GFD. The UMAP algorithm was applied using Euclidian metric, incorporating all markers except those used to identify non-granulocytes (Viability, CD45, SSC and FSC). A FlowSOM algorithm with elbow metaclustering was then performed on the same features. Gates were defined based on the FlowSOM clusters in combination with the UMAP output on the concatenated samples (**Fig. VI.5**). Clusters in which $\geq$ 40% of the cells were from a single patient were excluded from further analysis.

Each cluster was classified based on their feature expression. In complex cases, gating

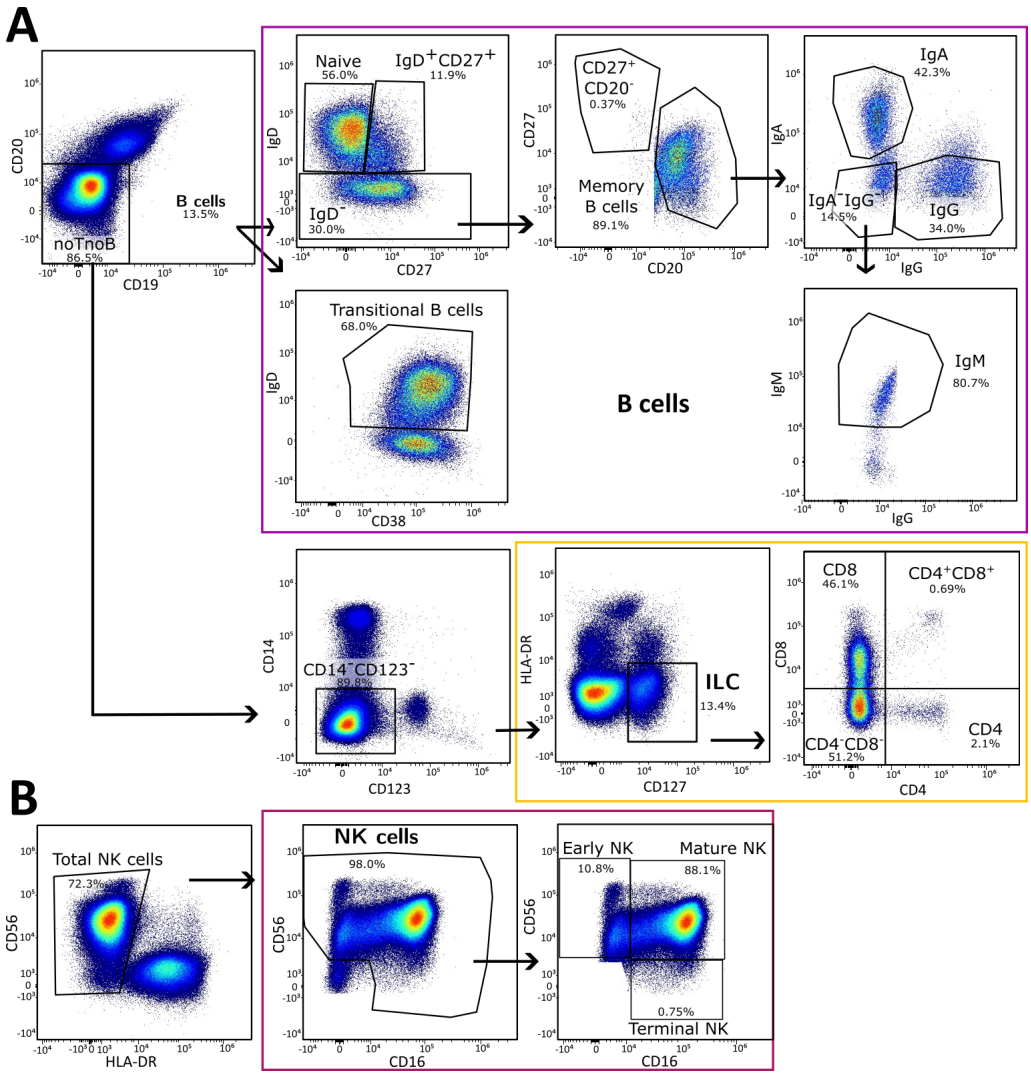

Figure VI.2: Identification of B and NK cells. *CD3-Tγδ- cells (identified as described in* ***Fig. VI.1*** *were further divided. (**A**) B cells ($CD20^+$ and $CD19^+CD20^-$) were categorized into transitional (IgD^+ $CD38^+$), naive (IgD^+CD27^-), IgD^+CD27^+ and IgD^-. The latter were subdivided into $CD27^+CD20^-$ and memory B cells ($CD20^+$). These subgroups were classified on the basis of their expression of IgA, IgG and IgM. Innate lymphoid cells (ILC) were identified as non-T non-B cells $CD14^-CD123^-HLA^-DR^-CD127^+$ and further subdivided based on CD8 and CD4 expression. (**B**) NK cells were defined as $CD56^+HLA^-DR^-$ cells and classified into: early ($CD56^+CD16^-$), mature ($CD56^+CD16^+$) and terminal ($CD56^-CD16^+$).*

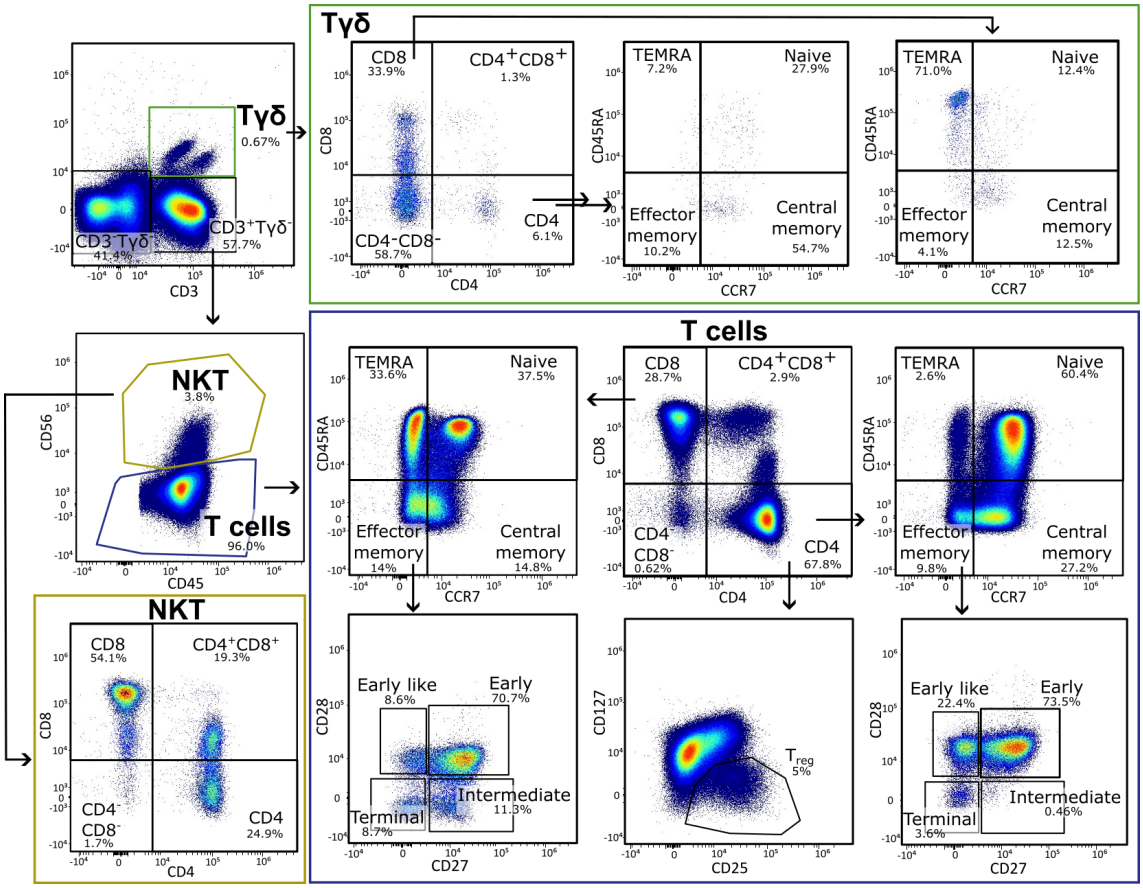

Figure VI.3: Identification of Tγδ, T and NKT cells. *Tγδ and CD3⁺Tγδ⁻ cells were identified as in* ***Fig. VI.1****. CD3⁺Tγδ- were further divided into T-cells (CD56⁻) and NKT cells (CD56⁺). Tγδ, T and NKT cells were further divided into CD8, CD8⁺CD4⁺, CD4 and CD8⁻CD4⁻. T_{reg} were identified within CD4⁺ T cells as CD127⁻CD25⁺. Last, CD4⁺ and CD8⁺ T and Tγδ cells were further divided into effector memory cells re-expressing CD45RA (TEMRA) (CD45RA⁺CCR7⁻), naive (CD45RA⁺CCR7⁺), central memory (CD45RA⁻CCR7⁺) and effector memory (CD45RA⁻CCR7⁻).*

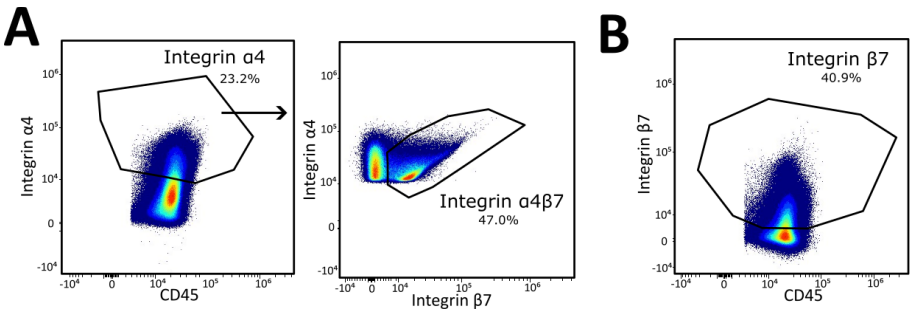

Figure VI.4: Identification of Integrin α4 and β7 expressing cells. *(**A**) Integrin α4⁺ cells were identified in each subset, and within these cells, Integrin β7⁺ cells (Integrin α4⁺β7⁺) were further selected. (**B**) Integrin β7⁺ cells were also identified across all subsets.*

strategies described in **Fig. VI.1**, **Fig. VI.2** and **Fig. VI.3** were overlaid with the clusters for validation. When multiple similar clusters were present, a heatmap was used to differentiate them. Finally, an empirical analysis of digital gene expression in R (EdgeR) was ran to compare clusters.

The same approach used with non-granulocytes was applied for Tγδ⁻CD3⁻ and Tγδ⁻CD3⁺ cells (**Fig. VI.6**). Additionally, the same analysis was performed within C-GFD group, stratifying samples based on the presence of atrophy (**Fig. VI.7**).

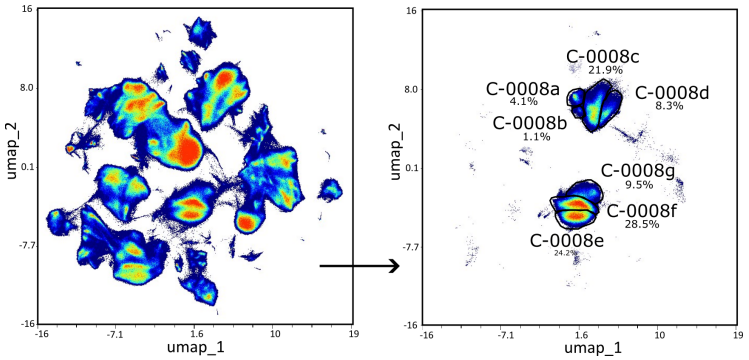

Figure VI.5: Division of FlowSOM clusters. *Clusters generated by FlowSOM algorithm were subdivided based on UMAP output.*

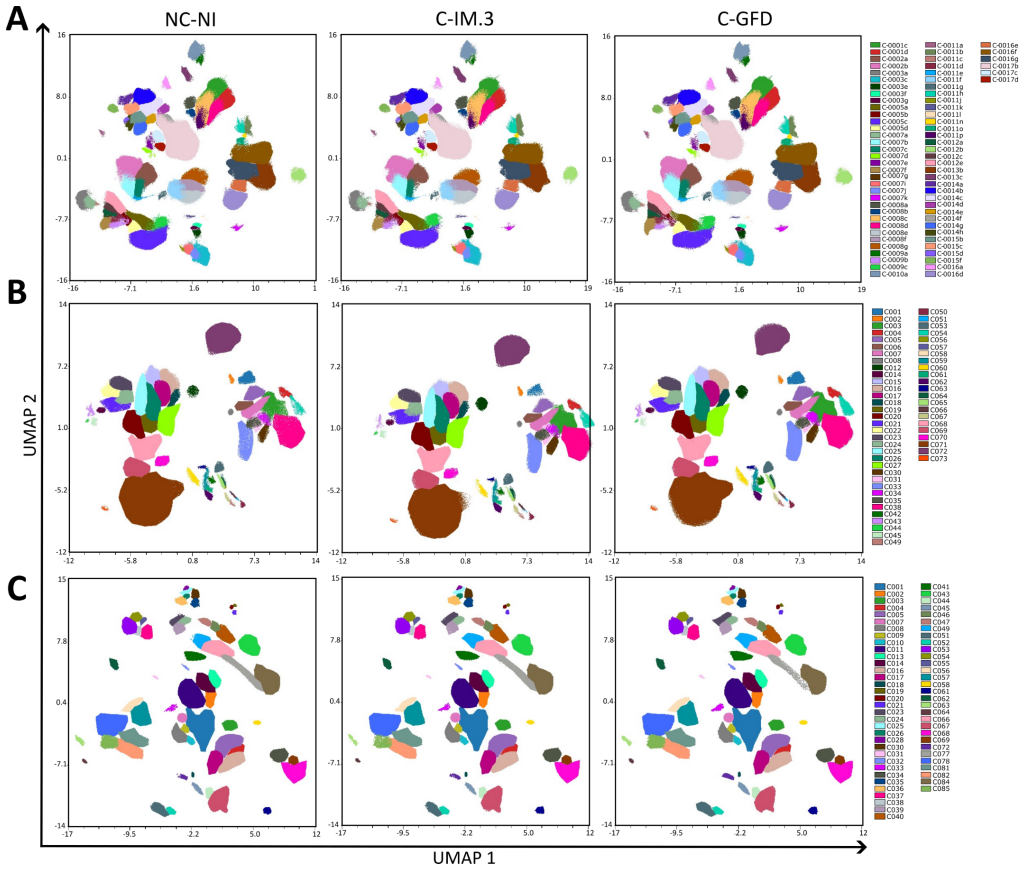

Figure VI.6: Cluster mapping across groups. *Patients were categorized into non-coeliac not inflamed (NC-NI) controls, coeliac patients with inflammation (Marsh 3) (C-I.M3) and coeliac patients on a gluten-free diet (C-GFD). Scatterplots display clusters identified using FlowSOM and UMAP algorithms on: (**A**) total cells, (**B**) T cells ($CD3^{+}T\gamma\delta^{-}$ and (**C**) no T cells ($CD3^{-}T\gamma\delta^{-}$).*

6.3 Results

6.3.1 Immune Cell Subsets and Marker Expression Profiles

No differences were observed in the distribution of most immune cells among the groups (**Tab. VI.1**). However,To understand the differences in immune profiles across patient groups, PBMC immune phenotype was compared between NC-NI controls, C-I.M3 and C-GFD patients. This comparison aimed to identify distinct immune markers and cell subset distributions that may reflect the underlying immunological alterations associated with CD and its treatment.

C-GFD patients showed fewer T$\gamma\delta$ CD4 cells compared to NC-NI controls (**Tab. VI.2**). This difference in T cell populations was further highlighted by distinct immune marker expression patterns observed among patient groups.

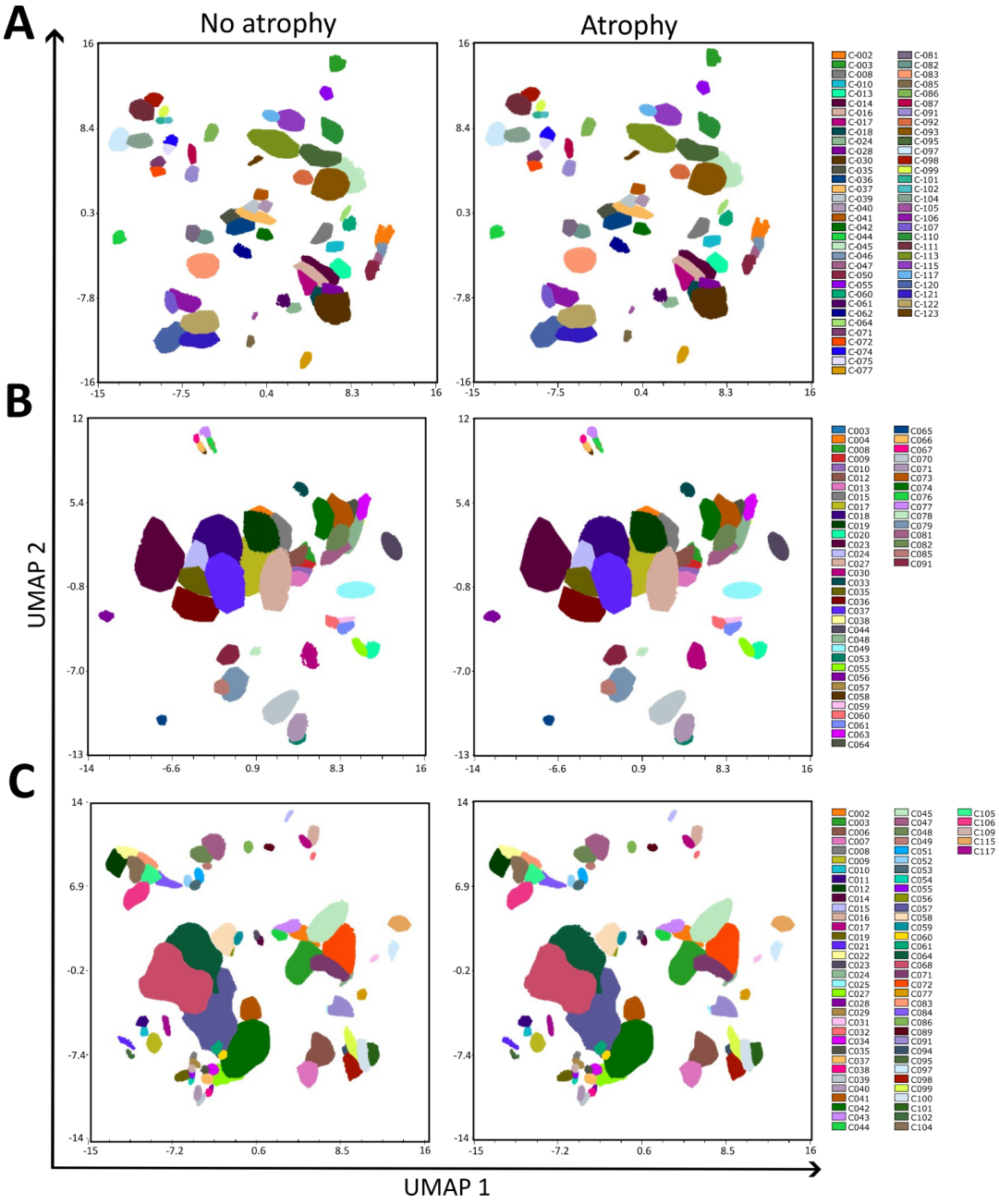

Figure VI.7: Immune cell clustering in coeliac patients on a gluten-free diet stratified by presence of atrophy. *Scatterplots show clusters identified using FlowSOM and UMAP algorithms on (**A**) total cells, (**B**) T cells (CD3$^+$ T$\gamma\delta^-$) and (**C**) no T cells (CD3$^-$ T$\gamma\delta^-$).*

	NC-NI		C-I.M3		C-GFD		ANOVA
	Mean	SD	Mean	SD	Mean	SD	
pDC	0.89	0.92	0.81	0.76	1.62	2.74	0.84
cDC	1.69	0.72	1.28	0.22	2.14	1.71	0.69
cDC1	0.01	0.01	0.05	0.07	0.02	0.02	0.44
$CD1c^{-}CD141^{-}$DC	1.20	0.73	0.80	0.35	1.57	1.37	0.60
cDC2	0.44	0.23	0.37	0.24	0.49	0.41	0.74
Total NK	18.33	11.18	19.72	9.23	25.27	15.89	0.63
Early NK	5.64	5.92	3.25	1.83	5.73	3.62	0.35
Mature NK	11.46	4.91	14.99	6.39	18.46	14.26	0.76
Terminal NK	0.80	0.91	1.17	1.60	0.75	0.93	0.99
Total ILC	9.52	11.75	11.03	13.14	7.66	5.28	0.82
ILC $CD4^{-}CD8^{+}$	1.81	1.89	3.06	3.56	2.04	1.41	0.79
ILC $CD4^{+}CD8^{+}$	0.01	0.01	0.01	0.02	0.03	0.05	0.79
ILC $CD4^{+}CD8^{-}$	0.16	0.11	0.10	0.07	0.14	0.16	0.74
ILC $CD4^{-}CD8^{-}$	7.55	9.88	7.85	9.52	5.46	3.96	0.87
B cells	11.89	8.74	11.05	11.13	14.06	9.33	0.86
$IgD^{+}CD27^{+}$	3.28	4.12	2.24	2.81	3.16	3.31	0.74
Naive B cells	3.62	2.12	3.34	2.06	6.25	4.90	0.51
Plasmoblasts	0.05	0.05	0.33	0.55	0.06	0.05	0.57
Memory B cells	4.22	2.34	3.95	4.08	3.71	2.07	0.62
IgA B cells	1.35	0.70	0.89	0.87	1.13	0.62	0.40
IgM B cells	0.82	1.30	0.29	0.27	0.49	0.34	0.36
IgG B cells	1.88	0.56	2.42	2.72	1.90	1.20	0.87
Transitional B cells	6.74	5.55	5.54	4.72	9.41	7.21	0.56
NKT	2.56	2.63	2.43	2.42	5.07	8.94	0.99
NKT $CD4^{+}CD8^{+}$	0.17	0.22	0.10	0.10	2.10	8.03	0.94
NKT CD8	1.39	1.18	1.86	2.30	2.26	3.46	0.99
NKT CD4	0.85	1.28	0.26	0.30	0.31	0.41	0.91
NKT $CD4^{-}CD8^{-}$	0.14	0.12	0.21	0.15	0.41	0.98	0.45
T cells	45.58	14.72	46.92	16.16	39.05	19.32	0.62
CD8 T cells	10.89	3.99	16.60	11.10	12.54	7.39	0.48
TEMRA CD8 T cells	2.25	1.31	7.13	8.66	3.98	2.34	0.41
Naive CD8 T cells	7.04	4.07	7.27	4.67	5.62	4.48	0.54
CM CD8 T cells	0.94	0.68	0.92	0.61	1.66	2.65	0.93
EM CD8 T cells	0.64	0.37	1.27	0.96	1.29	0.87	0.47
Early like EM CD8 T cells	0.06	0.04	0.06	0.08	0.08	0.08	0.75
Early EM CD8 T cells	0.35	0.21	0.59	0.56	0.54	0.38	0.61
Intermediate EM CD8 T cells	0.10	0.10	0.32	0.28	0.35	0.27	0.12
Terminal EM CD8 T cells	0.12	0.15	0.26	0.38	0.28	0.36	0.85
$CD4^{+}CD8^{+}$ T cells	0.54	0.37	0.66	0.61	0.66	0.56	0.98
CD4 T cells	33.08	11.62	28.12	15.55	24.75	12.96	0.32
TEMRA CD4 T cells	0.75	0.51	0.62	0.69	0.29	0.26	0.16
Naive CD4 T cells	17.43	11.13	15.31	14.71	12.94	8.81	0.69
CM CD4 T cells	11.63	4.53	8.85	3.64	9.09	8.68	0.29
EM CD4 T cells	3.26	1.39	3.34	2.92	2.43	1.91	0.46
Early like EM CD4 T cells	0.76	0.18	0.79	0.70	0.61	0.49	0.71
Early EM CD4 T cells	2.31	1.16	1.66	1.04	1.48	0.84	0.25
Intermediate EM CD4 T cells	0.04	0.04	0.12	0.19	0.07	0.19	0.98
Terminal EM CD4 T cells	0.15	0.13	0.73	1.07	0.25	0.68	0.73
T_{reg}	2.13	1.36	1.29	0.81	1.54	1.02	0.43
$CD4^{-}CD8^{-}$ T cells	1.11	0.64	1.53	0.81	1.11	0.66	0.72

Table VI.1: Peripheral blood mononuclear cells variability among groups. *Mean and Standard Deviation (SD) of the percentage of lymphocytes within the viable, $CD45^{+}$ singlet cell population. One-way ANOVA was used to compare the groups (p-values shown). Post-hoc Tukeys multiple comparisons tests were performed where the difference was statistically significant ($p<0.05$). C-GFD: Coeliac patients on a gluten-free diet; C-IM.3: Coeliac patients with active inflammation with Marsh 3; cDC: conventional dendritic cells; CM: Central memory, DC: Dendritic cells; EM: Effector memory; ILC: Innate lymphoid cells; NC-NI: Non-coeliac not inflamed; pDC: Plasmacytoid dendritic cells; TEMRA: effector memory cells re-expressing CD45RA; T_{reg}: Regulatory T cells.*

	NC-NI		C-I.M3		C-GFD		ANOVA	Tukey		
	Mean	SD	Mean	SD	Mean	SD		NC-NI vs C-I.M3	NC-NI vs C-GFD	C-I.M3 vs C-GFD
Tγδ	1.89	1.82	2.60	2.08	1.87	1.87	0.60			
Tγδ CD8	0.60	0.72	0.93	1.00	0.70	0.93	0.90			
Tγδ CD8 TEMRA	0.40	0.63	0.63	0.81	0.50	0.89	0.86			
Tγδ CD8 Naive	0.16	0.12	0.23	0.25	0.15	0.19	0.79			
Tγδ CD8 CM	0.02	0.02	0.03	0.02	0.03	0.04	0.34			
Tγδ CD8 EM	0.02	0.02	0.04	0.03	0.02	0.02	0.27			
Tγδ $CD4^+CD8^+$	0.05	0.06	0.03	0.04	0.06	0.12	0.85			
Tγδ CD4	0.25	0.15	0.20	0.17	0.15	0.26	**0.02**	0.43	**0.01**	0.11
Tγδ CD4 TEMRA	0.01	0.01	0.01	0.01	0.01	0.01	0.30			
Tγδ CD4 Naive	0.09	0.08	0.05	0.04	0.05	0.09	0.08			
Tγδ CD4 CM	0.12	0.06	0.12	0.14	0.07	0.13	0.15			
Tγδ CD4 EM	0.03	0.02	0.03	0.03	0.02	0.04	0.31			
Tγδ $CD4^-CD8^-$	0.98	1.02	1.43	0.97	0.96	0.93	0.31			
Basophils	0.12	0.15	0.09	0.02	0.12	0.07	0.49			
APC	15.70	10.00	13.28	7.72	9.33	8.02	0.28			
No classical monocytes	1.00	0.98	1.87	1.28	1.73	1.33	0.50			
Intermediate monocytes	0.73	0.98	0.58	0.43	0.29	0.25	0.39			
Classic monocytes	11.02	10.09	8.34	7.50	4.51	7.67	0.29			

Table VI.2: Peripheral γδ cells, basophils and monocytes among groups *Mean and Standard Deviation (SD) of the percentage of lymphocytes within the viable, $CD45^+$ singlet cell population. One-way ANOVA was used to compare the groups (p-values shown). Post-hoc Tukeys multiple comparisons tests were performed where the difference was statistically significant ($p < 0.05$).APC: Antigen presenting cells; C-GFD: Coeliac patients on a gluten-free diet; C-IM.3: Coeliac patients with active inflammation with Marsh 3; CM: Central memory, EM: Effector memory; NC-NI: Non-coeliac not inflamed; TEMRA: effector memory cells re-expressing CD45RA.*

Additionally, basophils from C-GFD expressed higher levels of Integrin α4 compared to controls, with C-I.M3 showing intermediate levels (**Fig. VI.8A**). Similarly, Integrin $\alpha4^+$ Integrin $\beta7^+$ followed a comparable pattern of expression in Tγδ CD4 naive cells, while in NKT cells the expression of this gut homing marker is clearly more abundant on C-I.M3 (**Fig. VI.8B**).

When considering CCR9 expression, C-I.M3 patients showed higher levels on IgM^+ B cells than controls (**Fig. VI.8C**), suggesting alterations in B cell populations in the presence of inflammation. This trend was also observed in memory $CD8^+$ T cells, where C-IM.3 patients expressed more CCR9 compared to both NC-NI and C-GFD patients (**Fig. VI.8C**). These findings point out to differences in cytokine receptor expression that might be related to the inflammatory environment present in C-I.M3 patients.

Further analysis of T cells revealed distinct patterns. TEMRA $CD8^+$ T cells in C-GFD patients showed lower CXCR5 expression than in C-I.M3 and controls (**Fig. VI.8D**). This suggests a potential functional shift in the T cell subsets in response to the dietary changes in C-GFD patients.

In terms of TLR4 expression, C-I.M3 patients demonstrated higher levels compared to both controls and C-GFD, particularly in memory B cells and IgG^+ B cells (**Fig. VI.8E**). This increase in TLR4 expression highlights the heightened immune response associated with active inflammation. Furthermore, TLR4 expression was also more pronounced on APC, specifically on intermediate monocytes (**Fig. VI.8E**). Looking at CXCR3 expression, C-I.M3 patients showed increased levels, particularly on EM $CD8^+$ T cells, with a more pronounced expression on early and early like subsets (**Fig. VI.8F**). On the other hand, CD2 expression was lower in intermediate EM $CD8^+$ T cells in coeliac patients (**Fig. VI.8G**).

Noteworthy, another finding of the study pertained to CD38 expression. C-I.M3 group showed increased CD38 expression on TEMRA $CD8^+$ T cells, terminal EM T cells and $CD4^+$ $CD8^+$ T cells, with significant differences observed when compared to C-GFD (**Fig. VI.8H**). This increase in CD38 expression in C-IM.3 was also observed when comparing terminal EM T cells and $CD4^+CD8^+$ T cells to controls, although the differences were marginal ($p = 0{,}054$

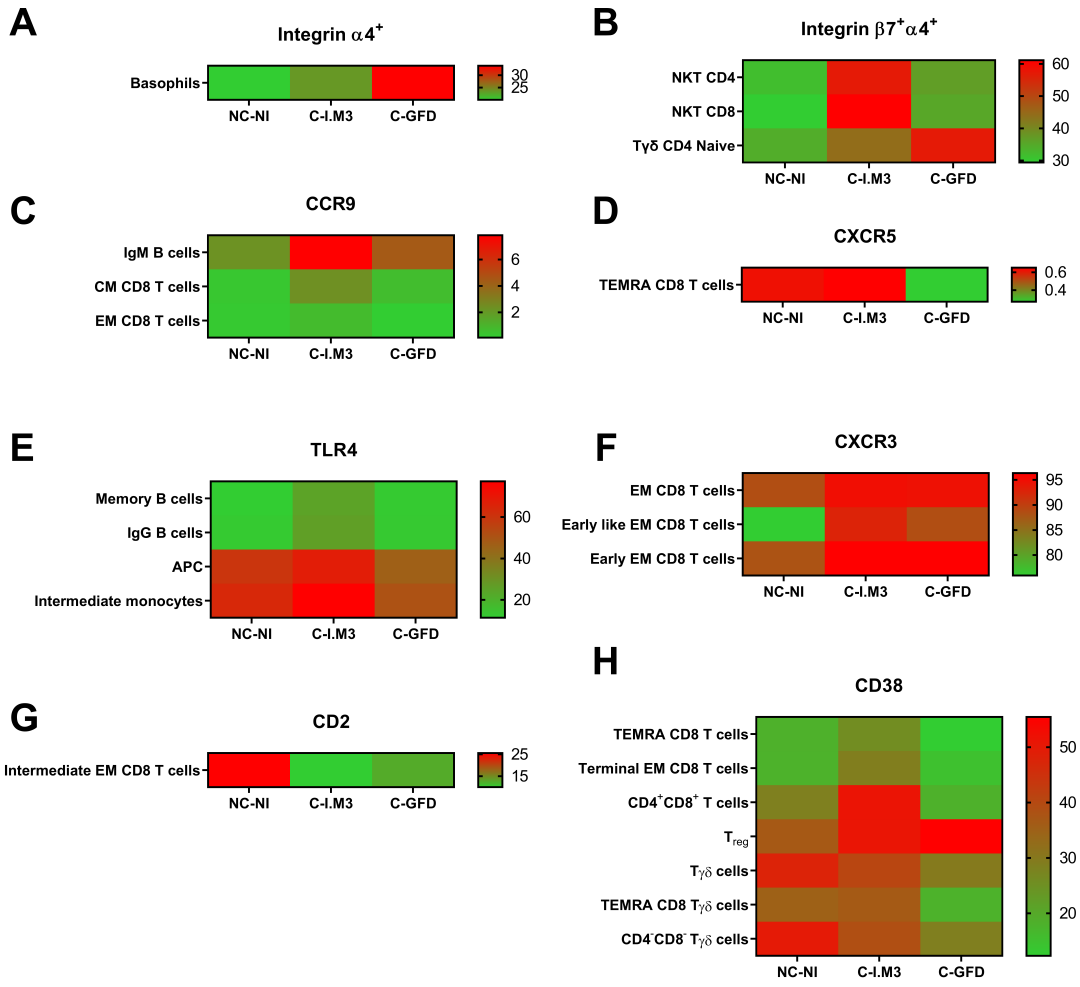

Figure VI.8: Peripheral immune markers in coeliac disease. *Differences in immune subsets between non-coeliac not inflamed (NC-NI) controls, coeliac patients with inflammation (Marsh 3) (C-I.M3) and coeliac patients on a gluten-free diet (C-GFD) are shown for the following markers: (**A**) Integrin $\alpha 4^+$ (**B**) Integrin $\beta 7^+$ Integrin $\alpha 4^+$ (**C**) CCR9$^-$, (**D**) CXCR5, (**E**) TLR4, (**F**) CXCR3, (**G**) CD2 and (**H**) CD38. Heatmap colors represent the median percentage of cells expressing each corresponding marker. For statistical analysis, ShapiroWilk normality test was assessed followed by an unpaired one-way ANOVA with uncorrected Fisher's LSD test and post-hoc Tukey's multiple comparisons test. Only markers that showed differentially expression ($p< 0.05$) are included. APC: Antigen presenting cells; EM: Effector memory; TEMRA: effector memory cells re-expressing CD45RA; T_{reg}: Regulatory T cells.*

and p = 0,64 respectively). C-GFD patients showed a significant increase in CD38 expression on T_{reg} compared to controls, with C-I.M3 patients showing a trend toward an increased expression (p = 0.09). In contrast, C-GFD T$\gamma\delta$ cells expressed lower levels of CD38 than controls, a pattern also observed in TEMRA CD8$^+$ T$\gamma\delta$ cells (p = 0.08), with C-GFD showing lower expression compared to C-I.M3 (p = 0.051). Additionally, CD4$^-$CD8$^-$ T$\gamma\delta$ cells in C-GFD patients exhibited a reduced CD38 expression compared to controls (**Fig. VI.8H**).

Of note, no significant differences were observed on Fas, CCR2 or Integrin $\beta 7$ expression across the three study groups, suggesting that these markers may not play a role in the observed peripheral immune changes in CD.

In summary, the targeted analysis of PBMC immune phenotypes revealed distinct immunological profiles among coeliac patient groups, reflecting disease activity and the effects of treatment. C-GFD patients exhibited a generally less activated immune state, characterized by reductions in specific T cell subsets and lower expression of activation markers such

as CD38. In contrast, C-I.M3 patients displayed features consistent with an inflammatory milieu, including elevated expression of gut-homing markers, pro-inflammatory receptors, and activation-associated molecules across multiple immune cell subsets. These findings underscore the differential modulation of the peripheral immune compartment in response to inflammation and dietary intervention in CD patients.

6.3.2 Unsupervised Clustering Analysis

While the preceding analyses focused on targeted comparisons of predefined immune markers and subsets, these approaches may overlook broader or unexpected cellular phenotypes. To complement these findings and explore the peripheral immune landscape more comprehensively, an unsupervised clustering analysis was performed. Leveraging the large number of circulating immune cells available in PBMC samples, this data-driven method enables the identification of differential expression patterns and phenotypic shifts that may not be captured through conventional gating strategies. Through this approach, we aimed to uncover subtle yet biologically relevant immune alterations across patient groups.

C-I.M3 patients showed an increase in a subset of plasmablasts, indicating a potential inflammatory shift. Conversely, C-GFD patients exhibited a decrease in classical monocytes (**Fig. VI.9A**) which may be associated with the immune suppression expected in this group. Interestingly, cDC2 were more abundant in C-GFD patients (**Fig. VI.9A**), further supporting the notion of a different immune profile in this group. When clusters were made from the $CD3^{+}T\gamma\delta^{-}$section, C-IM.3 patients showed an increase in some $CD4^{-}CD8^{-}$ T cells (**Fig. VI.9B**). Meanwhile clusters made from $CD3^{-}T\gamma\delta^{-}$cells showed that C-I.M3 patients had more plasmablasts compared to NC-NI and C-GFD patients, while classical and intermediate monocytes and some cDC were decreased in C-GFD patients. (**Fig. VI.9C**).

6.3.3 Effect of Atrophy on the Peripheral Immunome of C-GFD

		No atrophy		Atrophy		U Mann
		Mean	SD	Mean	SD	Whitney
% Cells	ILC $CD4^{+}CD8^{+}$	0,01	0,01	0,04	0,06	0,03
	NKT CD4	0,08	0,03	0,44	0,48	0,01
Fas	Early EM CD8 T cells	80,58	11,58	91,73	5,54	0,03
	TEMRA CD8 T cells	54,05	6,18	67,87	13,28	0,01
	NKT	55,58	6,57	65,17	9,46	0,05
$\alpha4^{+}\beta7^{+}$	CD8 T cells	33,70	13,90	49,67	13,82	0,04
Integrin $\beta7$	Intermediate EM CD8 T cells	29,20	20,89	48,14	8,90	0,04
	NKT CD4	68,68	8,48	45,30	25,56	0,03

Table VI.3: Effect of atrophy on peripheral blood mononuclear cells from coeliac disease patients on gluten-free diet. *Mean and Standard Deviation (SD) are shown only in the cases were the U Mann Whitney test was significant ($p < 0,05$). $\alpha4^{+}\beta7^{+}$: Integrin$\alpha4^{+}$Integrin$\beta7^{+}$, EM: Effector memory ILC: Innate lymphoid cells; TEMRA: effector memory cells re-expressing CD45RA.*

Given the observed differences in the peripheral immune profile of C-GFD and the presence of villous atrophy (Marsh score $\geq$ 3) in 68.4 % of the cohort (**Tab. IV.1**), the potential influence of this atrophy on the peripheral immune profile was next investigated to determine whether it leaves a detectable imprint in the blood. Notably, patients with atrophy showed higher levels of $CD4^{+}CD8^{+}$ ILC and $CD4^{+}$ NKT cells (**Tab. VI.3**). Additionally, these patients showed higher expression of Fas on early EM and TEMRA $CD8^{+}$ T cells, as well as on NKT cells. An elevation in the expression of Integrin $\alpha4^{+}$ Integrin $\beta7^{+}$ on $CD8^{+}$ T cells and Integrin $\beta7$ on intermediate EM $CD8^{+}$ T cells and NKT $CD4^{+}$ cells were also observed (**Tab. VI.3**).

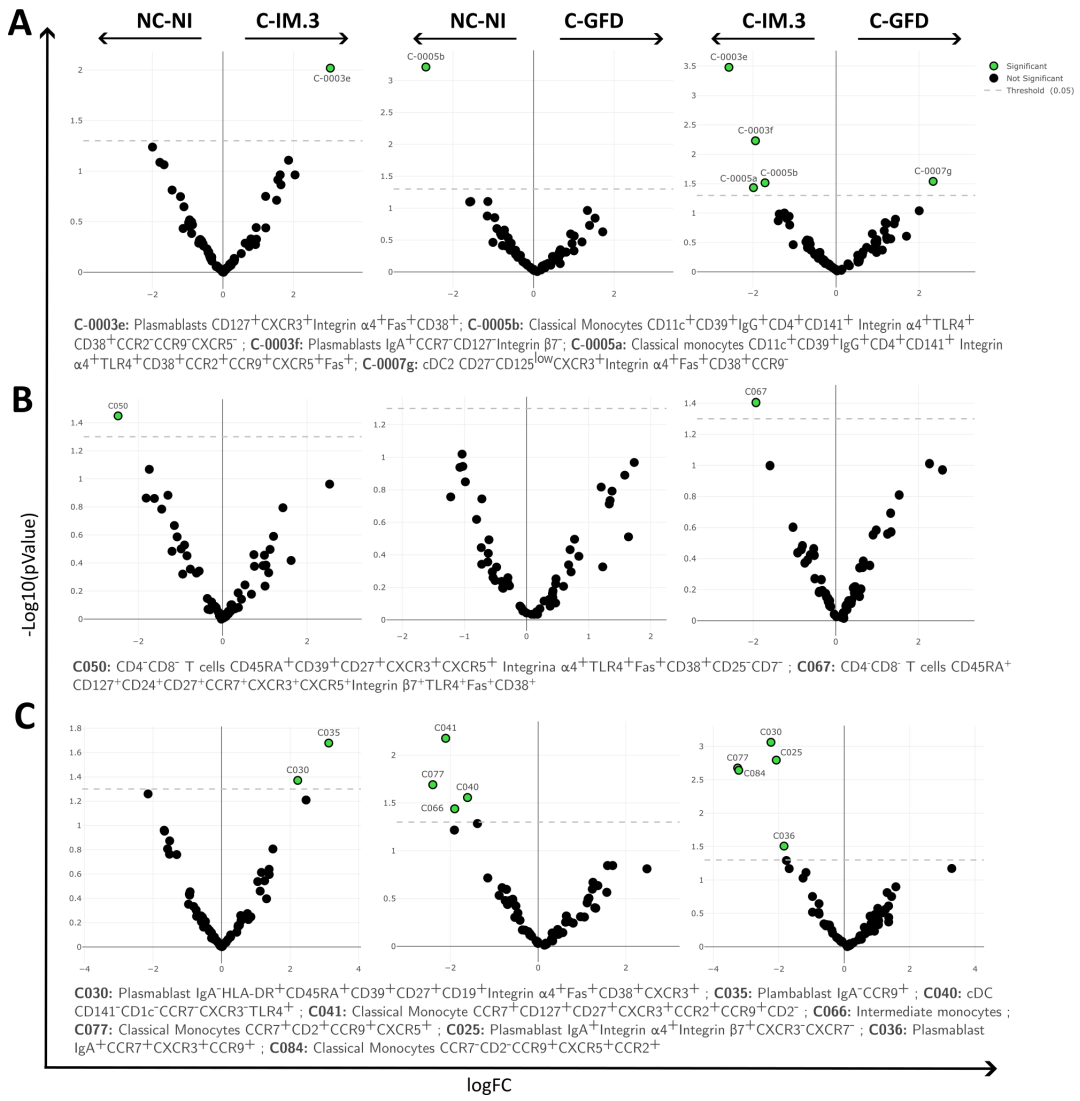

Figure VI.9: Differential cluster expression between groups. *Volcano plots illustrate differential expression of clusters using EdgeR analysis. Comparisons are made between non-coeliac not inflamed (NC-NI) controls, coeliac patients with inflammation (Marsh 3) (C-I.M3) and coeliac patients on a gluten-free diet (C-GFD). (**A**) total cells , (**B**) T cells ($CD3^+ T\gamma\delta^-$) and (**C**) no T cells ($CD3^- T\gamma\delta^-$). cDC: conventional dendritic cells.*

These changes suggest a shift in immune cell trafficking and a more active state on patients with an undergoing villous atrophy (**Fig. VI.10C**).

Further insights emerge from the unsupervised analysis, which revealed an increase in naive $CD4^+$ T cells in patients with atrophy, while certain plasmablast populations were downregulated (**Fig. VI.10A**). A more detailed examination of the $CD3^+T\gamma\delta^-$fraction showed a decrease in both naive $CD4^-CD8^-$ T cells and TEM $CD8^+$ T cells (**Fig. VI.10B**). Lastly, clustering of the CD3-$T\gamma\delta^-$ fraction indicated an increase in ILC $CD4^-CD8^-$ cells on patients with atrophy, further underscoring the distinct peripheral immune profile associated with villous atrophy.

6.3.4 Greater Expression of Integrina4, CD38 and TLR4 on Symptomatic Patients

Building on these findings, the analysis was extended to investigate whether differences in the immune profile were also associated with the presence or absence of symptoms in C-GFD

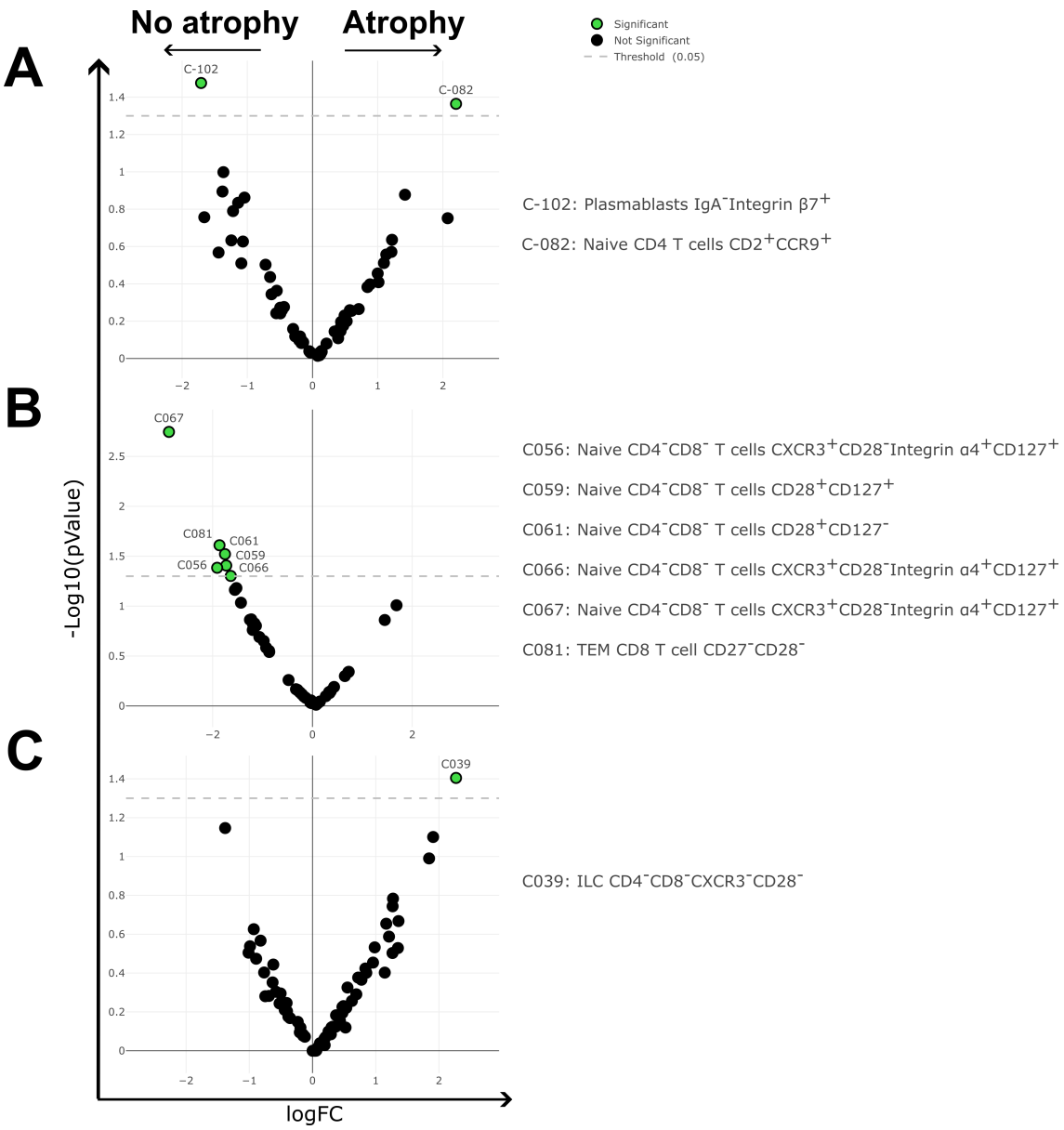

Figure VI.10: Differential cluster expression in coeliac patients on a gluten free diet stratified by atrophy. *Volcano plots illustrate differential cluster expressions using EdgeR analysis. Comparisons are made between coeliac disease patients on a gluten free diet with and without intestinal atrophy. (**A**) total cells, (**B**) T cells ($CD3^{+}T\gamma\delta^{-}$) and (**C**) no T cells ($CD3^{-}T\gamma\delta^{-}$). ILC: Innate lymphoid cells, TEM: Terminal effector memory.*

patients.

Symptomatic patients exhibited a decrease in ILC $CD4^+CD8^+$and NKT $CD4^+$ cells (see **Tab. VI.4**). In addition, they displayed a higher expression of Integrin $\alpha 4$ across various immune cell populations, including DC, terminal NK cells, ILC $CD4^-CD8^-$ cells, IgG B cells, NKT $CD4^+CD8^+$, T$\gamma\delta$ $CD4^+CD8^+$ and monocytes. This widespread increase in Integrin $\alpha 4$ expression may reflect alterations in cell adhesion or migration dynamics. Furthermore, an elevation in CD38 expression was observed in T$\gamma\delta$ CD4 naive cells, which could indicate a state of heightened activation in these cells

In contrast, asymptomatic C-GFD patients exhibited higher CCR2 levels on ILC $CD4^+$, T cells, T_{reg}, T$\gamma\delta$ CD4 CM cells and IgA B cells (**Tab. VI.4**). The increased CCR2 expression in these subsets may suggest differential chemokine signaling and trafficking patterns than in symptomatic patients with increased Integrin $\alpha 4$ expression. Additionally, CCR9 was more expressed in specific T cells subsets of asymptomatic patients, alongside with increased TLR4 expression on CD8 T cells and intermediate monocytes. Interestingly, this pattern was reversed in NKT $CD4^-CD8^-$ cells, highlighting a nuanced and complex interplay between immune regulation and symptom manifestation in C-GFD.

6.3.5 Time on GFD Decreased Migration Markers While Increasing Inflammation

Given the observed impact of villous atrophy and symptomatology on the peripheral immune profile of C-GFD patients, the next step was to investigate whether the duration of a GFD also shapes these immune parameters. Since long-term adherence to a GFD is essential for mucosal healing and symptom resolution, analyzing immune changes over time could provide insights into the dynamic adaptation of the immune system in response to gluten withdrawal.

Hence, the obtained results display a negative correlation between the time on a GFD and the percentage of circulating $CD4^+$ Naive T cells, as well as the expression of migration markers such as Integrin $\beta 7$ and Integrin $\alpha 4^+$ Integrin $\beta 7^+$, particularly on T cells and T$\gamma\delta$ cells (**Tab. VI.5**). On the other hand, there was a positive correlation between the time on GFD and the expression of CXCR5, TLR4 and CD38 in certain T$\gamma\delta$ cells as well as for CXCR3 and TLR4 in CD4 EM T cells (**Tab. VI.5**). These findings suggest that while some immune markers decline over time, others may become more prominent, reflecting a complex and dynamic immune reconfiguration in response to the dietary intervention.

6.3.6 Normalization of Inflammatory Mediators on GFD-Treated Patients

Last, to complete the characterization of the peripheral immune landscape in CD patients, plasma levels of different soluble immune mediators related to the immune response in the intestine were also analysed.

The obtained results revealed that plasma FABP2 levels were significantly higher in C-I.M3 patients (**Fig. VI.11**). In this cohort, patients with atrophy showed lower plasma levels of IFN-$\alpha 2$, IL-17A and CCL2 (**Fig. VI.12**). No significant differences were observed based on symptoms (**Fig. VI.13**). Additionally, time on GFD showed a negative correlation with plasma levels of CCL2 (**Fig. VI.14**).

6.4 Discussion

Given the observed alterations in the duodenal LP despite adherence to a GFD, as previously described in **Sec. 5.3**. It is particularly interesting to assess whether such persistent atrophy can be predicted on the circulating immunome. In fact, predicting the state of the mucosa in C-GFD without the need for invasive endoscopy would be highly valuable with a clear impact in monitor the mucosal healing in CD patients. In this context, the results in this chapter

		Asymptomatic		Symptomatic		T
		Mean	SD	Mean	SD	student
% Cells	ILC $CD4^+CD8^+$	0,06	0,08	0,01	0,01	0,04
	NKT CD4	0,60	0,62	0,18	0,20	0,03
Integrin α4	cDC	57,12	8,74	73,80	8,52	0,02
	$CD1c^-CD141^-$ DC	54,66	10,41	69,33	4,24	0,03
	Terminal NK	9,70	6,23	31,70	23,24	0,02
	ILC $CD4^-CD8^-$	5,37	2,64	11,04	5,42	0,03
	IgG B cells	66,00	22,10	84,93	16,46	0,04
	NKT $CD4^+CD8^+$	42,01	18,10	76,27	11,16	0,03
	T$\gamma\delta$ $CD4^+CD8^+$	36,24	20,68	64,06	6,74	0,02
	No classical monocytes	76,86	9,46	91,33	5,60	0,01
	Intermediate monocytes	86,64	15,61	89,53	17,64	0,04
	APC	67,98	13,03	85,48	5,33	0,04
$\alpha4^+\beta7^+$	Basophils	82,94	3,08	66,32	19,93	0,04
CCR2	ILC $CD4^+CD8^-$	7,79	4,03	3,33	2,84	0,04
	T cells	5,32	1,99	2,10	1,78	0,02
	CD4 T cells	8,14	4,48	3,06	3,31	0,03
	CD4 CM T cells	10,75	3,80	4,49	4,52	0,03
	CD4 EM T cells	23,12	11,23	8,84	6,19	0,02
	CD4 Early like EM T cells	30,94	8,88	11,64	6,63	0,00
	CD4 Early EM T cells	23,04	10,73	7,49	5,41	0,00
	T_{reg}	13,93	6,46	6,72	5,49	0,04
	T$\gamma\delta$ CD4 CM	31,16	8,85	19,72	5,73	0,04
	Intermediate monocytes	6,72	3,24	2,15	1,85	0,01
	IgA B cells	2,50	2,22	0,33	0,50	0,03
	CD8 Early EM T cells	6,13	6,12	1,46	0,76	0,03
	CD8 Terminal EM T cells	0,54	0,35	0,19	0,23	0,02
	$CD4^-CD8^-$ T cells	10,68	3,08	6,71	5,82	0,02
	CD8 Intermediate EM T cells	0,59	0,73	0,12	0,10	0,05
CCR9	NKT $CD4^-CD8^-$	1,42	1,03	6,65	6,17	0,02
	EM CD8 T cells	0,16	0,15	0,04	0,05	0,04
	EM CD4 T cells	23,12	11,23	8,84	6,19	0,02
	Terminal EM CD8 T cells	0,34	0,33	0,19	0,33	0,03
TLR4	ILC CD8	0,69	0,20	0,45	0,20	0,04
	NKT $CD4^-CD8^-$	4,48	3,04	13,14	7,72	0,04
	EM CD8 T cell	0,82	0,88	0,29	0,38	0,04
	Early EM CD8 T cells	0,99	1,25	0,18	0,22	0,01
	Terminal EM CD8 T cells	1,28	1,09	0,32	0,35	0,02
	Intermediate monocytes	65,38	20,13	41,65	13,98	0,03
CD38	T$\gamma\delta$ CD4 Naive	66,43	6,68	81,37	7,71	0,01

Table VI.4: Effect of symptoms on peripheral blood mononuclear cells from coeliac disease patients on a gluten free diet. *Mean and Standard Deviation (SD) are shown only when T student were significant ($p<0,05$). $\alpha4^+\beta7^+$: Integrin $\alpha4^+$Integrin $\beta7^+$; APC: Antigen presenting cells; cDC: Conventional dendritic cells; CM: Central memory; DC: Dendritic cells; EM: Effector memory; T_{reg}: Regulatory T cells.*

		Months GFD	
		Correlation	p value
% Cells	Naive CD4 T cells	-0,72	0,002
Integrin β7	IgA B cells	0,41	0,037
	CD8 T cells	-0,42	0,034
	CM CD8 T cells	-0,51	0,009
	EM CD8 T cells	-0,58	<,001
	Early like EM CD8 T cells	-0,61	<,001
	Early EM CD8 T cells	-0,58	<,001
	$CD4^+CD8^+$ T cells	-0,49	0,012
	Tγδ CD4	-0,44	0,031
	Tγδ CD4 CM	-0,45	0,031
Integrin β7	CD4 Naive T cells	-0,42	0,031
	EM CD4 T cells	-0,48	0,016
	Early EM CD4 T cells	-0,54	0,006
	Tγδ CD8 Naive	-0,47	0,019
	Tγδ CD4 Naive	-0,46	0,048
	Tγδ CD4 CM	-0,50	0,016
CCR2	NKT $CD4^-CD8^-$	-0,67	0,005
CCR9	Naive B cells	0,54	0,032
CXCR5	Tγδ CD4 Naive	0,75	0,005
TLR4	Early like EM CD8 T cells	0,59	0,045
	Tγδ $CD4^+CD8^+$	0,77	0,015
	NKT CD4	0,66	0,010
	TEMRA CD4 T cells	0,52	0,048
CXCR3	EM CD4 T cells	0,54	0,038
	Early like EM CD4 T cells	0,66	0,011
CD38	Tγδ CD4	0,54	0,048

Table VI.5: Correlation between peripheral blood mononuclear cells populations and time on a gluten free diet. *Only the cases were the Pearson correlation test were significant ($p < 0,05$) are shown. EM: Effector memory, CM: Central memory, TEMRA: Effector memory cells re-expressing CD45RA.*

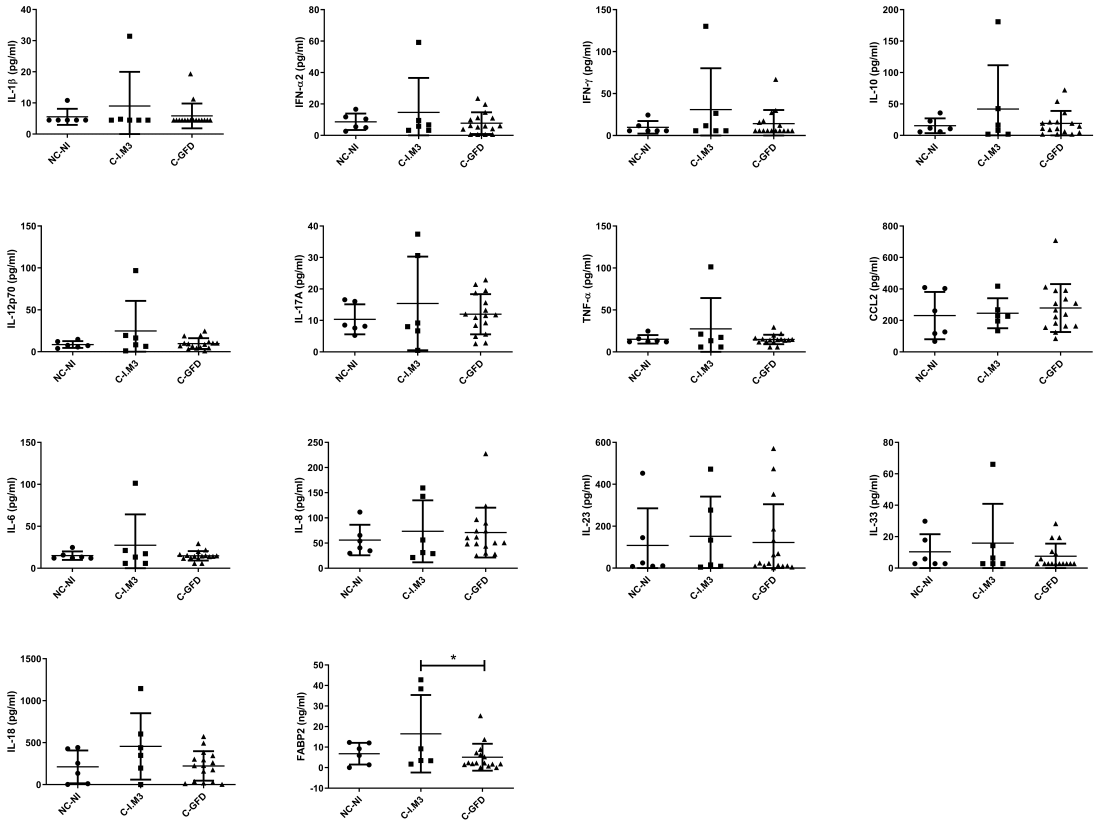

Figure VI.11: Plasma cytokines from coeliac disease patients. *Expression of IL-1β, IFN-α2, IFN-γ, IL-10, IL-12p70, IL-17A, TNF-α, CCL2, IL-6, IL-8, IL-23, IL-33, IL-18 and FABP2 of non-coeliac not inflamed (NC-NI) controls, coeliac patients with inflammation (Marsh 3) (C-I.M3) and coeliac patients on a gluten-free diet (C-GFD). One-way ANOVA with uncorrected Fishers LSD test was applied in all cases. P-values < 0.05 were considered significant (*p < 0.05). Data shown as pg/ml except for FABP2 which is in ng/ml.*

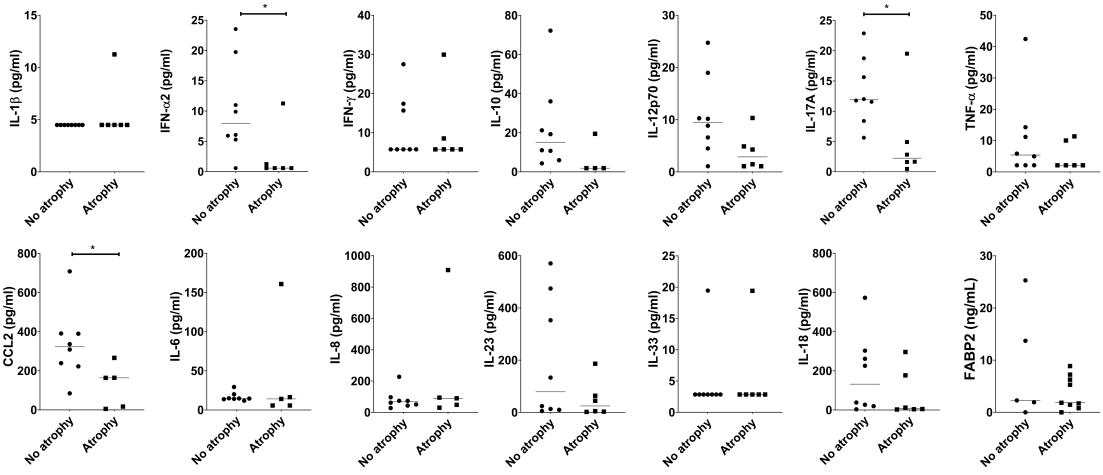

Figure VI.12: Plasma cytokines from coeliac disease patients on a gluten free diet stratified by atrophy. *Expression of IL-1β, IFN-α2, IFN-γ, IL-10, IL-12p70, IL-17A, TNF-α, CCL2, IL-6, IL-8, IL-23, IL-33, IL-18 and FABP2 on plasma samples from coeliac patients on a gluten-free diet. Patients were stratified based on the presence of gut atrophy. Unpaired Mann-Whitney U test was performed in all cases. P-values < 0.05 were considered significant (*p < 0.05). Data shown as pg/ml except for FABP2 which is in ng/ml.*

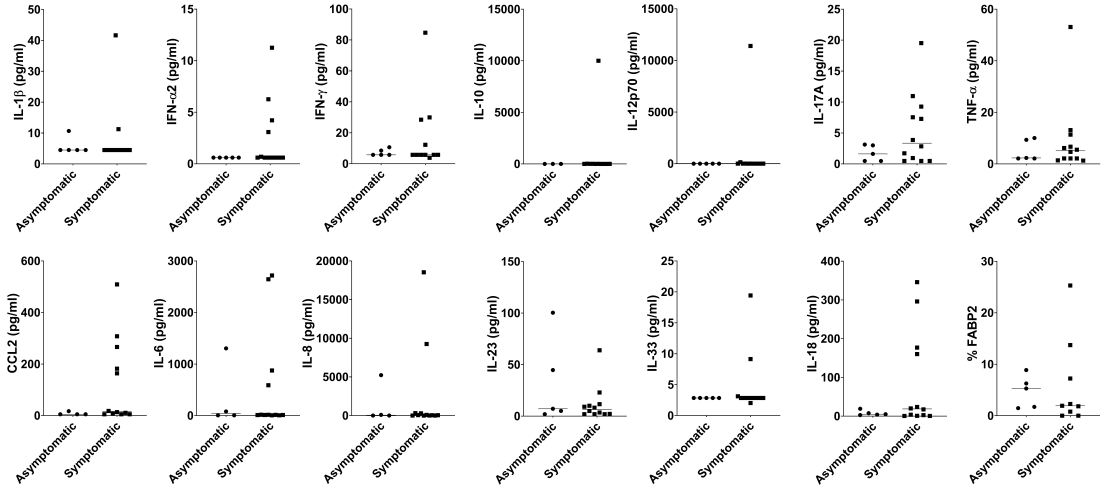

Figure VI.13: Plasma cytokines from coeliac disease patients on a gluten free diet stratified by symptoms. *Expression of IL-1β, IFN-α2, IFN-γ, IL-10, IL-12p70, IL-17A, TNF-α, CCL2, IL-6, IL-8, IL-23, IL-33, IL-18 and FABP2 on plasma samples from coeliac patients on a gluten-free diet. Patients were based on the presence of symptoms. Unpaired Mann-Whitney U test was performed in all cases. P-values < 0.05 were considered significant (*p < 0.05). Data shown as pg/ml except for FABP2 which is in ng/ml.*

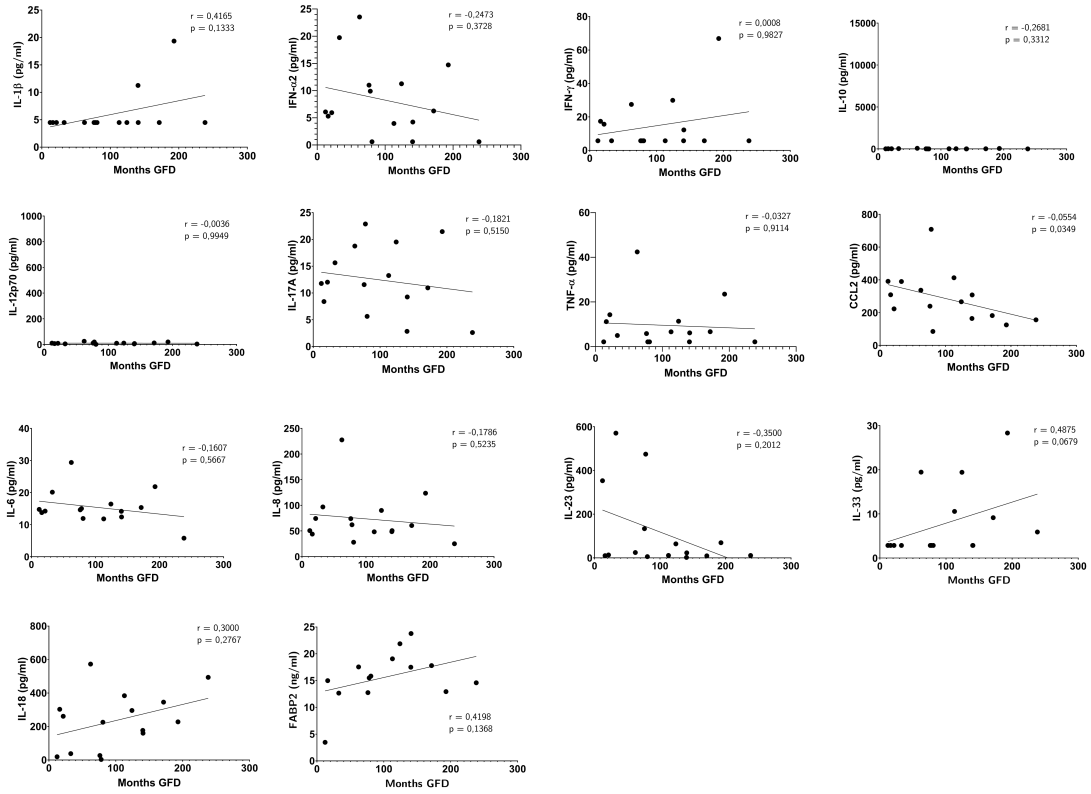

Figure VI.14: Correpation between plasma cytokines and time on a gluten free diet. *Expression of IL-1β, IFN-α2, IFN-γ, IL-10, IL-12p70, IL-17A, TNF-α, CCL2, IL-6, IL-8, IL-23, IL-33, IL-18 and FABP2 on plasma samples from coeliac patients on a gluten-free diet. Spearman test was performed for the time on GFD (months) and cytokine or FABP2 levels. P-values < 0.05 were considered significant. Data shown as pg/ml except for FABP2 which is in ng/ml.*

have revealed that the peripheral immune response in CD is not only altered during the active phase of the disease, but it also undergoes long-term modulation following gluten withdrawal as occurs in the LP.

In C-GFD PBMC a reduction in T$\gamma\delta$ CD4 cells and CD38 expression on total T$\gamma\delta$ cells can be observed, alongside an expansion of CD38$^+$ T_{reg}. These changes suggest the presence of immunoregulatory mechanisms that may contribute to immune recovery after gluten removal. However, this modulation appears to be reversible, as previous studies have shown that a short-term gluten challenge reactivates gut-homing T$\gamma\delta$ T cells (CD103$^+$ Integrin $\beta7^{hi}$ CD38$^+$)[56,215].

During the active phase of the disease in newly diagnosed patients, the immune profile follows the expected patterns, characterized by a sustained immune activation. The over-expression of TLR4 in B cells and intermediate monocytes agrees with previous findings on mRNA[171,169]. Similarly, the increased CXCR3 expression in EM CD8 T cells reinforces the established role of the CXCR3 C-X-C motif chemokine ligand 10 axis in the immune cell recruitment observed in CD[216]. Moreover, the heightened CCR9 expression levels in B cells and memory CD8 T cells suggest an enhanced gut trafficking, while the elevated CD38 expression across various T cell subsets further supports the inflammatory state characterizing active disease. These findings align with reports of increased circulating CD8 CD38$^+$ T cells following gluten challenge in CD patients[56,215]. Together, these results confirm the extensive immune activation and recruitment of immune cells observed in CD.

Unsupervised clustering analysis provides additional insights, revealing distinct immune subsets shifts that complement the traditional analysis. Notably, plasmablast expansion in C-I.M3 patients and monocyte depletion in C-GFD patients emerge as key differentiating features between the inflammatory and post-GFD states. Further studies in a larger cohort are needed to confirm if this latest feature can be used as a biomarker to assist in the diagnosis of CD patients who are already on a GFD and are hesitant to reintroduce gluten for diagnostic purposes. If these results are validated, a blood test biomarker might be possible in these cases, providing an easy and non-invasive technique.

Despite negative serology and good adherence to the diet, many CD patients have persistent atrophy as previously discussed. The results of this study, evidenced that the peripheral immune system retains signs of this activation, an increase in ILC CD4$^+$CD8$^+$ and NKT CD4 cells, along with a heightened Fas expression on certain T cell subsets and NKT cells. Additionally, the upregulation of Integrin $\alpha4^+$ and Integrin $\beta7$ on CD8$^+$ T cells and CD4$^+$ NKT cells in patients with mucosal atrophy suggests an increased migration of active immune cells to the intestine. Nevertheless, the unsupervised clustering analysis does not fully support all these findings. Therefore, larger studies are needed to validate these results and specifically examine these markers and cell subsets.

Even if the results of supervised analysis could not always be confirmed with an unsupervised analysis the combination of both methodologies broadens our understanding of immune differences in CD. While supervised analysis relies on predefined gating strategies and may overlook unexpected cellular subpopulations[208], unsupervised methods enable the data-driven identification of immune subsets without predefined gating constraints[217]. However, mathematically optimal clustering does not always align with biological meaningfulness[218]. In the context of this study, unsupervised analysis reveals previously unappreciated variations in immune subsets, such as the increase in naive CD4$^+$ T cells in patients with mucosal atrophy. Nonetheless, the lack of validation for some of these findings underscores the need to integrate both approaches to ensure robust and biologically meaningful conclusions. Future validation in independent cohorts, using manual gating strategies, will be essential to confirm the relevance of these immune subsets. Additionally, expanding the study to NC individuals on a GFD, such as family members of CD patients, could provide further insights into immune modulation in the absence of gluten exposure.

The impact of symptomatology on the immune activation in C-GFD patients further high-

lights heterogeneity within this group. Symptomatic patients exhibit an increased expression of inflammatory markers, mirroring the immune activation observed in C-I.M3 patients and reinforcing the association between persistent immune activation and symptomatology. Interestingly, asymptomatic patients show elevated CCR2, CCR9 and TLR4 expression levels on some subsets which might be a reflection of the ongoing mucosal inflammation and atrophy even in patients without symptoms. A larger cohort of C-GFD patients, grouped by the presence or absence of atrophy and further subdivided in symptomatic and asymptomatic groups, would be of great value to elucidate this point. This could determine whether there is a peripheral immune signature of CD that is independent of mucosal atrophy and related to extraintestinal symptomatology.

The time on GFD also appears to modulate the immune migration and inflammatory marker expression, contributing to immune quiescence in long-term treated patients. It has been confirmed that the correlations are exclusively to the time on GFD, as markers do not consistently increase or decrease with age. The negative correlation between the time on GFD and Integrin $\beta7$ and Integrin $\alpha4^+$ Integrin $\beta7^+$ expression suggests a progressive decline in immune cell trafficking over time, likely reflecting improvements in the mucosal status after the initiation of the GFD (**Tab. IV.1**) Additionally, a longer time on the diet correlates with a decrease in $CD4^+$ naive T cells, indicating a shift in T cell composition over time. However, some inflammatory pathways persist despite a prolonged GFD adherence, as evidenced by the positive correlation between time on GFD and CXCR5, TLR4, and CD38 expression in certain $T\gamma\delta$ and T cell subsets. This suggests that the mechanisms of immune surveillance may remain active even in long-term treated patients, possibly contributing to the persistent atrophy observed in many patients. A longitudinal study of the same patients from the moment of diagnosis while still consuming gluten, followed over time on a GFD, would be valuable to corroborate these findings.

Plasma immune mediators further illustrate the effects of dietary treatment. Inflammatory markers generally normalize in C-GFD patients, with C-I.M3 patients showing higher FABP2 levels, indicative of a gut barrier dysfunction. Additionally, the negative correlation between time on GFD and CCL2 plasma levels further supports the notion that a prolonged dietary treatment dampens systemic inflammation. Notably, patients with atrophy exhibit reduced plasma IFN-$\alpha2$, IL-17A, and CCL2 levels, suggesting a paradoxical immune downregulation in the presence of mucosal damage.

Overall, these results highlight distinct immune alterations associated with active disease, atrophy, symptomatology, and dietary intervention. While atrophy and persistence of symptoms are linked to immune activation, prolonged adherence to a GFD leads to a reduction in migratory capacity and normalization of inflammatory biomarkers. However, the persistent elevation of markers such as CXCR3, CD38, and TLR4 in specific subsets suggests that some aspects of immune activation may endure despite dietary treatment. Thus lack of validation in unsupervised clustering analysis suggests that the differences in immune subsets may be subtle. These findings underscore the need for further research into the long-term immunological consequences of CD and the potential for targeted immunomodulatory interventions.

7

Discussion

The persistent immune dysfunction in CD, emphasizing the need to rethink disease management beyond the dietary intervention alone. Despite the adherence to a GFD and a partial immune normalization, many patients continue to exhibit persistent atrophy, IEL abnormalities, altered PBMC profiles, and ongoing LP activation, emphasizing the need for improved disease monitoring strategies. These findings support the hypothesis that persistent mucosal atrophy in CD patients on a GFD may be associated with immune alterations at both the mucosal and systemic levels.

7.1 Regional Variations at the Gut Immune System

A deeper understanding of the gut immune system is considered essential for unraveling its complex role in health and disease. Notably, the characterization of IEL across the gut has highlighted the duodenum as a particularly unique compartment, where an expansion of both T cells and $CD7^+$ NK-like cells has been observed. Furthermore, it has been suggested that IEL exhibit a non-inflammatory phenotype[144]. In agreement with this, in this thesis, low IL-15Rα expression and reduced NKG2D levels in T$\gamma\delta$ cells were identified in health. These findings align with previous reports in which an immunoregulatory function has been attributed to the duodenum[122,82]. These findings on the immunoregulatory environment of the duodenum, characterized by low IL-15Rα expression and a reduced inflammatory signaling, provide a compelling context for the understanding of the pathophysiology of CD, which predominantly affects the small intestine. The immune quiescence observed in the duodenal mucosa may play a critical role in maintaining tolerance to dietary antigens, including gluten in CD patients and other antigens in the general population. Disruptions to this balance could contribute to disease onset.

7.2 CD Prevalence and Impact of Dietary Intervention

Immune alterations may be manifested differently across age groups. Notably, such differences might partially explain the higher prevalence of CD in children compared to adults, as described in previous studies[28,24]. This intriguing issue raises the possibility that more cases are diagnosed in children than in adults. One possible reason for this could be that some children may adapt to a gluten-containing diet over time if they were not diagnosed, which could further explain the lower prevalence in adults. Another possibility is that the gradual introduction of solid foods makes the disease easier to identify in children. Indeed, children report greater rates of both gastrointestinal and extraintestinal symptom resolution as compared to adults following a GFD[219]. Tapsas et al. described that younger children suffer primarily from gastrointestinal symptoms and growth failure, and adolescents from extra-intestinal manifestations[220]. Therefore, adults may normalize their manly extra-intestinal symptoms and unconsciously adopt a reduced-gluten containing diet, leading to underdiagnosis. The higher prevalence in children underscores the importance of early screening and diagnosis.

The impact of early versus late dietary intervention on immune recovery has also been explored, with findings suggesting that earlier initiation of a GFD may lead to more effective immune normalization[221]. Greater immune plasticity in younger individuals might be a potential explanation, whereas delayed diagnosis and late GFD initiation appear to be associated with prolonged immune dysregulation, altered gut-homing marker expression, and long-term consequences for immune homeostasis. Histological recovery, defined by the resolution of villous atrophy resolution, seems to be more likely in patients who begin a GFD earlier, whereas those with delayed intervention may experience persistent mucosal abnormalities despite strict dietary adherence[195].

7.3 Epithelial Barrier and Microbiota Alterations in CD

Epithelial integrity has been described as a crucial factor in CD, with intestinal permeability being regulated by enterocytes through tight junction proteins. Disruptions in these structures, particularly those mediated by zonulin, have been shown to increase permeability and facilitate the translocation of gluten peptides, thereby triggering immune responses[222]. Moreover, IEC and macrophages can express MHCII in addition to cDC, shaping the function of previously primed mucosal $CD4^+$ T cells, including those producing IL-10, a key immunoregulatory cytokine. Dietary proteins have been shown to enhance MHCII expression by IEC, a process necessary to sustain IL-10-producing T_{reg} cells in the intestinal LP. Furthermore, a subset of $CD4^+CD8^+$ IEL whose development depends on MHCII expression by IEC, has been proposed to help maintain intestinal tolerance to the microbiota[223]. Beyond epithelial barrier dysfunction, microbial dysregulation has also been implicated in CD pathogenesis. Early-life factors such as cesarean delivery and antibiotic exposure have been associated with increased disease susceptibility[222]. Moreover, high-resolution microbiome analyses in treated CD patients have revealed significant inter-individual variability, emphasizing the role of the microbial composition in immune activation and disease progression[224].

7.4 Immune Dysregulation in Active CD Patients

The increased NKG2D expression in $CD4^+$ and $CD4^+CD8^+$ IEL, particularly in those with Marsh 3, suggest a potential role for this receptor in disease progression. Therefore, NKG2D could be considered a therapeutic target in cases where villous atrophy persists despite adherence to a GFD.

However, a non-inflammatory, regulatory phenotype may still be maintained in the duodenum. Despite the well-established role of IL-15 in CD pathogenesis, no increase in IL-15Rα

expression has been detected in duodenal IEL from CD patients. These results are in agreement with the previously proposed immunoregulatory role of IEL[122,82].

Given the apparent absence of a functional IL-15 receptor in IEL, this supports the theory that other cytokines -such as IL-7- may play a more prominent role in CD pathogenesis in the IEL compartment[160]. However, while IL-15Rα expression has remained unchanged in IEL, an increased expression has been observed in the $CD45^-$ fraction, presumably corresponding to IEC. This finding has been interpreted as further evidence of IL-15 trans-presentation from IEC to IEL. The discrepancy between increased IL-15Rα expression in IEC and unchanged levels in IL-2Rβ in IEL might be explained by receptor internalization. In active CD patients, it is possible that the IL-15 signal on the IEL has been already internalized, which could account for the inability to detect it. This hypothesis aligns with the known mechanisms of cytokine receptor trafficking and signaling, where the binding of the ligand often leads to receptor internalization as part of the signaling process.

Single-cell RNA sequencing and intracellular flow cytometry could be used to determine whether IL-15Rα is internalized upon ligand binding in IEL, providing insights into receptor trafficking mechanisms. Additionally, immunofluorescence microscopy could help visualize IL-15Rα localization and its potential interaction with IL-2Rβ in situ. Functional studies using organoid or organ-on-chip models, where IEC-IEL interactions can be closely monitored, would allow controlled manipulation of IL-15 signaling and its downstream effects[225].

Beyond the IEL compartment, in the LP from active CD patients (C-I.M3) a pro-inflammatory innate-like profile has been observed, characterized by an expansion of NK cells, ILC and Tγδ cells[197,166,168]. This immune shift is accompanied by a reduction in total T cells, $CD4^+$ T cells, T_{reg} and $CD4^+CD8^+$ T cells, along with increased levels of IL-18 and IL-12p70 in the biopsy milieu, reflecting cytokine changes in the duodenal environment. Alterations in peripheral blood immune cells further reinforce the pro-inflammatory nature of active CD. An elevated expression of gut-homing receptor CCR9 has been reported, along with an increase in the activation marker CD38, highlighting systemic immune activation in affected patients

This aligns with earlier studies showing a higher frequency of $CCR9^+$ T cells in PBMC from untreated CD patients and a reduction in IEL and LPMC T cells. However, the thesis results indicate a persistent elevation of CCR9 expression in some GFD-treated patients LPL[226,227]. This discrepancy might be due to differences in patient demographics, duration of GFD, or the high-resolution analysis provided by flow cytometry. Notably, CCR9 has been shown to inhibit T_{reg} development[228] which may further contribute to mucosal inflammation despite gluten exclusion. Additionally, methodological differences, particularly the use of flow cytometry, may have affected the results compared to previous studies. By enabling precise quantification and detailed phenotyping of immune cells, flow cytometry allows for the identification of subtle immune alterations that might otherwise go undetected, underscoring the complexity of immune regulation in CD.

7.5 Immune Alterations in GFD Treated Patients

Distinct immunological features of CD persist despite dietary adherence. IEL continue to exhibit an expansion of Tγδ cells, regardless of GFD adherence, mucosal status, or the presence of symptoms, as previously described[142,51]. Nevertheless, a trend toward normalization in the proportions of $CD3^-$ and Tγδ cells has been observed, correlating with the duration of GFD adherence.

Changes in the peripheral immune system further reflect the impact of GFD, with reductions in $CD4^+$ Tγδ cells and CD38 expression on total Tγδ cells, alongside with an expansion of $CD38^+$ T_{reg}. However, these modifications appear to be easily reversible, as a short-term gluten challenge has been shown to induce a reactivation of gut-homing Tγδ T cells ($CD103^+$ Integrin $\beta7^{hi}$ $CD38^+$)[56,215]. Additionally, a reduction in a specific monocyte population in peripheral

blood has been identified as a potential hallmark of the immune profile in CD patients adhering to a GFD. Unsupervised clustering analysis has further revealed that patients on a GFD with atrophic mucosa exhibit a reduction in classical monocytes, accompanied by an increase in cDC2 on peripheral blood. This expansion of cDC2 may represent an attempt to compensate for the altered immune homeostasis, potentially influencing the mechanisms oral tolerance in these patients. Given that specific populations of migratory cDC likely contribute to the induction of oral tolerance in different anatomical locations[223], the observed immune shifts could reflect a broader adaptation to chronic antigenic exposure. Additionally, CX3CR1-expressing macrophages have been shown to form transepithelial protrusions that facilitate the transfer of luminal antigens to neighboring $CD103^+$ cDC, a process essential for the induction of oral tolerance[229]. Future research should investigate whether these expanded peripheral cDC2 originate from CD103+ cDC in the LP, which may encounter and process antigens in a distinct manner. Additionally, validating their expansion in GFD-treated patients with atrophic mucosa could offer further insights into their role in immune regulation.

Cytokine levels generally normalize with long-term GFD adherence; however, increased FABP2 levels in the duodenal microenvironment suggest persistent alterations in intestinal permeability. Furthermore, a prolonged GFD adherence has been associated with lower plasma CCL2 levels. Differences in immune regulation between patients with ongoing mucosal atrophy and those achieving mucosal healing have also been reported, with atrophic patients exhibiting lower levels of IFN-α2, IL-17A, and CCL2, indicating a distinct regulatory immune response.

In symptomatic GFD-treated patients, persistent immune activation has been reported despite prolonged gluten exclusion. However, the resolution of symptoms does not necessarily coincide with full immune normalization. Asymptomatic CD patients exhibit elevated Fas and Perforin-high expression in IEL, suggesting an increased cytotoxic potential without active inflammation. These observations raise the possibility of irreversible changes in the IEL compartment, requiring further investigation. Furthermore, a higher CCR2, CCR9, and TLR4 expression has been detected in multiple immune subsets in PBMC of asymptomatic patients, reflecting again distinct immune regulation patterns compared to symptomatic individuals.

These immune dynamics highlight the need for a deeper understanding of gut-localized antigen processing and T cell homing. This is essential to clarifying how oral tolerance is maintained. Specialized $MHCII^+AIRE^+ROR\gamma t^+$ APC, expressing $\alpha v\beta 8$, may contribute to tolerance by migrating from the LP to neonatal mesenteric lymph nodes, while the diversification of microbiota at weaning supports immune maturation. T_{reg} play a key role in tolerance, yet their rapid turnover in the small intestine contrasts with the long-lasting nature of oral tolerance, suggesting that memory-like T_{reg} in secondary lymphoid organs sustain mucosal immune regulation[223]. Murine models indicate that gliadin-specific $CD4^+$ T cells are scarce in the gut, where T_{reg} and effector Th cells predominate, highlighting a balance between tolerance and inflammation. Moreover, an intact microbiota may favor the development of food allergen-specific $ROR\gamma t^+$ $FOXP3^+$ T_{reg}, underscoring the role of commensal bacteria in shaping immune tolerance. Understanding these mechanisms may provide insights into persistent immune alterations in CD despite adherence to a GFD[223].

7.6 Nutritional Alterations in GFD

Dietary factors further shape intestinal health and the development of symptoms. Children with CD who adhere to a GFD also report a high prevalence of functional gastrointestinal disorders (FGID), regardless of whether their diet consists of natural or processed gluten-free foods. The development of FGID appears to be linked to overall caloric intake and dietary fat percentage rather than the specific composition of the GFD[230]. The underlying causes of these symptoms remain unclear, but one possible factor is the consumption of ultra-processed gluten-free foods, which tend to have lower protein content and higher levels of fats and additives. This dietary

imbalance could influence gut function and overall health, potentially contributing to FGID development. The rising popularity of GFD extends beyond CD patients, as many individuals without the pathology have also adopted a GFD, often under the assumption that it offers health benefits[62].

The increased availability of gluten-free products has facilitated the rising trend of GFD adoption, but has also raised concerns about nutritional quality[62]. While a naturally GFD -free from processed foods, breaded products, pastries, and sauces- can be nutritionally beneficial, many manufactured gluten-free products compensate for the absence of gluten by incorporating higher levels of fats, salt, and refined carbohydrates[231,232]. This shift in macronutrient composition has potential long-term health implications, particularly for individuals with CD, who are already at an increased risk of cardiovascular disease[233]. Further research is needed to clarify whether strict GFD adherence mitigates or exacerbates cardiovascular disease risk in CD patients[234].

The nutritional composition of a GFD not only influences metabolic health but may also have implications for immune function in individuals with CD. As dietary patterns shift due to the consumption of processed gluten-free products, the resulting macronutrient imbalances or incorporation of other antigens could contribute to systemic inflammation and immune dysregulation. Given that CD is an immune-mediated disorder, these dietary changes may influence immune cell activity and gut-associated lymphoid tissue responses. Indeed, in symptomatic GFD-treated patients, persistent immune alterations have been observed, including increased gut-homing markers in $CD8^+$ T cells and memory B cells, alongside reduced CXCR3 and CD38 expression on T_{reg} cells from the LP. On the other hand, a longer period of adherence to a GFD adherence has been associated with increased expression of gut-homing markers (Integrins $\alpha 4$, $\beta 7$, CCR9, CCR2) and inflammatory markers (CD2, CD38) within the LP.

At first glance, this might seem paradoxical, but several explanations could account for this phenomenon. Chronic immune stimulation could be driven by non-gluten-related factors, such as microbial-derived immune modulators, epithelial barrier dysfunction, or other dietary components. With time on GFD, immune cells may gradually repopulate the LP as part of mucosal healing. The increase in gut-homing markers could reflect a compensatory homing of lymphocytes to restore gut immune homeostasis. However, the persistence of inflammatory markers suggests that regulatory pathways involved in mucosal healing may not be fully functional, leading to ongoing immune activation despite gluten exclusion.

The consumption of ultra-processed gluten-free foods may contribute to the persistence of low-grade inflammation in CD patients, even in the absence of gluten exposure. This could occur through multiple mechanisms, including increased intestinal permeability and alterations to the microbiota. Given the already elevated intestinal permeability in CD patients[235], such dietary patterns could exacerbate immune activation and blocking mucosal healing. To test this hypothesis, a longitudinal study could compare CD patients on a minimally processed, fiber-rich GFD with those consuming a processed-food GFD. Over time, markers of epithelial integrity, inflammatory cytokine profiles, and gut microbiota composition could be assessed to determine whether dietary patterns influence ongoing inflammation and immune dysregulation in GFD-treated CD patients.

7.7 Disease Management

The observed immune heterogeneity among GFD-treated CD patients underscores the importance of personalized disease monitoring. Persistent immune activation in individuals with mucosal atrophy or ongoing symptoms suggests that adjunctive therapeutic strategies may be necessary beyond GFD alone. Biomarkers such as Integrin $\alpha 4\beta 7$ and TLR4 expression could potentially help in identifying patients at risk for incomplete immune recovery, allowing for more targeted interventions.

Monitoring immune recovery in CD patients on GFD could be enhanced by incorporating these immunological markers. Flow cytometry-based tests, such as peripheral blood T cell analysis, show promising results[51]. This technique could provide valuable insights into the efficacy of GFD adherence and help clinicians to assess the need for additional interventions.

Advances in imaging techniques have also shed light on the monitoring of physiological and microbial changes on C-GFD patients. Recent research using magnetic resonance imaging (MRI) has provided new insights into how GFD affects gut function and microbiome in CD patients. After one year of GFD, gut symptoms, bowel water, and gut transit improved in patients, but without returning to a normal state. Interestingly, the GFD reduced some beneficial gut bacteria, suggesting a potential need for prebiotic treatments to counteract these negative impacts[236].

In conclusion, the complex interplay between diet, immune function, and gut health in CD patients necessitates a multifaceted approach to treatment and monitoring. By combining advanced imaging techniques, immunological markers, and personalized dietary interventions, clinicians may be better equipped to manage the diverse manifestations of CD and improve long-term outcomes for patients.

7.8 Persistent Villous Atrophy

In this work, a partial normalization of immune responses has been reported in patients on a GFD, leading to reduced inflammation and restoration of certain immune subsets, particularly within the LP. However, despite strict dietary adherence, the presence of a persistent villous atrophy in 68.4% of CD patients has been shown, even though the duodenal immune infiltrate in the LP largely normalizes, except for elevated T$\gamma\delta$ cells. Notably, while the majority of patients exhibited atrophy, its severity was lower at diagnosis (**Tab. IV.1**). This supports the hypothesis that adults require more time to recover than children, possibly due to a prolonged exposure to damage over time.

Given that most CD patients still display persistent villous atrophy, in agreement with our findings and others[66,237,238,239,240,241], it is important therefore to highlight at this point RCD. RCD is defined as CD with persistent symptoms of malabsorption and villous atrophy despite at least 12 months of strict adherence to a GFD. With a prevalence of 0.3-1% among CD patients. RCD can be classified into 2 subtypes, with different diagnostic criteria, prognosis, and response to therapy. Type I is characterized by villous atrophy with an IEL population similar to that seen in cCD. In contrast, Type II is defined by aberrant clonal T cell expansion in the gastrointestinal tract, involving $CD3^-$ cells with cytosolic CD3 expression, and is associated with a poorer prognosis and an increased risk of developing ulcerative jejunoileitis or enteropathy-associated T cell lymphoma (EATL)[242,243]. Neoplastic cells are aberrant IEL, whose differentiation in T cells was interrupted by outstanding IL-15 stimulation, acquiring an intermediate phenotype with NK cells. Those neoplastic cells are indeed highly cytotoxic in the intestinal mucosal, inducing severe injury and severe clinical malabsorption. Additionally, aberrant IEL acquire mutations in the JAK1-STAT3 pathway that provide them with a survival advantage and promote progression towards EATL[244]. These mutations enhance their autonomous production of cytokines and promote clonal expansion[245].

In terms of treatment, RCD can be challenging, as it does not respond to the conventional GFD. Management includes nutritional support and the use of immunosuppressive therapies, such as corticosteroids. Type I RCD responds well to immunosuppression and the prognosis is good. Second line therapies generally include multimodality chemotherapy to eliminate the aberrant IEL. If symptoms worsen, high-dose chemotherapy followed by autologous stem cell transplantation (ASCT) is recommended[243]. However, no treatment is effective to cure type II RCD or prevent EATL development. Sequential treatment with cladribine and ASCT can induce clinical and histologic responses and possibly delay EATL development. Future therapies

that target and eliminate aberrant T cells are needed, as the persistence of those non-dividing cells might function as a reservoir for clinical relapse and fuel EATL development[244].

Having described therefore RCD, this raises an interesting question. Does the patients with mucosal atrophy despite GFD[66,237,238,239,240,241] have RCD or, on the contrary, at risk of developing that condition? The findings of this research show that more than half of CD patients still exhibit persistent villous atrophy despite strict adherence to a GFD for an average of 7 ± 5 years, and this raises an important question regarding the definition of RCD. Previous studies have shown that up to 50% of CD patients on a GFD continue to experience symptoms after 6 to 12 months, a condition termed non-responsive CD[239]. A GFD results in seroconversion to negative in more than 80% of patients within 6 months[246]. However, in adults, the recovery of mucosal histological is delayed and not universal. Only one third of patients present a normal villous architecture within 2 years, two thirds within 5 years, and 90 % by 9 years[237,238,241]. Notably, 30-40 % of patients are slow responders, taking more than 5 years to achieve a complete histological remission[240,247].

These findings suggest that persistent villous atrophy may not be an exclusive indicator of RCD but rather, it may reflect a more complex form of CD that does not fit the traditional definition of refractoriness. Consequently, the question arises as to whether the concept of RCD should be redefined, considering that the persistence of villous atrophy could be a marker of prolonged damage rather than a definitive indication of clinical refractoriness, possibly representing a slower or more insidious progression of the disease.

7.9 Methodological Considerations and Study Limitations

While this work provides valuable insights into immune alterations in CD patients, it also raises important methodological and interpretative considerations that need to be addressed. Immune profiling in CD is inherently complex, and no single methodological approach can fully capture the intricacies of immune dysregulation. Functional assays should be integrated to better elucidate the basis mechanistic of the observed immune alterations across all immune compartments. A deeper understanding of these mechanisms could pave the way for more targeted therapeutic approaches and improved biomarkers for monitoring disease activity and response to the treatment response.

The IEL enrichment procedure and the associate technical complexities pose significant challenges for flow cytometry analyses, introducing potential variations in cell purity and viability that could subtly influence immunological interpretations. Further optimization of IEL isolation methods is needed to preserve functional diversity and enhance data accuracy. Moreover, cryopreservation approaches have been shown to impact IEL cytokine responses, highlighting the necessity for specialized culture conditions that consider the distinct characteristics of these cells. These findings emphasize the plasticity of IEL under varying experimental conditions and reinforce the need for optimized activation protocols, distinct from those used for PBMC, in order to enhance the reproducibility and reliability of IEL-based studies.

Patient heterogeneity represents a major limitation, compounded by the studys relatively small sample size. The insufficient number of isolated cells precluded comprehensive unsupervised analysis of LPL and limited the scope of T$\gamma\delta$ IEL investigations. Additionally, the absence of mandatory patient follow-up protocols and the tendency of asymptomatic individuals to avoid medical consultations introduce potential selection biases that may skew research findings.

Another key limitation is the lack of GFD adherence questionnaires for control groups, which represents a significant mechanism of verification. The absence of standardized dietary assessment tools hinders a more precise correlation between immune alterations and dietary patterns, potentially affecting the interpretation of results. Future studies should incorporate validated dietary assessment methods to ensure a more rigorous evaluation of the impact of

GFD adherence on immune parameters.

7.10 Future Directions and Lessons Learned

Future research should focus on longitudinal studies with diverse patient cohorts, standardized cell isolation protocols, and comprehensive functional assays to track the immune evolution over extended periods of GFD adherence. Integrating advanced immunological techniques with detailed clinical observations will provide valuable insights into the long-term effects of GFD on immune function and gut health. Additionally, exploring adjuvant therapies to address persistent immune dysregulation could help to develop more effective treatment strategies for CD patients who do not fully respond to a GFD alone.

In this context, the need for personalized dietary or immunomodulatory interventions is becoming increasingly apparent. For patients with persistent symptoms or immune activation despite strict GFD adherence, exploring microbiota state and additional dietary modifications, such as avoiding FODMAP, might be beneficial. However, any dietary changes should be carefully monitored and implemented under professional guidance to ensure nutritional adequacy.

The findings of this thesis highlight the complexity of immune regulation in CD, demonstrating that despite strict adherence to a GFD, many patients continue to experience villous atrophy and immune activation. This suggests that while initial immune normalization occurs, it may be followed by unresolved chronic inflammation, potentially driven by microbial modulators or by other dietary antigens. These insights underscore the urgent need for personalized therapeutic strategies beyond gluten exclusion, targeting immune dysregulation to improve the long-term outcomes for CD patients.

8

Conclusions

- Despite strict adherence to a gluten-free diet, 68.4% of coeliac disease patients continue to show villous atrophy.
- Increased NKG2D expression on intraepithelial lymphocytes correlates with villous atrophy, suggesting its potential as a target for immunotherapies.
- IL-15 receptors are not elevated on intraepithelial lymphocytes from coeliac disease patients suggesting that other cytokines contribute to their cytotoxicity.
- Gluten free diet restores the immune balance in lamina propria lymphocytes. However, symptomatic patients exhibit increased gut-homing and inflammatory markers, which further rise with prolonged adherence to the diet.
- Villous atrophy and persistent symptoms are associated with peripheral immune activation, whereas longer adherence to gluten free diet reduces migratory capacity but increases the presence of inflammatory biomarkers.
- The rise in inflammatory markers in both the mucosal and peripheral immune system with prolonged adherence to a gluten free diet may reflect an initial immune normalization, followed by unresolved chronic inflammation potentially linked to microbial drivers or other dietary antigens.

References

1. Sollid LM, Jabri B. *Triggers and drivers of autoimmunity: lessons from coeliac disease*. Nature Reviews Immunology 4 2013;13:294–302.
2. Raiteri A, Granito A, Giamperoli A, Catenaro T, Negrini G, Tovoli F. *Current guidelines for the management of celiac disease: A systematic review with comparative analysis*. World Journal of Gastroenterology 1 2022;28:154–75.
3. Ludvigsson JF, Yao J, Lebwohl B, Green PHR, Yuan S, Leffler D. *Coeliac disease: complications and comorbidities*. Nature Reviews: Gastroenterology & Hepatology 4 2025;22:252–64.
4. Al-Toma A, Volta U, Auricchio R, et al. *European Society for the Study of Coeliac Disease (ESsCD) guideline for coeliac disease and other gluten-related disorders*. United European Gastroenterology Journal 5 2019;7:583–613.
5. Ludvigsson JF, Leffler DA, Bai JC, et al. *The Oslo definitions for coeliac disease and related terms*. Gut 2013;62:43–52.
6. Rubio-Tapia A, Murray JA. *Classification and management of refractory coeliac disease*. Gut 4 2010;59:547–57.
7. Megiorni F, Pizzuti A. *HLA-DQA1 and HLA-DQB1 in Celiac disease predisposition: practical implications of the HLA molecular typing*. Journal of Biomedical Science 2012;19:88.
8. Abadie V, Sollid LM, Barreiro LB, Jabrì B. *Integration of genetic and immunological insights into a model of celiac disease pathogenesis*. Annual Review of Immunology 2011;29:493–525.
9. Al-Toma A, Goerres MS, Meijer JWR, Peña AS, Crusius JBA, Mulder CJ. *Human Leukocyte Antigen-DQ2 Homozygosity and the Development of Refractory Celiac Disease and Enteropathy- Associated T-Cell Lymphoma*. Clinical Gastroenterology and Hepatology 3 2006:315–9.
10. Dubois P, Trynka G, Franke L, et al. *Multiple common variants for celiac disease influencing immune gene expression*. Nature Genetics 2010;42:295–302.
11. Asri N, Mohammadi S, Jahdkaran M, Rostami-Nejad M, Rezaei-Tavirani M, Mohebbi S. *Viral infections in celiac disease: What should be considered for better management*. Clinical and Experimental Medicine 2024;25:25.

12. Reale A, Trevisan M, Alvisi G, Palù G. *The silent enemy: Celiac disease goes viral*. Journal of Cellular Physiology 4 2018;233:2693–4.

13. Matera M, Guandalini S. *How the Microbiota May Affect Celiac Disease and What We Can Do*. Nutrients 12 2024;16:1882.

14. Pes GM, Bibbò S, Dore MP. *Coeliac disease: beyond genetic susceptibility and gluten. A narrative review*. Annals of Medicine 1 2019;51:1–16.

15. Verdú EF, Schuppan D. *Co-factors, Microbes, and Immunogenetics in Celiac Disease to Guide Novel Approaches for Diagnosis and Treatment*. Gastroenterology 5 2021;161:1395–1411.e4.

16. Ruiz-Carnicer Á, Segura V, Lourdes Moreno M de, Coronel-Rodríguez C, Sousa C, Comino I. *Transfer of celiac disease-associated immunogenic gluten peptides in breast milk: variability in kinetics of secretion*. Frontiers in Immunology 2024;15:1405344.

17. Rahmani S, Galipeau H, Clarizio A, et al. *Gluten dependent activation of CD4+ T cells by MHC class II-expressing epithelium*. Gastroenterology 6 2024;167:1113–28.

18. Dunne MR, Byrne G, Chirdo FG, Feighery C. *Coeliac Disease Pathogenesis: The Uncertainties of a Well-Known Immune Mediated Disorder*. Frontiers in Immunology 2020;11:1374.

19. Fitzpatrick M, Antanavicuite A, Provine NM, Garner LC, Soilleux EJ, Klenerman P. *O43 The phenotype and TCR repertoire of intestinal CD8+ T cells is altered in coeliac disease*. Gut 2021;70:A24.

20. Shalimar DM, Das P, Sreenivas V, Gupta SD, Panda SK, Makharia GK. *Mechanism of villous atrophy in celiac disease: role of apoptosis and epithelial regeneration*. Archives of Pathology & Laboratory Medicine 9 2013;137:1262–9.

21. Rizzi A, Gioacchino MD, Gammeri L, et al. *The Emerging Role of Innate Lymphoid Cells (ILCs) and Alarmins in Celiac Disease: An Update on Pathophysiological Insights, Potential Use as Disease Biomarkers, and Therapeutic Implications*. Cells 14 2023;12:1910.

22. Giuffré M, Gazzin S, Zoratti C, et al. *Celiac Disease and Neurological Manifestations: From Gluten to Neuroinflammation*. International Journal of Molecular Sciences 24 2022;23:15564.

23. Voisine J, Abadie V. *Interplay Between Gluten, HLA, Innate and Adaptive Immunity Orchestrates the Development of Coeliac Disease*. Frontiers in Immunology 2021;12:674313.

24. Singh P, Arora A, Strand TA, et al. *Global Prevalence of Celiac Disease: Systematic Review and Meta-analysis*. Clinical Gastroenterology and Hepatology 6 2018;16:823–836.e2.

25. Celdir MG, Jansson-Knodell CL, Hujoel IA, et al. *Latitude and Celiac Disease Prevalence: A Meta-Analysis and Meta-Regression*. Clinical Gastroenterology and Hepatology 6 2020;20:E1231–E1239.

26. Mariné M, Farre C, Alsina M, et al. *The prevalence of coeliac disease is significantly higher in children compared with adults*. Alimentary Pharmacology & Therapeutics 4 2010;33:477–86.

27. Jansson-Knodell CL, Hujoel IA, West CP, et al. *Sex Difference in Celiac Disease in Undiagnosed Populations: A Systematic Review and Meta-analysis*. Clinical Gastroenterology and Hepatology 10 2019;17:1954–1968.E13.

28. Arau B, Dietl B, Sudrià-Lopez E, et al. *A Population-Based Cross-Sectional Study of Paediatric Coeliac Disease in Catalonia Showed a Downward Trend in Prevalence Compared to the Previous Decade*. Nutrients 24 2023;15:5100.

29. King J, Jeong J, Underwood FE, et al. *Incidence of Celiac Disease Is Increasing Over Time : A Systematic Review and Meta-analysis*. The American Journal of Gastroenterology 4 2020;115:507–25.

30. Lunet N, Azevedo A. *On the comparability of population-based and hospital-based*. Gaceta Sanitaria 6 2009;23:564.

31. Kvamme JM, Sørbye SW, Florholmen J, Halstensen TS. *Population-based screening for celiac disease reveals that the majority of patients are undiagnosed and improve on a gluten-free diet*. Scientific Reports 2022;12:12647.

32. Castaño M, Gómez-Gordo R, Cuevas D, Núñez C. *Systematic Review and Meta-Analysis of Prevalence of Coeliac Disease in Women with Infertility*. Nutrients 8 2019;11:1950.

33. Mahadev S, Laszkowska M, Sundström J, et al. *Prevalence of Celiac Disease in Patients With Iron Deficiency Anemia-A Systematic Review With Meta-analysis*. Gastroenterology 2 2018;155:374–382.E1.

34. Caio G, Volta U, Sapone A, et al. *Celiac disease: a comprehensive current review*. BMC Medicine 1 2019;17:142.

35. Husby S, Koletzko S, Korponay-Szabó IR, et al. *European Society Paediatric Gastroenterology, Hepatology and Nutrition Guidelines for Diagnosing Coeliac Disease 2020*. Journal of Pediatric Gastroenterology and Nutrition 1 2020;70:141–56.

36. Rubio-Tapia A, Ludvigsson JF, Brantner TL, Murray JA, Everhart JE. *The Prevalence of Celiac Disease in the United States*. The American Journal of Gastroenterology 10 2012;107:1538–44.

37. Christophersen A, Ráki M, Bergseng E, et al. *Tetramer-visualized gluten-specific CD4+ T cells in blood as a potential diagnostic marker for coeliac disease without oral gluten challenge*. United European Gastroenterology Journal 4 2014;2:268–78.

38. Sarna VK, Lundin KEA, Mørkrid L, Qiao SW, Sollid LM, Christophersen A. *HLA-DQ-Gluten Tetramer Blood Test Accurately Identifies Patients With and Without Celiac Disease in Absence of Gluten Consumption*. Gastroenterology 4 2017;154:886–896.e6.

39. Villanacci V, Vanoli A, Leoncini G, et al. *Celiac disease: histology-differential diagnosis-complications. A practical approach*. Pathologica 3 2020;113:186–96.

40. Marsh MN. *Gluten, major histocompatibility complex, and the small intestine. A molecular and immunobiologic approach to the spectrum of gluten sensitivity ('celiac sprue')*. Gastroenterology 1 1992;102:330–54.

41. Oberhuber G, Granditsch G, Vogelsang H. *The histopathology of coeliac disease: time for a standardized report scheme for pathologists*. European Journal of Gastroenterology & Hepatology 10 1999;11:1185–94.

42. Corazza GR, Villanacci V, Zambelli C, et al. *Comparison of the interobserver reproducibility with different histologic criteria used in celiac disease*. Clinical Gastroenterology and Hepatology 7 2007;5:838–43.

43. Ebert EC. *Activation of human intraepithelial lymphocytes reduces CD3 expression*. Clinical and Experimental Immunology 3 2003;132:424–9.

44. Lockhart A, Mucida D, Bilate AM. *Intraepithelial Lymphocytes of the Intestine*. Annual Review of Imunology 1 2024;42:289–316.

45. Burgueño-Gómez B, Escudero-Hernández C, Pedro R de, et al. *Duodenal lymphogram as a complementary tool in the diagnosis of celiac disease in adults*. Revista Española de Enfermedades Digestivas 6 2020;112:434–9.

46. Isasi C, Colmenero I, Casco F, et al. *Fibromyalgia and non-celiac gluten sensitivity: a description with remission of fibromyalgia*. Rheumatology International 2014;34:1607–12.

47. Prasad S, Singh P, Singh A, et al. *Reproductive functions and pregnancy outcome in female patients with celiac disease*. Journal of Gastroenterology and Hepatology 7 2024;39:1310–7.

48. García-Hoz C, Crespo L, Pariente R, Andrés AD, Rodríguez-Ramos R, Roy G. *Intraepithelial Lymphogram in the Diagnosis of Celiac Disease in Adult Patients: A Validation Cohort*. Nutrients 8 2024;16:1117.

49. Martín-Cardona A, Carrasco A, Arau B, et al. *$\gamma\delta+$ T-Cells Is a Useful Biomarker for the Differential Diagnosis between Celiac Disease and Non-Celiac Gluten Sensitivity in Patients under Gluten Free Diet*. Nutrients 14 2024;16:2294.

50. Polanco I, Montoro M, Fernández F, Arranz E. *Protocolo para el diagnóstico precoz de la enfermedad celiaca*. Gobierno de Canaria, España: Ministerio de Sanidad, Servicios Sociales e Igualdad, Servicio de Evaluación del Servicio Canario de la Salud (SESCS) 2018.

51. Roy G, Fernández-Bañares F, Corzo M, Gómez-Aguililla S, García-Hoz C, Núñez C. *Intestinal and blood lymphograms as new diagnostic tests for celiac disease*. Frontiers in Immunology 2023;13:1081955.

52. Mayassi T, Ladell K, Gudjonson H, et al. *Chronic Inflammation Permanently Reshapes Tissue-Resident Immunity in Celiac Disease*. Cell 5 2019;176:967–981.E19.

53. Leffler DA, Schuppan D. *Update on serologic testing in celiac disease*. The American Journal of Gastroenterology 12 2010;105:2520–4.

54. Brottveit M, Beitnes ACR, Tollefsen S, et al. *Mucosal Cytokine Response After Short-Term Gluten Challenge in Celiac Disease and Non-Celiac Gluten Sensitivity*. The American Journal of Gastroenterology 5 2013;108:842–50.

55. Camarca A, Radano G, Mase RD, et al. *Short wheat challenge is a reproducible invivo assay to detect immune response to gluten*. Clinical and Experimental Immunology 2 2012;169:129–36.

56. Fernández-Bañares F, López-Palacios N, Corzo M, et al. *Activated gut-homing CD8 T cells for coeliac disease diagnosis on a gluten-free diet*. BMC Medicine 1 2021;19:237.

57. Biesiekierski JR. *What is gluten?* Journal of Gastroenterology and Hepatology S1 2017;32:78–81.

58. Sollid LM, TyeDin JA, Qiao SW, Anderson RP, Gianfrani C, Koning F. *Update 2020: nomenclature and listing of celiac disease-relevant gluten epitopes recognized by CD4+ T cells*. Immunogenetics 2020;72:85–8.

59. Brouns F, Geisslitz S, Guzman C, et al. *Do ancient wheats contain less gluten than modern bread wheat, in favour of better health?* Nutritional Bulletin 2022;47:157–67.

60. Kivelä L, Verdu EF, Caminero A, et al. *Current and emerging therapies for coeliac disease*. Nature Reviews Gastroenterology & Hepatology 2020;18:181–95.

61. Kurppa K, Paavola A, Collin P, et al. *Benefits of a gluten-free diet for asymptomatic patients with serologic markers of celiac disease*. Gastroenterology 3 2014;147:610–617.E1.

62. Kim HS, Patel KG, Orosz E, et al. *Time Trends in the Prevalence of Celiac Disease and Gluten-Free Diet in the US Population: Results From the National Health and Nutrition Examination Surveys 2009-2014*. JAMA Internal Medicine 11 2016;176:1716–7.

63. Herfarth HH, Martin CF, Sandler RS, Kappelman MD, Long MD. *Prevalence of a gluten free diet and improvement of clinical symptoms in patients with inflammatory bowel diseases*. Inflammatory Bowel Diseases 7 2014;20:1194–7.

64. Aljada B, Zohni A, ElMatary W. *The Gluten-Free Diet for Celiac Disease and Beyond*. Nutrients 2021;13:3993.

65. Penny HA, Baggus EMR, Rej A, Snowden JA, Sanders DS. *Non-Responsive Coeliac Disease: A Comprehensive Review from the NHS England National Centre for Refractory Coeliac Disease*. Nutrients 1 2020;12:216.

66. Fernández-Bañares F, Beltrán B, Salas A, et al. *Persistent Villous Atrophy in De Novo Adult Patients With Celiac Disease and Strict Control of Gluten-Free Diet Adherence: A Multicenter Prospective Study (CADER Study)*. The American Journal of Gastroenterology 5 2021;116:1036–43.

67. Lahdenperä A, Ludvigsson J, FälthMagnusson K, Högberg L, Vaarala O. *The effect of gluten-free diet on Th1-Th2-Th3-associated intestinal immune responses in celiac disease*. Scandinavian Journal of Gastroenterology 5 2011;46:538–49.

68. Wieser H, Ruiz-Carnicer Á, Segura V, Comino I, Sousa C. *Challenges of Monitoring the Gluten-Free Diet Adherence in the Management and Follow-Up of Patients with Celiac Disease*. Nutrients 7 2021;13:2274.

69. Bykova SV, Sabelnikova EA, Novikov AA, Baulo EV, Khomeriki SG, Parfenov AI. *Zonulin and I-FABP are markers of enterocyte damage in celiac disease*. Therapeutic Archive Journal 4 2022;94:511–6.

70. Mowat AM. *To respond or not to respond - a personal perspective of intestinal tolerance*. Nature Reviews Immunology 6 2018;18:405–15.

71. Koumbi L, Giouleme O, Vassilopoulou E. *Non-Celiac Gluten Sensitivity and Irritable Bowel Disease: Looking for the Culprits*. Current Developments in Nutrition 12 2020;4:nzaa176.

72. Skodje GI, Sarna VK, Minelle IH, et al. *Fructan, Rather Than Gluten, Induces Symptoms in Patients With Self-Reported Non-Celiac Gluten Sensitivity*. Gastroenterology 3 2017;154:529–539.E2.

73. Li Z, Zhang L, Li L, Du Z. *Evaluation of Serum Levels of Copper and Zinc in Patients with Celiac Disease Seropositivity: Findings from the National Health and Nutrition Examination Survey*. Biological Trace Element Research 2022;201:683–8.

74. Punshon T, Jackson BP. *Essential micronutrient and toxic trace element concentrations in gluten containing and gluten-free foods*. Food Chemistry 2018;252:258–64.

75. Raehsler SL, Choung RS, Marietta E, Murray JA. *Accumulation of Heavy Metals in People on a Gluten-Free Diet*. Clinical Gastroenterology and Hepatology 2 2017;16:244–51.

76. Gaylord A, Trasande L, Kannan K, et al. *Persistent organic pollutant exposure and celiac disease: A pilot study*. Environmental Research 2020;186:109439.

77. Zevallos VF, Raker V, Tenzer S, et al. *Nutritional Wheat Amylase-Trypsin Inhibitors Promote Intestinal Inflammation via Activation of Myeloid Cells*. Gastroenterology 5 2017;152:1100–1113.E12.

78. Schnedl WJ, Mangge H, Schenk M, Enko D. *Non-responsive celiac disease may coincide with additional food intolerance/malabsorption, including histamine intolerance*. Medical Hypotheses 2020;146:110404.

79. Deora NS, Deswal A, Mishra HN. *Alternative Approaches Towards Gluten-Free Dough Development: Recent Trends*. Food Engineering Reviews 2014;6:89–104.

80. Marín-Sanz M, Barro F. *RNAi silencing of wheat gliadins alters the network of transcription factors that regulate the synthesis of seed storage proteins toward maintaining grain protein levels*. Frontiers in Plant Science 2022;13:935851.

81. Sánchez-León S, Marín-Sanz M, Guzmán-López MH, Gavilán-Camacho M, Simón E, Barro F. *CRISPR/Cas9-mediated multiplex gene editing of gamma and omega gliadins: paving the way for gliadin-free wheat*. Journal of Experimental Botany 22 2024;75:7079–95.

82. Mowat AM, Agace WW. *Regional specialization within the intestinal immune system*. Nature Reviews Immunology 10 2014;14:667–85.

83. Pabst O, Mowat AM. *Oral tolerance to food protein*. Mucosal Immunology 3 2012;5:232–9.

84. Agace WW, McCoy KD. *Regionalized Development and Maintenance of the Intestinal Adaptive Immune Landscape*. Immunity 2017;46:532–48.

85. Mörbe U, Jørgensen PH, Jørgensen PB, et al. *Human gut-associated lymphoid tissues (GALT); diversity, structure, and function*. Mucosal Immunology 14 2021;4:793–802.

86. Bjornson-Hooper ZB, Fragiadakis GK, Spitzer MH, et al. *A Comprehensive Atlas of Immunological Differences Between Humans, Mice, and Non-Human Primates*. Frontiers in Immunology 2022;13:867015.

87. Gibbons DL, Spencer J. *Mouse and human intestinal immunity: same ballpark, different players; different rules, same score*. Mucosal Immunology 2 2011;4:148–57.

88. Robinson JP, Ostafe R, Iyengar SN, Rajwa B, Fischer R. *Flow Cytometry: The Next Revolution*. Cells 14 2023;12:1875.

89. Nolan JP. *The evolution of spectral flow cytometry*. Cytometry 10 2022;101:812–7.

90. Cossarizza A, Chang HD, Radbruch A, et al. *Guidelines for the use of flow cytometry and cell sorting in immunological studies (third edition)*. European Journal of Immunology 12 2021;51:2708–3145.

91. Bruggner RV, Bodenmiller B, Dill DL, Tibshirani R, Nolan GP. *Automated identification of stratifying signatures in cellular subpopulations*. Proceedings of the National Academy of Sciences of the United States of America 26 2014;111:E2770–E2777.

92. Feher K, Kirsch J, Radbruch A, Chang HD, Kaiser T. *Cell population identification using fluorescence-minus-one controls with a one-class classifying algorithm*. Bioinformatics 23 2014;30:3372–8.

93. Johnsson K, Wallin J, Fontes M. *BayesFlow: latent modeling of flow cytometry cell populations*. BMC Bioinformatics 2016;17:25.

94. Gong L, Cretella A, Lin Y. *Microfluidic systems for particle capture and release: A review*. Biosensors and Bioelectronics 2023;236:115426.

95. Gong Y, Fan N, Xu Y, Yang X, Peng B, Jiang H. *New advances in microfluidic flow cytometry*. Electrophoresis 8 2019;40:1212–29.

96. Ask EH, Tschan-Plessl A, Hoel HJ, Kolstad A, Holte H, Malmberg KJ. *MetaGate: Interactive Analysis of High-Dimensional Cytometry Data with Meta Data Integration*. bioRxiv 2023.

97. Ghaleb TA, Mohammed MA, Ramadan E. *Automated analysis of flow cytometry data: a systematic review of recent methods*. 2016 2nd International Conference on Open Source Software Computing (OSSCOM) 2016.

98. Ugawa M, Ota S. *Recent Technologies on 2D and 3D Imaging Flow Cytometry*. Cells 24 2024;13:2073.

99. necik K, Meric A, König LM, Theis FJ. *FlowVI: Flow Cytometry Variational Inference*. bioRxiv 2023.

100. Saeys Y, Gassen SV, Lambrecht BN. *Computational flow cytometry: helping to make sense of high-dimensional immunology data*. Nature Reviews Immunology 2016;16:449–62.

101. Bernardo D, Durant L, Mann ER, et al. *Chemokine (C-C Motif) receptor 2 mediates dendritic cell recruitment to the human colon but is not responsible for differences observed in dendritic cell subsets, phenotype, and function between the proximal and distal colon*. Cellular and Molecular Gastroenterology and Hepatology 1 2016;2:22–39.e5.

102. Bernardo D, Marin AC, Fernández-Tomé S, et al. *Human intestinal pro-inflammatory CD11chighCCR2+CX3CR1+ macrophages, but not their tolerogenic CD11cCCR2CX3CR1 counterparts, are expanded in inflammatory bowel disease*. Mucosal Immunology 4 2018;11:1114–26.

103. Mann ER, Bernardo D, English NR, et al. *Compartment-specific immunity in the human gut: properties and functions of dendritic cells in the colon versus the ileum*. Gut 2 2015;65:256–70.

104. Martínez-López M, Iborra S, Conde-Garrosa R, et al. *Microbiota Sensing by Mincle-Syk Axis in Dendritic Cells Regulates Interleukin-17 and -22 Production and Promotes Intestinal Barrier Integrity*. Immunity 2 2019;50:446–461.e9.

105. Park LM, Lannigan J, Jaimes MC. *OMIP-069: Forty-Color Full Spectrum Flow Cytometry Panel for Deep Immunophenotyping of Major Cell Subsets in Human Peripheral Blood*. Cytometry 10 2020;97:1044–51.

106. Olivares-Villagómez D, Kaer LV. *Intestinal Intraepithelial Lymphocytes: Sentinels of the Mucosal Barrier*. Trends in Immunology 4 2018;39:264–75.

107. Cheroutre H, Lambolez F, Mucida D. *The light and dark sides of intestinal intraepithelial lymphocytes*. Nature Reviews Immunology 7 2011;11:445–56.

108. Vandereyken M, James OJ, Swamy M. *Mechanisms of activation of innate-like intraepithelial T lymphocytes*. Mucosal Immunology 5 2020;13:721–31.

109. Escudero-Hernández C, Montalvillo E, Antolín B, et al. *Different Intraepithelial CD3+ Cell Numbers in Crohn's Disease and Ulcerative Colitis*. Inflammatory Bowel Diseases 3 2020;26:e14–e15.

110. Lutter L, Konijnenburg DPH van, Brand EC, Oldenburg B, Wijk F van. *The elusive case of human intraepithelial T cells in gut homeostasis and inflammation*. Nature Reviews Gastroenterology & Hepatology 10 2018;15:637–49.

111. Lebwohl B, Sanders DS, Green PHR. *Coeliac disease*. The Lancet 10115 2017;391:70–81.

112. Vaquero L, Bernardo D, León F, Rodríguez-Martín L, Alvarez-Cuenllas B, Vivas S. *Challenges to drug discovery for celiac disease and approaches to overcome them*. Expert Opinion on Drug Discovery 10 2019;14:957–68.

113. Waldmann TA, Waldmann R, Lin JX, Leonard WJ. *The implications of IL-15 trans-presentation on the immune response*. Advances in Immunology 2022;156:103–32.

114. Quéméner A, Morisseau S, Sousa RP, et al. *IL-15Rα membrane anchorage in either cis or trans is required for stabilization of IL-15 and optimal signaling*. Journal of Cell Science 5 2020;133:jcs236802.

115. Abadie V, Kim SM, Lejeune T, et al. *IL-15, gluten and HLA-DQ8 drive tissue destruction in coeliac disease*. Nature 7796 2020;578:600–4.

116. Malamut G, Cording S, Cerf-Bensussan N. *Recent advances in celiac disease and refractory celiac disease*. F1000Research 2019;8:969.

117. Abadie V, Discepolo V, Jabri B. *Intraepithelial lymphocytes in celiac disease immunopathology*. Seminars in Immunopathology 4 2012;34:551–6.

118. Sabatino AD, Ciccocioppo R, D'Alò S, et al. *Intraepithelial and lamina propria lymphocytes show distinct patterns of apoptosis whereas both populations are active in Fas based cytotoxicity in coeliac disease*. Gut 3 2001;49:380–6.

119. Hüe S, Mention JJ, Monteiro RC, et al. *A direct role for NKG2D/MICA interaction in villous atrophy during celiac disease*. Immunity 3 2004;21:367–77.

120. Lindfors K, Ciacci C, Kurppa K, et al. *Coeliac disease*. Nature Reviews Disease Primers 1 2019;5:3.

121. Fernández-Bañares F, Carrasco A, Martín A, Esteve M. *Systematic review and meta-analysis: Accuracy of both gamma delta+ intraepithelial lymphocytes and coeliac lymphogram evaluated by flow cytometry for coeliac disease diagnosis*. Nutrients 9 2019;11:1992.

122. Kunisawa J, Takahashi I, Kiyono H. *Intraepithelial lymphocytes: their shared and divergent immunological behaviors in the small and large intestine*. Immunological Reviews 1 2007;215:136–53.

123. Lamers K, Steele MA, Cangiano LR. *A novel method for isolation and flow cytometry analysis of intraepithelial lymphocytes from colon biopsies*. JDS communications 5 2023;4:433–7.

124. Roberts AI, Lee L, Schwarz E, et al. *Cutting Edge: NKG2D Receptors Induced by IL-15 Costimulate CD28-Negative Effector CTL in the Tissue Microenvironment*. The Journal of Immunology 10 2001;167:5527–30.

125. Taunk J, Roberts AI, Ebert EC. *Spontaneous cytotoxicity of human intraepithelial lymphocytes against epithelial cell tumors*. Gastroenterology 1 1992;102:69–75.

126. Binda E, Erhart D, Schenk M, Zufferey C, Renzulli P, Mueller C. *Quantitative isolation of mouse and human intestinal intraepithelial lymphocytes by elutriation centrifugation*. Journal of Immunological Methods 1 2009;344:26–34.

127. Carrasco A, Mañé J, Santaolalla R, et al. *Comparison of lymphocyte isolation methods for endoscopic biopsy specimens from the colonic mucosa*. Journal of Immunological Methods 1-2 2013;389:29–37.

128. Yonemoto Y, Nemoto Y, Morikawa R, et al. *Single cell analysis revealed that two distinct, unique CD4+ T cell subsets were increased in the small intestinal intraepithelial lymphocytes of aged mice*. Frontiers in Immunology 2024;15:1340048.

129. Prakhar P, Prakhar P, Gonzalez V, González V, Park JH, Park JH. *High-yield enrichment of mouse small intestine intraepithelial lymphocytes by immunomagnetic depletion of EpCAM+ cells*. STAR protocols 1 2022;3:101207.

130. Hatano R, Yamada K, Iwamoto T, et al. *Antigen presentation by small intestinal epithelial cells uniquely enhances IFN-γ secretion from CD4+ intestinal intraepithelial lymphocytes*. Biochemical and Biophysical Research Communications 4 2013;435:592–6.

131. James OJ, Vandereyken M, Marchingo JM, et al. *IL-15 and PIM kinases direct the metabolic programming of intestinal intraepithelial lymphocytes*. Nature Communications 2021;12:4290.

132. León F, Roy G. *Isolation of human small bowel intraepithelial lymphocytes by annexin V-coated magnetic beads*. Laboratory Investigation 2004;84:804–9.

133. Swamy M, Abeler-Dörner L, Chettle J, et al. *Intestinal intraepithelial lymphocyte activation promotes innate antiviral resistance*. Nature Communications 2015;6:7090.

134. James OJ, Vandereyken M, Swamy M. *Isolation, Characterization, and Culture of Intestinal Intraepithelial Lymphocytes*. Methods of Molecular Biology 2020;2121:141–52.

135. Barros RDM, Roberts NA, Dart RJ, et al. *Epithelia Use Butyrophilin-like Molecules to Shape Organ-Specific $\gamma\delta$ T Cell Compartments*. Cell 2016;167:203–218.E17.

136. Ebert EC. *Tumour necrosis factor-alpha enhances intraepithelial lymphocyte proliferation and migration*. Gut 5 1998;42:650–5.

137. Fujihashi K, Yamamoto M, McGhee JR, Beagley KW, Kiyono H. *Function of $\alpha\beta$ TCR+ intestinal intraepithelial lymphocytes: Th1-and Th2-type cytokine production by CD4+ CD8 and CD4+ CD8+ T cells for helper activity*. International Immunology 1993:1473–81.

138. Lundqvist C, Melgar S, Yeung MMW, Hammarström S, Hammarström ML. *Intraepithelial lymphocytes in human gut have lytic potential and a cytokine profile that suggest T helper 1 and cytotoxic functions*. The Journal of Immunology 5 1996;157:1926–34.

139. Jo M, Me G, Goodrich ME, Eichelberger H, Dw M, McGee DW. *Polarized secretion of IL-6 by IEC-6 intestinal epithelial cells: differential effects of IL-1 beta and TNF-alpha*. Immunological Investigations 4 1996;25:333–40.

140. Bernardo D, Garrote JA, Fernández-Salazar L, Riestra S, Arranz E. *Is gliadin really safe for non-coeliac individuals? Production of interleukin 15 in biopsy culture from non-coeliac individuals challenged with gliadin peptides*. Gut 6 2007;56:889–90.

141. Escudero-Hernández C, Salvador-Peña A, Bernardo D. *Immunogenetic Pathogenesis of Celiac Disease and Non-celiac Gluten Sensitivity*. Current Gastroenterology Reports 7 2016;18:36.

142. Fernández-Bañares F, Crespo L, Núñez C, et al. *Gamma delta intraepithelial lymphocytes and coeliac lymphogram in a diagnostic approach to coeliac disease in patients with seronegative villous atrophy*. Alimentary Pharmacology & Therapeutics 7 2020;51:699–705.

143. Núñez C, Carrasco A, Corzo M, Pariente R, Esteve M, Roy G. *Chapter 12 - Flow cytometric analysis of duodenal intraepithelial lymphocytes (celiac lymphogram): A diagnostic test for celiac disease*. Ed. by Castellanos-Rubio A, Galluzzi L. Vol. 179. Academic Press, 2023:143–55.

144. Mayassi T, Jabri B. *Human intraepithelial lymphocytes*. Mucosal Immunology 5 2018;11. doi: 10.1038/s41385-018-0016-5:1281–9.

145. León F. *Flow cytometry of intestinal intraepithelial lymphocytes in celiac disease*. Journal of Immunological Methods 2 2011;363:177–86.

146. Antonangeli F, Soriani A, Cerboni C, Sciumè G, Santoni A. *How mucosal epithelia deal with stress: Role of NKG2D/NKG2D ligands during inflammation*. Frontiers in Immunology 2017;8:1583.

147. Adlercreutz EH, Weile C, Larsen J, et al. *A gluten-free diet lowers NKG2D and ligand expression in BALB/c and non-obese diabetic (NOD) mice*. Clinical and Experimental Immunology 2 2014;177:391–403.

148. Costes LMM, Lindenbergh-Kortleve DJ, Berkel LA van, et al. *IL-10 signaling prevents gluten-dependent intraepithelial CD4 cytotoxic T lymphocyte infiltration and epithelial damage in the small intestine*. Mucosal Immunology 2 2018;12:479–90.

149. Mandile R, Maglio M, Mosca C, et al. *Mucosal Healing in Celiac Disease: Villous Architecture and Immunohistochemical Features in Children on a Long-Term Gluten Free Diet*. Nutrients 18 2022;14:3696.

150. Schmitz F, Kooy-Winkelaar Y, Wiekmeijer AS, et al. *The composition and differentiation potential of the duodenal intraepithelial innate lymphocyte compartment is altered in coeliac disease*. Gut 8 2015;65:1269–78.

151. Vitale S, Santarlasci V, Camarca A, et al. *The intestinal expansion of TCR$\gamma\delta$ and disappearance of IL4 T cells suggest their involvement in the evolution from potential to overt celiac disease*. European Journal of Immunology 12 2019;49:2222–34.

152. Pagliari D, Cianci R, Frosali S, et al. *The role of IL-15 in gastrointestinal diseases: a bridge between innate and adaptive immune response*. Cytokine Growth Factor Review 5 2013;24:455–66.

153. Bernardo D, Garrote JA, Allegretti Y, et al. *Higher constitutive IL15Rα expression and lower IL-15 response threshold in coeliac disease patients*. Clinical and Experimental Immunology 1 2008;154:64–73.

154. Jabri B, Abadie V. *IL-15 functions as a danger signal to regulate tissue-resident T cells and tissue destruction*. Nature Reviews Immunology 12 2015;15:771–83.

155. Allard-Chamard H, Mishra HK, Nandi M, et al. *Interleukin-15 in autoimmunity*. Cytokine 2020;136:155258.

156. Pennington DJ, Silva-Santos B, Shires J, et al. *The inter-relatedness and interdependence of mouse T cell receptor $\gamma\delta+$ and $\alpha\beta+$ cells*. Nature Immunology 10 2003;4:991–8.

157. Hu MD, Ethridge AD, Lipstein R, et al. *Epithelial IL-15 Is a Critical Regulator of $\gamma\delta$ Intraepithelial Lymphocyte Motility within the Intestinal Mucosa*. The Journal of Immunology 2 2018;201:747–56.

158. Zhu Y, Cui G, Miyauchi E, et al. *Intestinal epithelial cell-derived IL-15 determines local maintenance and maturation of intra-epithelial lymphocytes in the intestine*. International Immunology 5 2019;32:307–19.

159. Aghamohamadi E, Kokhaei P, Rostami-Nejad M, et al. *Serum Level and Gene Expression of Interleukin-15 Do Not Correlate with Villous Atrophy in Celiac Disease Patients*. Genetic Testing and Molecular Biomarkers 8 2020;24:502–7.

160. Santos AJM, Unen V van, Lin Z, et al. *A human autoimmune organoid model reveals IL-7 function in coeliac disease*. Nature 2024;632:401–10.

161. Branchi F, Wiese JJ, Heldt C, et al. *The combination of clinical parameters and immunophenotyping of intraepithelial lymphocytes allows to assess disease severity in refractory celiac disease*. Digestive and Liver Disease 12 2022;54:1649–56.

162. Mascarel A de, Belleannée G, Stanislas S, et al. *Mucosal intraepithelial T-lymphocytes in refractory celiac disease: a neoplastic population with a variable CD8 phenotype*. The American Journal of Surgical Pathology 5 2008;32:744–51.

163. Schiepatti A, Maimaris S, Scarcella C, et al. *Flow cytometry for the assessment and monitoring of aberrant intraepithelial lymphocytes in non-responsive celiac disease and non-celiac enteropathies*. Digestive and Liver Disease 5 2023;56:795–801.

164. Stonier SW, Schluns KS. *Trans-presentation: a novel mechanism regulating IL-15 delivery and responses*. Immunology Letters 2 2009;127:85–92.

165. Ciszewski C, Discepolo V, Pacis A, et al. *Identification of a γc Receptor Antagonist That Prevents Reprogramming of Human Tissue-resident Cytotoxic T Cells by IL15 and IL21*. Gastroenterology 3 2020;158:625–637.E13.

166. Dieckman T, Schreurs M, Mahfouz A, et al. *Single-Cell Analysis of Refractory Celiac Disease Demonstrates Inter- and Intra-Patient Aberrant Cell Heterogeneity*. Cellular and Molecular Gastroenterology and Hepatology 1 2022;14:173–92.

167. Lindeman I, Sollid LM. *Single-cell approaches to dissect adaptive immune responses involved in autoimmunity: the case of celiac disease*. Mucosal Immunology 1 2021;15:51–63.

168. Unen V van, Li N, Molendijk I, et al. *Mass Cytometry of the Human Mucosal Immune System Identifies Tissue- and Disease-Associated Immune Subsets*. Immunity 5 2016;44:1227–39.

169. Ghasiyari H, RostamiNejad M, Amani D, et al. *Diverse Profiles of Toll-Like Receptors 2, 4, 7, and 9 mRNA in Peripheral Blood and Biopsy Specimens of Patients with Celiac Disease*. Journal of Immunology Research 1 2018;2018:7587095.

170. Herrera MG, Pizzuto M, Lonez C, et al. *Large supramolecular structures of 33-mer gliadin peptide activate toll-like receptors in macrophages*. Nanomedicine : Nanotechnology, Biology and Medicine 4 2018;14:1417–27.

171. Brynychova I, Hoffmanová I, Dvorak M, Dankova P. *Increased Expression of TLR4 and TLR7 but Not Prolactin mRNA by Peripheral Blood Monocytes in Active Celiac Disease*. Advances in Clinical and Experimental Medicine 5 2016;25:887–93.

172. Park SJ, Shin JI. *Interleukin-21-mediated TLR4 activation in celiac disease*. Digestive Diseases and Sciences 2013;58:2425.

173. Lammers KM, Lu R, Brownley J, et al. *Gliadin induces an increase in intestinal permeability and zonulin release by binding to the chemokine receptor CXCR3*. Gastroenterology 1 2008;135:194–204.E3.

174. Lammers KM, Brownley J, Lu R, et al. *Gliadin Binding to CXCR3 Causes Zonulin Release and Increased Intestinal Permeability*. Journal of Pediatric Gastroenterology and Nutrition 4 2006;43:E72.

175. Lammers KM, Khandelwal S, Chaudhry F, et al. *Identification of a novel immunomodulatory gliadin peptide that causes interleukin-8 release in a chemokine receptor CXCR3-dependent manner only in patients with coeliac disease*. Immunology 2011;132:432–40.

176. Schaerli P, Loetscher P, Moser B. *Cutting Edge: Induction of Follicular Homing Precedes Effector Th Cell Development*. The Journal of Immunology 11 2001;167:6082–6.

177. Velaga S, Herbrand H, Friedrichsen M, et al. *Chemokine Receptor CXCR5 Supports Solitary Intestinal Lymphoid Tissue Formation, B Cell Homing, and Induction of Intestinal IgA Responses*. The Journal of Immunology 5 2009;182:2610–9.

178. Winter S, Loddenkemper C, Aebischer A, et al. *The chemokine receptor CXCR5 is pivotal for ectopic mucosa-associated lymphoid tissue neogenesis in chronic Helicobacter pylori-induced inflammation*. Journal of Molecular Medicine 2010;88:1169–80.

179. Cárdeno A, Magnusson MK, QuidingJärbrink M, Lundgren A. *Activated T follicular helper-like cells are released into blood after oral vaccination and correlate with vaccine specific mucosal B-cell memory*. Scientific Reports 2018;8:2729.

180. Ciccocioppo R, D'Alo S, Sabatino AD, et al. *Mechanisms of villous atrophy in autoimmune enteropathy and coeliac disease*. Clinical and Experimental Immunology 1 2002;128:88–93.

181. Morimoto Y, Hizuta A, Ding EX, et al. *Functional expression of Fas and Fas ligand on human intestinal intraepithelial lymphocytes*. Clinical and Experimental Immunology 1 1999;116:84–9.

182. Sabatino AD, Ciccocioppo R, D'Alo S, et al. *Intraepithelial and lamina propria lymphocytes show distinct patterns of apoptosis whereas both populations are active in Fas based cytotoxicity in coeliac disease*. Gut 3 2001;49:380–6.

183. Glaría E, Valledor AF. *Roles of CD38 in the Immune Response to Infection*. Cells 1 2020;9:228.

184. Pré MF du, Berkel LA van, Ráki M, et al. *CD62LnegCD38 expression on circulating CD4 T cells identifies mucosally differentiated cells in protein fed mice and in human celiac disease patients and controls*. The American Journal of Gastroenterology 6 2011;106:1147–59.

185. Zühlke S, Risnes LF, DahalKoirala S, Christophersen A, Sollid LM, Lundin KEA. *CD38 expression on gluten-specific T cells is a robust marker of gluten re-exposure in coeliac disease*. United European Gastroenterology Journal 10 2019;7:1337–44.

186. Binder C, Cvetkovski F, Sellberg F, et al. *CD2 Immunobiology*. Frontiers in Immunology 2020;11:1090.

187. Gonsky R, Deem RL, Young HA, Targan SR. *CD2 mediates activation of the IFNγ intronic STAT binding region in mucosal T cells*. European Journal of Immunology 5 2003;33:1152–62.

188. Escudero-Hernández C, Martín Á, Pedro Andrés R de, et al. *Circulating Dendritic Cells from Celiac Disease Patients Display a GutHoming Profile and are Differentially Modulated by Different GliadinDerived Peptides*. Molecular Nutrition & Food Research 6 2020;64:1900989.

189. Yuan J. *CCR2: A characteristic chemokine receptor in normal and pathological intestine*. Cytokine 2023;169:156292.

190. Pathak M, Lal G. *The Regulatory Function of CCR9 Dendritic Cells in Inflammation and Autoimmunity*. Frontiers in Immunology 2020;11:536326.

191. Gorfu G, RiveraNieves J, Gawaz M, Ley K. *Role of β7 integrins in intestinal lymphocyte homing and retention*. Current Molecular Medicine 7 2009;9:836–50.

192. Schweighoffer T, Tanaka Y, Tidswell M, et al. *Selective expression of integrin alpha 4 beta 7 on a subset of human CD4+ memory T cells with Hallmarks of gut-trophism*. The Journal of Immunology 2 1993;151:717–29.

193. Marsch DS, Marchbank T, Playford RJ, Jones AW, Thatcher R, Davison G. *Intestinal fatty acid-binding protein and gut permeability responses to exercise*. European Journal of Applied Physiology 5 2017;117:931–41.

194. Fernández-Bañares F, Farrais S, Planella M, et al. *Coeliac Disease in Elderly Patients: Value of Coeliac Lymphogram for Diagnosis*. Nutrients 9 2021;13:2984.

195. Rodríguez-Martín L, Ayala LMV, Martín MH, Alegre SV. *Assessing mucosal recovery in celiac disease - Time to diagnosis and histological severity as determining factors*. Revista Española de Enfermedades Digestivas 7 2024;116:356–61.

196. Nijeboer P, Gils T van, Reijm M, et al. *Gamma-Delta T Lymphocytes in the Diagnostic Approach of Coeliac Disease*. Journal of Clinical Gastroenterology 5 2019;53:e208–e213.

197. Abadie V, Han AS, Jabri B, Sollid LM. *New Insights on Genes, Gluten, and Immunopathogenesis of Celiac Disease*. Gastroenterology 1 2024;167:4–22.

198. Ciacci C, Bai JC, Holmes G, et al. *Serum anti-tissue transglutaminase IgA and prediction of duodenal villous atrophy in adults with suspected coeliac disease without IgA deficiency (Bi.A.CeD): a multicentre, prospective cohort study*. The Lancet. Gastroenterology & Hepatology 11 2023;8:1005–14.

199. Gong C, Saborit C, Long X, et al. *Serological Investigation of Persistent Villous Atrophy in Celiac Disease*. Clinical and Translational Gastroenterology 12 2023;14:e00639.

200. Schiepatti A, Maimaris S, Raju SA, et al. *Persistent villous atrophy predicts development of complications and mortality in adult patients with coeliac disease: a multicentre longitudinal cohort study and development of a score to identify high-risk patients*. Gut 11 2023;72:2095–102.

201. Ventura I, Rodriguez B, Suescum S, et al. *More Than Three Years for Normalisation of Routine Laboratory Values after Gluten Withdrawal in Paediatric Coeliac Patients*. Children (Basel, Switzerland) 9 2023;10:1580.

202. Palma GD, Nadal I, Collado MC, Sanz Y. *Effects of a gluten-free diet on gut microbiota and immune function in healthy adult human subjects*. British Journal of Nutrition 8 2009;102:1154–60.

203. Sanz Y. *Effects of a gluten-free diet on gut microbiota and immune function in healthy adult humans*. Gut Microbes 3 2010:135–7.

204. Sangineto M, Graziano G, DAmore S, et al. *Identification of peculiar gene expression profile in peripheral blood mononuclear cells (PBMC) of celiac patients on gluten free diet*. PLOS ONE 5 2018;13:e0197915.

205. Ramírez-Sánchez AD, Chu X, Modderman R, et al. *Single-Cell RNA Sequencing of Peripheral Blood Mononuclear Cells From Pediatric Coeliac Disease Patients Suggests Potential Pre-Seroconversion Markers*. Frontiers in Immunology 2022;13:843086.

206. Chao P. *Application of Flow Cytometry in Functional Analysis of Immune Cells*. International Journal of Clinical and Experimental Medicine Research 4 2023;7:595–8.

207. McKinnon K. *Flow Cytometry: An Overview*. Current Protocols in Immunology 1 2018;120:5.1.1–5.1.11.

208. Paterson J, Ailles LE. *High Throughput Flow Cytometry for Cell Surface Profiling*. Methods in Molecular Biology 11 2018;1678:111–38.

209. Liu P, Pan Y, Chang HC, et al. *Comprehensive evaluation and practical guideline of gating methods for high-dimensional cytometry data: manual gating, unsupervised clustering, and auto-gating*. bioRxiv 1 2024;26:bbae633.

210. McInnes L, Healy JJ. *UMAP: Uniform Manifold Approximation and Projection for Dimension Reduction*. arXiv: Machine Learning 2018.

211. Stolarek I, Samelak-Czajka A, Figlerowicz M, Jackowiak P. *Dimensionality reduction by UMAP for visualizing and aiding in classification of imaging flow cytometry data*. iScience 10 2022;25:105142.

212. Weijler L, Kowarsch F, Wödlinger M, et al. *UMAP Based Anomaly Detection for Minimal Residual Disease Quantification within Acute Myeloid Leukemia*. Cancers 4 2022;14:898.

213. Gassen SV, Callebaut B, Helden MJ van, et al. *FlowSOM: Using self-organizing maps for visualization and interpretation of cytometry data*. Cytometry 7 2015;87:636–45.

214. Goh WWB, Wang W, Wong L. *Why Batch Effects Matter in Omics Data, and How to Avoid Them*. Trends in Biotechnology 6 2017;35:498–507.

215. López-Palacios N, Pascual V, Castaño M, et al. *Evaluation of T cells in blood after a short gluten challenge for coeliac disease diagnosis*. Digestive and Liver Disease 11 2018;50:1183–8.

216. Bondar C, Araya RE, Guzmán L, Rua EC, Chopita NA, Chirdo FG. *Role of CXCR3/CXCL10 axis in immune cell recruitment into the small intestine in celiac disease*. PLOS ONE 2014;9:e89068.

217. Baumgaertner P, Sankar M, Herrera F, et al. *Unsupervised Analysis of Flow Cytometry Data in a Clinical Setting Captures Cell Diversity and Allows Population Discovery*. Frontiers in Immunology 2021;12:633910.

218. Olsen LR, Pedersen CB, Leipold MD, Maecker HT. *Getting the Most from Your High-Dimensional Cytometry Data*. Immunity 3 2019;50:535–6.

219. Sansotta N, Amirikian K, Guandalini S, Jericho H. *Celiac Disease Symptom Resolution*. Journal of Pediatric Gastroenterology and Nutrition 1 2018;66:48–52.

220. Tapsas D, Hollén E, Stenhammar L, Fälth-Magnusson K. *The clinical presentation of coeliac disease in 1030 Swedish children: Changing features over the past four decades*. Digestive and Liver Disease 1 2016;48:16–22.

221. Szakács Z, Mátrai P, Hegyi P, et al. *Younger age at diagnosis predisposes to mucosal recovery in celiac disease on a gluten-free diet: A meta-analysis*. PLOS ONE 11 2017;12:e0187526.

222. Cukrowska B, Sowiska A, Biera JB, Czarnowska E, Rybak A, -Chlebowczyk UG. *Intestinal epithelium, intraepithelial lymphocytes and the gut microbiota*. World Journal of Gastroenterology 42 2017;23:7505–18.

223. Cerovic V, Pabst O, Mowat A. *The renaissance of oral tolerance: merging tradition and new insights*. Nature Reviews Immunology 2024;25:42–56.

224. Slager J, Simpson HL, Gacesa R, et al. *High-resolution analysis of the treated coeliac disease microbiome reveals strain-level variation*. bioRxiv 2024.

225. Simpson HL, Smits E, Moerkens R, et al. *Human organoids and organ-on-chips in coeliac disease research*. Trends in Molecular Medicine 2 2025;31:117–37.

226. Olaussen RW, Karlsson MR, Lundin KEA, Jahnsen J, Brandtzaeg P, Farstad IN. *Reduced Chemokine Receptor 9 on Intraepithelial Lymphocytes in Celiac Disease Suggests Persistent Epithelial Activation*. Gastroenterology 7 2007;132:2371–82.

227. Papadakis KA, Prehn JL, Moreno ST, et al. *CCR9Positive lymphocytes and thymus-expressed chemokine distinguish small bowel from colonic Crohn's disease*. Gastroenterology 2 2001;121:246–54.

228. Evans-Marin HL, Cao AT, Yao S, et al. *Unexpected Regulatory Role of CCR9 in Regulatory T Cell Development*. PLOS ONE 7 2015;10:e0134100.

229. Mazzini E, Massimiliano L, Penna G, Rescigno M. *Oral tolerance can be established via gap junction transfer of fed antigens from CX3CR1 macrophages to CD103 dendritic cells*. Immunity 2 2014;40:248–61.

230. Nastro FF, Serra MR, Cenni S, et al. *Prevalence of functional gastrointestinal disorders in children with celiac disease on different types of gluten-free diets*. World Journal of Gastroenterology 46 2022;28:6589–98.

231. Khoury DE, Balfour-Ducharme S, Joye IJ. *A Review on the Gluten-Free Diet: Technological and Nutritional Challenges*. Nutrients 10 2018;10:1410.

232. Melini V, Melini F. *Gluten-Free Diet: Gaps and Needs for a Healthier Diet*. Nutrients 1 2019;11:170.

233. Wang Y, Chen B, Ciaccio EJ, et al. *Celiac Disease and the Risk of Cardiovascular Diseases*. International Journal of Molecular Sciences 12 2023;24:9974.

234. Schmucker C, Eisele-Metzger A, Meerpohl JJ, et al. *Effects of a gluten-reduced or gluten-free diet for the primary prevention of cardiovascular disease*. Cochrane Database of Systematic Reviews 2 2022;2:CD013556.

235. Gan J, Nazarian S, Teare J, Darzi A, Ashrafian H, Thompson AJ. *A case for improved assessment of gut permeability: a meta-analysis quantifying the lactulose:mannitol ratio in coeliac and Crohn's disease*. BMC Gastroenterology 2022;22:16.

236. Costigan CM, Warren FJ, Duncan AP, et al. *One year of gluten free diet impacts gut function and microbiome in celiac disease*. Clinical Gastroenterology and Hepatology 24 2024;S1542-3565:1048–6.

237. Hære P, Höie O, Schulz T, Schönhardt I, Ráki M, Lundin KEA. *Long-term mucosal recovery and healing in celiac disease is the rule - not the exception*. Scandinavian Journal of Gastroenterology 2016;51:1439–46.

238. Lanzini A, Lanzarotto F, Villanacci V, et al. *Complete recovery of intestinal mucosa occurs very rarely in adult coeliac patients despite adherence to gluten-free diet*. Alimentary Pharmacology & Therapeutics 12 2009;29:1299–308.

239. Malamut G, Soderquist CR, Bhagat G, Cerf-Bensussan N. *Advances in Non-responsive and Refractory Celiac Disease*. Gastroenterology 1 2024;167:132–47.

240. Pekki H, Kurppa K, Mäki M, et al. *Performing routine follow-up biopsy 1 year after diagnosis does not affect long-term outcomes in coeliac disease*. Alimentary Pharmacology & Therapeutics 11 2017;45:1459–68.

241. Rubio-Tapia A, Rahim MW, See JA, Lahr BD, Wu TT, Murray JA. *Mucosal recovery and mortality in adults with celiac disease after treatment with a gluten-free diet*. The American Journal of Gastroenterology 6 2010;105:1412–20.

242. Green PHR, Paski S, Ko CW, Rubio-Tapia A. *AGA Clinical Practice Update on Management of Refractory Celiac Disease: Expert Review*. Gastroenterology 5 2022;163:1461–9.

243. Scarmozzino F, Pizzi M, Pelizzaro F, et al. *Refractory celiac disease and its mimickers: a review on pathogenesis, clinical-pathological features and therapeutic challenges*. Frontiers in Oncology 2023;13:1273305.

244. Machado MV. *Refractory Celiac Disease: What the Gastroenterologist Should Know*. International Journal of Molecular Sciences 19 2024;25:10383.

245. Cording S, Lhermitte L, Malamut G, et al. *Oncogenetic landscape of lymphomagenesis in coeliac disease*. Gut 3 2022;71:497–508.

246. Mulder CJJ, Wierdsma NJ, Berkenpas M, Jacobs MAJM, Bouma G. *Preventing complications in celiac disease: our experience with managing adult celiac disease*. Best Practice & Research in Clinical Gastroenterology 3 2015;29:459–68.

247. Gils T van, Nijeboer P, Wanrooij RL van, Bouma G, Mulder CJJ. *Mechanisms and management of refractory coeliac disease*. Nature Reviews Gastroenterology & Hepatology 10 2015;12:572–9.